MOERAKI TOWNSHIP: INSTABILITY ASSESSMENT

A thesis

submitted in partial fulfilment

of the requirements for the Degree

of

Master of Science in Engineering Geology

in the

University of Canterbury

by

M.K. MOLINEAUX

University of Canterbury

1983

FRONTISPIECE

Moeraki township established along the northern coastline of Moeraki Peninsula, South Island, New Zealand. Salient varied relief in the township area is attributed to well delineated, deep-seated mass movement developed along the coastline. Oblique view looking inland west to the Southern Alps.

(Photograph courtesy New Zealand Geological Survey)

ABSTRACT

Moeraki township has within its boundaries active mass movement jeopardizing housing and roading which necessitates comprehensive instability investigations for hazard mitigation.

Geomorphological research identified salient deep-seated slope failure encompassing the entire township area developed within Tertiary mudstones; subsequent shallow instability amidst juxtaposed slide blocks has been accelerated by man and poses a major threat to residential development.

Tertiary mudstone units in the field area are subject to strain "softening" and were characterized as over-consolidated, blue-grey, silty clays containing an abundance of smectites. In-situ softening appeared expedited by high ground water pressures and yields a cohesive plastic clay of low strength prone to slope failure.

Investigations were concentrated in two areas where active mass movement was threatening housing and roading. Severe damage in the two study areas was caused by well delineated cohesive flow-slide behaviour moving at rates in excess of 15 cm per year principally via "drained" failure in response to rising ground water levels. Comparatively stable mudstone regolith/colluvium at low slope angles exhibited "creep" deformation in the order of 2 cm to 4 cm per year, sufficient to damage building foundations.

Incipient slope failure was assessed utilizing classical limit equilibrium analyses (Janbu, Generalised Procedure of Slices) and highlighted the inadequacies of such methods in dealing with real world scenarios such as "progressive slope failure".

Data was collated to develop a model for evolving slope failure within mudstone; principle criteria controlling shallow instability were concluded as:

1) extent of terrain activity
2) ground water pressure.

Mass movement susceptibility plans (scale 1:1000) were compiled for the township area based on the preceding failure model. Terrain evaluation was by subjective assessment of three factors; geology, geomorphology and hydrology. Finally, concise recommendations on land use zoning are outlined.

CONTENTS

Page

Page

LIST OF FIGURES

CONTENTS OF MAP ENCLOSURE

ACKNOWLEDGEMENTS

My sincere thanks to the countless people who have encouraged, advised and assisted me during the time it took to complete this project; the following in particular deserve special mention.

Mr B. Paterson (NZGS) who initiated the project and provided perceptive discussion throughout.

The Waitaki County Council for continued financial support.

Mr D.H. Bell and Dr Pettinga (University of Canterbury) for encouragement, astute supervision, and patient editing of thesis drafts.

Mr B. Lockerbie (Waitaki County Council) without whose support and endless patience the field work undertaken would have proven impossible.

Mr A. Greig and J. Hermann (University of Otago) who managed to instruct me in some of the mysteries of surveying.

Glen Coates (University of Canterbury) for endeavouring to teach me the intricacies of grain-size analysis and the "Texas". Albert Downing for his photographic skills; Arthur Nichols plus J. van Dyke for maintenance in the wake of my testing programme and Mark Foley for inspired assistance with clay mineralogy and triaxial testing.

Dr R. Davis (University of Canterbury) for enlightenment on 'slip circles' and all things mathematical.

Mr and Mrs Kedsley and Moeraki township residents who made me so welcome and provided invaluable local knowledge pertaining to slope stability problems.

Mrs Brenda Carter who patiently deciphered a cryptic scrawl into something resembling a thesis.

To Chris, Gay, Fin, Sossy, Rats, Binky, Buttons and Bryce, sincere appreciation for assistance which 'kept me going'.

Special thanks to my parents without whose encouragement and faith, the project would not have been possible.

CHAPTER ONE

INTRODUCTION

1.1 INTRODUCTION

The township of Moeraki, situated in the South Island, New Zealand, is located on a sequence of well defined slope failures, and has within its boundaries areas of active slope deformation posing a threat to housing and/or roading. This project was undertaken to delineate zones susceptible to mass movement, and in doing so, to establish a sound basis for guidelines on future residential development. The relevance of this research to the local authority (Waitaki County Council) becomes apparent if reference is made to the statutory provisions in the Town and Country Planning Act (1977) relating to this type of contingency.

1.2 THESIS OBJECTIVES

1. To compile detailed engineering geological maps (scale 1:1000) of Moeraki township which delineate the following features in relation to housing and roading:
   a) the extent and activity of mass movement
   b) bedrock geology
   c) drainage paths, springs etc ....

2. To determine geotechnical properties of the surficial materials most prone to instability.

3. To study in detail two regions where active slope failure is affecting housing and/or roading and subsequently suggest remedial options.

4. To develop a hazard or mass movement susceptibility map for the township area which may provide guidelines for land-use zoning.

1.3 MOERAKI PENINSULA

1.3.1 Location

Moeraki township is established along the northern coastline of Moeraki Peninsula which is located on the east coast of the South Island, New Zealand, approximately 75 km north of Dunedin (Fig. 1.1).

Topography of the peninsula is generally subdued and undulatory to the south with higher relief restricted to the north and northeastern sections; the highest point being Moeraki Trig Station (154.6 m) located in the far north-western corner.

Moeraki township is situated about 1 km east of State Highway 1; it lies between 45°22' South Long. and 170°50' to 170°52' East and borders 1.7 km of coastline covering an area of roughly 9.7 km.

Published maps of the area used during the investigation are:

- NZ Topographical Map 1:63360 Interim Series NZMS 1, Sheet 146, Moeraki.
- NZ Geological Map, 1:250,000, Sheet 23, Oamaru.

All metric grid references for specific locations are in terms of GEODETIC DATUM 1949.

False Origin, Observation Point
700 000 mN , 300 000 mE

References quoted are to the nearest 50 m and in the format (Easting,Northing) with each graticule abridged to four figures, ie. Moeraki township jetty (317650E,750250N) is abbreviated to (7650E,0250N).

1.3.2 Geological Setting

The peninsula is bisected north-south by predominatly easterly dipping blue-grey glauconitic silty mudstones. Overlying and flanking these to the east and west are pyroclastic basaltic tuffs and agglomerates. The sequence is extensively intruded

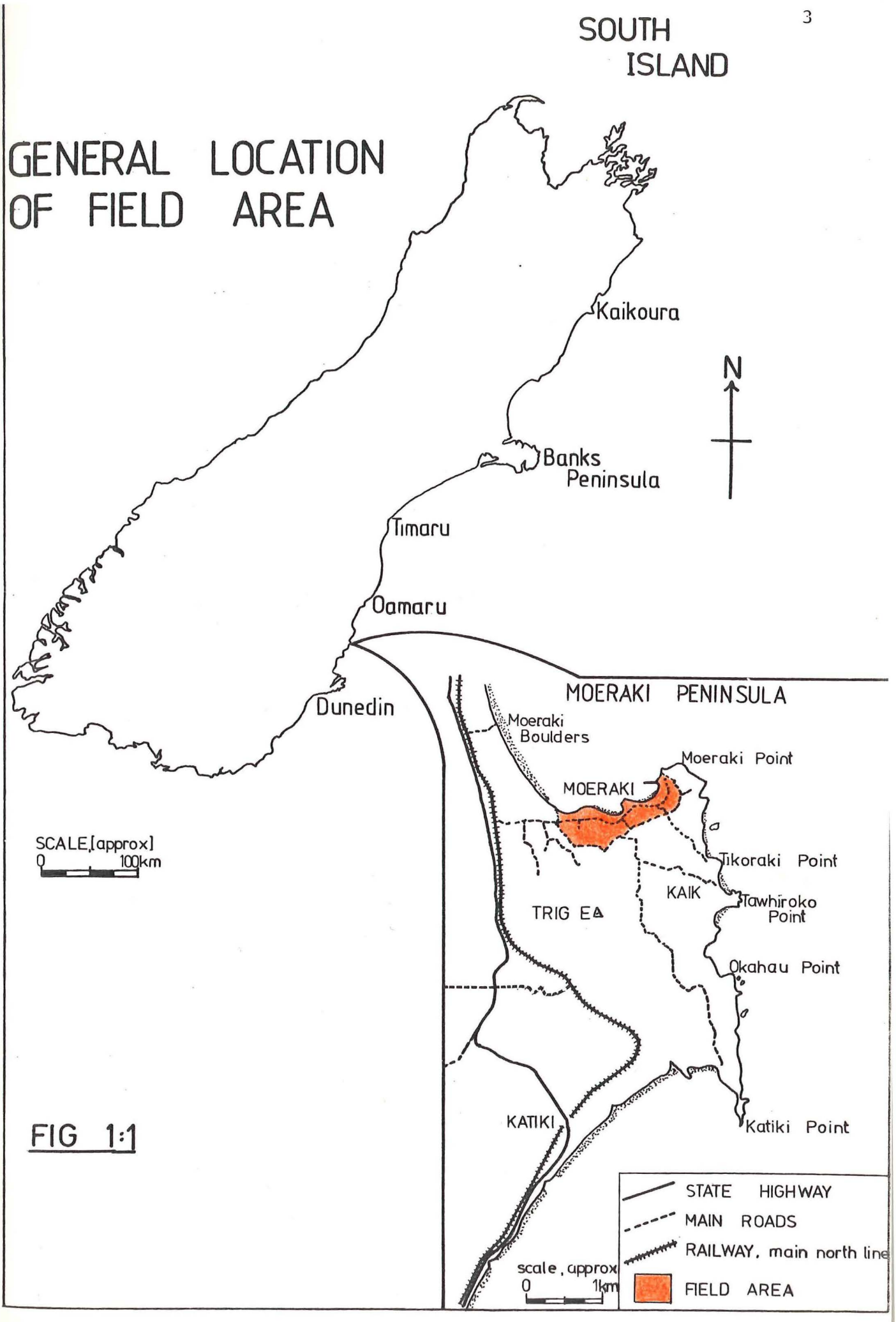
SOUTH ISLAND
GENERAL LOCATION OF FIELD AREA
Kaikoura
N
Banks Peninsula
Timaru
Oamaru
Dunedin
SCALE, [approx]
0 100km
MOERAKI PENINSULA
Moeraki Boulders
Moeraki Point
MOERAKI
Tikoraki Point
KAIK
Tawhiroko Point
TRIG E
Okahau Point
KATIKI
Katiki Point
scale, approx
0 1km
STATE HIGHWAY
MAIN ROADS
RAILWAY, main north line
FIELD AREA

FIG 1:1

by dolerite sills and associated dyke complexes.

Higher relief to the north and east of the peninsula is associated with two extensive dolerite sills which form resistant caps and prevent erosion of softer underlying mudstone.

Intrusive sheet and dyke complexes appear to control degradation along the northern coast, where isolated dolerite outcrops form three resistant headlands separating bays eroded into mudstone. The eastern coast is essentially linear due to the influence of a resistant intrusive sheet in the south, and numerous dyke structures in the north.

The entire northern coastline has a markedly varied topography attributed to a series of adjacent slides varying in scale, and delineated by prominent headscarps (relief up to 20 m), which are developed within the mudstone formations. Subsequent erosion of dislocated slide blocks has produced a hummocky morphology predominantly sloping northward, on which the township of Moeraki is established.

Drainage patterns etched into higher relief on the peninsula show some structural control in a southwest-northeasterly direction. Altered topography along the northern coastline has caused irregular drainage networks and surface ponding. The only significant catchment area influencing groundwater lies to the southwest of the township proper.

1.3.3 Vegetation

Vegetation covering the peninsula is predominantly grassland cultivated for rural use, with patches of exotic shrub occurring toward the central region. Pre-European vegetation was coastal Broadleaf-Podocarp forest, containing broadleaf *(Griselina littoralis)*, totara *(Podocarpus totara)*, kowhai *(Sophora microphylla)*, kawa ka *Libocedrus bidwillie)*, rimu *(Dacrydium cupressinum)*, and silver beech *(Nothofagus menziesii)* (Mr B. Lockerbie, *pers.comm.*).

Isolated remnants of native bush occur within the township, together with clusters of exotic trees (mainly conifers).

1.3.4 Climate

The nearest New Zealand Meteorological Station to the peninsula is located at Trotters Creek (Lat. 45°23' South, Long. 170°49' East) approximately 3 km inland and south-west of the study area.

Records from 1908 to 1980 show a mean annual rainfall for the area of 623 mm (NZ Meteorological Office, Wellington).

August and September on average are the driest months, with November and December the wettest, but there is little seasonal variation. A Moeraki station established closer to the township area (Lat. 45°22' South, Long. 170°50' East) was operative from 1895 to 1942, and has records showing the peninsula as consistently drier than Trotters Creek with mean annual rainfall roughly 100 mm lower. Averaged data from this station confirms August is generally the driest month with December and January the wettest.

Rainfall is typically of low concentration but of prolonged duration rather than short storms of high intensity. Compared to further inland, the peninsula area has fewer sunshine hours (1600-1800) each year, due to increased cloud cover and less rainy days. Incident radiation is also low, being between 300-320 cals. cm^2/day. The prevailing wind for most of the year is north-easterly with south-westerlies associated with the majority of rain. During winter months (June, July, August) occasional frosts occur in shaded areas freezing ground to depths of 8-10 cm. The climate is broadly classified as subhumid and mesothermal. Daily rainfall and temperature readings for the study area were recorded by Mr and Mrs Kedsley (Pembroke Street)(refer Appendix 2).

1.3.5 Land Use

In the main, the peninsula is extensively farmed, with the only significantly populated areas being Moeraki township along the northern coastline and small isolated holiday settlements situated beside the east coast. Moeraki township is bounded within two tarsealed roadways; Haven Street essentially following the peninsula's northern shoreline and Tenby Street extending roughly parallel to this along higher

ground, the intersection of the two defining the township's western margin. The township area's District Scheme is comprised of three land-use zones; residential, rural B and industrial (Fig. 1.2).

1.4 HISTORY OF INSTABILITY

The district was first settled by Europeans at Onekakara Bay on 26th December 1836. In 1858 Moeraki township was laid out by the Provincial Government and in 1863 a survey plan was produced (McDonald, 1940). It was reported "heavy traffic and constant slips made upkeep of the road very expensive" and in May 1875 it was described as "nearly impassable".

By February 1977, a rail link connecting Moeraki fishing depot to the main trunk line was established; the track followed the coast, crossing to Tawitiatauka Point by a curving viaduct and continued to a station located near the jetty (Moeraki Centenary Souvenir, 1936). In 1878 piles supporting the viaduct had moved seaward 1.2 m. Subsequent remedial measures were finally abandoned and the line taken up in October 1879 (McDonald 1940). Erosion problems continued in this area as Benson (1946b) notes:

> "although in a very sheltered spot wave action cuts back the low mudstone cliff at the rate of a few feet per year and the present shoreline is not only a hundred yards inland of its position in 1860, but, is nearly fifty yards inland of the former position of the railway embankment."

Maintenance of the main road proved difficult, until in 1880 it was described as resembling "stairs" in places and was threatened with closure.

Stability problems have intensified to the present day with increasing urban growth. The main road, Haven Street, is subject to severe, sudden subsidence following rainfall, which on occasions creates a traffic hazard and some housing areas are threatened or have been damaged by shallow slope failures.

WAITAKI COUNTY DISTRICT PLANNING MAP OF MOERAKI

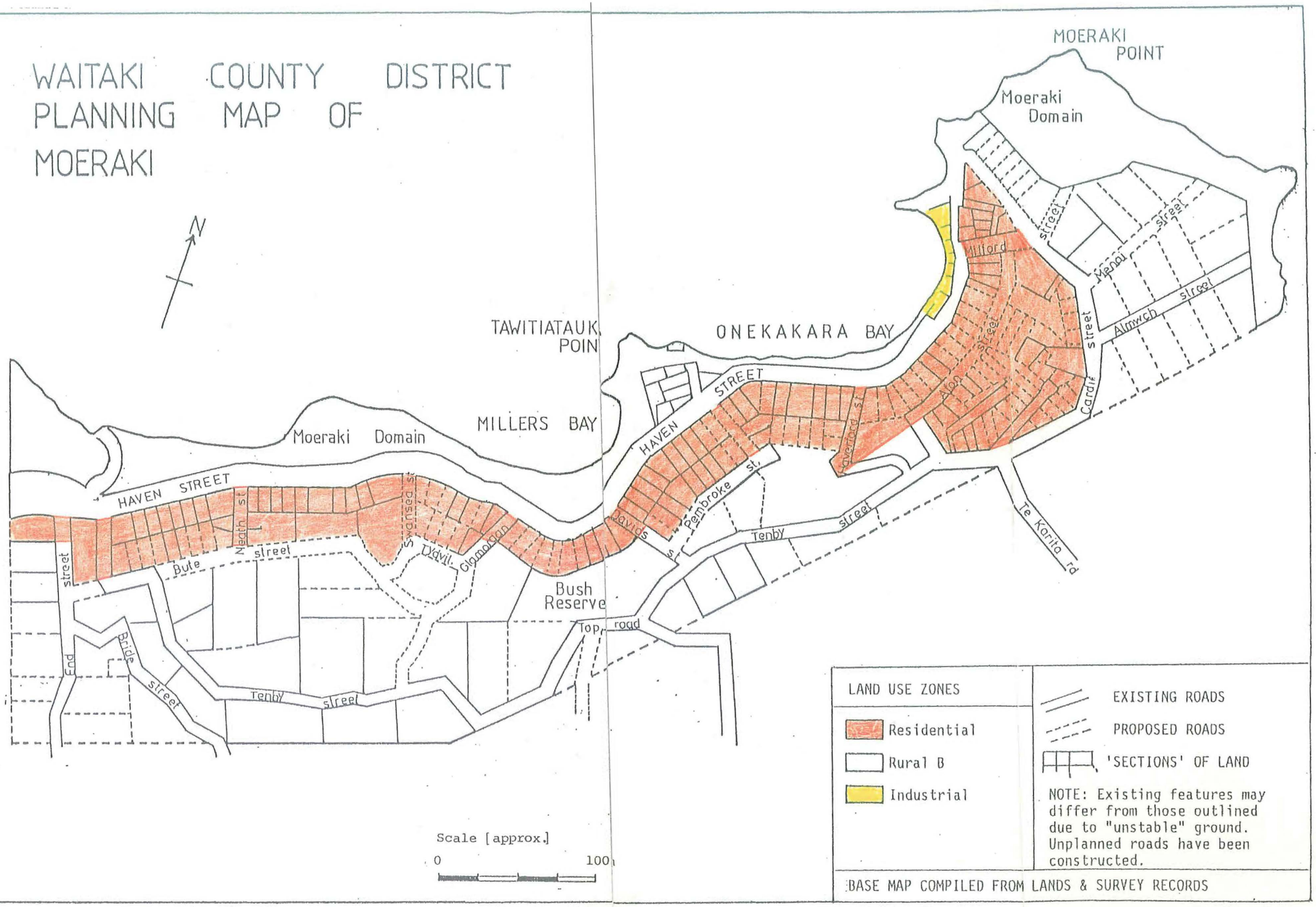

LAND USE ZONES	
Residential	EXISTING ROADS
Rural B	PROPOSED ROADS
Industrial	'SECTIONS' OF LAND
	NOTE: Existing features may differ from those outlined due to "unstable" ground. Unplanned roads have been constructed.

BASE MAP COMPILED FROM LANDS & SURVEY RECORDS

FIGURE 1.2

date?

1.5 PREVIOUS RESEARCH

Mantell (1850) in his paper on the geology of North Otago, was the first to describe the Hampden "clays" as the Onekakara "beds".

> "At Onekakara a green, gritty marl crops out beneath the blue clay; layers of iron pyrites occur at intervals in it. The water that flows through this bed is highly charged with salts and of extremely disagreeable flavour."

Hector (1862) produced a geological report, which was followed by a fuller classification of geological formations in 1866 (Hector).

Traill (1869) described fossils from Hampden and concluded the clays could not be younger than Miocene.

Haast (1873) having reported on the Shag Point coal fields, produced a geological map and in collaboration with Hutton (1875), concluded the Moeraki Boulder Beds, Hampden Clays and Waiarekan Tuffs were Upper Miocene.

Hector (1877) published a classification of New Zealand geological formations which differed considerably by placing all formations from Shag Point to the Kakanui River in the Cretaceo-Tertiary group.

Cox (1883) in a brief report on Shag Valley first defined the fault, which formed the valley, that is now known as part of the Waihemo Fault Complex.

McKay (1887) produced two reports on North-east Otago confirming a fault but showing conclusively the major structure lay to the south-west side of the Blue Mountains rather than the north-east side as shown by Cox (1883). McKay's, Onekakara clays (the upper part of which is now correlated with the Hampden Formation, the lower the Kurinui Formation) differs from Mantell's (1850) Onekakara "beds" which are equivalent to the Moeraki Formation (Brown, 1959) (refer Appendix 1, NZ Geological Time Scale).

In the early 1900s the age of the Hampden beds was placed by various workers between Eocene and Miocene and not finally confirmed until Finlay and Marwick's (1940) foraminifera work accurately determined them as Eocene.

Benson (1940, 1941, 1942, 1943, 1944, 1945, 1946a, 1946b) analysed in detail the igneous rocks and tectonic environment of eastern Otago; his 1943 paper describes Moeraki Peninsula geology in detail and the 1946b publication briefly highlights the extent of instability affecting the township area.

Coombs and Dickey (1965) briefly review the volcanic rocks exposed on the peninsula.

Paterson (1980) prepared a concise unpublished report for the Waitaki County Council, highlighting the extent of mass movement influencing housing and/or roading. Following this Tonkin and Taylor (1982) adopted a "broad brush" approach to stability assessment and produced a land hazard map (scale 1:5000) in association with a land-use management plan for the Moeraki township.

CHAPTER TWO

GEOLOGY

2.1 INTRODUCTION

Chapter two attempts a concise geological outline depicted in four parts. The first is a summary of regional geology in conjunction with a generalised description of geological history. Parts two and three deal specifically with the Moeraki Peninsula; the second describing stratigraphy with particular reference to those formations outcropping within the field area, and the third outlines structure. The final part, is a synthesis of Quaternary geology providing background information pertinent to deep-seated instability developed along Moeraki Peninsula's northern coastline.

2.2 REGIONAL GEOLOGY

Regionally, two structural blocks are recognized, separated by the northwest-southeast trending Waihemo Fault Complex. A block to the northeast, stretching from the Kakanui River to Shag Point with its western edge forming the Kakanui Range, and a second block to the southwest extending south of Shag Point and inland to the east (Fig. 2.1).

Basement of the northeastern block is mica schist, which regionally dips northeast, and was eroding during the Cretaceous to a peneplain.

Towards the coast, the block is covered with remnants of Late Cretaceous and Tertiary sediments (mudstones, siltstones, sandstones and limestones) which include igneous rocks associated with volcanic activity during the Eocene and Oligocene. The sequence is covered by a variable mantle of Quaternary deposits (outwash fans and terrace gravels).

REGIONAL GEOLOGY

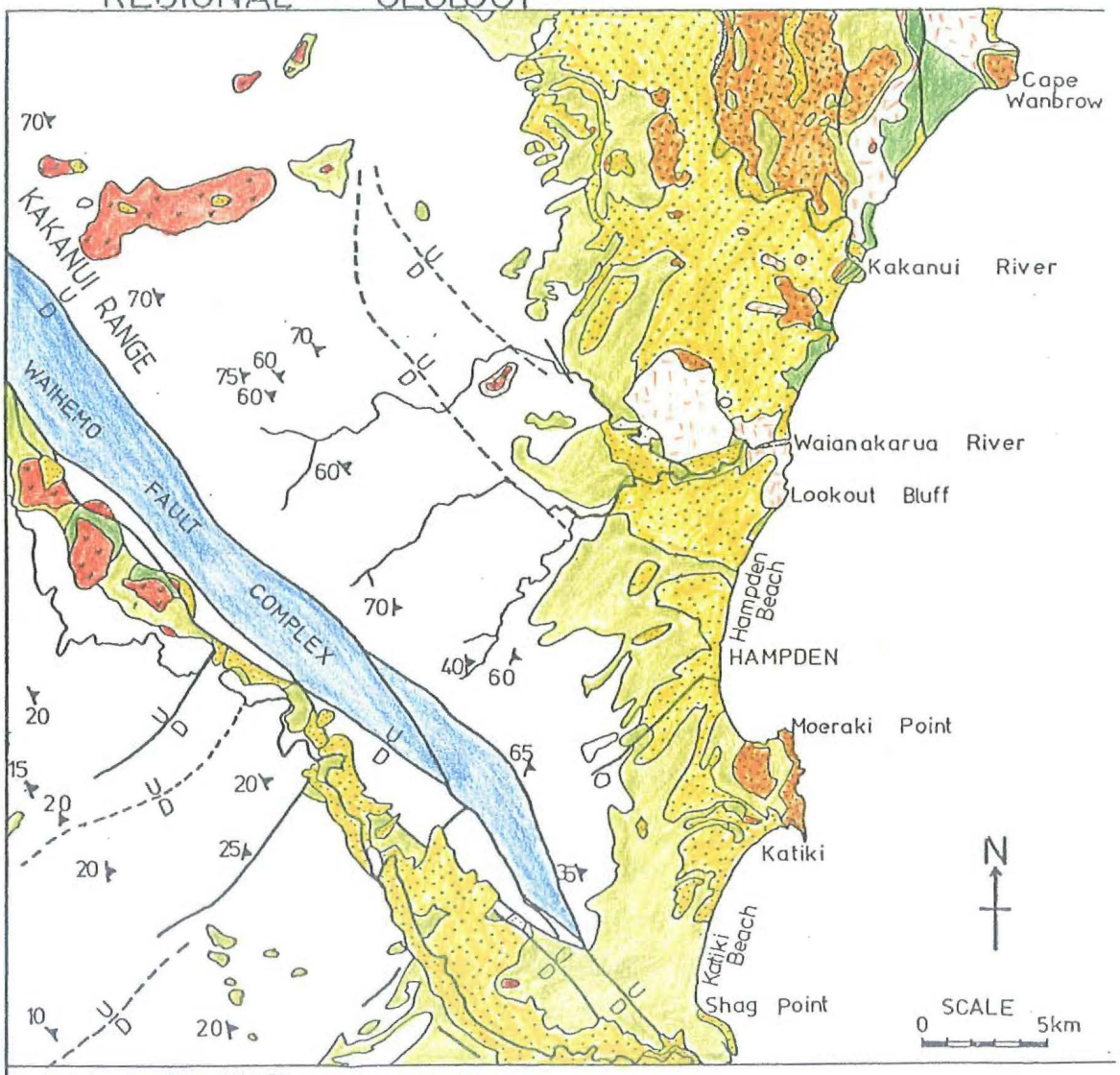

LEGEND

Age	General lithology.
Pleistocene	Till, outwash and terrace gravels.
Pliocene	Basaltic intrusives.
Oligocene	Siltstones and sandstones. [Some glauconitic]
	Bedded tuff, basaltic breccia, pillow lava and columnar basalt sills.
	Limestone
Eocene	Tuff basalt and tachylite breccia, dolerite sills and basalt dykes.
Late Cretaceous	Dark grey sandstones, siltstones and mudstones. [Some glauconitic]
	Greywacke breccia. Siltstone with coal seams.
Middle Triassic	Greywacke and argillite.
?	Quartzo-feldspathic schists.

SYMBOLS

D/U — Fault

D - Downthrown block.

Strike and dip

Based on A.Mutch 1963. Sheet 23 Geol Map of N.Z 1 : 250,000

FIG 2:1

The southwestern block is lithologically similar to, and correlates with sediments of the northeastern block up until the Tertiary, but the Cretaceous peneplain is less uniform in dip due to a series of northeast-southwest striking faults.

The two structural units probably originated during the Cretaceous when faulting along the line of the present Shag Valley formed a downthrown block to the northeast. Erosion of the uplifted southwestern area then exposed underlying mica schists with streams draining the region depositing thick sequences of conglomerate over the lower northeastern terrain (Shag Point Group). Quartz sandstones and finer grained conglomerates (Herbert Formation) were laid down in the east. Subsequent depression of the uplifted block resulted in deposition of a transgressive sequence (Katiki, Otepopo and Moeraki Formations) across the northwest-southeast trending fault complex. Two distinct paleogeographical provinces emerged with sediments of both regions yielding separate formations throughout the Tertiary; the succession of the northeastern block relatively continuous while the southwestern block showing a complete break during the Whaingaroan, and resuming again from the Duntroonian, (possibly associated with igneous activity to the northeast, Brown, unpublished bulletin). Erosion during the Miocene developed a peneplain onto which Pliocene volcanics were extruded (mainly in the southwest). Reverse faulting along the Waihemo complex followed, elevating the western section of the northeastern block to form the Kakanui Range.

Mutch (1963) notes Late Quaternary transcurrent fault movement occurs along the Wharekuri Fault about 70 km northwest of Moeraki Peninsula. Wellman (1979) estimates an annual uplift rate of 0.1 mm along the coastal region, increasing inland to 0.2 mm/year although substantial margins of error (up to 50%) may be associated with these figures.

A geological history synthesis is shown in Fig. 2.2.

SYNTHESIS OF REGIONAL GEOLOGICAL HISTORY. [PRE-QUATERNARY]

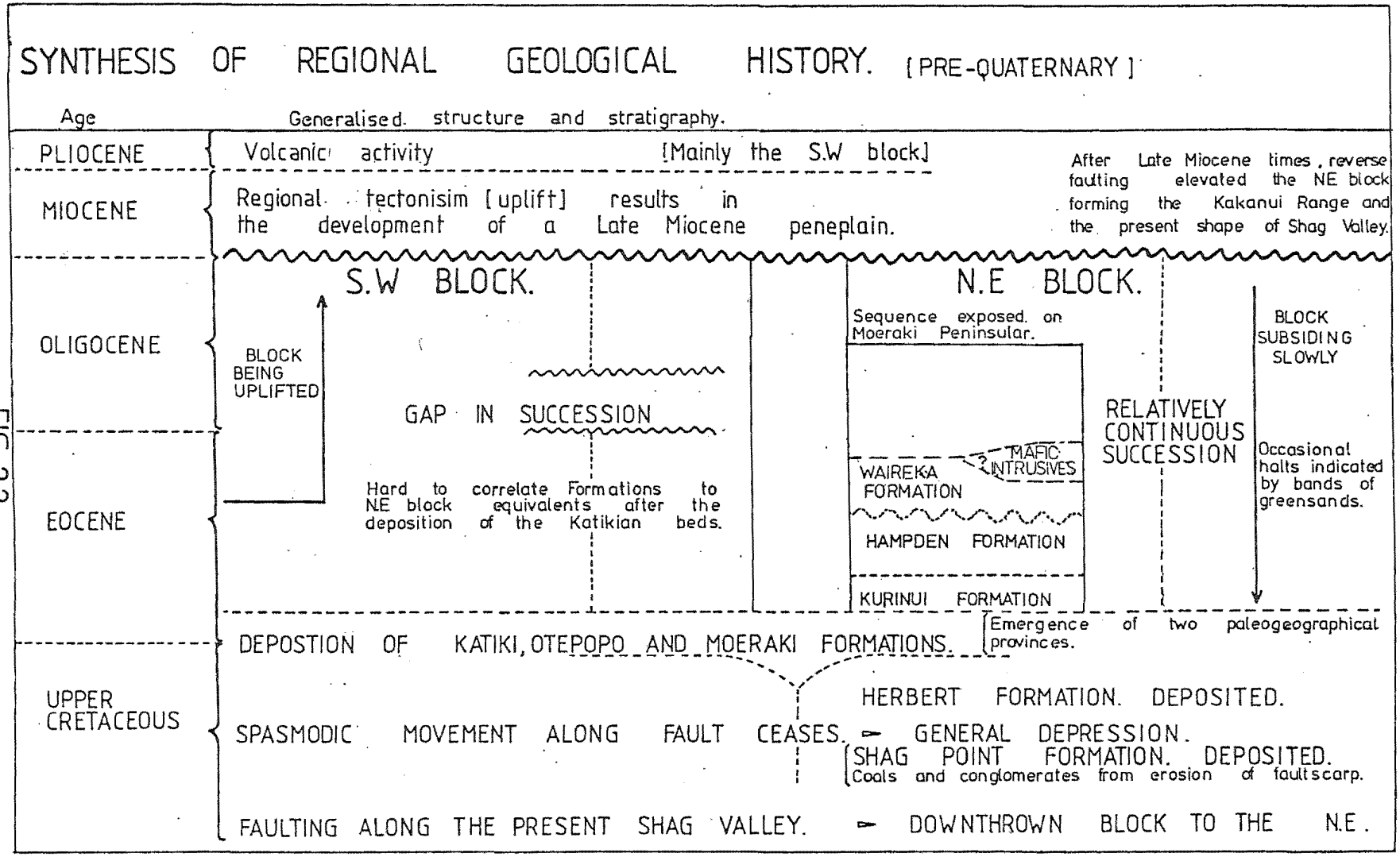

FIG 22

2.3 STRATIGRAPHY

Dark grey-black glauconitic mudstones and siltstones of the Moeraki Formation containing septarian concretions are exposed along Hampden Beach to the north, and are inferred to extend southward underneath the sequence exposed on Moeraki Peninsula.

Conformably resting on these are dark-grey mudstones of the Kurinui Formation.

KURINUI FORMATION (Benson, 1943)

Age: Heretaungan (Brown, 1959)

Distribution: Exposed along the shorewave platform in the north-west and south-west corners of the peninsula (Fig. 2.3).

Content: Dark blue-grey, homogeneous, jointed, indurated gluconitic silty-mudstone containing occasional greensand bands.

No actual contact between the Kurinui and underlying Moeraki Formation is exposed.

Type Locality: Coastal section between Big Kuri Stream and Park Gulch, north of Hampden.

Further to the east, along the peninsula's northern coastline, the overlying uniform blue-grey mudstones of the Hampden Formation are exposed.

HAMPDEN FORMATION (McKay, 1877)

The Formation, although not defined by McKay is evidently the upper part of his "Onekakara Beds"; the lower part correlated to the Kurinui Formation.

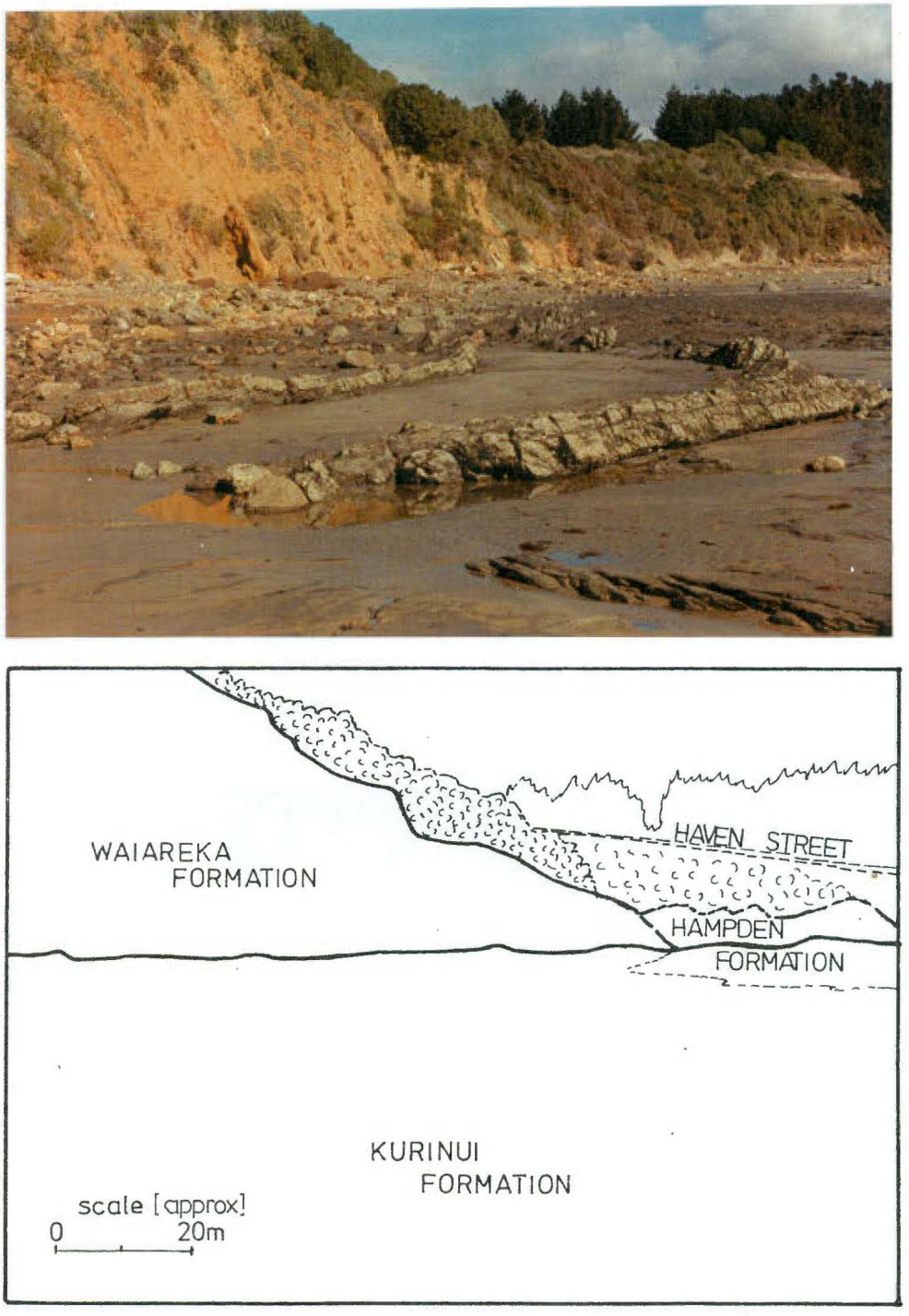

Fig.2.3: Sequence exposed along northwestern shore platform of the Moeraki Peninsula; note backtilted folded greensand bands within Kurinui Formation. Viewing southwest from 6700E,0450N.

Age: Regarded as the temporary Standard Sequence for the Bortonian Stage (Finlay and Marwick, 1940).

Distribution: Exposed along the northern coastline east of the Kurinui Formation, again on the east coast and in some prominent mass movement headscarps to the south. It is inferred to continue from the northern coast through to the southern coast, bisecting the peninsula (Fig. 2.4).

Content: Dark blueish-grey, homogeneous, jointed, indurated, silty-mudstone containing some gluconitic and smaller calcareous and pyritic concretions.

Type Locality: Coastal cliffs north from Park Gulch to 500 m north-north-east of Kakaho Creek, North Otago.

Exposed to the east and west of the Kurinui and Hampden mudstone formation are igneous rocks of the Waiareka Volcanics.

WAIAREKA VOLCANIC FORMATION (Hector, 1884)

Age: Arnold.
Finlay and Marwick (1940) place the tuffs in the Kaiatan Stage but at least part is younger, extending into the Runangan (Brown, unpublished bulletin). Precise ages of mafic dykes and sill intrusions associated with these sediments is in doubt (Coombs and Dickey, 1965).

Distribution: Waiareka Volcanics are exposed along the north-west and eastern coasts with occasional outcrops either side of the mudstone formations bisecting the peninsula (Fig. 2.4).

Content: Reddish-brown, massive or stratified, poorly indurated, calcareous coarse basaltic tuff containing decomposed basalt and trachylite fragments. The tuffs are unconformable with the underlying Formations (Gage, 1957).

MOERAKI PENINSULA GEOLOGY

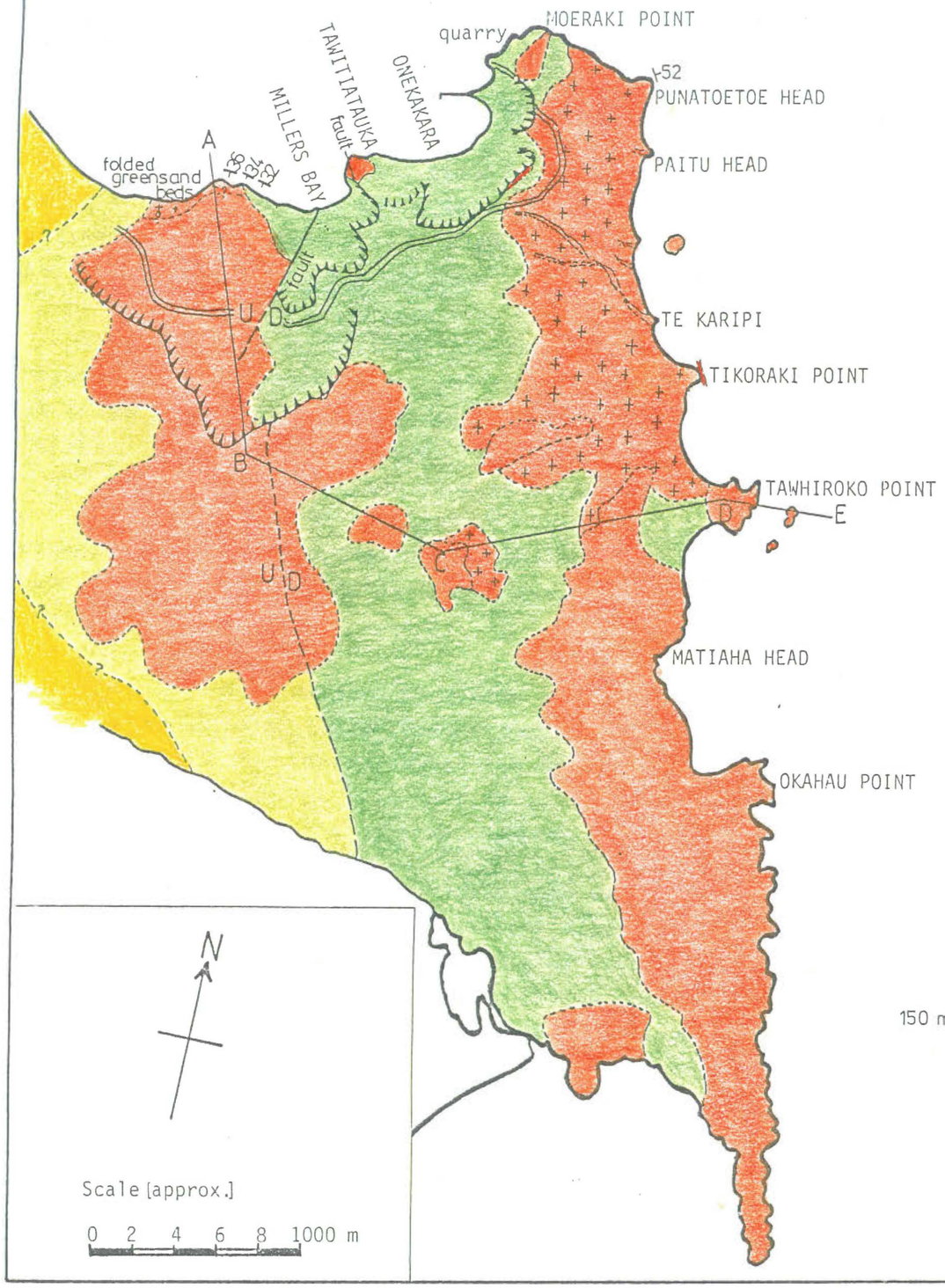

REFERENCE

GEOLOGICAL LEGEND

Lithology	Formation	Age (Stage)
Basalt and Dolerite intrusive sheets and dykes	WAIAREKA FORMATION	KAIATIAN
Reddish-brown basaltic tuff	WAIAREKA FORMATION	RUNANGAN
Dark blue-grey silty mudstone	HAMPDEN FORMATION	BORTONIAN
Dark blue-grey silty mudstone with occasional greensand bands	KURINUI FORMATION	HERETAUNGAN
Dark grey-black glauconitic mudstones and siltstones	MOERAKI FORMATION	?

- dip and strike
- U/D fault (U-upthrown block)
- Principal escarpments depicting mass movement
- Tenby Street delineating Moeraki township

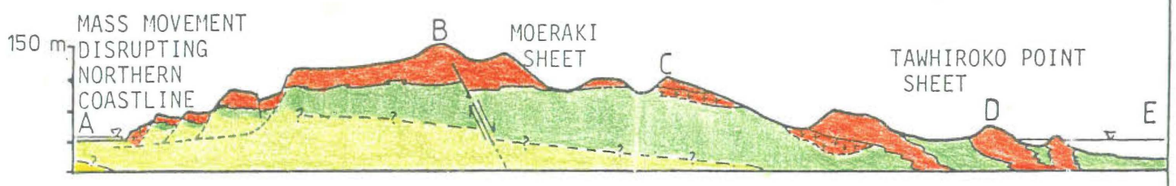

Fig. 2.4: Generalised Geology Map of Moeraki Peninsula

Type Locality:Hillside immediately west of Lorne, Oamaru (Marwick, 1926).

Mafic intrusions associated with the Waiareka Volcanics occur as dyke swarms or large sill like sheets, both characterised by porcellanization if intruded into the mudstone units. The petrographic similarity and field association with Waiareka tuffs is evidence for a Waiareka correlation, however since their precise age is in doubt (Coombs and Dickey, 1965) the intrusives are described separately.

Intrusives can be divided into three groups; dykes, the Tawhiroko Sheet and the more extensive Moeraki Dolerite Sheet (Fig. 2.4).

Dykes, usually less than 10 m in width, occur singly, in pairs or as a series of overlapping structures, possibly originating from a single fracture in the basement rock (Benson, 1943). Those of significance outcropping along the northern coastline are:

1) A large dyke exposed by quarry excavations at Moeraki Point (7800E,0600N) comprised of medium grained, non vesicular olivine dolerite. About 15.5 m thick, it dips east at 35^{o} and has clearly porcellanized the adjacent Hampden mudstone.

2) A dyke exposed on the beach to the west of Tawitiatauka Point (6400E,0550N) dipping at 30^{o} south-south-east and consisting of coarse grained olivine dolerite which Benson (1943) considers may have been a feeder to the intrusive Main Moeraki Sheet.

A small, well exposed, sill like intrusion, dipping gently eastward and estimated to have been about 47 m thick, outcrops at Tawhiroko Point (Tawhiroko Point Sheet). Its high apalite content and advanced mineral differentiation suggests it was intruded separately and independent of an adjacent Main Moeraki Sheet exposed to the west. Benson (1943) notes it is possibly genetically affiliated with that dyke striking south-

southeast through Tikoraki Point (refer Fig. 2.4).

The Main Moeraki Sheet includes intrusive mafic rocks in the west of Moeraki township extending from the coast to Trig E, together with those outcropping at Tawitiatauka Point; remnants of the same sheet occur along the cliffed coastline from Matiaha Head southward plus two patches 1 km east of Trig E (Fig. 2.4).

The differential Moeraki Sheet is about 60 m thick and composed of micrographic quartz dolerite at the top (Trig E and two adjacent hills) and massive olivine dolerite at its base (exposed at Tawitiatauka Point and along the northwest coast of the peninsula) (Benson, 1943). Western margins of the intrusion are either in contact with or adjacent to the Kurinui Formation and invade the Hampden Formation at Tawitiatauka Point. To the southeast of the peninsula, the sheet intrudes Hampden mudstone and Waiareka Volcanics.

2.4 STRUCTURE

The Kurinui and Hampden Formations, dipping approximately 10° east-north-east, outcrop and extend from the northern to southern coastline bisecting the peninsula (Fig.2.4).

Flanking the mudstone units in the east and west is the Waiareka Formation. Bedding within the volcanics is well exposed in some coastal areas, however the overall structure is masked by shallow mass movement.

Exposed in the north and southeast of the peninsula are the two intrusive sheets; Benson (1943) infers the sheets characteristic bulbous margins as a reflection of the overlying muds 'plasticity' at the time of intrusion.

In the northwest, the Kurinui Formation is uplifted laterally adjacent to Hampden mudstone by a northeast-southwest trending normal fault.

Greensand banding within the Kurinui mudstones outcrops along the northwestern shore platform; banding is folded and dips 30^{o} to 60^{o} south, contrary to estimated regional dip (Fig. 2.3). Structure is accounted for by "rotational deformation" associated with deep-seated instability which encompasses the entire northwestern section of the peninsula. Based on this information plus geomorphological evidence, geology exposed along the shore platform from Tawitiatauka Point westward is not in-situ but modified by extensive deep-seated "gravity movement" delineated in Fig. 2.4.

2.5 QUATERNARY SYNTHESIS

Regional uplift during Miocene times resulted in extensive degradation, stripping cover from elevated portions of a Cretaceous erosion surface and causing peneplanation of relatively soft Tertiary sediments. This regional setting of subdued relief was subsequently modified by glacio-eustatic related effects and tectonism during the Quaternary.

Evidence of penultimate and earlier Pleistocene glaciations (outwash fans, terrace gravels) outcrops inland of Moeraki Peninsula to the north, west and south. Absence of glacial remnants on the peninsula itself may reflect partial marine submergence or its existence as a topographical 'high' during this time.

Sediments representing a marine beach were identified, 3 m above present sea level along the eastern coast of Moeraki Peninsula and beside Katiki Beach further to the south. Older, 15 m, elevated bench horizons, can be discerned at Shag Point and along Hampden Beach. These raised bench sands provide evidence for a Hawera coastline prior to Final Glaciation comprised of embayments developed in soft Tertiary rock separating prominent headlands protected by more competent materials (Moeraki Point, Shag Point).

Remnants of the final Hawera Glaciation occur along Katiki Beach and Hampden Beach but are not present on Moeraki Peninsula.

Deep-seated, large scale, slope movement extensively altered subdued topography along Moeraki Peninsula's northern coastline during the Quaternary. Triggering of instability is attributed to fluctuating climatic and base level controls in conjunction with seismotectonic effects (associated with uplift).

CHAPTER THREE

GEOMORPHOLOGY

3.1 INTRODUCTION

This chapter comprises a geomorphological rather than geotechnical appraisal of instability affecting the northern coastline of Moeraki Peninsula. Mass movement is evaluated in seven principal sections. The first, landform association, provides a generalised overview of slope failure; the second explains classification used in depicting instability and the third outlines mapping approach plus description of mapping units. Parts four, five and six describe specific slides with their inter-relationships synthesised in a final section on geomorphological evolution.

3.2 LANDFORM ASSOCIATION

Present day morphology of Moeraki Peninsula has principally evolved by erosion of the soft mudstone units which extend from its northern to southern coastlines. Degradation of these incompetent sediments has yielded local topographical highs in the northwest and east of the peninsula where resistant Waiareka Volcanics are exposed; the highest relief occurring in the northwest (Trig E) and foremost ascribed to tectonic uplift (faulting). Elsewhere topography is low and hummocked.

Peninsula drainage is not dominated by any single catchment or river, and is generally via shallow, meandering, unbraided streams. Surface runoff from areas of higher relief shows some structural control in a southwest-northeasterly direction.

The peninsula's southern coastline forms a smooth arc to the southwest; cut into Hampden mudstone it has a gentle subdued topography. A cliffed eastern coastline, trends roughly north-south and is essentially linear being comprised

of competent volcanics which hinder retrogression. In the north the peninsula coast consists of three adjacent bays eroded into mudstone and separated by resistant mafic intrusives. Morphology neighbouring the entire northern shoreline has an acutely varied relief attributable to a sequence of deep-seated, slope failures on which the township of Moeraki is established.

Cadastral surveys for the township disclose differences which can only be attributed to recent earth movements (1863 to 1981) *pers.comm.* R. Petre. Brewster (1981) notes discrepancies in the order of 2 m (Tenby Street, End Street area) over a period from 1890 to the present. Petre (1981) commenting on cadastral data (Davids Road area) observed little or no difference disclosed from 1863 to 1922 with clear indication of movement from 1922 to 1975. Petre subsequently qualifies this information noting further detailed investigation would be required to ascertain if inconsistencies are due to earth movement or survey difference (refer to Appendix 9 for reports by Washbunton, Park, Brewster and Petre).

Assuming survey discrepancies are from slope deformation, the problem arises of whether differences indicate shallow regolith/colluvial movement or deep-seated deformation. Generally surficial displacement is seasonal (movement increasing during winter months) and of smaller magnitude than "constant" deep-seated movement, if considered over a reasonable data base (0s of years).

Slope instability affecting the Moeraki Peninsula's northern coastline occurs on a variety of scales and has a complex history of episodic reactivation. The township is located amidst a series of prominent deep-seated slides which in some areas are being degraded by currently "active" shallow slope deformation jeopardizing roading and housing.

Data pertaining to mass movement affecting the township has been collated from surface geology and geomorphology mapping in conjunction with stereoscopic analyses. Shallow slope failure is depicted on detailed (scale 1:1000) engineering

geology plans whilst deep-seated instability is delineated on a more generalised map (scale 1:5000) and described in terms of three principal features:

1) Moeraki Slide
2) Davids Road Failure
3) Eastern Slide Complex.

3.3 MASS MOVEMENT CLASSIFICATION

3.3.1 Introduction

Mass movement classification is an attempt to categorise material that has moved downslope, usually according to similar morphology or genesis. Its aim is the provision of an adequate framework about which we can accumulate common experience for use in controlling and avoiding slope failure. All classification imposes arbitrary boundaries on natural continuums and therefore requires the definition of a consistent terminology to avoid ambiguity.

Sharpe (1938) used rate of movement and water content as criteria to describe slope failure. Carson and Kirkby (1972) expanded the idea to produce a simple, comprehensive classification in terms of three movement processes, slides, flows and heaves, which they defined (Fig. 3.1). Superficially this method unites different phenomena but in practice not enough adequate terminology is provided.

Varnes (1958) proposed a mass movement description based on failure mechanisms which he listed as, slides, flows, and falls. The system was modified in (1978) to include toppling and lateral spreading along with terminology describing failure surface, rate of movement and type of material (Fig. 3.2).

The Varnes (1978) method has been adopted for this study due to its emphasis on description rather than catagorization of a slope failure. Principal criteria used in classification are:

1) Mechanism and mode of movement
2) Type of material involved.

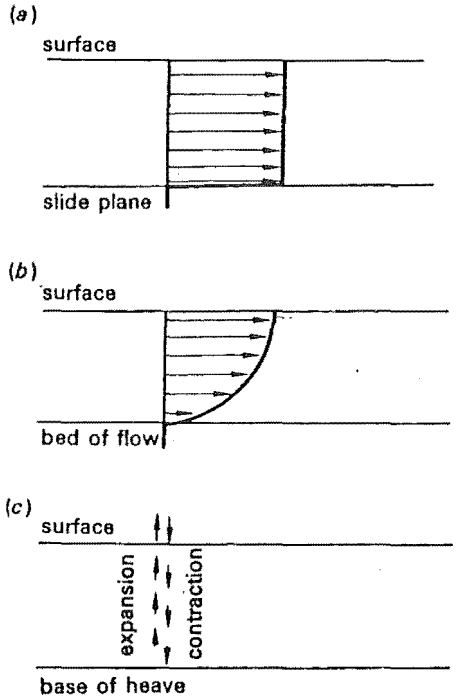

Fig. 3.1: Velocity profiles for "ideal" movement types. (a) Pure slide. (b) Pure flow. (c) Pure heave (Carson and Kirkby, 1972, Fig.5.1).

TYPE OF MOVEMENT			TYPE OF MATERIAL		
			BEDROCK	ENGINEERING SOILS	
				Predominantly coarse	Predominantly fine
FALLS			Rock fall	Debris fall	Earth fall
TOPPLES			Rock topple	Debris topple	Earth topple
SLIDES	ROTATIONAL	FEW UNITS	Rock slump	Debris slump	Earth slump
	TRANSLATIONAL	FEW UNITS	Rock block slide	Debris block slide	Earth block slide
		MANY UNITS	Rock slide	Debris slide	Earth slide
LATERAL SPREADS			Rock spread	Debris spread	Earth spread
FLOWS			Rock flow (deep creep)	Debris flow	Earth flow (soil creep)
COMPLEX			Combination of two or more principal types of movement		

Fig.3.2: Abbreviated Varnes classification of slope movements (Varnes, 1978, Fig.2.2).

Only relevant terminology is defined, some with slight modification to that proposed by Varnes.

3.3.2 Material

Four terms are used in describing material at the moment of incipient slope failure. Soft rocks often exhibit continuous gradation between soil and bedrock which necessitates minor alteration to terminology adopted by Varnes.

Bedrock:

Bedrock refers to in-situ rock "mass" (as opposed to rock material) as if a rigid cohesive body of interlocking particles welded or cemented together, plus interstial gas or liquid which may not be separated by such gentle means as agitation in water.

Engineering Soil:

Soil or rock "mass" behaving as if loose, unconsolidated or poorly cemented aggregates of solid particles, together with interstial gas or liquid, which may be separated by such gentle means as agitation in water. Engineering soil is further subdivided into Debris and Earth depending on "in-situ grain size characteristics" at the time of failure.

Debris:

Material in which 20% to 80% of fragments are greater than 2 mm and the remainder less than 2 mm (Schroder, 1971).

Earth:

Connotes material in which 80% or more of fragments are smaller than 2 mm (Schroder, 1971).

Example:

Mudstone regolith with a laboratory grain size analysis of 10% sand, 50% silt and 40% clay may exist in-situ at 60% intact blocks of mudstone within an ambient matrix of fine degraded material hence would be classified as DEBRIS not earth.

3.3.3 Mechanisms of Movement

Movement between bodies is relative and therefore refers only to the materials in relative motion, ie. a slide refers to motion between stable and moving ground, however the term flow refers to the distribution and relative movement of

particles within a moving mass (Fig. 3.3).

Slide:

True slide movement consists of shear strains and displacement along one or several surfaces that are visible or may reasonably be inferred within a relatively narrow zone (Varnes, 1978). Bedrock discontinuities (joints, faults, bedding) often structurally control failure.

Flows:

The term "flow" is applied to material indicating a similar distribution of velocities to that of a viscous fluid. Bedrock "flow" deformation is commonly along many large or small fractures without concentration of displacement along a single through-going discontinuity (Varnes, 1978). Movement is generally slow and constant with time often manifested by folding, bending or bulging of the slide mass.

Shallow-seated "flow" behaviour commonly has slip surfaces within the moving mass usually not visible or short lived, with the boundary between moving mass and material in place, a sharp surface of differential movement or a diffuse zone of shear (Varnes, 1978).

Creep is recognized as a variety of flow behaviour which requires further distinction. It commonly results in imperceptible permanent downslope movement unconfined by lateral shear boundaries and as defined by Varnes (1978) is "deformation under constant stress."

Toppling:

Forward rotation of material about some pivot point below, under the action of gravity and forces exerted by adjacent material or fluid. Tilting without collapse (Varnes, 1978).

3.3.4 Mode of Failure

The mode prefix refers to geometry or manifestation of the failure mass, a description which is important to stability analysis and remedial design.

Rotational:

Movement essentially rotational about an axis parallel to that slope. The surface of rupture is often spoon shaped and movement in the head region mostly vertical with tension cracks concentric in plan and concave toward the direction of movement (Varnes, 1978).

A degree of rotation occurs within the bulk of slope failures and the term is only applied if the majority of the failure surface is curved.

Rotational movement decreases the driving moment and restores equilibrium to the failed material.

Translational:

Movement essentially out, or down and out, along a more or less planar or gently undulatory surface with little rotational movement (Varnes, 1978).

Failures are commonly structually controlled by surfaces of weakness and the slide mass broken into sequences of independently tilted units.

The prefix is only applied if material has undergone considerable lateral displacement.

Translational movement does not restore equilibrium within the failure mass; movement will continue if the basal shear surface is sufficiently inclined and as long as shear resistance along this surface remains lower than the more or less constant driving force (Varnes, 1978).

Complex:

Slope failures which involve more than one mode of movement either within various parts of the moving mass or at different stages in their development (Varnes, 1978).

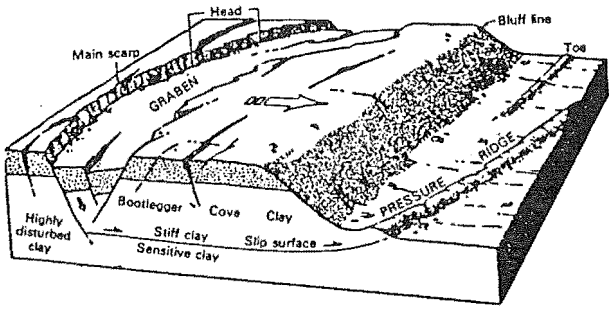

(a) Translational block slide

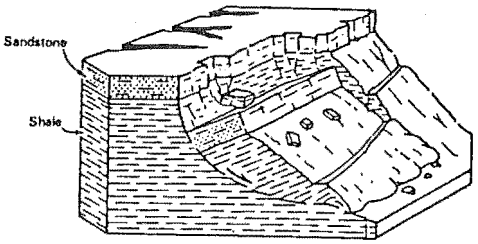

(b) Rotational block slide

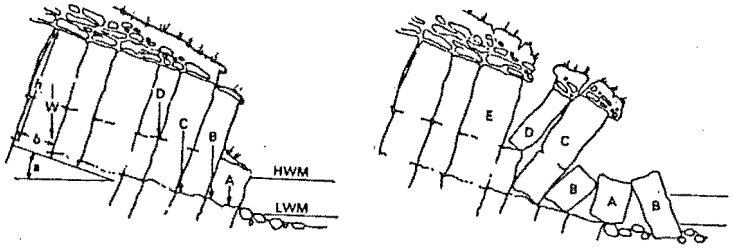

(c) Toppling failure

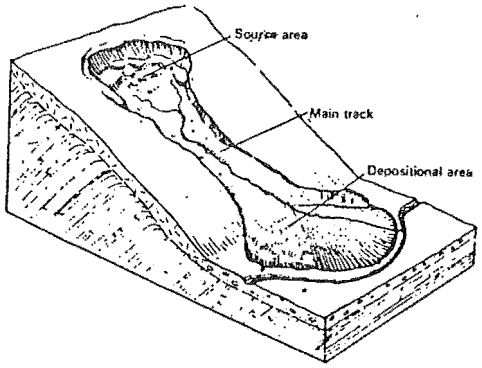

(d) Debris flow

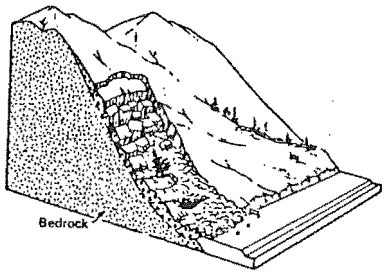

(e) Debris slide

Fig.3.3: Principal slope failure mechanisms and modes as illustrated by Varnes (1978, Fig.2.1).

Slide disruption is described by the terms block for material comprising few moving coherent units and broken for rock fractured into numerous aggregates insignificant in relation to size of the slope failure. Multiple refers to two or more slides each with a curved slip surface tangential to a common generally deep-seated slip sole (Varnes, 1978).

3.3.5 Terrain Activity

Subjective assessment of terrain "activity" is given where appropriate, to distinguish currently active and inactive slope deformation plus indentify areas prone to further slope failure (ie. dormant).

Slopes are classified as "inactive" if there is no evidence of displacement within the last cycle of seasons. They may be "dormant" in which case the causes of failure remain and movement may be renewed or they may be "stabilized" in which case factors essential to movement have been removed naturally or by human activity (Varnes, 1978).

"Active" slopes are those currently moving or those which have moved during the last cycle of seasons and may be qualified by terms relating to direction and rate of failure.

Direction of movement is described as:

1) advancing - downslope movement
2) retrogressive - retreating movement
3) extending - simultaneous advancing and retreating movement.

When possible overall rates of displacement are estimated and described (Fig. 3.4).

3.3.6 Classification

Classification lists inferred mass movement processes to the fullest extent possible in the order of Activity, Mode, Material, Mechanism and refers to the most recent moment of incipient failure, ie if material fails via one method, stabilizes and subsequently reactivates via another method, it is classified according to the most "recently active" processes since these are the most relevant when considering ensuing

reactivation or remedial options.

Slope failure often cannot be attributed to a single mechanism and so requires double classification in which case the dominant mechanism is listed last.

Example: A "slowly extending, translational, debris, flow-slide" would be an active slope failure advancing and retrogressing less than 1.5 m/yr that originated in unconsolidated material where 20-80% of fragments were greater than 2 mm and failed predominantly as a slide exhibiting some flow behaviour with significant lateral displacement.

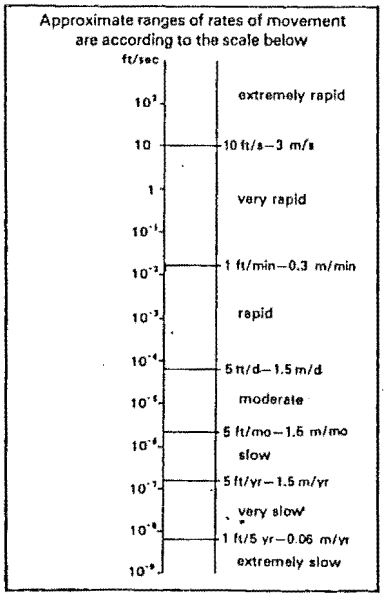

Fig.3.4: Rate of movement scale.
(Varnes, 1978, Fig.2.1)

3.4 ENGINEERING GEOLOGICAL MAPPING

3.4.1 Approach

Engineering geological mapping was conducted on a scale sufficient to depict detail of any mass movement affecting housing and/or roading (scale 1:1000). Shallow slope failures causing damage are developed within a series of coherent bedrock "blocks", dislocated by deep-seated slope movement. To avoid confusion between the extent of deep-seated failure and shallow instability, the two mass movement phenomena are outlined on separate maps; deep-seated instability at a scale of 1:5000 (Fig. 3.5) and shallow slope failure at a scale of 1:1000 (refer map enclosure, engineering geology maps).

Objectives of mapping include:

1) The delineation of "active" and "stabilized" slope movement in relation to housing and roading.
2) The provision of a basis for mass movement susceptibility plans.

Since no suitable topographical plots are available a geomorphological approach to mapping was adopted which also facilitated the correlation of features mapped to those in the field. Base plans were compiled directly from aerial photography. Detailed engineering geological base maps were prepared from:

Aerial Surveys Ltd
Ref No 664/16, 17, 18, 19, 20, scale 1:1000, flown in 1978. Distortion was minimised by the considerable overlapping within the photographic sequence.

The smaller scale map depicting deeper-seated slope failure was compiled from:

NZ Aerial Mapping
Ref No 1355/27, 28 scale 1:5000, flown in 1947. The map portrays morphology prior to extensive regrading carried out to enable residential development, hence highlights the extent of some debris flow-slide features not present on the larger scale engineering geology plans.

Fig. 3.5: Geomorphological map delineating deep-seated instability.

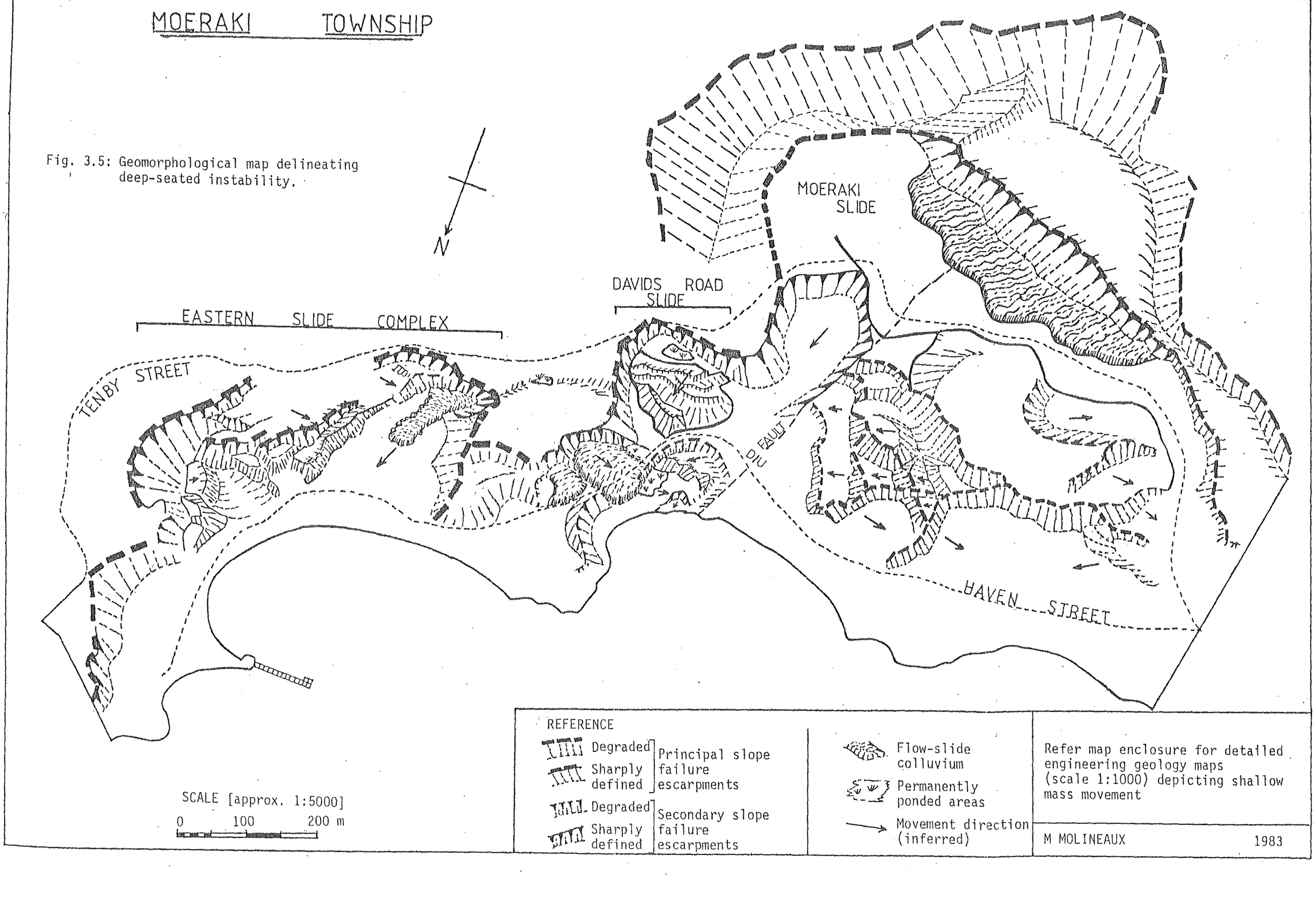

Description of mass movement was aimed at providing sufficient information on activity, mechanism, and mode of failure to enable design of tentative remedial measures should housing or roading be threatened. Drainage paths or areas of ponding feeding individual slopes are easily identified from changes in relief drawn on the maps. Culverts, along with flow direction, size and construction methods are plotted; ineffectual ones, periodically blocked by siltation are denoted "S".

3.4.2 Bedrock Units

Four lithological units are identified within the field area (refer Appendix 7, McLean 1976, description methodology).

1. A very soft, moderately strong, blue-grey GLAUCONITIC SILTY MUDSTONE with very wide, slightly rough defects and occasional folded greensand banding; Kurinui Formation.

2. A very soft, moderately strong, blueish-grey SILTY MUDSTONE with moderate to widely spaced, slightly rough defects and no obvious structure; Hampden Formation.

3. A very soft, very weak, reddish-brown COARSE BASALTIC TUFF, massive or stratified; Waiareka Formation.

4. A hard, very strong, black BASALT and DOLERITE with widely and closely spaced smooth defects; Waiareka Formation.

The two mudstone formations (Kurinui, Hampden) are lithologically similar and field evidence suggests equivalent in susceptibility to mass movement, therefore for engineering geological mapping purposes, both are grouped together forming one unit.

The two extreme engineering rock types within the Waiareka Formation are also considered as one mapping unit since both appear stable with regard to shallow slope failure; the tuff attributed to its coarse texture yielding a high permeability and the basalt or dolerite due to its in-situ hardness and strength.

3.4.3 Surficial Deposits

The extent of surficial deposits was not mapped for the following reasons:

1. The complex history of slope failure combined with mans' influence on original topography would make the distinction between in-situ regolith and colluvial deposits an excessively difficult task.

2. The mapping of surficial deposits (colluvium, regolith) would not provide much additional insight into the susceptibility of areas to shallow slope failure, since
   a) the geotechnical properties of colluvium and weathered regolith are similar, and
   b) the aerial extent of surficial deposits derived from one rock type is largely confined to the area of that lithology ie. do not get mudstone colluvium resting on the Waiareka Formation.

An engineering geological description of a typical surficial deposit associated with the mudstone lithologies is as follows (refer to McLean 1976 for description methodology).

Light, reddish-brown, homogeneous (moderately weathered, CLAYEY SILT with rare SAND; CH)

- (soft; moist:) unbedded; silty, subangular to subrounded quartz; clay; highly plastic.

Interspersed paleosols are common, consisting of ... Dark brownish black, homogeneous, CLAYEY, SILT with rare SAND; OH

- (very soft; wet;) partly to highly organic; silty, subangular to subrounded quartz; clay; highly plastic.

Surficial deposits associated with the Waiareka Formation are, in the main, derived from weathered basalt and dolerite and comprise ...

Light brownish-red, non bedded, (moderately weathered), SILTY, fine to coarse SAND, with some clay; CL

- loose; (dry;) uniformly graded; sand, angular to subangular, feldspar and iron oxides, silt,

subangular to subrounded feldspar and iron oxides; clay; moderately plastic.

Note: Properties such as weathering, moisture content and strength vary considerably, are site specific and so are bracketed in the descriptions above.

3.4.4 Geomorphic Symbols

Mass movement superimposed on a number of scales necessitates a hierachy of geomorphic symbols for mapping purposes.

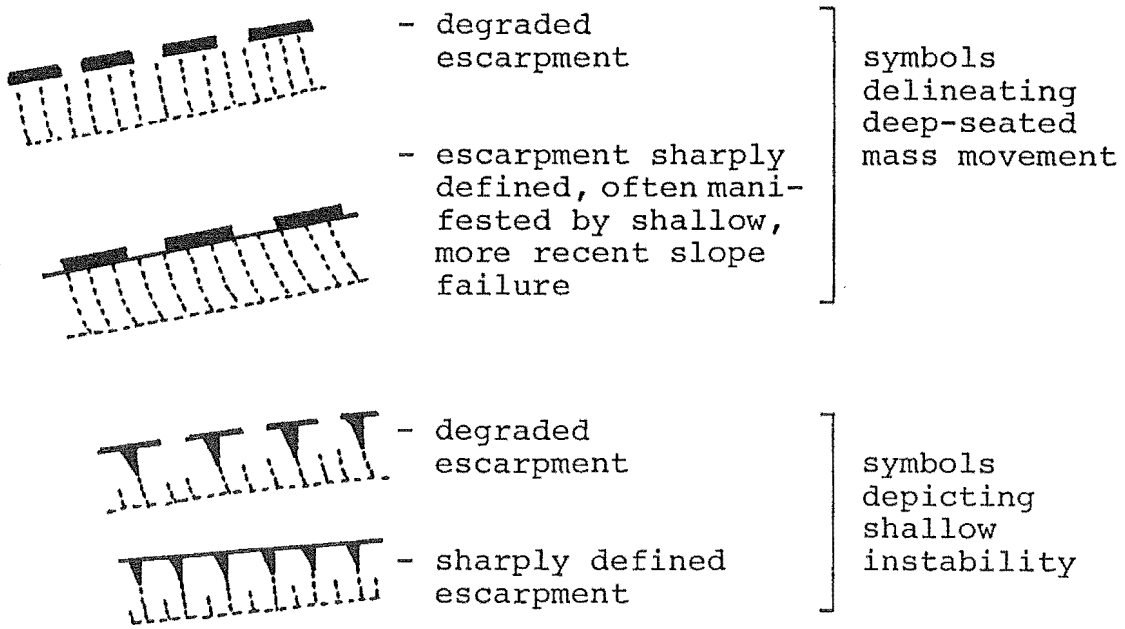

The blocks associated with each deep-seated failure are outlined in heavy ink on the detailed engineering geological maps enhancing correlation to the smaller scale 1:5000 plan (refer map enclosure for engineering geology maps scale 1:1000 and Fig. 3.5, scale 1:5000).

3.5 MOERAKI SLIDE

3.5.1 Introduction

The Moeraki Slide is a large scale, partially obscured feature encompassing the northwestern margin of the peninsula. The slope failure extends southwest about 1 km from the northern coastline rising to 120 m above sea level, covering an area of 6.5×10^4 square metres. Its failure mass affects topography over the entire western half of Moeraki township (west of Davids Road)(Fig. 3.6).

Bedrock geology in the immediate vicinity comprises the Kurinui, Hampden plus Waiareka Formations, the structure of which has been confused by slope deformation. Waiareka Volcanics are well exposed covering the bulk of the failure mass. The underlying Hampden mudstones do not outcrop within the slide body or along the northwestern shore platform and their presence is assumed masked by mass displacement (inferred, partially rotational along the coast, Fig. 3.6). Beneath this unit lies the Kurinui Formation, prominently exposed along the shore platform and visibly deformed (principally by mass movement). To the east, the slide mass is cut by a distinct northeast-southwesterly trending normal fault downthrowing the Kurinui Formation so it lies laterally adjacent to the Hampden mudstones.

3.5.2 Morphology

Extensive alteration of topography to facilitate residential development has partially removed "original" slide morphology. In addition, relief in some areas is veiled in dense vegetation.

An asymmetrical "principal escarpment" varying in height (up to 25 m) can be discerned approximately 1 km south of the northern coastline; it is degraded and thus difficult to ascertain in parts (Fig. 3.7 and 3.8). Further to the north a distinctive semi-circular "secondary escarpment" is developed within competent Waiareka Volcanics; altering in height (up to 20 m) the central region is manifested by more recent shallow mass movement yielding a talus apron of volcanic debris. Adjacent to the talus colluvium deep-seated slope failure has developed a zone of

THE MOERAKI SLIDE

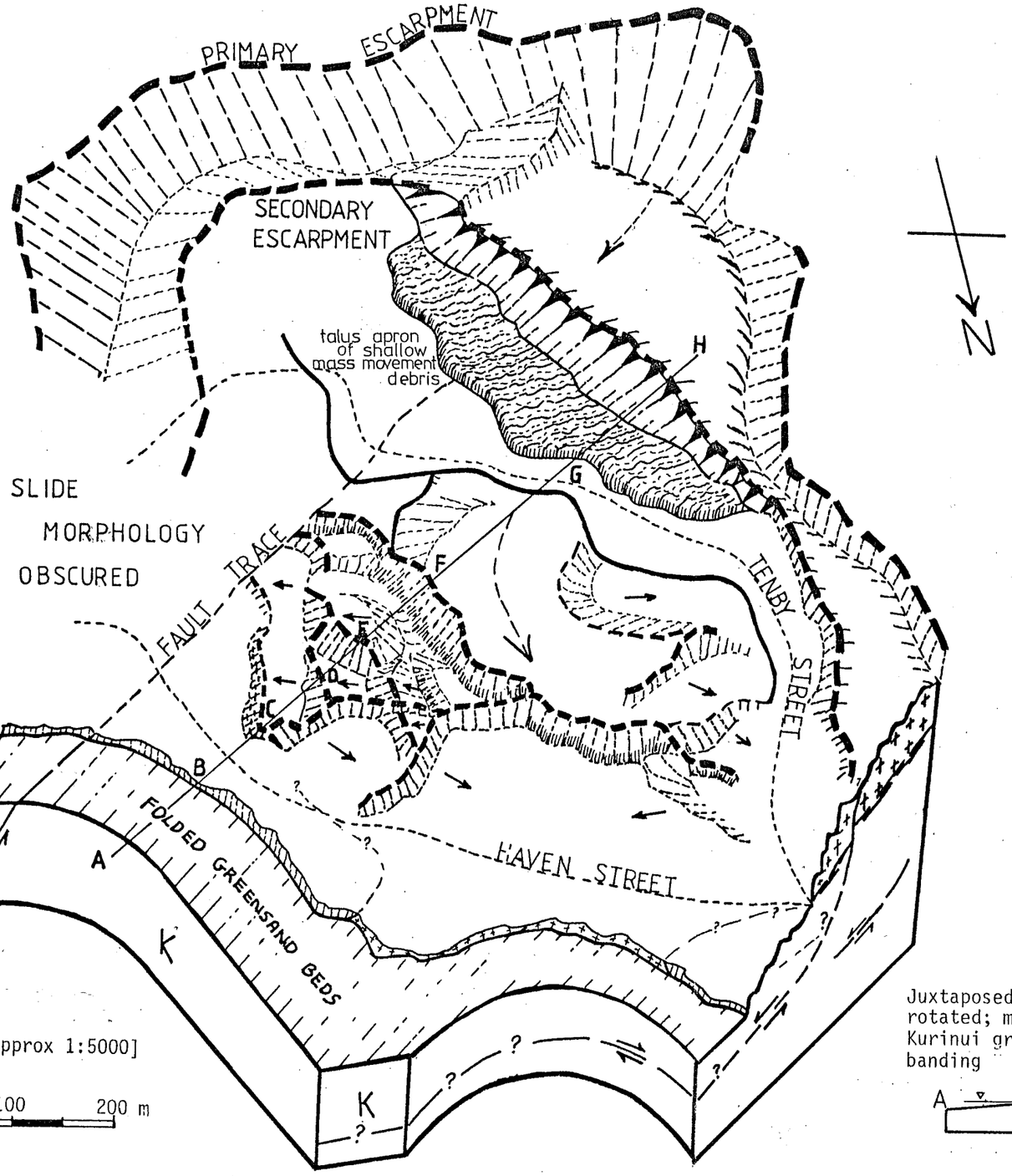

Fig.3.6: Hypothetical schematic diagram of the Moeraki Slide.

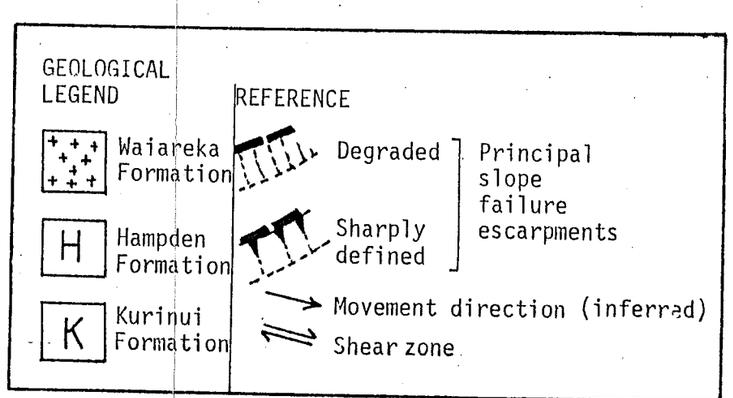

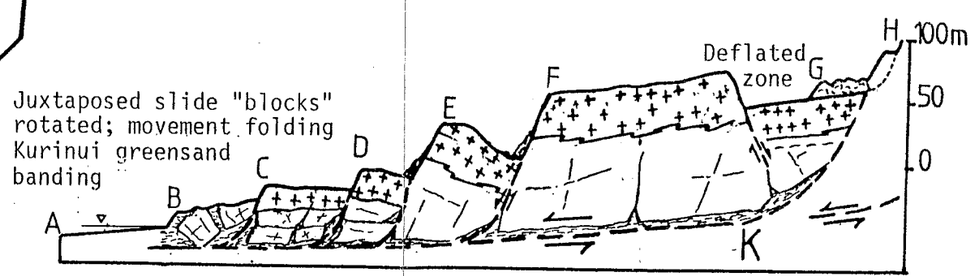

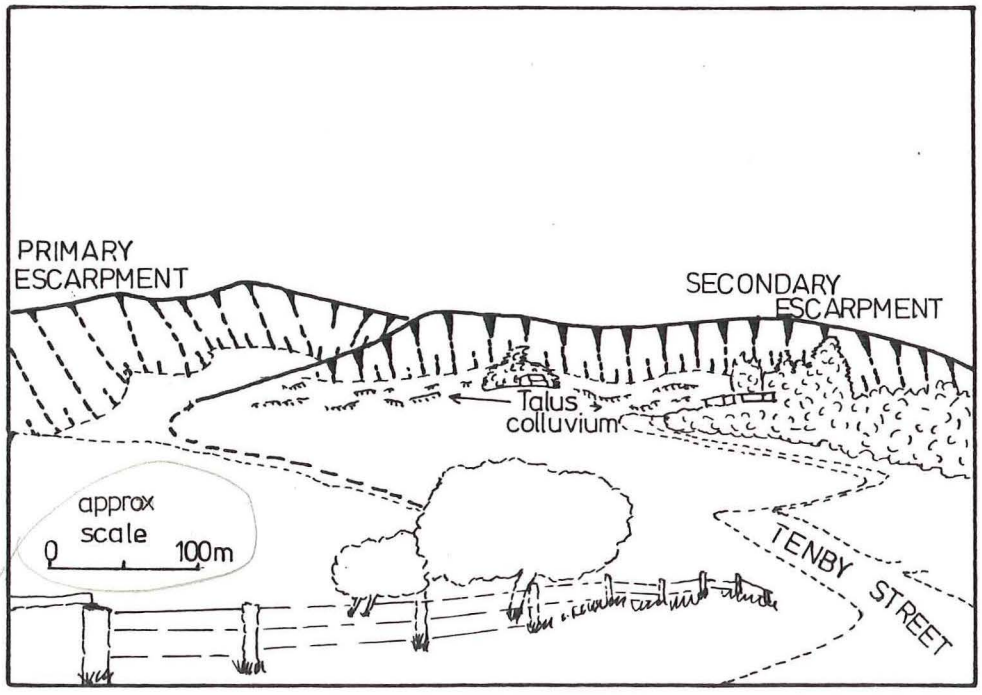

Fig.3.7: Principal escarpments of the Moeraki Slide; the degraded primary scarp delineating the first phase of instability and the secondary scarp, subsequent slope failure within the original slide mass. Note highlighting of the secondary escarpment by more recent shallow mass movement amassing talus colluvium. Looking southwest from 7350E,0100N.

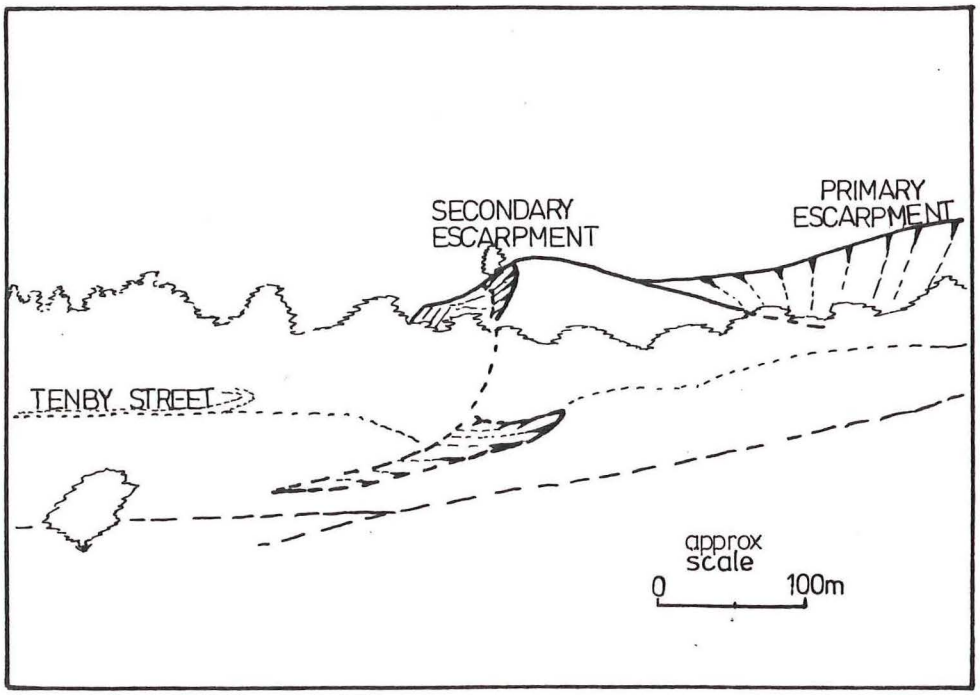

Fig.3.8: Primary and secondary escarpments of the Moeraki Slide looking east from 6100E,0100N.

Photo on Fig 3.6?

deflation, narrowing to the west. Neighbouring this depression and extending northward to the coast lies the majority of failed material. To the east slide mass topography has been obliterated by subsequent shallower mass movement. In the west the slide body, bulk, comprises a rectangular region of high undulatory relief bounded by distinct escarpments. The remaining failure mass is sheared into a series of tilted "blocks" facing northeast and northwest producing a hummocked relief down to the peninsula's northern coastline.

Permeable Waiareka Volcanics absorb excess rainfall preventing runoff ponding despite the varied relief, consequently the area is well drained.

3.5.3 Failure Mechanism and Mode

No subsurface data on the landslide has been obtained by either direct (drillhole core or excavations) or indirect means (seismic refraction ...) hence all comments regarding subsurface geometry of the slide mass and movement mechanisms are only inferred.

Mechanism

Two principal mechanisms of movement are identified.

1) Sliding: via defined bedrock discontinuities (jointing, bedding) and propagating rupture (shear) zones.

2) Flow: deep-seated gravitational "creep" movement amidst broad zones; via numerous large or small fractures without significant concentration of displacement along a single discontinuity.

The slide is clearly deep-seated with its basal shear surface extending unexposed beyond the peninsula's northern coastline (Fig. 3.6). The principal failure plane is most probably developed within the Kurinui Formation and need not be structurally controlled but could merely propagate through the comparatively incompetent and fractured mudstone unit. However bedding and/or greensand banding within the sequence, being zones associated with permeability changes (hence

variation in pore pressure and strength) could influence movement.

Mode

Slide geometry is that of a complex multiple block failure with predominantly translational displacement in the head region developing a rotational element toward the toe.

Two major phases of instability are recognized:

1) The first, delineated by a "principal escarpment", involved translational movement to the northeast reorientating geologic structure (faulting, bedding, jointing) within the failure mass more to the north.

2) The second episode depicted by a "secondary escarpment" initiated amidst the "original" failure mass. Movement appears translational with a rotational element to the northwest generating a deflated zone (graben structure) situated in the slides head region which narrows to the west (Fig. 3.6).

Initial movement most likely sheared the slide body into numerous coherent "blocks", reducing rock mass strength and increasing permeability, thus facilitating the subsequent secondary slope failure.

Secondary movement may be coincident with bedding or rock mass defects reorientated by the first episode of instability. Following these two major periods of slope failure the slide mass has probably undergone several episodes of minor isolated movement to evolve present day topography.

However, it must be emphasised the degradation and cryptic nature of some terrain comprising the slide means failure mode and mechanisms postulated are only tentative.

Suggested Failure Model

The following failure model is suggested for the Moeraki Slide.

1) Precursor gravitational "creep" movement amidst the Kurinui Formation causing flexural toe bulging and subsidence further upslope; possibly induced by horizontal stress relaxation (fluctuating base levels, coastal erosion, localised instability) and associated with regional uplift (seismo tectonic effects). Creep movement would be facilitated by inherent mudstone properties (latent strain release) plus the "load" effect of brittle, Waiareka Volcanics on underlying less competent sediments.

2) Continued creep movement via a propagating translational rupture zone (possibly structurally controlled) culminating in the first episode of slope failure.

3) A second major phase of predominently translational movement further shearing the slide mass into a sequence of coherent "blocks" individually bound by caps of resistant Waiareka Volcanics.

4) Subsequent, minor and isolated, reactivation of the slides toe region. Segregated failures expedited amidst heavily fractured and/or weathered mudstone, rotating juxtaposed slide "blocks" to form the present day hummocky topography.

3.5.4 Stability

Current slide "activity" is difficult to ascertain solely from data collated.

Individual blocks comprising the failure mass are assumed "inactive" with regard to sudden, massive slide failure. Cadestral data suggests some areas are subject to significant "creep" displacement; the delineation and verification of which would require detailed investigation of Moeraki cadestral survey information. Likelihood of rapid reactivation of the Moeraki Slide (in part or as a whole) in response to present coastal erosion or adverse climatic fluctuation is thought minimal considering depth to basal shear zone plus protection furnished by the Waiareka Formation (absorbing surface runoff

and minimising local coastal retrogression).

Active subordinate slope failure is mainly confined to two areas:

1) A debris flow-slide laterally controlled by a fault boundary which erodes Moeraki Slide morphology in the east.

2) Surficial mass movement causing gradual retrogression of the principal "secondary escarpment".

The present absence of major active shallow instability is attributed in part to the permeable blanket of Waiareka Volcanics absorbing surface runoff thus minimising infiltration into the underlying incompetent mudstone formations.

3.6 DAVIDS ROAD SLIDE

3.6.1 Introduction

The Davids Road Slide is a smaller scale feature, located east of and adjacent to the Moeraki Slide, affecting topography in the central region of the township (Fig. 3.9). The slope failure stretches 250 m southwest from the northern coastline, rising to an elevation of 50 m above sea level and covers an area of 3.5×10^4 square meters (Fig. 3.9).

Bedrock geology in the failure proximity comprises homogeneous Hampden mudstones which outcrop along the shore platform to the north and amidst slide escarpments in the south. A northeast-southwest trending normal fault, down-throwing the underlying Kurinui Formation is recognized to the east, beyond the current slide boundaries (within the Moeraki Slide).

3.6.2 Morphology

Morphology of the upper slide region is partially masked by dense vegetation whilst its lower section has been regraded for roading and recreation purposes. Principal escarpments developed within Hampden mudstone delineate the slide in the east and south (varying in height from 5 to 15 m); its western margin plus morphology having been obscured by more recent mass movement. The failure mass is rectangular and can be broadly divided into two equal parts by Haven Street and separated by a sharp change in height; an upper section broken into a series of well defined tilted blocks of comparatively low relief sloping to the northeast and a lower coastal section of more gentle topography. Degradation of slide mass escarpments in the upper region has infilled a narrow depression forming a flat triangular section to the centre of the slide body; often associated with "ponding" from surface runoff draining the encompassing higher relief.

Permanent ponding from runoff accumulation occurs in deflated zones (graben structures) at the head and toward the coastal section of the slide mass.

DAVIDS ROAD SLIDE

Fig.3.9: Hypothetical Schematic diagram of the Davids Road Slide

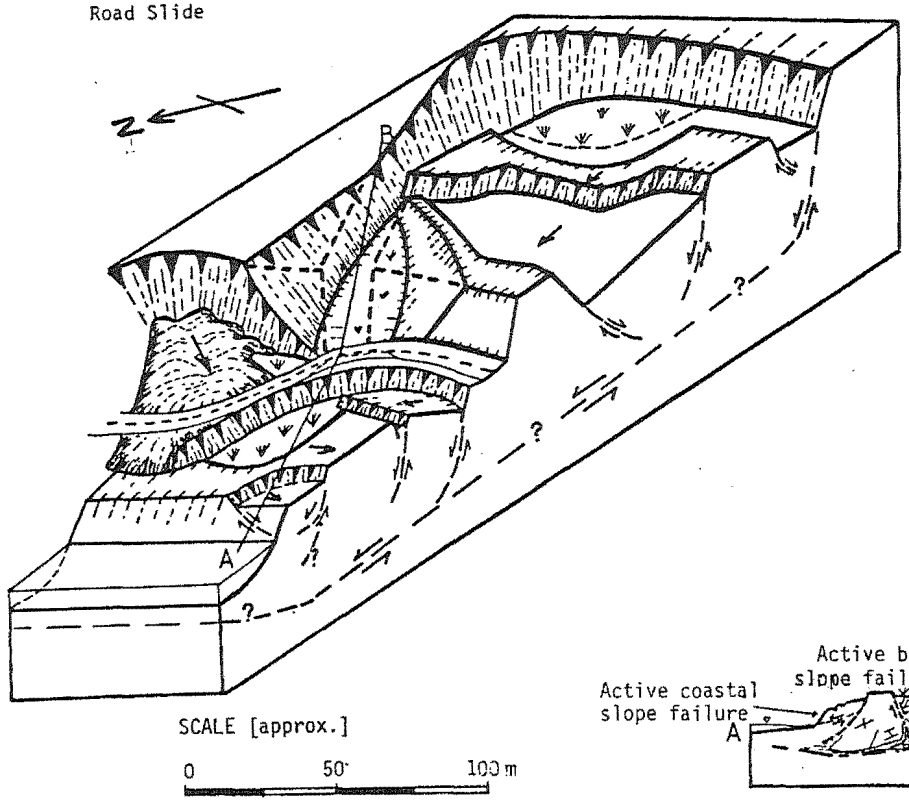

REFERENCE

- Principal slope failure escarpment
- Movement direction (inferred)
- Shear zone
- Permanently ponded areas
- Volume eroded following initial movement

Refer map enclosure for surveyed profile presented with geomorphological interpretation of shallow borehole data.

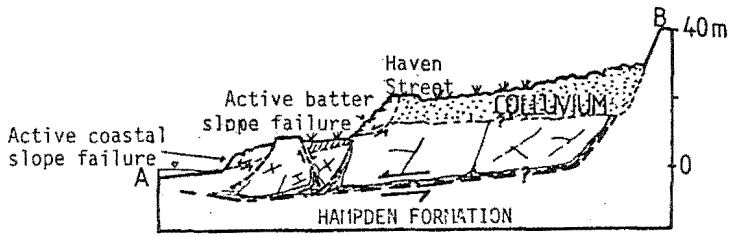

All unvegetated scarps are gradually eroding resulting in continual accumulation of talus debris.

3.6.3 Failure Mechanism and Mode

Limited subsurface data relating to shallow slope failure (<10 m) has been collected from five auger holes plus one drill hole. No information pertaining to the principal basal shear surface of the Davids Road Slide is known hence only speculative comment can be made on failure mechanisms and modes.

Mechanism

Two prime mechanisms of failure are recognized:

1) Sliding: controlled by discrete bedrock discontinuities (bedding, jointing) plus spreading rupture (shear) zones.

2) Flow: plastic "creep" displacement amidst many large or small discontinuities forming "broad" zones of deformation.

The Davids Road failure is shallower than the neighbouring Moeraki Slide but nevertheless moderately deep-seated with its basal shear surface extending, unexposed, beneath the peninsula's northern coastline. As disclosed along the shore platform the Hampden Formation is relatively homogeneous with no obvious inherent lithological variation which could dictate failure mode. Hence the principal basal shear zone may simply propagate through relatively incompetent fissured mudstone possibly partially controlled or coincident with a bedding plane parting.

Mode

Slide mass geometry is that of a complex multiple block failure. Movement appears mainly translational in the head region, tantamount to estimated regional dip, with significant rotational displacement towards the toe.

Principal slide morphology most likely developed from a single episode of instability with subsequent reactivation of isolated patches occurring periodically.

Suggested Failure Model

A concise hypothetical failure model is suggested for the Davids Road Slide.

1) Creep deformation amidst the Hampden Formation probably incited by fluctuating base levels (glacio-eustatic effects), coastal erosion and regional uplift (seismo tectonic influences) producing a steadily propagating basal rupture zone (possibly structurally controlled).

2) On going "creep" displacement culminating in translational slope failure and the shearing of coherent mudstone into juxtaposed slide "blocks".

3) Subsequent minor episodes of reactivation in the toe region; isolated failures rotating "blocks" amidst heavily fractured and/or weathered mudstone.

4) Human interference, removing vegetation, regrading topography and concentrating drainage resulting in accelerated shallow instability within the failure mass.

3.6.4 Stability

Present day slide "activity" is difficult to deduce from the information known. A comprehensive cadastral survey data investigation to ascertain displacement trends and magnitudes is required before any conclusive statement on slide stability could be made.

Bearing this in mind "blocks" comprising the slide mass are assumed "inactive" in regard to abrupt, massive slope failure, but prone to shallow creep movement.

Hazardous subsidiary instability occurs in two regions and is principally ascribed to concentration of drainage.

1) A Haven Street batter slope failure which subsides along well defined rupture zones jeopardizing traffic.

2) A coastal slope failure encroaching land used for recreation purposes.

Extensive altering of current topography (via shallow instability or man's activities) in conjunction with adverse climatic conditions could feasibly reactivate the Davids Road Slide. Sudden slope failure (in part or as a whole) would most likely be preceded by accelerated "creep" movement easily discerned by conventional survey methods (accurate to ±1 cm).

3.7 EASTERN SLIDE COMPLEX

3.7.1 Introduction

The Eastern Slide Complex is a partially concealed large scale feature affecting the eastern Moeraki township. The composite slope failure extends southward 300 m from the peninsula's northern coastline rising to a height of 50 m above sea level and covering an area of 8.6×10^4 square metres. Instability is delineated by a prominent amphi-theatre escarpment and comprises three, related, adjacent slope failures; the Motor Camp Slide, the Tenby Street Failure and the Rotational Slide (Fig. 3.10).

Bedrock geology in the "failure complex" vicinity consists of homogeneous Hampden mudstones which outcrop along the northern shore platform and within scarps further to the south. No evidence of tectonic folding or faulting which may influence mass movement was identified. Mafic intrusions flank the "complex" to the east and west (Moeraki Point, Tawitiatauka Point) together with an affiliated dyke, striking east-north-east which outcrops amidst the principal asymmetrical escarpment (central section).

3.7.2 Motor Camp Slide

The Motor Camp Slide forms the western section of the Eastern Slide Complex. Stretching 280 m southward from the peninsula's northern coastline the failure covers an areas of approximately 4.3×10^4 square metres.

Slide morphology has been extensively altered to facilitate residential development.

A distinctive eliptical escarpment, open to the north and vacillating in height (5 to 20 m) encloses the failure mass.

Shallow mass movement has eroded and manifested the scarp to the south accumulating aprons of colluvial debris over the slide's upper section. Slide body relief is low and gently undulatory, sloping down to the peninsula's northern coastline.

THE EASTERN SLIDE COMPLEX

3.10: Hypothetical schematic diagram of Eastern Slide Complex

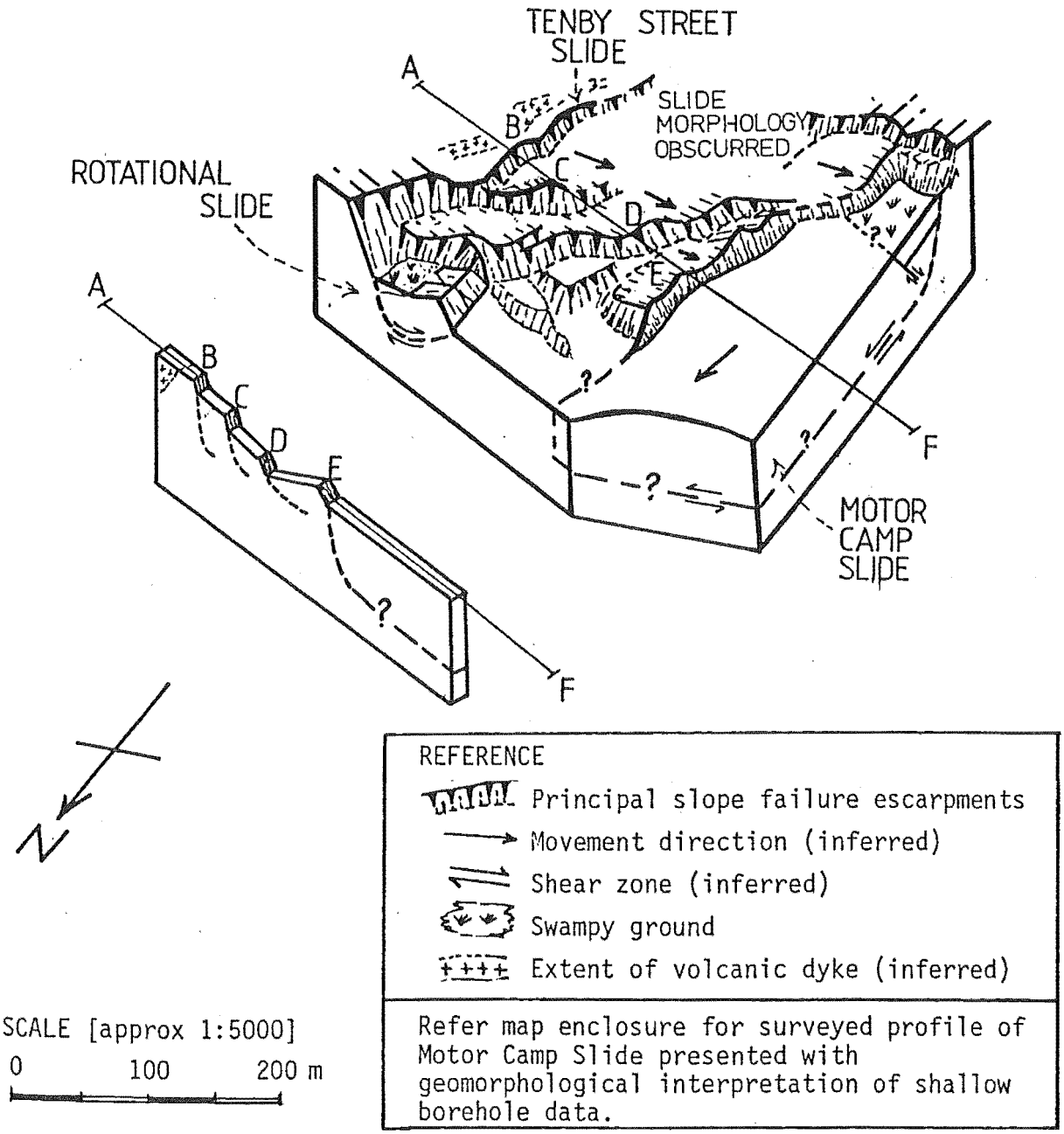

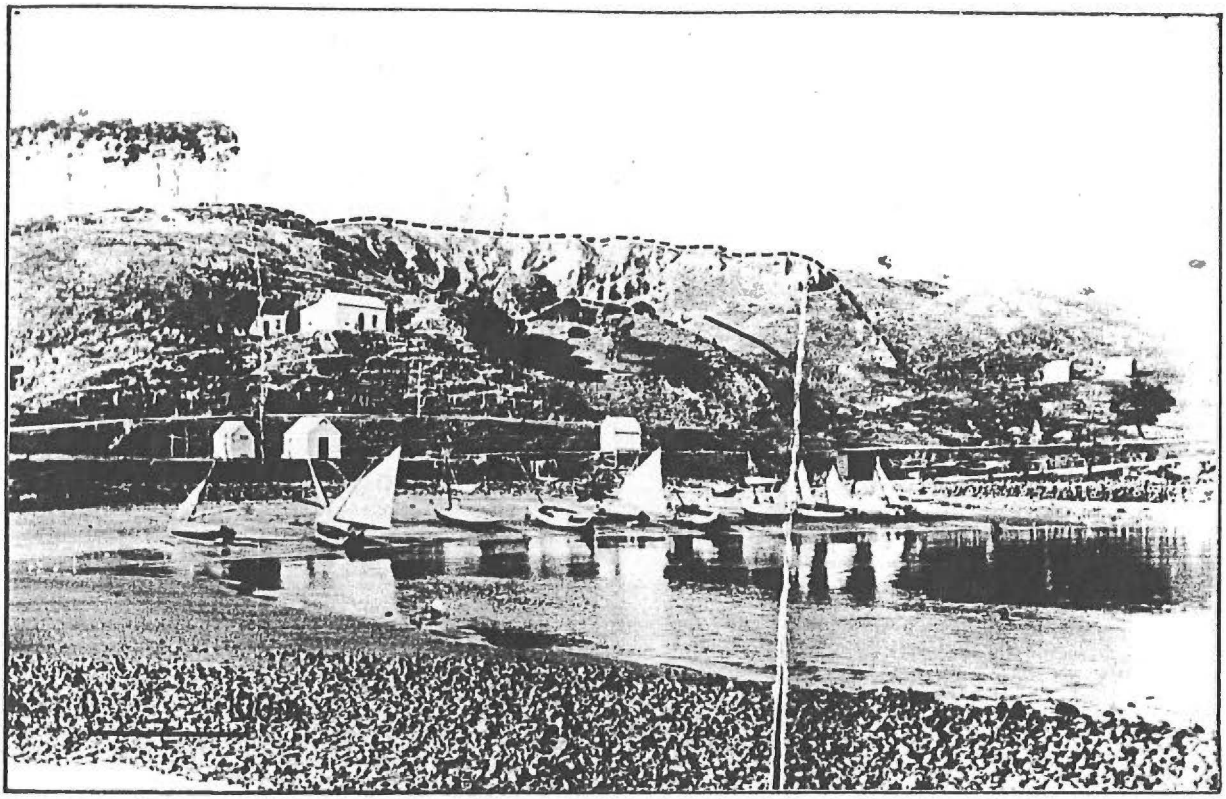

Fig.3.11: Salient amphitheatre escarpment encompassing the Eastern Slide Complex (dashed line) prior to extensive residential development in the area; the Rotational Slide plus Tenby Street Failure are obscurred with Motor Camp Slide movement direction denoted by the arrow. Note degradation of the central scarp region. Looking southwest from 7800E, 0200N.

Photograph courtesy Mr P. Kedsley (dated pre 1930's).

The area is comparatively free draining with precipitation runoff draining higher relief causing temporary ponding in deflated zones amidst the slides head region.

Failure Mechanism and Mode

Limited information pertaining to shallow mass movement was collated from four auger holes. No data concerning the principal basal shear surface are available for the Motor Camp Slide so all comment regarding subsurface geometry of the slide mass and mechanism of failure is speculative.

Sliding via discrete bedrock discontinuities (joints, bedding) or propagating rupture zone is inferred to be the chief failure mechanism.

The slide appears moderately deep-seated with its basal failure plane unexposed and probably extending beneath the northern coastline. Developed amidst homogeneous mudstone with no apparent lithological variation, the principal shear surface may simply propagate through incompetent fractured mudstone, conceivably, partially governed by or coincident with a bedding plane parting.

Motor Camp Slide geometry is obscured, however the slide is tentatively described as a translational block failure. Movement was to the north, probably shearing coherent mudstone into individual "blocks"; although no tangible evidence supports this apart from an inferred graben structure at the slide mass head (Fig. 3.10, refer to surveyed cross section of the Motor Camp Area in map enclosure). Instability most probably initiated from precursory "creep" movements evolving a basal shear zone with continued deformation culminating in complete slope failure. The resultant slide mass possibly of "juxtaposed blocks" may have subsequently reactivated, periodically, as isolated slope failures.

Stability

The Motor Camp Slide is assumed "inactive". However this speculative hypothesis requires verification from cadestral survey analyses utilizing the maximum data base (1890 to 1983).

Apart from significant regolith/colluvial "creep" deformation, two areas of subsidiary "active" mass movement are recognized:

1) Shallow slope failures amidst the slides principal escarpment to the south.

2) Coastal erosion plus affiliated subsidence of Haven Street in the north.

The influence of minor coastal and headscarp retrogression on large scale reactivation (in part or as one unit) of the Motor Camp Slide is considered minimal in view of the failure's deep-seated origin.

3.7.3 Tenby Street Failure

The Tenby Street Failure, forms the central region of the Eastern Slide Complex. The slide extends 150 m northwest of the amphitheatre escarpment delineating the "slide complex", covering an area of 3.3×10^4 square metres.

Slide morphology has been virtually eradicated to enable urban development. Nevertheless a sequence of degraded essentially linear escarpments trending northeast-southwest and varying in height (2 to 15 m) can be discerned within the failure mass; intervening sections are tilted and facing the northwest (Fig. 3.12).

Precipitation drainage off high relief results in temporary ponding in deflated areas.

Failure Mechanism and Mode

No subsurface information, either direct or indirect, relating to the slide is known. Hence all comment pertaining to failure mechanism and mode is speculative. Slope failure appears to have involved two main mechanisms.

1) Sliding: via defined bedrock discontinuities (jointing and along advancing shear zones).

2) Flow: slow plastic "creep" deformation across broad zones with limited concentration of movement along any single bedrock failure.

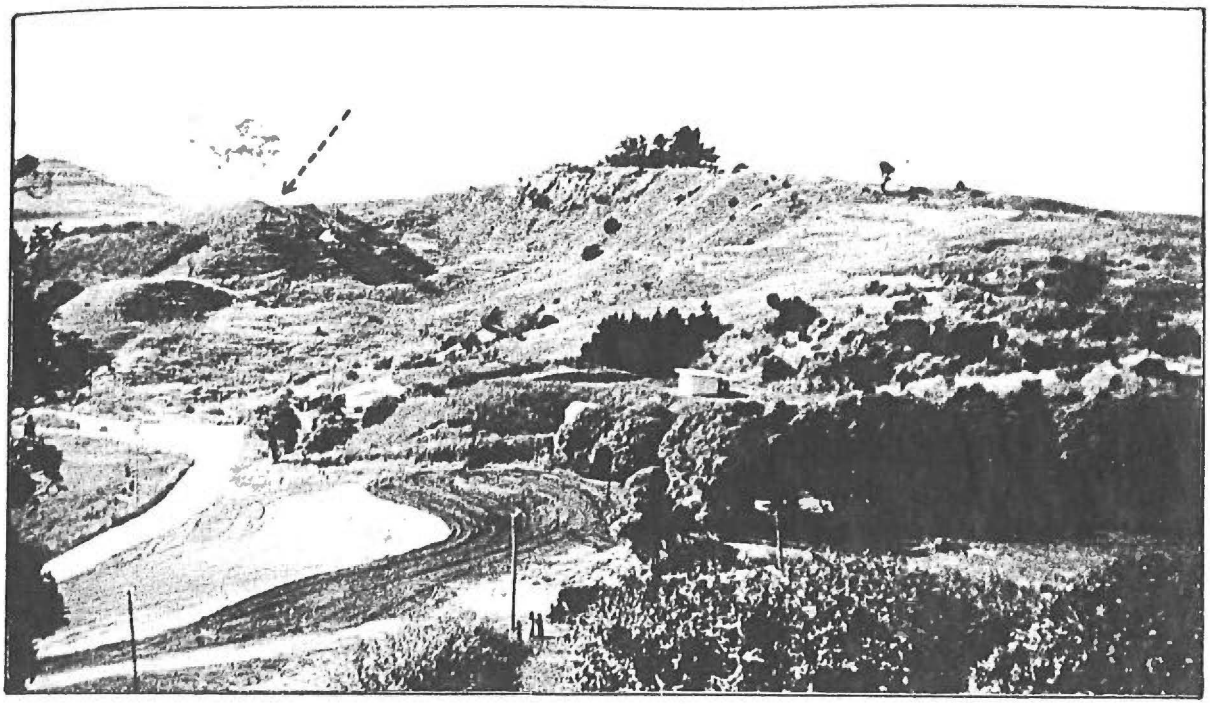

(a)

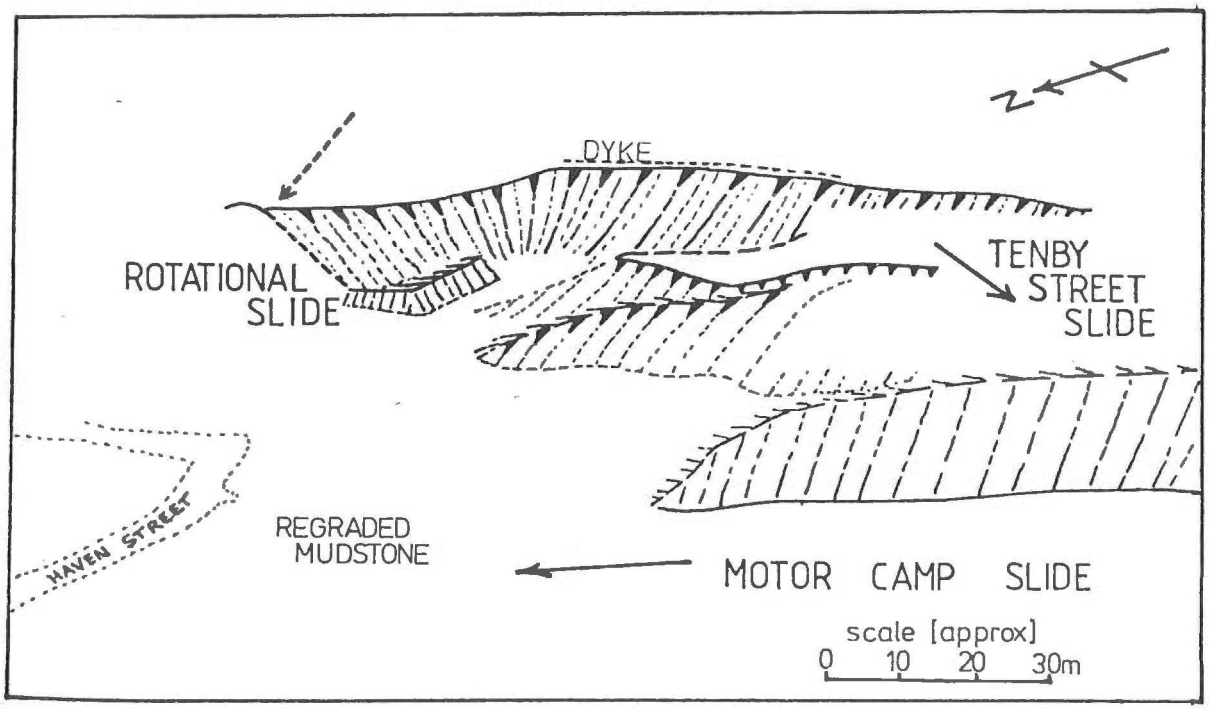

(b)

Fig.3.12: Eastern Slide Complex, central section; partially showing principal escarpments delineating the three related slides. Dotted arrow denotes that section of the scarp subsequently eroded by a large debris flow-slide amassing colluvium onto rotated slide blocks; inferred location of the volcanic dyke is also highlighted (refer map enclosure, engineering geology maps). Note regrading of mudstone to facilitate expansion of Motor Camp accommodation has begun. Viewing southeast from 7550E,0400N.

Photograph courtesy Mr P. Kedsley (dated about 1940's).

The slide seems moderately deep-seated with its principal basal rupture zone plunging, unexposed, to the northwest.

Northwesterly movement was against estimated regional dip emphasising the incompetence of the Hampden mudstone.

Original slide morphology is mostly obscured but slide mode can be inferred as a Rotational multiple block failure.

Instability was most likely initiated as "creep" displacement due to relaxation of horizontal stress when the adjacent region failed (Motor Camp Slide). Continued precursory creep probably sufficiently weakened material to yield episodes (at least three) of rotational slide-flow slope failure forming a sequence of tilted blocks subsiding to the northwest. Retrogression is possibly structurally controlled by the mafic dyke striking east-north-east (Fig. 3.10).

Stability

Individual blocks comprising the failure mass are assumed "inactive" however this requires cadastral survey verification. If extensive alteration of present topography occurs (via active shallow slope failure or man's actions) in conjunction with adverse climatic conditions, reactivation of the Tenby Street Failure may result. Sudden slope failure would be preceded by accelerated "creep" movement and delineated by tension cracking.

No active shallow instability occurs within the slide region, but some surficial "creep" is expected.

3.7.4 Rotational Slide

The Rotational Slide, covers an area of 1×10^4 square metres and forms an eastern boundary to the "composite slide complex".

A steep, prominent, semi-circular escarpment, varying in height (5 to 15 m) encompasses the failure mass. The scarp's lateral margin, to the north, has been eroded by more recent mass movement amassing colluvium over the slide body.

The failure mass comprises back tilted coherent "blocks" facing northwest.

Drainage off high relief is concentrated in the deflated zone adjacent to the slide's principal escarpment, causing an area of permanently swampy ground.

Failure Mechanism and Mode

No subsurface data pertaining to failure mass geometry is known nor considered necessary to establish movement mechanism and mode.

The main mechanism of slope failure appears to be sliding via a rupture zone extending through intensely fractured Hampden mudstone.

The slide is moderately shallow-seated with its basal shear surface, unexposed, obviously semi-circular and consequently not structurally controlled.

The slide is a rotational block failure, with lateral movement essentially in a west-north-westerly direction.

Slope failure was probably via a single episode of abrupt rapid movement, triggered by unfavourable climatic conditions. Displacement has sheared the failure mass into two discernible "blocks", both predominently back tilted. Equilibrium was most likely restored within the slide mass upon failure and there is no evidence of subsequent episodic reactivation.

Stability

The moderately shallow-seated slide is assumed "stablised" and ensuing reactivation along the original basal shear zone seems unlikely under the present conditions.

Shallow mass movement is actively degrading the front face of slide mass "blocks" but apart from this the only slope deformation identified is via surficial "creep" displacement. Mass movement is expedited by drainage concentration (runoff ponding) producing localised high groundwater levels amidst the failure mass.

3.8 GEOMORPHOLOGICAL EVOLUTION

The extensive deep-seated slope failures evolved along the Moeraki Peninsula's northern coastline highlight the incompetence and inherent instability within the Kurinui and Hampden Formations.

Similar deep-seated mass movement is well documented; Abbotsford Landslide (Coombs and Norris, 1981), Mt. Vulcan Slide (Smale *et.al.*, 1982), Utiku Landslide (Ker, 1970) and the Waipoapoa Landslide (Pettinga, in prep.)

The similar mode and failure mechanisms of the Davids Road and Motor Camp Slides supports a hypothesis for common structural control governing their basal shear zones.

Slip surfaces for both the Utiku and Abbotsford Slides were recognised as thin, planar clay layers coincident to bedding. Minor lithological variations (mm thick in the Utiku case) are difficult to identify and may exist as inherent zones of weakness within the Hampden and Kurinui mudstones.

Rock mass defects of lithologies in the study area probably in part govern main escarpment morphology, especially those secondary scarps developed following an initial movement phase.

Events responsible for triggering each episode of slope movement are the subject of considerable speculation.

The deep-seated Moeraki Slide probably initiated as "gravitational creep" deformation in response to relaxation of horizontal stress (principally by coastal erosion) and/or seismo-tectonic effects associated with regional uplift. Mass movement would have influenced geologic structure along the peninsula's northern coastline such that fluctuating climatic conditions and base level controls (glacio-eustatic effects) most likely triggered further episodic slope failure during the Quaternary.

Instability could be associated with a period of extremely heavy precipitation and runoff which Stout (1971) notes occurs between 1300 and 1700 years B.P.

A precise chronology of instability is difficult to infer without absolute dating of selected samples due to the absence of peri-glacial deposits.

A generalised outline of the geomorphological evolution of Moeraki Peninsula is portrayed in Fig. 3.13.

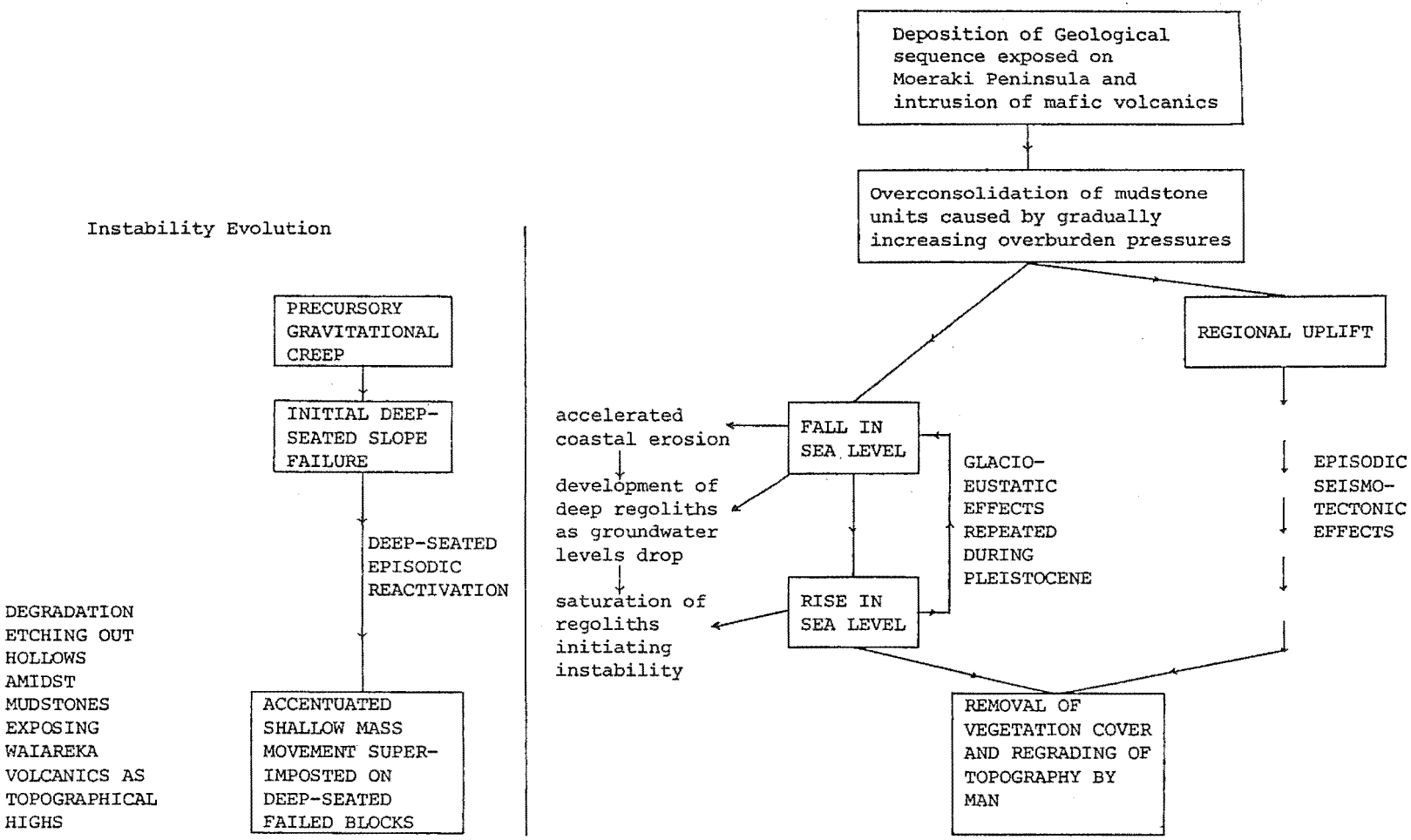

Fig.3.13: Hypothetical geomorphic evolution of Moeraki Peninsula with particular reference to mass movement.

CHAPTER FOUR

ENGINEERING GEOLOGY

4.1 INTRODUCTION

Engineering geology of the township area is discussed in five parts. A generalised summary of approach adopted for instability investigations is outlined in the first part; the second and third parts deal with "characterization" of mudstone and volcanic formations furnishing accounts on geotechnical proterties, weathering and clay mineralogy. Differences within lithologies relating to shallow slope failure are highlighted in a synthesis comprising the fourth section and the final part deals with discussion on "active processes" under the headings mass movement, hydrology and coastal erosion.

4.2 INVESTIGATION PROGRAMME

Investigations on land stability in the Moeraki township involved engineering geological mapping, field monitoring programmes together with detailed geotechnical testing and can be summarised into three successive stages (Fig. 4.1).

Stage I

Reconnaissance, which essentially comprised a literature review, preliminary mapping and some geotechnical testing, was undertaken to delineate the extent of instability plus formulate tentative ideas on failure mechanisms. From the conclusions of this initial investigation it was decided a general appraisal of mass movement would not be sufficient to understand slope processes affecting the township area. For this reason the approach adopted was to concentrate research on two "active" areas of slope deformation causing damage to roading. The conclusions drawn from these studies were subsequently applied to assess slope failure over the whole of Moeraki township.

The Motor Camp and Davids Road areas were chosen for detailed study, because:

Fig. 4.1: Investigation Programme Synthesis

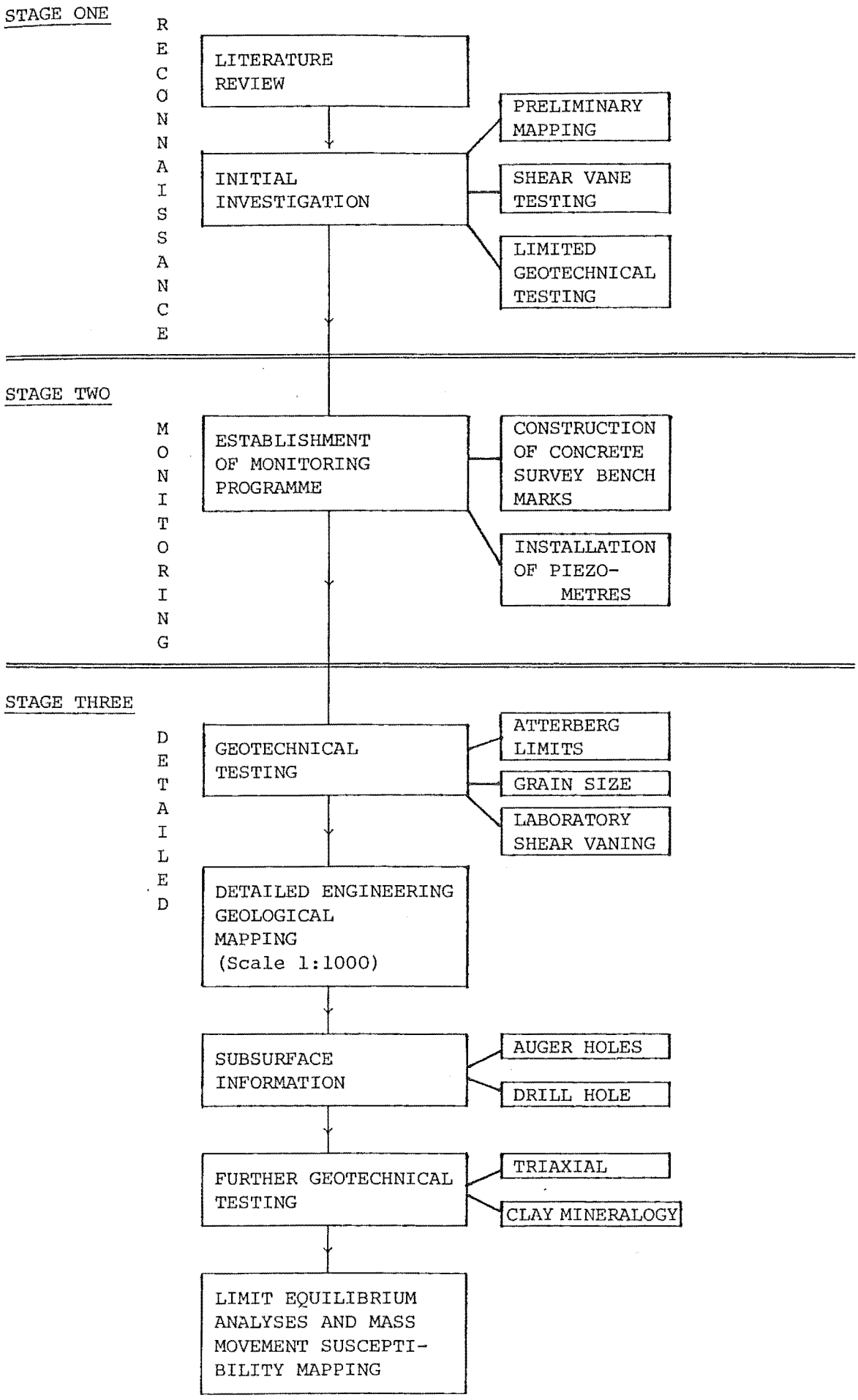

1) Slope processes at both localities were resulting in severe damage to roading (Haven Street).

2) Each region of instability was a well defined, individual problem.

3) Different mechanisms and modes of slope movement occurred in each area providing a broad spectrum of processes to study.

Stage II

A monitoring programme was commenced prior to any further investigations in order to obtain a maximum data base (two winters). Survey networks were established in both study areas, during July 1981, to evaluate rates and nature of ground movements. Standpipe piezometers (P_1, P_2 and P_3) were installed in September 1981, to record groundwater pressures.

Stage III

Remoulded samples collected during piezometer installation were tested between November 1981 to January 1982 to establish geotechnical parameters for Hampden Formation regolith and colluvium.

Field work for compilation of engineering geological maps was carried out during January 1982 to April 1982.

Tentative failure models for the Motor Camp and Davids Road areas were developed and for verification of these, six hand augered holes and one borehole were put down in February 1982.

A series of, consolidated, undrained, triaxial tests with pore pressure measurement to determine effective stress parameters were performed on regolith samples from an area of active slope deformation. The results were subsequently used for limit equilibrium analyses to assess the relative effects of falling ground water levels on "active" slope failure.

The survey monitoring programme was completed in August 1982, providing a data base of one year with sufficient information to:

1) Delineate unstable areas and their rates of movement.

2) Identify any correlation between ground movement and rainfall.

Information from stability investigations was collated and applied in the preparation of mass movement susceptibility plans for the township area (scale 1:1000).

4.3 CHARACTERIZATION OF THE HAMPDEN FORMATION

4.3.1 Introduction

The Hampden Formation is characterized in three major sections. The first recounting geotechnical parameters of both weathered and unweathered mudstone (consistency limits, grain-size analyses, density and clay mineralogy). Secondly, weathering peculiarities are described and thirdly, strength parameters of material involved in shallow instability are considered.

Apart from occasional greensand bedding, the Kurinui Formation is lithologically similar to the Hampden mudstones, hence this chapter is tacitly assumed to typify behaviour for both formations.

4.3.2 Consistency Limits

Cohesive soils vary from solid state when dry to semi-solid, plastic and finally liquid upon increasing water content. Atterberg (1911) subdivided this continuum via arbitrary boundaries into "consistency limits" for a soil, two of which Casagrande (1932) specified in terms of standardized test procedures (Atterberg Limits).

1) The liquid limit, corresponding to the moisture content above which a soil readily becomes a liquid.

2) The plastic limit, correlating to the water content below which the soil begins to crumble.

The difference between these two extremes is the range of water content over which a soil behaves plastically and is a direct reflection of composition and shear strength (Casagrande, 1932).

The lowermost boundary of soil consistency between solid and semi-solid behaviour is defined by the standardized test determining Skrinkage Limit.

Testing of the Hampden Formation was on remoulded samples taken from piezometer installations (P_1, P_2, P_3), auger hole 1,

along with stiff, dry weathered material exposed in slope failure escarpments and random samples from brecciated zones along the shore platform.

Extensive Atterberg and Shrinkage Limit testing was carried out to establish the degree of variation in remoulded properties within profiles (refer Appendix 3 for test methodology).

Atterburg Limits

Liquid and plastic limits showed no distinct variation with depth or soil texture (ie. softened profile horizons); liquid limit (LL) varying between 32% to 87% and plastic limit (PL) from 19% to 45%.

Hydroscopic water (H_W) is water absorbed on soil colloids and their associated ions (Spangler and Handy, 1973), at room humidity, and was determined as a routine measurement (refer Appendix 3). The parameter provides a quick, direct reflection of relative swelling clay content between samples (assuming constant air humidity). It was correlated with principal soil parameters to speculatively ascertain their relationships with swelling clay mineral content.

The range of plastic behaviour (PI) and liquid limit both increased with growing abundance of swelling clays (inferred from H_W), whilst the plastic limit showed no correlation to H_W, and thus appears an independent parameter (Fig. 4.3). The presence of carbonaceous material within paleosol and swamp horizons increased liquid limits without significantly altering plasticity index.

Tests on stiff, dry weathered regoliths showed anomalously low liquid limits (refer Appendix 3).

Swelling clays absorb moisture increasing the quantity of water a soil assimilates before exhibiting liquid behaviour, hence the affinity of H_W with LL and PI. These tentative correlations agree with Bouchardt (1977) who concluded smectite clays were indirectly related to both LL and PI, but that PL showed no consistent relationship to clay mineral type.

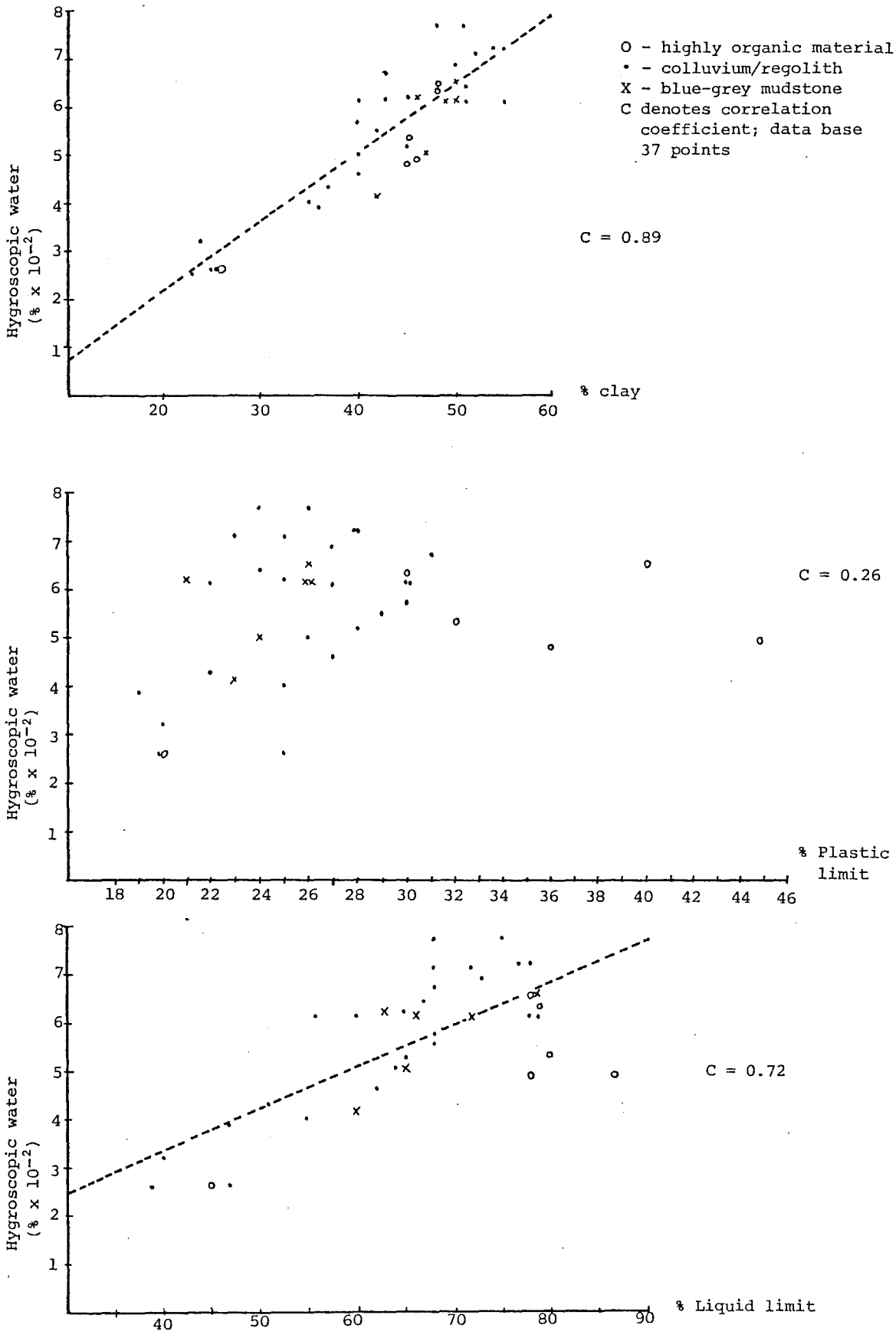

Fig.4.2: Regression correlations between hygroscopic water content and consistency parameters for Hampden mudstone.

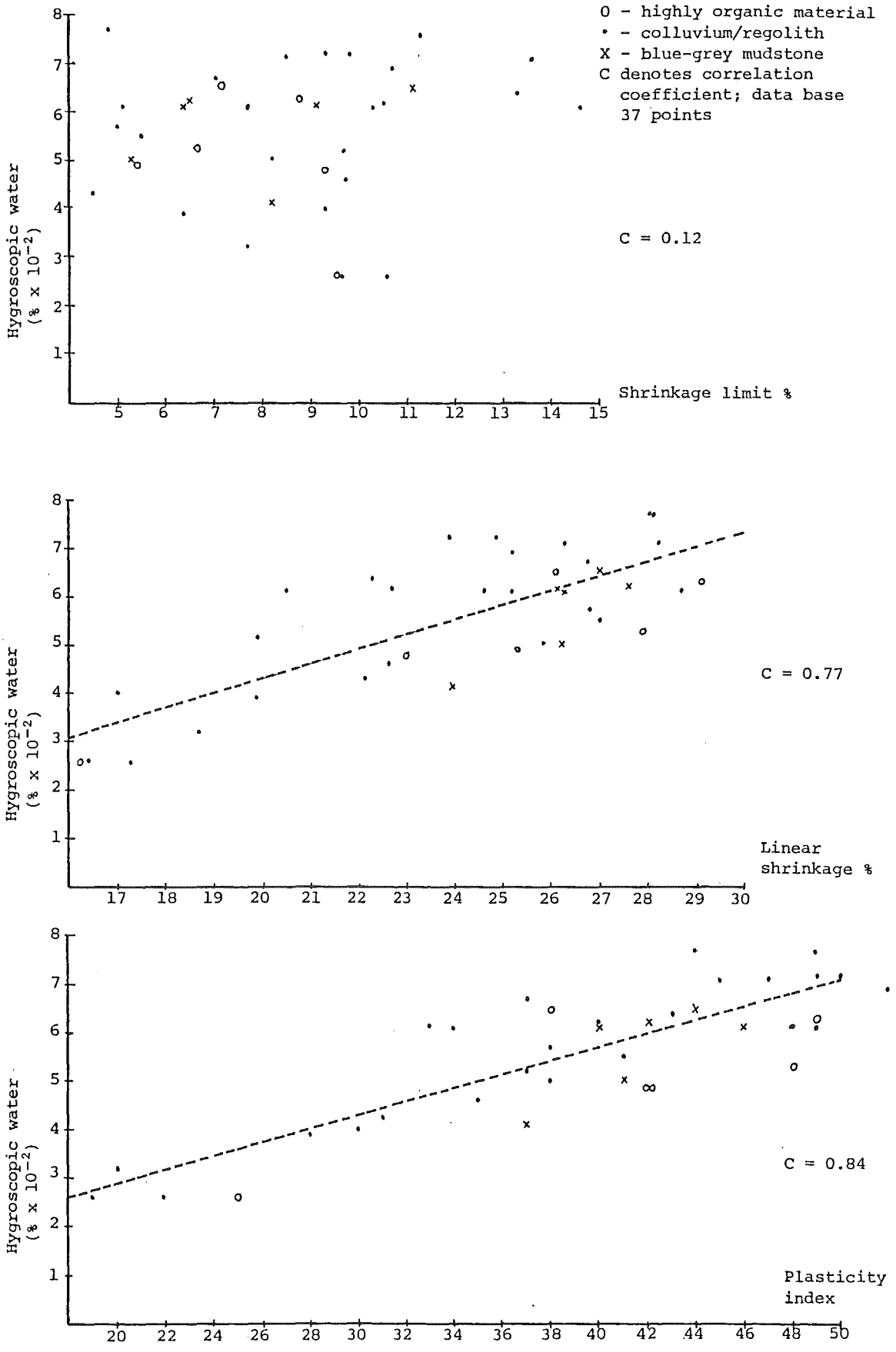

Fig.4.3: Retrogression correlations between hygroscopic water content and consistency parameters for Hampden mudstone.

The anomalously low, LL, values for dried regolith are ascribed to a welding together of active clay particles upon drying rather than change in mineralogy due to degradation.

Arman (1970) noted organic fibres "fix" free water along with organic micelles increasing soil moisture which accounts for the relationship between high LL and carbonaceous material (Fig. 4.2).

Shrinkage Limits

Shrinkage limits (SL) varied from 4.8% to 14.6% and showed no consistent correlation with other parameters (PL, LL, PI, H_W) (Fig. 4.3).

Shrinkage limits are influenced by particle arrangement or structure, consequently the degree of sample disturbance during preparation and testing is reflected in the numerical value obtained. For thoroughly disturbed clay pastes, a low SL indicates a dispersed structure while a high SL indicates a flocculated structure (Winterkorn and Fang, 1975).

Linear shrinkage (L_S) shows good correlation to H_W, thus appears influenced by the quantity of swelling clays present. Excess carbonaceous material present in some samples did not appear to alter this relationship (Fig. 4.3).

4.3.3 Grain-Size Analyses

True size analyses of samples containing high percentages of clay cannot be measured since analytical techniques do not differentiate between variation in size, shape and density (the latter dependent on mineral and extent of cation adsorption, Lewis, 1981).

Grain-size distributions show the Hampden Formation as uniformly graded with amounts of sand varying from 2% to 13%, silt from 37% to 67%, and clay from 23% to 55%.

Sand fraction percentages seem consistent whilst clay quantity varied with amount of silt.

Carbonate content, was estimated from 50 gm samples and varied between 3% to 7% for weathered regolith and 9% to 12% for unweathered mudstone (refer Appendix 4 for methodology).

4.3.4 Density

Density was determined using a Balloon Densometer with 30 gm balloon, 200 mm diameter x 50 mm rings allowing large representative sampling with a minimum of disturbance to in-situ structure (methodology, NZS 4402, Part 2, 1981).

Bulk density of weathered overburden showed no relationship to depth or texture, varying from 1.530 t/m^3 to 1.888 t/m^3 but good correlation to moisture content (Fig.4.4a). Partially softened blue-grey brecciated horizons exposed along the shore platform had bulk densities of 1.065 t/m^3 and 1.124 t/m^3. Bulk densities of relatively unweathered mudstone were 1.105 t/m^3 and 1.085 t/m^3; the anomolously lower densities attributed to open discontinuities amidst material tested.

Two exceptions occur to the well defined relationship between weathered overburden bulk density and moisture content, which are principally attributed to erroneous water content measurement (in the order of 10%). The presence of dry, hard mudstone fragments amongst moist ambient mud matrix, affects moisture content based on bulk samples. Hutchinson (1970) notes differences in water percentages between softened mudsone and hard inclusions of up to 9%, resulting in significant moisture content error if the sample is considered on a bulk basis.

4.3.5 Clay Mineralogy

The clay fraction is a size term, referring to grains finer than two microns, the bulk of which are laminated flake shaped particles known as clay minerals.

Mineralogy was identified by X-ray diffraction using a Phillips X-ray diffractometer with CvKα radiation maintained by a 1^{o} divergence slit, a 0.2 mm receiving slit and a 1^{o} anti-scatter slit. A Norelco tube was run at 34 Kv and 34 mA and diffraction patterns recorded at a scan rate of 1^{o} min (refer Appendix 5 for methodology).

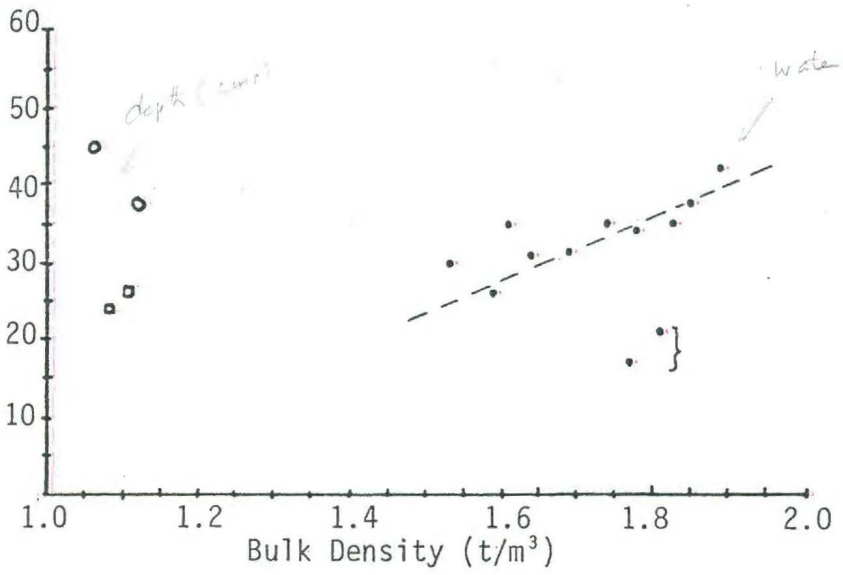

Fig.4.4(a): Analysis of field density data.

Fig.4.4(b): Balloon Densometer

Materials analysed were sampled from a profile of Hampden Formation regolith exposed along the shore platform in the Davids Road area and consisted of:

1) softened mudstone,
2) weathered regolith, containing hard mudstone inclusions within an ubiquitous softened matrix (yielding characteristic lumpy texture),
3) similar textured but unweathered horizons; exposed between coherent "blocks" of blue-grey mudstone,
4) unweathered Hampden mudstone,
5) stiff, dry, weathered mudstone regolith.

Objectives of analyses were.

1) To identify mineralogy.

2) To ascertain any significant changes in mineralogy associated with the development of specific weathering textures (ie. softened horizons).

As quantitative analyses were not carried out relative changes within mineral groups relating to different horizons within the profile are not hightlighted.

The following mineral assemblages were indentified:
Illite, Kaolinite, Vermiculite and Smectites.
Dried regoliths showed regular and random interlayering of Vermiculite, Smectite and Illite.

No variation associated with texture or depth was identified. Mineralogy of blue-grey mudstone was similar to yellow-brown regoliths tested.

It should be noted variation in PH, ion concentration and organic material will alter abundance and clay mineral type within materials hence analyses performed only provide a reflection of lithological mineralogy.

Based on visual appraisal of diffractogram peak intensity and area, smectites appear to comprise the majority of

the clay fraction followed by Kaolinite, then Illite with Vermiculite a minor constituent.

4.3.6 Weathering

Weathering is the total effect of all processes which bring about the decay and disintegration of rocks providing that no large scale transport of loosened products is involved; ie. such as wind or rain wash which are essentially erosional (Holmes, 1965).

Identification of active weathering mechanisms plus their associated products is complicated by mass movement history of the township area. Repeated slope failure, on various scales, has confused geologic structure and hence establishment of textures developed in-situ or as a result of downslope movement, is difficult in some regions.

Weathering results in a continuous, transient gradation between rock and soil, thus all descriptions in terms of rigid classifications are arbitrary.

The Fookes *et.al.* (1971) scheme based on texture was adopted for in-situ field classification (Fig. 4.5). The "state" of weathering for thoroughly remoulded samples when structure and texture are destroyed, is described in terms of oxidation (mottling and gleying). Mottling is specified via contrast, size and abundance; gleying often related to organic material in terms of weak, moderate or strongly gleyed (refer Appendix 7). Both are indicative of chemical weathering and the presence of iron.

Field exposure showed mudstone lithologies prone to slaking. In view of this no standardized slaking tests were felt necessary since the results would

1) merely confirm conclusions that these formations are susceptible to slaking,
2) provide no further insight into the mechanisms of slope instability.

Changes in geotechnical properties associated with weathering are inferred from slope stability investigation in the two detailed study area.

N.I.R.R.*		Grade	Degree of decomposition	Field recognition (after Fookes & Horswill 1969)		Engineering properties (after Little 1969)
Index† value	Classification			Soils (i.e. soft rocks)	Rocks (i.e. hard rocks)	
12 11	Residual soil	VI	Soil	The original soil is completely changed to one of new structure and composition in harmony with existing ground surface conditions.	The rock is discoloured and is completely changed to a soil in which the original fabric of the rock is completely destroyed. There is a large volume change.	Unsuitable for important foundations. Unstable on slopes when vegetation cover is destroyed, and may erode easily unless a hard cap present. Requires selection before use as fill.
10		V	Completely weathered	The soil is discoloured and altered with no trace of original structures	The rock is discoloured and is changed to a soil, but the original fabric is mainly preserved. The properties of the soil depend in part on the nature of the parent rock.	Can be excavated by hand or ripping without use of explosives. Unsuitable for foundations of concrete dams or large structures. May be suitable for foundations of earth dams and for fill. Unstable in high cuttings at steep angles. New joint patterns may have formed. Requires erosion protection.
9 8	Badly weathered	IV	Highly weathered†	The soil is mainly altered with occasional small lithorelicts of original soil. Little or no trace of original structures.	The rock is discoloured; discontinuities may be open and have discoloured surfaces and the original fabric of the rock near the discontinuities is altered; alteration penetrates deeply inwards, but corestones are still present.	Similar to grade V. Unlikely to be suitable for foundations of concrete dams. Erratic presence of boulders makes it an unreliable foundation for large structures.
7 6 5	Weathered	III	Moderately weathered‡	The soil is composed of large discoloured lithorelicts of original soil separated by altered material. Alteration penetrates inwards from the surfaces of discontinuities.	The rock is discoloured; discontinuities may be open and surfaces will have greater discolouration with the alteration penetrating inwards; the intact rock is noticeably weaker, as determined in the field, than the fresh rock.	Excavated with difficulty without use of explosives. Mostly crushes under bulldozer tracks. Suitable for foundations of small concrete structures and rockfill dams. May be suitable for semipervious fill. Stability in cuttings depends on structural features, especially joint attitudes.
4	Fresh	II	Slightly weathered	The material is composed of angular blocks of fresh soil, which may or may not be discoloured. Some altered material starting to penetrate inwards from discontinuities separating blocks.	The rock may be slightly discoloured; particularly adjacent to discontinuities which may be open and have slightly discoloured surfaces; the intact rock is not noticeably weaker than the fresh rock.	Requires explosives for excavation. Suitable for concrete dam foundations. Highly permeable through open joints. Often more permeable than the zones above or below. Questionable as concrete aggregate.
3		I	Fresh rock	The parent soil shows no discolouration, loss of strength or other effects due to weathering.	The parent rock shows no discolouration, loss of strength or any other effects due to weathering.	Staining indicates water percolation along joints; individual pieces may be loosened by blasting or stress relief and support may be required in tunnels and shafts.

*The N.I.R.R. Classification is given for comparative purposes and the Grade Figures given throughout the text are those in the third column.
†Total Index Value obtained by adding together the index value for lustre, hardness and consistency and state of crystallization.
‡The ratio of original soil or rock to altered material should be estimated where possible.

Fig.4.5: Weathering classification adopted for in-situ field description; according to Fookes *et.al.* (1971).

Slaking

Slaking encompasses all processes causing the disaggregation of materials by an increase in strain from the ingress of water.

Intact unweathered Hampden mudstone slakes via a continuum of mechanisms to form a "softened" cohesive clay of the same mineralogy.

Slaking phenomena occur simultaneously on a number of scales. The influence and effect of various mechanisms on material depend on:

1) Permeability and porosity which control the entry, retention and mobility of pore fluids.

2) Cementation and consolidation (stress history) which determine the resistance to tensional forces induced by slaking.

3) Mineralogy. The adsorption of ions or molecules plus solution of cement being significant in the slaking process.

Processes involved in slaking can be broadly classified into two categories (Fig. 4.6).

1) Intra-Particle swelling.
2) Inter-Particle swelling.

Intra-particle swelling involves rapid disaggregation principally controlled by permeability, porosity, cementation and consolidation; processes comprise:

Air Breakage

Tensional failure attributed to air trapped and pressurized by the rapid ingress of water usually within a dry mass (voids mainly air filled).
Terzaghi and Peck (1936), Taylor and Spears (1970), Badger *et.al.* (1956).
The mechanism is dependent on void size rather than void volume (ie. capillary pressure is inversly proportional to pore radius).

PROCESS	MECHANISM	DOMINANT CONTROLS
INTRA-PARTICLE SWELLING	AIR BREAKAGE	consolidation, cementation; permeability, porosity
INTER-PARTICLE SWELLING	CHEMICAL DISSOLUTION	clay mineralogy
	IONIC DISPERSION	

Fig.4.6: Synthesis of slaking processes.

Inter-particle swelling is a slower process of disaggregation, primarily dependent on clay mineralogy and hence influenced by chemical weathering; processes comprise:

Chemical Dissolution

Chemical dissolution, as proposed by Nakano (1967) refers to the ability of an ubiquitous solution to form hydrogen bonds with originally absorbed water molecules (predominantly around clay minerals), thus causing an increase in strain. Total evaporation is unnecessary and the process may occur in response to fluctuating vapour pressures (or ground water levels). The practical implications of this being "softening" of mudstone may proceed till the chemical potential of absorbed water becomes equal to that of the ground water as active surface of mudstone clay particles are exposed and water molecules absorbed (Nakano, 1967).

Ionic Dispersion

Dispersion may result by repulsion of similarly charged clay micelles; individual mineral charges relating to their atmosphere of exchangeable absorbed ions. The ease of dispersion/disaggregation is dependent on clay type plus dominant cation, ie. clays of hydrated cations such as Na prove the easiest to disperse, followed by K, followed by Mg. Properties of the ambient pore fluid are not significant due to the excessively high ionic concentrations required before dispersion is reduced (Badger *et.al.*, 1956).

Stress Relief

Stress relief may result in brittle tensional fracture or jointing when the difference between effective vertical and horizontal stress exceeds the materials' peak strength. Fracturing is classified into two groups:

1) Systematic joints, occurring in ordered sets, with sub-planar surfaces over lengths of several metres.

2) Non Systematic joints, or fissures occurring in more or less random orientations with irregular or concoidal surface over short lengths (1 cm to 50 cm). (Skempton and Petley, 1967).

Both systematic and non-systematic jointing through the mudstone units are attributed mainly to stress relief, plus to a lesser degree, seismotectonic effects and slope instability.

Systematic jointing as mapped within the Hampden and Kurinui Formations extends for tens of metres, maintaining essentially constant strike. Mudstone fissuring intensifies towards the ground surface forming profiles of disaggregated "blocks"; fracture concentration and depth being influenced by ground water fluctuation and mass movement.

Effects of stress relief are related to consolidation history.

Over-consolidation causes deformation of flexible clay particles which, if not strained beyond their elastic limit, is partially recoverable. Thus clay rich materials may contain latent strain energy, the amount dependent on consolidation pressure, diagenisis and clay fraction properties (Bjerrum, 1967).

Stress relief fracturing increases permeability facilitating weathering and the release of latent strain stored within isolated mudstone "blocks". The higher the recoverable strain the higher the potential volume and moisture content of fully degraded clay, ie. moisture content of intact Hampden mudstone is about 24% in contrast to 40% in the "softened" weathered state where latent strain has been released.

Oxidation

Oxidation involves the combination of elements with oxygen or the removal of electrons and is the dominant chemical weathering process degrading mudstone formations. Most significant is the reaction of pyrite with oxygen rich ground water yielding ferrous sulphate and sulphuric acid.

$$FeS_2 + H_2O + 7(O) \rightarrow FeSO_4 + H_2SO_4$$

The ferrous sulphate may combine further with water to produce limonite and sulphuric acid (Morgenstern, 1970). The brownish-yellow stain of limonite is common but mostly dehydrates to hematite exposed as large red stains along fissures (Fig. 4.7).

$$FeSO_4 + 2H_2O \rightarrow \underset{\text{limonite}}{Fe(OH)_2} + H_2SO_4$$

$$2He(OH)_2 \rightarrow \underset{\text{hematite}}{Fe_2O_3} + H_2O$$

Hematite accounts for the yellowish brown colour of weathered Hampden and Kurinui Formations (Fig. 4.8).

Percolating solutions containing calcium carbonate from dissolved cement or foraminifera react with sulphuric acid (produced by degradation of pyrite) to form gypsum which may crystallize out as selenite (Chandler, 1972).

$$H_2SO_4 + CaCO_3 + 2H_2O \rightarrow Ca:SO_4:2H_2O + H_2CO_3$$

Precipitation of gypsum often concentrated along fractures, results in significant volume increase aiding mechanical breakdown of mudstone.

Weathering Model

The weathering of intact mudstone, ultimately to a plastic cohesive clay via the mechanisms described, is referred to as "softening" and within the field area appears a continuum which may be divided into three successive stages (Fig. 4.9).

Weathering processes (slaking, stress relief, oxidation) are interdependent and act simultaneously, with the significance of each method in an area relating to local conditions.

Slaking: the principal "softening" mechanism, predominantly via intra-particle swelling (chemical dissolution); accelerated in areas of high ground water and pore pressure (desiccation is not essential).

Fig.4.7: Hematite and limonite oxidation along relict joint (dotted) within the Hampden Formation (7850E,0550N).

Scale

0 2 cm

Fig.4.8: Weathered yellow-brown Kurinui mudstone exposed along the peninsula's north-western shore platform (6900E,0450N).

Scale

0 4m

WEATHERING MODEL FOR IN-SITU SOFTENING OF MUDSTONE

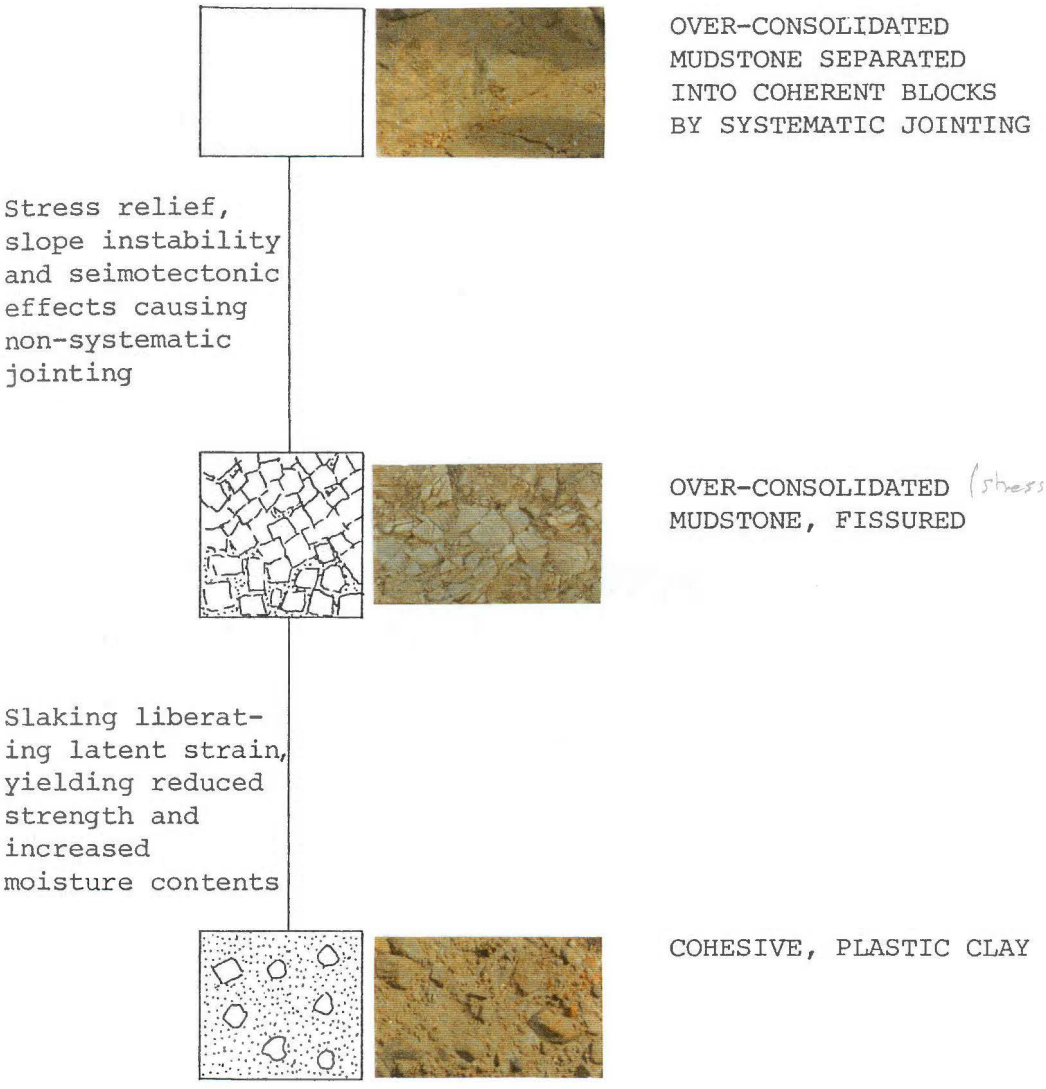

Fig.4.9: Schematic representation of "model" for in-situ mudstone softening; note absence of oxidation in all three stages.

Stress relief: by increasing permeability, exposing a larger surface area and contributing to slaking by strain release.

Oxidation: by dissolution of calcareous cement, reaction with Fe and precipitation of gypsum weakening inter-particle bonding.

Oxidation is not essential to the "softening" process, but is accentuated by increasing area exposed to reaction hence oxidation zoning often broadly correlates to the three stage weathering "model".

Regolith Development

Mudstone regolith is defined as that zone of in-situ yellow-brown overburden which rests on blue-grey unweathered mudstone; depths vary between 1 m to 7 m with the disaggregated mantle often characterized by a sharp basal bedrock overburden boundary.

In-situ profile development can be broadly divided into three stages based on weathering characteristics (Fig.4.10).

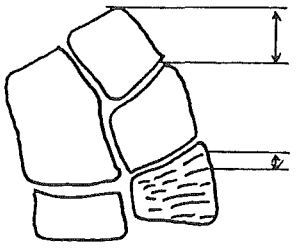

Stage One (Slightly Weathered)

Blue-grey mudstone broken into coherent blocks by fissuring; spacing >1000 mm. No shrinkage cracking. No significant oxidation or precipitation of gypsum observed. Carbonate content approximately 9% to 12%, field moisture content 24% to 27%.

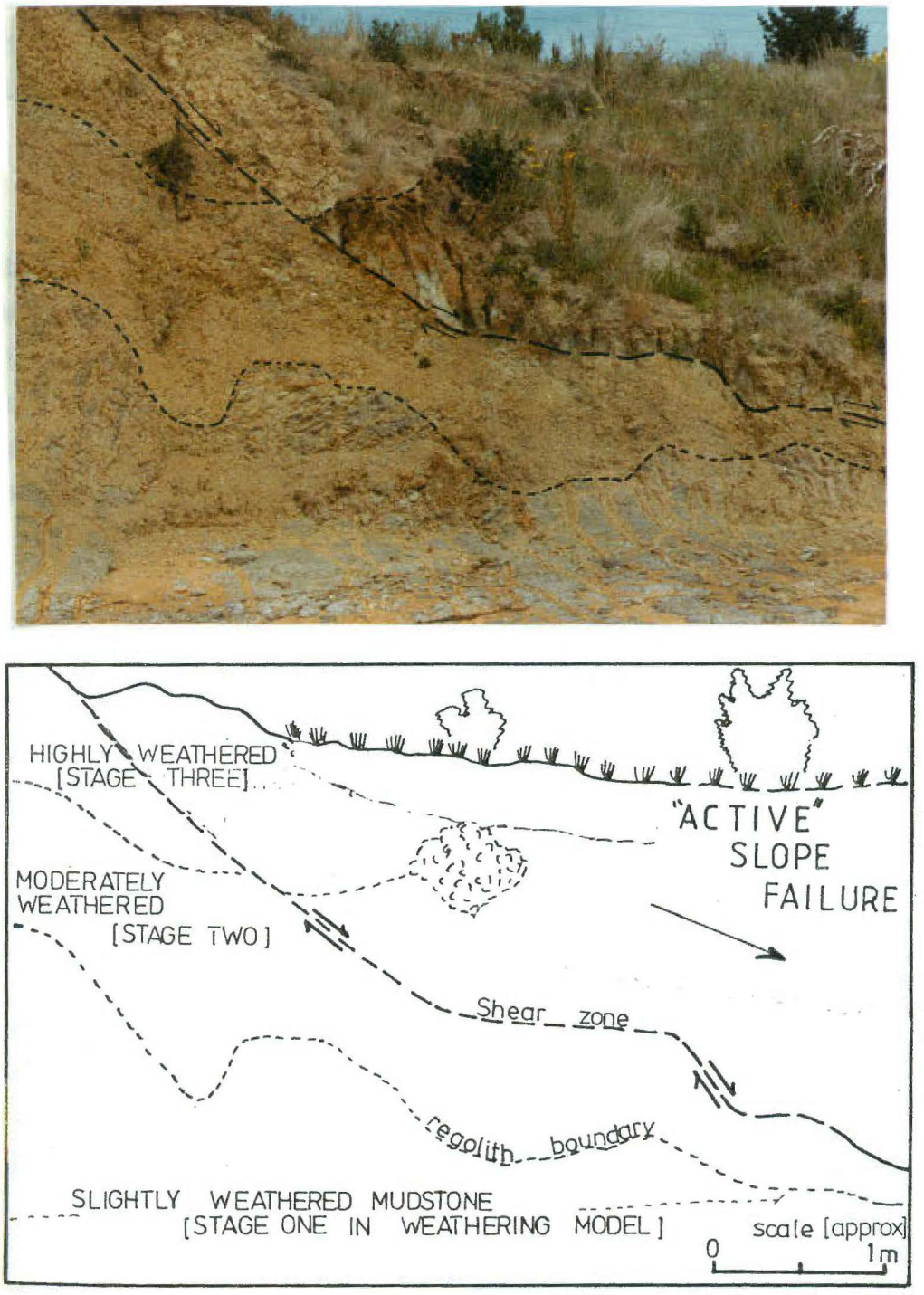

Fig.4.10: Weathering zones classified according to Fookes *et.al.* (1971) correlated with stages comprising the regolith development "model". View from the shore platform, Davids Road area (7250E,0350N).

Stage Two (Moderately Weathered)

Grey-brown fissured clay. Fissure spacing 10 mm to 100 mm and shrinkage cracking spaced at 1 mm to 2 mm. Oxidation concentrated along major fissures in zones composed of limonite and/or hematite. Gypsum crystals rare.

Stage Three (Highly Weathered)

Light-yellow-brown fissured clay; containing solid lithorelics (up to 30 mm) within a matrix of fine silty clay which appears remoulded. Oxidation occurs as lithorelic skins (1 mm to 5 mm); varied mottled patches within the ambient matrix occur together with occasional gelyed zones. Gypsum crystals common. Carbonate content approximately 3% to 7% and field moisture percentage varying between 24% to 41%.

Regolith development appears initiated above the water table where disintegration of mudstone is accelerated by desiccation (inducing slaking) and oxidation (Fig. 4.11). Hence sharp basal contacts between regoliths and underlying mudstones probably represent the lowest surface of relict ground water tables; a hypothesis supported by oxidised regolith lithorelics anomalously present in reducing conditions, below current water table fluctuations.

Relatively continuous, horizontal, "softened horizons" occur within both regolith and relatively unweathered mudstone which may depict remnants of systematic joints along which ground water has accelerated the softening (via slaking) process.

X.R.D. clay mineral analyses showed no significant leaching trends down the regolith profile tested or distinct changes in mineralogy associated with different textures.

4.3.7 Strength

Strength is defined in terms of total or effective stress depending on the assumed drainage condition.

If undrained, Coulomb's equation defines strength in terms of total stress:

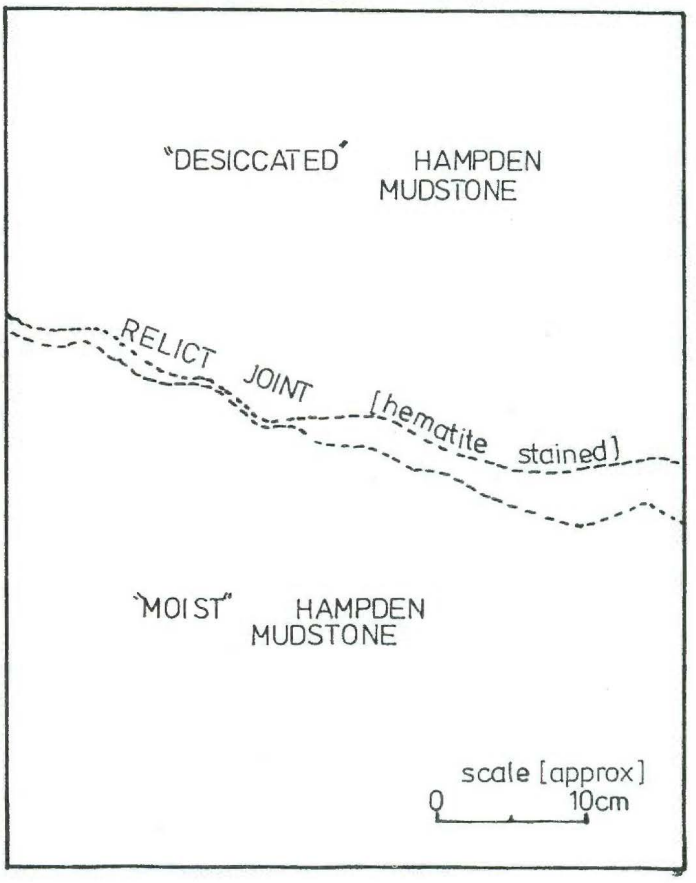

Fig.4.11: Oxidised relict joint dividing desiccated from moist in-situ mudstone. Accelerated slaking above the zone of saturation enhances development of yellow-brown regolith from blue-grey mudstone (7850E,0550N).

$\tau = c + \sigma n \text{ Tan } \phi$

τ = shear strength

c = cohesion

σn = normal stress

ϕ = angle of internal friction

If drained conditions prevail, strength is specified by Terzagli's equation in terms of effective stress parameters:

$\tau' = c' + (\sigma n' - \mu) \text{Tan } \phi'$

c' = effective cohesion

$\sigma n'$ = effective normal stress

ϕ' = effective anlge of internal friction

μ = pore pressure

and τ' = effective shear strength

The relatively large clay content (approximately 45%) of Hampden mudstones influences their strength in a number of ways.

1) Cohesion is increased. Physio-chemical attraction is concentrated within the clay fractions due to the high surface area plus anisotropic charge of clay micelles (stress history and diagenisis also influence cohesion).

2) The angle of internal friction may be considerably reduced. (Upon alignment of flake shaped minerals, predominantly confined to the clay fraction.)

3) Strength in partially saturated material is supplemented by negative pore pressures (capillary suction) or alternately reduced by positive pressures both of which are maximised within the clay fraction; capillary suction due to the large contact area between particles and positive pressures due to slow drainage within fine grained materials. Hence, ostensibly, the high undrained strength of desiccated mudstone is attributed to capillary suction, whilst the comparatively low saturated strength to positive pore pressure.

Most important to slope stability assessment and the determination of relevant strength parameters is the changes in strength associated with weathering.

Changes in Strength Associated with Weathering (Softening Process)

Consider a hypothetical block of intact, overconsolidated mudstone containing latent strain and confined by all around pressure. Stress relief jointing fractures the mudstone into a number of individual, disaggregated "blocks". Skempton and Petley (1967) make the following tentative conclusions on strength along systematic joints:

1) The majority of cohesion along the joint surface is destroyed (c' reduced by 90% from intact value) without causing much reorientation of particles (ϕ' reduced by only 1.5^{o}).

2) Fractures can be considered at residual strength, especially at low confining pressures. Small shearing movements in the order of a few millimetres along original fractures are sufficient to orientate particles within a boundary layer reducing ϕ to its residual value and polishing the surface.

Following fracturing the processes of mudstone softening are accelerated with individual defects actings as stress concentrators allowing latent strain release. The increase in strain and moisture content associated with softening decreases the strength within each block well below peak, ie. if cohesion or peak strength is not exceeded the softening process does not perpetuate.

Expansion of fissured clay to its full potential is generally prevented by surrounding confining stresses. If slope movement or jointing allows liberation of all latent strain, the material becomes "normally consolidated" and the mass reaches its "fully softened strength". Skempton (1970) notes at this stage strength parameters are equivalent to peak strength of the same clay had it not been subjected to overconsolidation. Strain required to reduce an overconsolidated clay to the "fully softened" condition, or approximately to this state, is several times greater than the strain to peak strength, but is nevertheless, not large and considerably less

than that corresponding to residual strength (Skempton, 1970). It seems probable that once strength has fallen to the "fully softened value", or close to it, there are no principal shear surfaces but instead a complex of minor shears such as Riedel, thrust and displacement shears (Skempton, 1966) which are not linked into a smooth continuous surface. Particle reorientation will have occurred along these minor ruptures as demonstrated by Morgenstein and Tachalenko (1967); note the effects of such fabric is incorporated into the "fully softened strength" (Skempton, 1970).

Once a principal slip surface has formed subsequent movements are concentrated along it without fundamental change in the pattern of rupture (displacement shears), the orientation of particles with increasing strain ultimately reducing strength to the residual value. Shear zones within the Hampden mudstone (consisting of thrust, Riedel and principal slip surfaces) exposed along the shore platform were sharply defined, sub-planar and commonly less than 5 cm wide (Fig.4.12).

The characteristic behaviour of over-consolidated clay rich material produces a distinctive stress-strain relationship important in the assessment of slope instability (Fig. 4.13). The significant reduction in strength with increasing strain (peak to fully softened to residual) yields susceptibility to a certain variety of slope deformation peculiar to over-consolidated clays ("progressive slope failure" refer Chapter Five, Motor Camp Area).

Strength Determination

Reconnaissance investigations involved in-situ undrained strength determination at standard intervals down three exploratory boreholes (adjacent to holes 1, 3 and P_2) utilizing a Geonor hand held shear-vane (refer Appendix 6 for methodology plus analysed data).

Undrained strength showed no correlation to depth and only a broad relationship to moisture content.

Results are of limited accuracy due to plant debris and small mudstone"blocks" within ambient regolith/colluvium matrix

Fig.4.12: Well delineated sub-planar basal shear zone (arrowed) exposed along the northwestern shore platform. View looking south from 6900E,0450N.

0 4 m

Scale

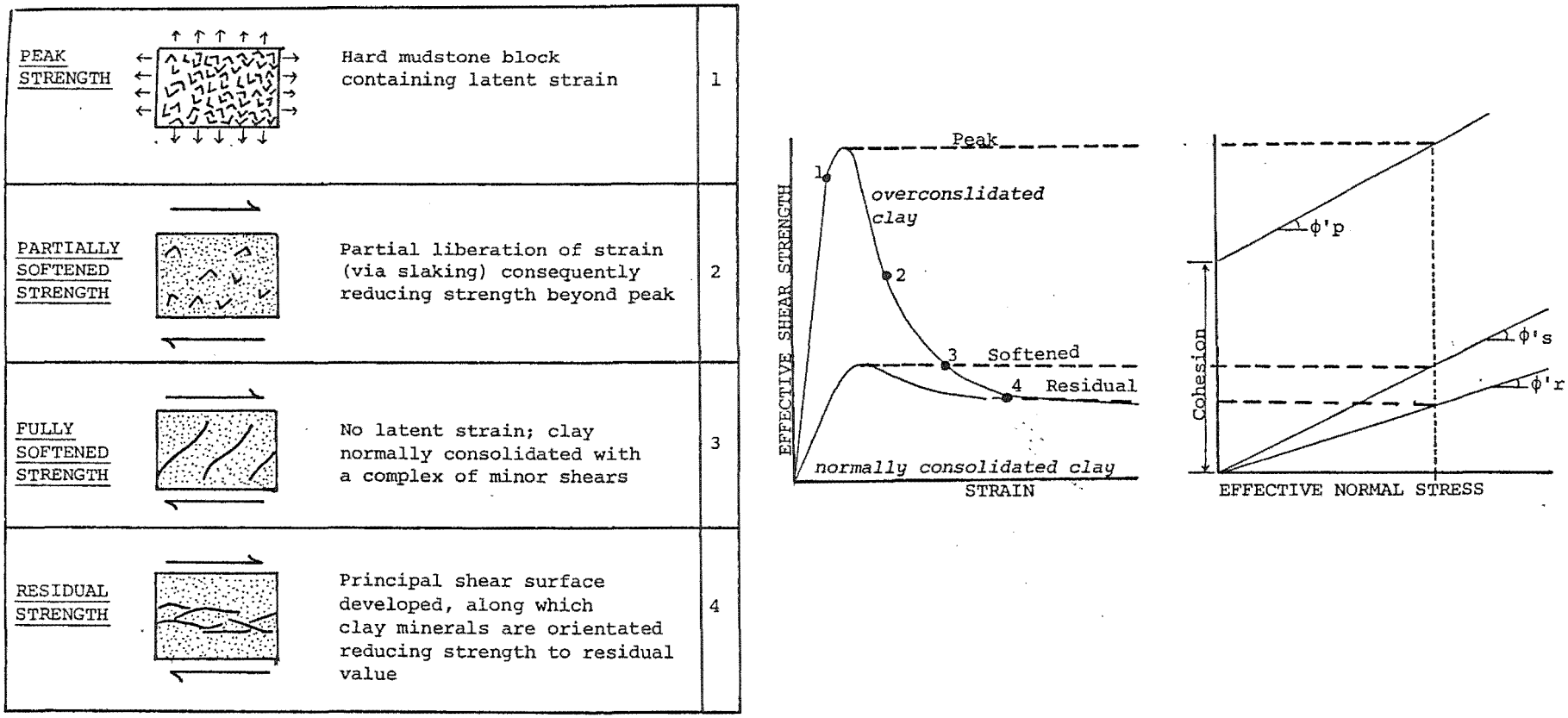

Fig.4.13: Stress-strain characteristics and associated strength parameters for over-consolidated clays; note significant strength reduction from peak to residual with comparatively small increase in strain.

disrupting shear-vane action and hindering relevant moisture content determination (refer section 4.3.4).

Two general conclusions are made:

1) Remoulded, undrained strength of mudstone colluvium/ regoliths are in the order of 1.5 t/m^2 to 4 t/m^2 (14.8 kPa to 39.2 kPa).

2) Horizons rich in organic matter had significantly higher moisture contents and consequently lower undrained strengths.

Laboratory vaning was subsequently carried out to verify these conclusions, the accuracy of results increased due to:

1) Thorough remoulding, and removal of plant debris ensuring an even sample texture and thus facilitating accurate vane strength plus moisture content determination.

2) Application of a controlled strain rate until failure.

Thorough remoulding of material caused high water content yielding low undrained strengths, the correlation of which compared favourably with extrapolated in-situ field vane results (Fig. 4.14). The relatively large changes in moisture content in comparison with shear strength are attributed to absorption of water by swelling clay minerals. Presence of organic material appears to increase weathered mudstones capacity for water assimilation thereby reducing cohesion (ie. undrained vane strength directly reflects cohesion since ϕ is assumed zero, Fig. 4.14). This data is in apparent conflict with more detailed research by Arman (1970) who concludes both unconfined compressive and triaxial shear strength of organic soils increases with organic content.

In the field situation paleosols and swamps most likely exist as regions of water concentration, which would reduce strength; thus they may be regarded zones of weakness amidst ubiquitous regolith and colluvium.

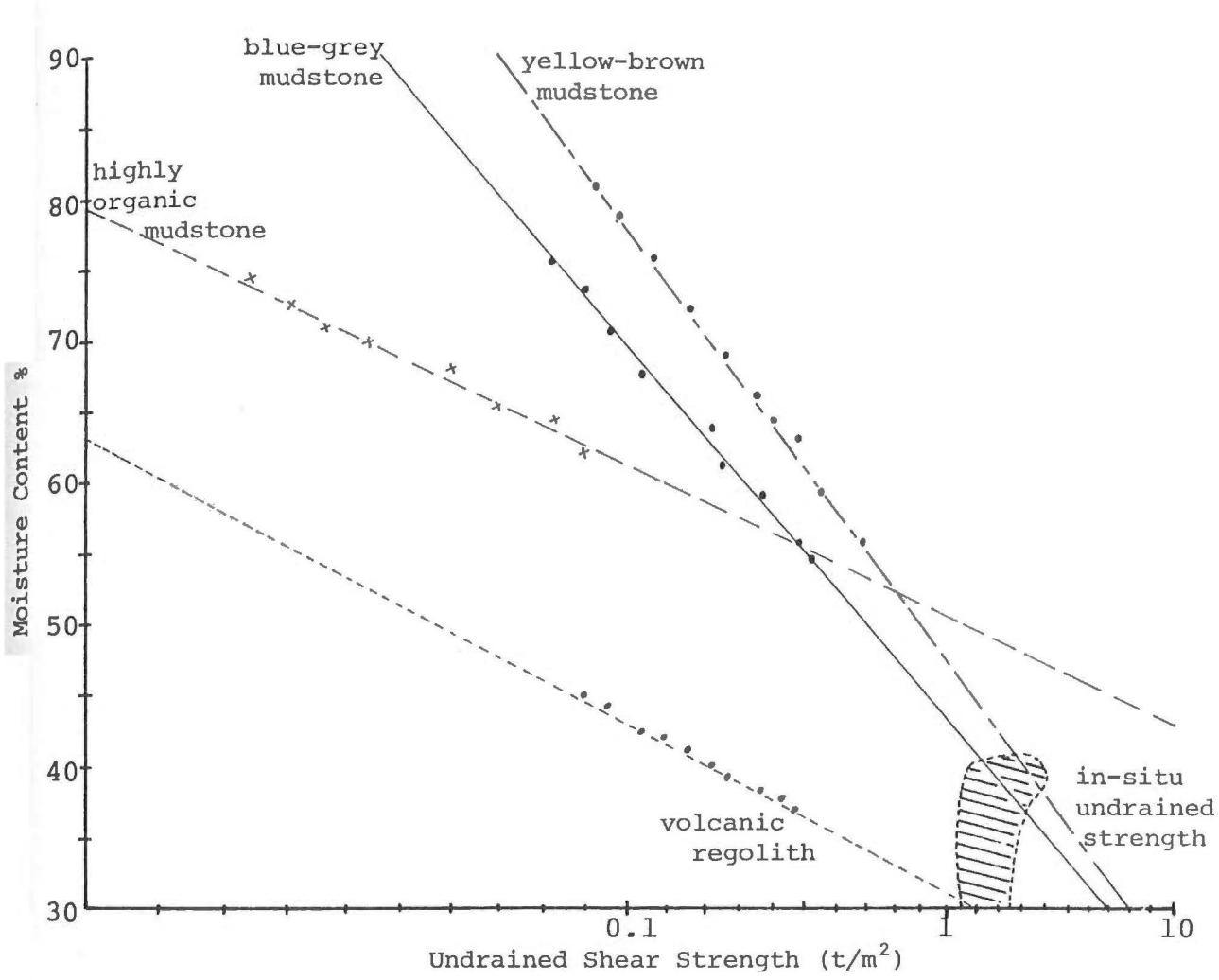

Fig. 4.14(a): Correlation of shear vane data.

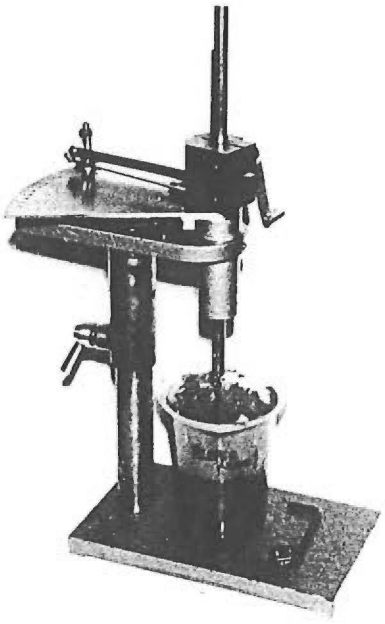

Fig.4.14(b): Geonor Laboratory Shear Vane

Effective stress parameters for limit equilibrium analyses were determined from consolidated, undrained triaxial tests incorporating pore pressure measurement.

Parameters are used in assessing currently "active" regions plus areas of incipient failure.

First time slides within over-consolidated clay rich materials such as the Hampden Formation, occur well below peak strength (Skempton, 1964; Bjerrum, 1967) often approaching the "fully softened" value (Skempton, 1970, 1977). For this reason undisturbed samples for in-situ strength determination were obtained from "softened" mudstone amidst the failure mass of an active slope failure (School Slip, refer Chapter Five). Specimens were collected in 35 mm silicone greased cores from a 1.5 m deep pit.

Confining pressure (effective pressures of 100, 150 and 350 kPa) were sufficiently high to minimise the influence of any partially softened "blocks" within the core matrix. Stress-strain plots showed no pronounced peak upon failure, indicating "plastic" deformation characteristic of "softened" mudstone rather than the pronounced peak associated with over-consolidated (non softened) material.

A graphical plot of shear strength versus normal stress produced two plausible sets of effective stress parameters for softened Hampden mudstone (Fig. 4.15).

$\phi' = 17^{o}$ $\quad c' = 8$ kPa

$\phi = 18^{o}$ $\quad c' = 0$

Triaxial testing could not strain samples sufficiently to obtain the residual strength. Undisturbed sampling of clearly defined shear zones most likely at the residual value proved impractical and therefore no effective residual strength parameters are known.

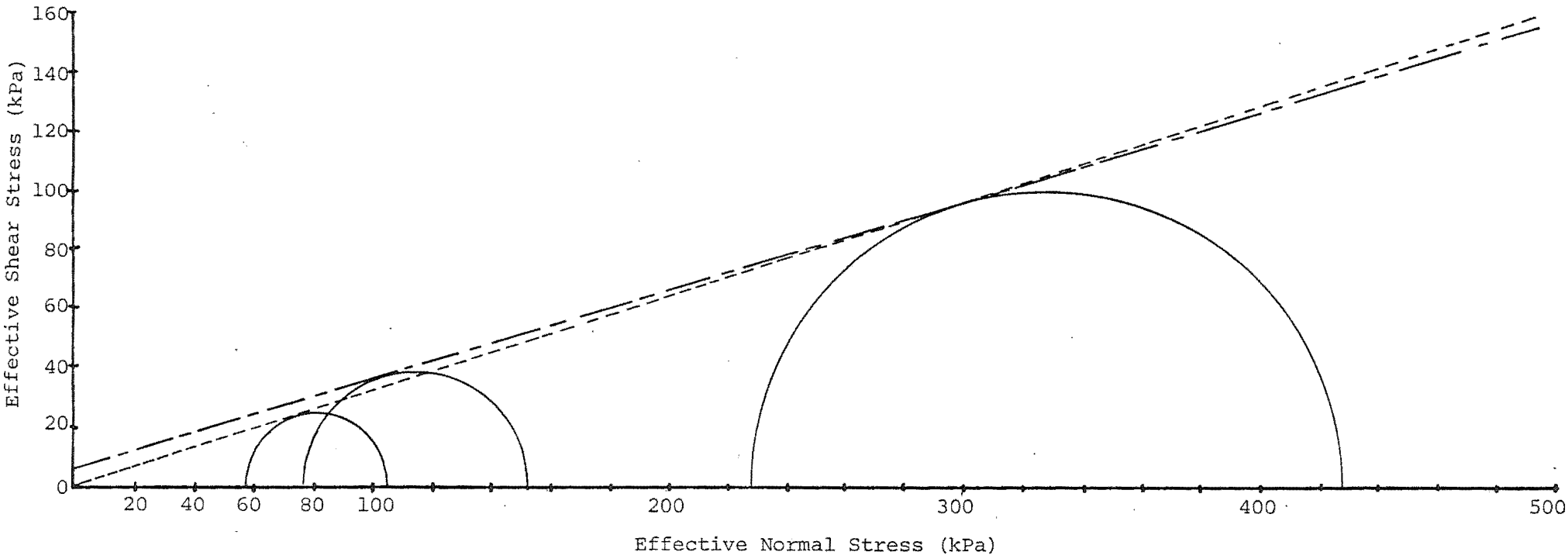

Fig.4.15: Graphical plot of triaxial data showing two most plausible interpretations representing effective strength parameters. (——-—— $\phi'=17^{o}, c'=8$ kPa) (-------- $\phi'=18^{o}, c'=0$)

4.4 CHARACTERIZATION OF THE WAIAREKA FORMATION

4.4.1 Introduction

Characterization of the Waiareka Formation is described in seven concise sections; consistency limits, grain-size analyses, density, clay mineralogy, weathering, regolith development, and strength.

No mass movement damaging housing and/or roading was identified within the formation hence description of the unit is based on limited geotechnical testing and is outlined purely for comparative purposes. No boreholes or profiles were necessary since regoliths are shallow (1 cm to 100 cm) and proved homogeneous lacking any horizon or textural development.

4.4.2 Consistency Limits

Testing of the Waiareka Formation was on ten remoulded, random samples collected from shallow pits without reference to depth or any regolith horizonal structure.

Atterberg Limits

Liquid Limits vary between 29% to 43% and the plastic limits from 17% to 20%.

Correlations between principal soil mechanics parameters and hygroscopic water content (H_W) followed fundamental patterns disclosed from testing of the Hampden Formation; the limited data base means relationships are only tentative.

Plasticity index and liquid limit both increased corresponding to increases in swelling clay content (H_W) and plastic limit appeared independent of H_W (Fig. 4.16).

Shrinkage Limits

Shrinkage limits varied widely from 6.5% to 13.9% showing an "apparent" correlation to H_W. The relationship is contradictory to that found within the Hampden mudstone and is speculatively ascribed to the insufficient data base.

Linear shrinkage appears controlled by swelling clay content.

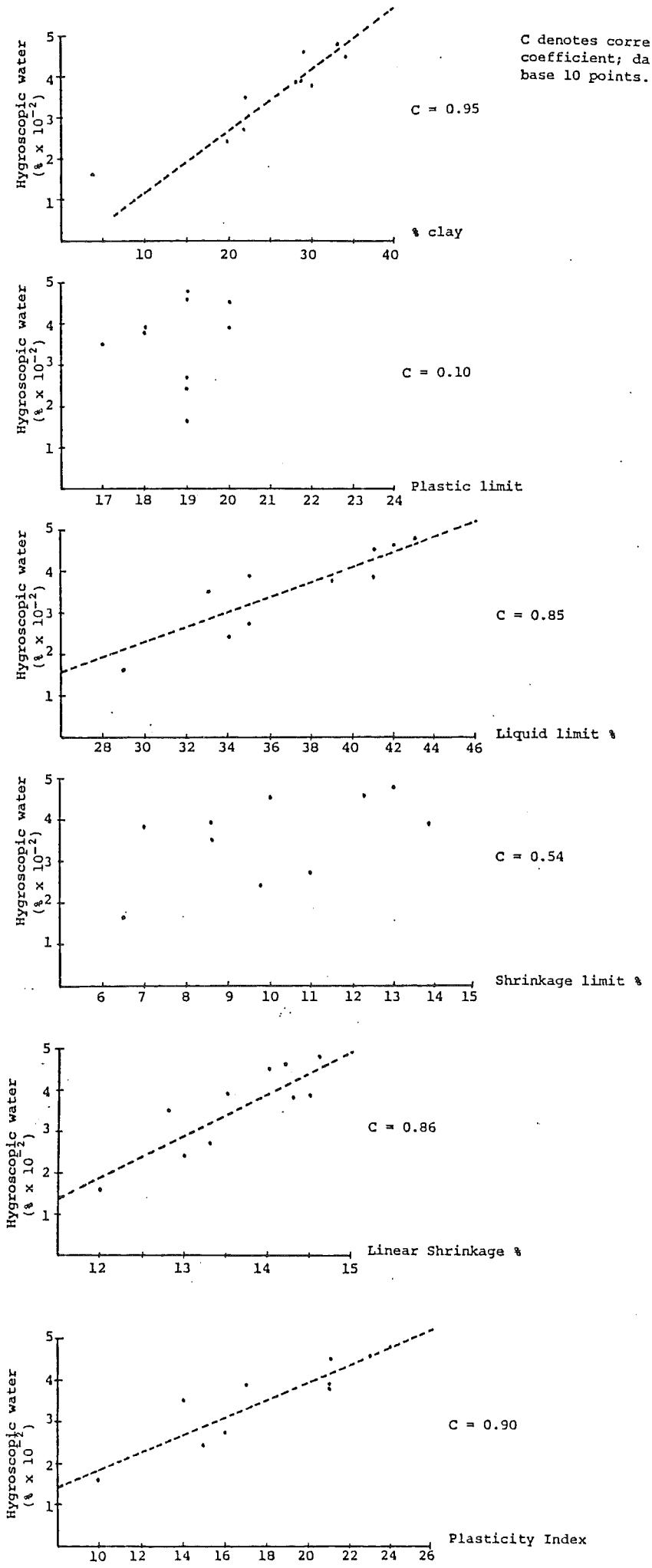

Fig.4.16: Regression correlations between hygroscopic water content and consistency parameters for Volcanic regoliths.

4.4.3 Grain-Size Analyses

Grain-size analyses done by pipette and sieve techniques showed volcanic regoliths were well graded with amounts of sand varying from 25% to 57%, silt from 25% to 53%, and clay from 14% to 35%. No one coarse size fraction appears to predominate, implying each is composed of equally unstable minerals, equivalent in susceptibility to weathering breakdown.

4.4.4 Density

Density of volcanic regoliths was determined using a Balloon Densometer with 30 gm balloon, 200 mm diameter x 50 mm rings . Bulk densities of 1.484 t/m^3 and 1.460 t/m^3 were determined, associated with moisture contents in the vicinity of 15%; low densities being indicative of a sandy open textured soil structure (methodology, NZS 4402, Part 2, 1981).

4.4.5 Mineralogy

Clay mineralogy was identified by X-ray diffraction (refer Appendix 5 for methodology). Four randomly collected sandy regolith samples overlying the Moeraki Intrusive Sheet were tested with the principal aim of providing an insight into the materials geotechnical behaviour.

The clay mineral assemblage identified is:
Vermiculite, Illite, Smectite and Halloysite.

As no quantitative analyses were attempted, relative changes within individual mineral groups reflecting selective weathering of specific unstable minerals are not highlighted. Based on visual comparison of diffractogram peak intensity and area, smectites appear in significantly larger quantities within the clay fraction than either vermiculite or illite, with halloysite a minor constituent.

4.4.6 Weathering

Lithologic diversity within the Waiareka Volcanics (bedded tuffs, breccias, dykes and sills) results in a variety of significant weathering processes. Volcanic composition is chiefly mafic, consequently the Formation contains unstable minerals which readily degrade, ultimately to clay predominantly via chemical reaction (hydrolysis, oxididation alteration and

recrystallization).

The coarser grained igneous intrusives (Moeraki Sheet) generally break down more rapidly than their finer grained equivalents (dykes) ie.intergranular surface area increases with a decrease in grain-size hence more energy is required to disintegrate finer material (Birkland, 1980). Degradation of minerals such as biotite to clays causes expansion that eventually shatters intact rock into aggregates of coarse fragments. This type of mechanical disintegration induced by chemical weathering has formed shallow gradational regoliths over the intrusive Moeraki Sheet exposed in the west. In comparison, finer grained dykes weather slowly forming weathering skins as chemical attack proceeds inward grain by grain.

Chemical Weathering

The transformation of primary minerals, such as feldspar, amphiboles and micas, found in unweathered rock, into silicate clays involves two processes; alteration and recrystallization.

Alteration

Alteration occurs when soluble constituents are removed or substituted in crystal lattices by percolating solutions (via oxidation, hydrolysis). Once formed, alteration of 2:1 clays from one variety to another is expedited by relatively weak interlayer bonding and their structural similarity.

Example:

Illite → montmorillonite (smectite) by replacement of K^+ with Mg^{2+} (oxidation).

Alteration of 2:1 clays to the 1:1 variety involves greater structural reorganization and is irreversible.

Recrystallization

Clay minerals may crystallize out within solutions containing certain ion concentrations, the type and genisis of mineral dependent on Si content, cation concentration and PH (Birkland, 1980).

Mineralogy will continue changing via these two processes until an assemblage in equilibrium with environmental conditions is reached (Fig. 4.17).

Oxidation

Iron oxidation produces the distinctive reddish colouring associated with weathered volcanics.

Jointing

Jointing, of secondary importance to weathering, is attributed to stress relief, freeze thaw action combined with slope movement and accelerates degradation by increasing the surface area exposed to chemical attack.

Regolith Development

Regoliths are characteristically reddish-brown in colour, sandy, shallow (generally <1.5 m) and relatively homogeneous with no distinct horizonal development. Bedrock-regolith interface is usually gradational, often becoming appreciably deeper along relict rock defects.

Development is a long-term process controlled predominantly by the rate of chemical weathering.

4.4.7 Strength

In-situ strength was not established for Waiareka Volcanic regoliths. Undrained strengths of remoulded overburden was determined by laboratory vaning ostensibly for comparison with remoulded mudstone (Fig. 4.14). Relatively low clay content yields low cohesion with the majority of strength attributed to high internal friction developed within the sand fraction.

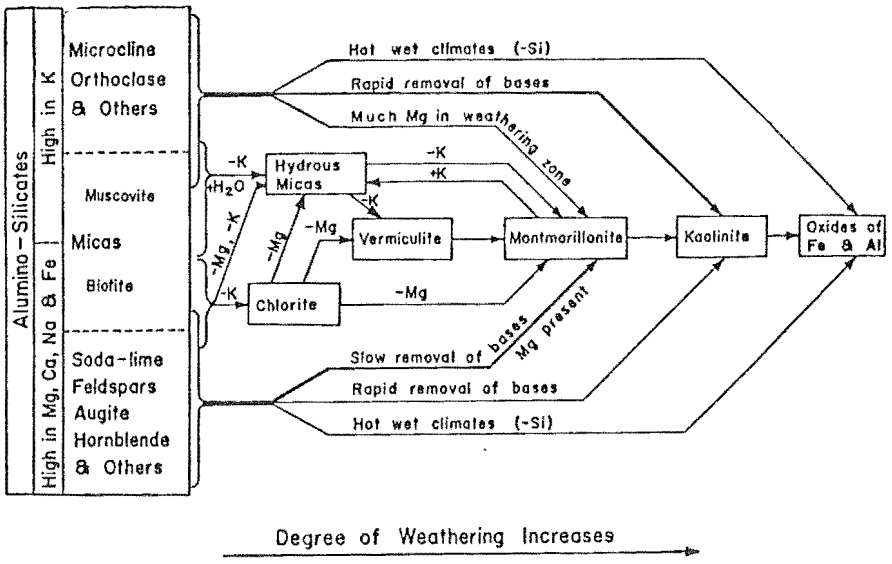

Fig.4.17: Schematic representation of general conditions for the formation of various silicate clays and oxides. In each case, genesis, is accompanied by removal of soluble elements such as K, Na, Ca, and Mg (Buckman and Brady, 1969, Fig.4.7).

4.5 SYNTHESIS OF LITHOLOGICAL CHARACTERIZATION

Geotechnical testing has established the Hampden mudstone as a silty-clay containing abundant smectites (11% sand, 42% silt, 47% clay). Compositional variation between unweathered and weathered mudstone is negligible with the degree of variance reflected by mean deviation in the plot PI versus clay percentage (Fig. 4.18). Regoliths are categorised "CH" according to the Unified Soil Classification System and described as "inorganic clays of high plasticity, fat clays" (refer to Fig. 4.19 for positioning on Casagrande plot, LL v PI).

Mudstone progressively "softens" to a cohesive, plastic material, the properties of which relate to the clay mineral fraction (Fig. 4.20). Smectite, vermiculite, illite and kaolinite comprise the clay component which has a "normal activity" as defined by Skempton (1953)(Fig. 4.21). Softening of mudstone is associated with water absorption causing increased strains plus elevated in-situ moisture content (30% to 40%), thus reducing strength and raising the mudstone susceptibility to slope failure (undrained softened strength about 1.5 t/m^2 to 4 t/m^2).

In contrast, regoliths developed from the Waiareka Formation are shallower and sandy (38% sand, 36% silt, 26% clay), the low clay content influencing geotechnical parameters (Fig. 4.20), in-situ moisture contents (about 15%) and strengths (sand causing high ϕ but low c).

Based on limited geotechnical data volcanic regolith composition appears homogeneous ie. little mean deviation in the plot PI v clay % (Fig. 4.18).

Utilizing the Unified Soil Classification System, volcanic regoliths are "CL" or "inorganic clays of low to medium plasticity"; Skempton categorises the clay fraction as "inactive" (Fig. 4.21). High permeability is not conducive to the development of excess pore pressures, consequently in spite of low cohesion, the regoliths are not susceptible to shallow slope failure.

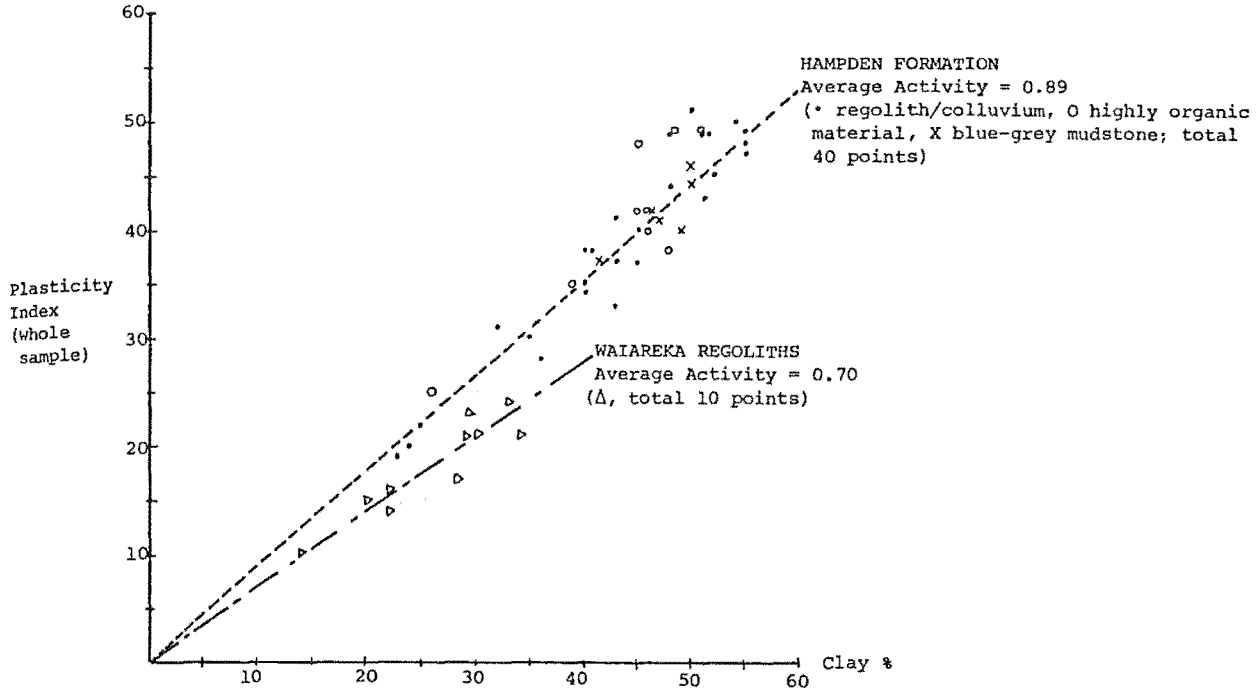

Fig.4.18: Activity plot for Hampden Formation and Waiareka regoliths; note small mean deviation indicative of homogeneous mineralogy.

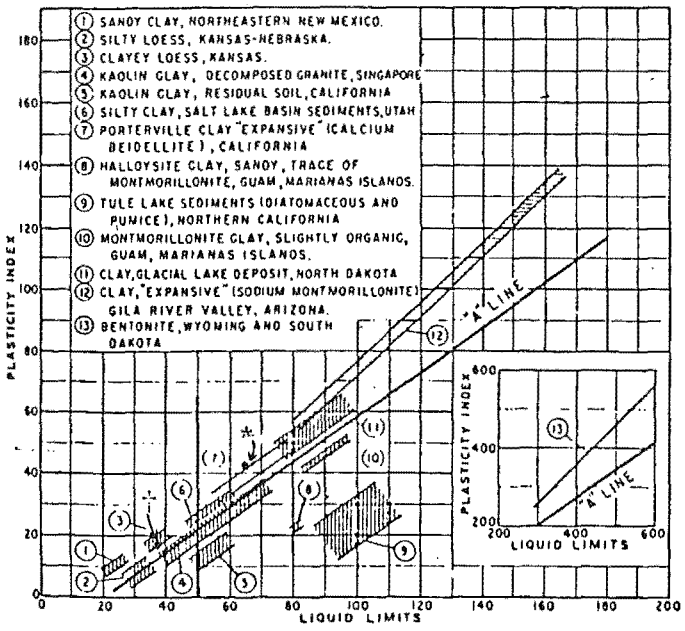

Fig.4.19: Casagrande plot showing relative positioning of Hampden Formation (*) and Volcanic regoliths (†) (USBR Manual 1974).

		No Tested	Sand %	Silt %	Clay %	Plastic Limit (PL%)	Liquid Limit (LL%)	Plasticity Index (PI)	Shrinkage Limit (SL%)	Linear Shrinkage (L_S%)	Activity PI/ % CLAY
HAMPDEN FORMATION	BLUE GREY MUDSTONE	6	10	43	47	24	67	42	7.8	26.2	0.89
	REGOLITH/ COLLUVIUM	25	7	50	43	26	64	38	8.9	23.6	0.88
	HIGHLY ORGANIC	9	7	49	44	36	76	40			0.91
		6							7.8	24.6	
WAIAREKA FORMATION	REGOLITH	10	38	36	26	19	37	18	10.1	13.6	0.69

Fig.4.20: Summary of grain-size and consistency parameters for the Hampden and Waiareka Formations.

CLASSIFICATION	ACTIVITY	GROUP	COMMENT
INACTIVE CLAYS	<0.5	1	Apart from Kayolin generally late-glacial or post glacial clays
	0.5→0.75	2	Clays derived from normal weathering
NORMAL CLAYS	0.75→1.25	3	Marine and esturine clays with predominance of illite
ACTIVE CLAYS	1.25→2.0	4	Contain appreciable organic colloids
	>2.0	5	Bentomitic clays

Fig.4.21: Classification of clay fraction according to Skempton (1953).

4.6 ACTIVE PROCESSES

4.6.1 Mass Movement

Active mass movement, generally via slow cohesive deformation, occurs amidst both mudstone formations exposed in the east of Moeraki township jeopardizing housing and roading in places (Fig. 4.22). Current slope failure is principally attributed to progressive "softening" of coherent mudstone resulting in:

1) A reduction in permeability.
2) A significant decrease in strength (increased strain lowering strength well below peak).
3) A rise in moisture content.

The softening process is accelerated by increasing ground water pressures (levels). Many mudstone slopes probably exist in a meta-stable state, capable of failure should their threshold ultimately be exceeded by prolonged heavy rain or localised concentrated drainage. This is reflected by the significant rise in shallow failure over the last fifty years following the removal of vegetation, growing housing density, and introduction of a water scheme.

Current active mass movement is classified into three main groups.

Debris Flow Slides

Debris flow slides comprise the bulk of active slope displacement occurring within the field area; they are often manifested as composite failure complexes affecting areas in the vicinity of 500 square metres. Instability commonly evolves as shallow (3 m to 4 m) lobe-shaped debris slides which upon downslope movement via plastic deformation, partially degrade and exhibit some flow behaviour. Slope failure is usually preceded by tension cracking, concentric in plan and concave toward the direction of movement. Salient slide morphology comprises a rafted block plus graben which reduces to hummocked topography of low relief accompanying flow movement within the slide mass.

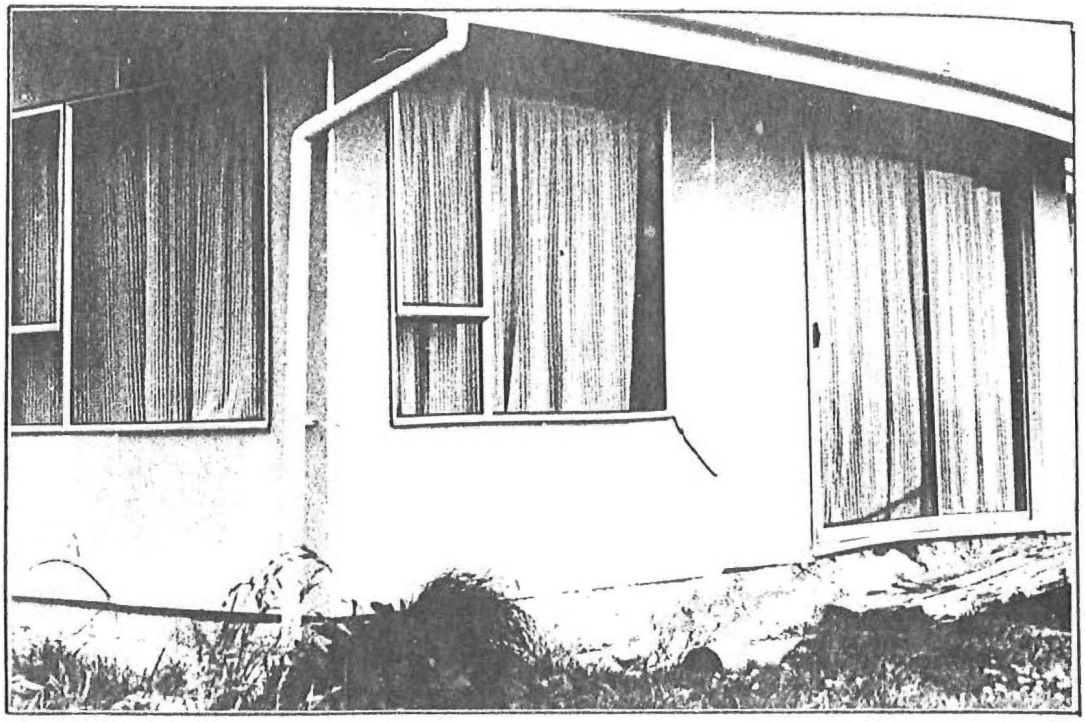

Fig.4.22(a): August 1981

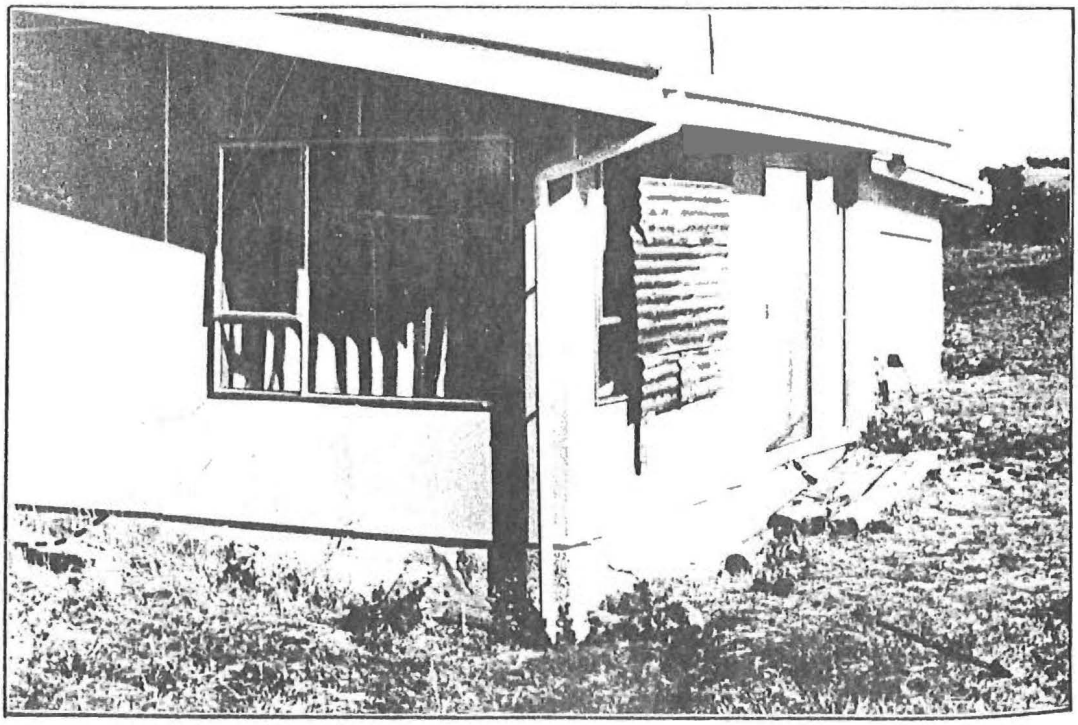

Fig.4.22(b): August 1982

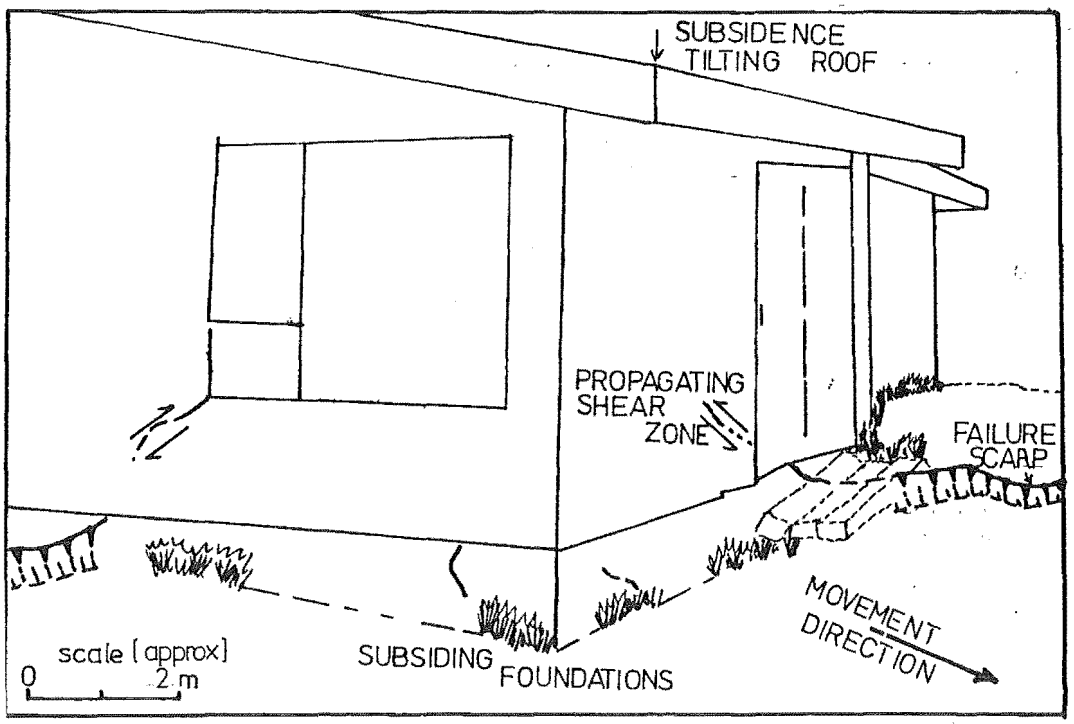

Fig.4.22(c): Incipient slope failure amidst Hampden mudstone damaging housing. Note broken window and buckled sliding door; continuing deformation will culminate in abrupt slope failure probably triggered by excessively heavy rainfall. (7800E,0450N)

Mudstone profiles consist of disaggragated coherent "blocks", and thus are susceptible to shallow rotational, rather than translational, movement. Failure within low angled slopes results in greater horizontal movement for each unit of vertical offset in the centre portion of the slide than in the head region. Hence despite curved failure surfaces, movement is predominantly translational (Fig. 4.23). In contrast, failure of higher angled slopes is associated with more rotational displacement creating back tilted zones adjacent to principal escarpments.

Apart from raised ground water levels, wind blown, mature trees appear to weaken mudstone colluvium/regolith and facilitate shallow slides (Fig. 4.24).

Creep

Significant "en-masse" creep movement, potentially hazardous to housing and/or roading, occurs over the majority of mudstone slopes subject to periods of saturation. Movement produces a dynamic hummocked terrain of low relief associated with desiccation cracking and frequently responsible for tilting of surface structures (Fig. 4.25).

Toppling

Toppling failure is confined to steep, unvegetated coastal mudstone faces. Failure is sudden, preceded by deep tension cracking and produces a talus apron of colluvial debris as the cliff face retrogresses.

4.6.2 Hydrology

Hydrology within the study area is complicated by variable topography and the effects of "superimposed" slope failure.

Moeraki township can be divided into two broad hydrological regimes, based on lithology:

1) An area to the east, comprising the Hampden and Kurinui Formations which is poorly drained, with numerous spring fed ponds.

2) An area to the west based on the Waiareka Formation, well drained and with no permanent ponding.

Fig.4.23(a): Typical mudstone regolith profile comprising disaggregated coherent "blocks". Profiles usually lack continuous zones of significant weakness hence basal shear surfaces often propagate along a rotational arc; note oxidised yellow-brown relict joints (7550E,0300N).

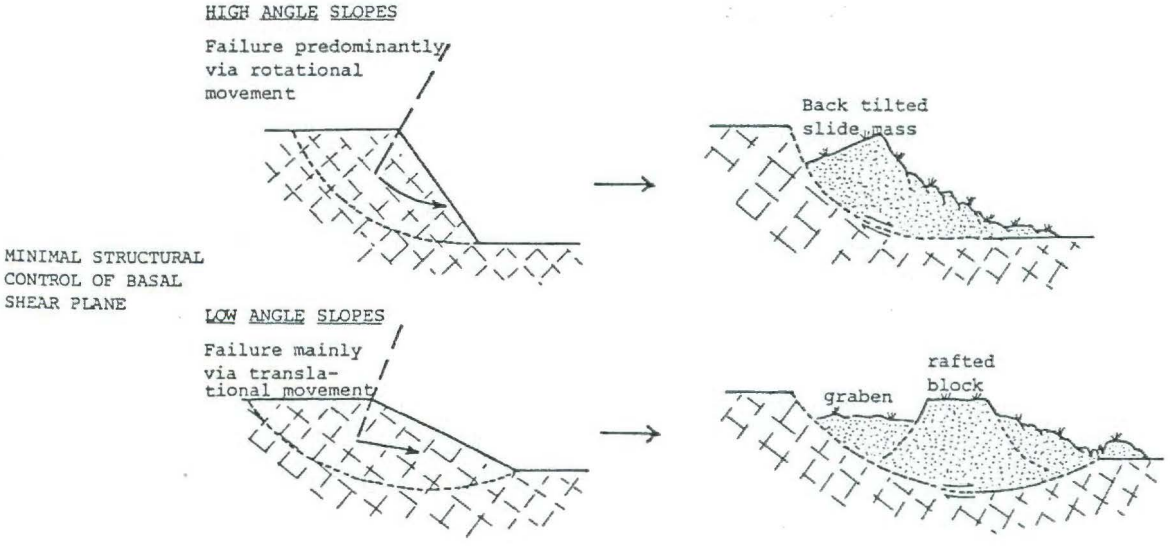

Fig.4.23(b): Characteristic morphology associated with failure of high and low angle mudstone slopes in the field area.

Fig.4.24: Wind blown trees accentuating development of a shallow debris slide. Looking north from 7000E,0350N.

0 4 m

Scale

Fig.4.25: Severe housing foundation damage attributed to mass "creep" deformation. (7050E,0250N).

0 2 m

Scale

Ground water flow is recharged by rainfall via "overland flow" and "through flow", the mechanisms of which are reviewed and compared for both regimes (Fig.4.26).

Overland flow refers to flow physically over a hillslope and occurs either when material is saturated or its infiltration rate is exceeded.

Permeability of weathered mudstone, exposed in the east, is increased by non-systematic jointing. Upon heavy rainfall, swelling clays absorb water closing fissures, thus creating a comparatively impervious surface which promotes overland flow.

In contrast, volcanic regoliths disclosed to the west are sandy, contain little clay and are permeable so overland flow is rare, only occurring during intense rainfall exceeding regolith infiltration rates.

Through flow refers to water diverted laterally within a material and can occur amidst any permeable zone or above any impermeable interface; it is normally unsaturated flow except near a flowing stream and at the base of each permeable horizon (Carson and Kirkby, 1972).

Mudstone profiles contain horizons of varying permeability producing complex through flow patterns. Softened, impermeable layers if relatively continuous, may result in perched water tables or confine more previous zones, leading to the development of excess pore pressures. Horizons high in organic content (paleosols, swamps) are generally more permeable than ubiquitous regolith/colluvium and can act as aquifers within the profile. Through flow decreases with depth as jointing becomes less frequent and overburden pressures increase.

Waiareka Formation regoliths are comparatively homogeneous with through flow unimpeded and expedited by their sandy texture. Flow amidst unweathered intrusive volcanic material is concentrated along jointing and thus decreases with depth.

Through flow in both hydrological regimes is complicated by dykes which channel ground water (via jointing) and/or

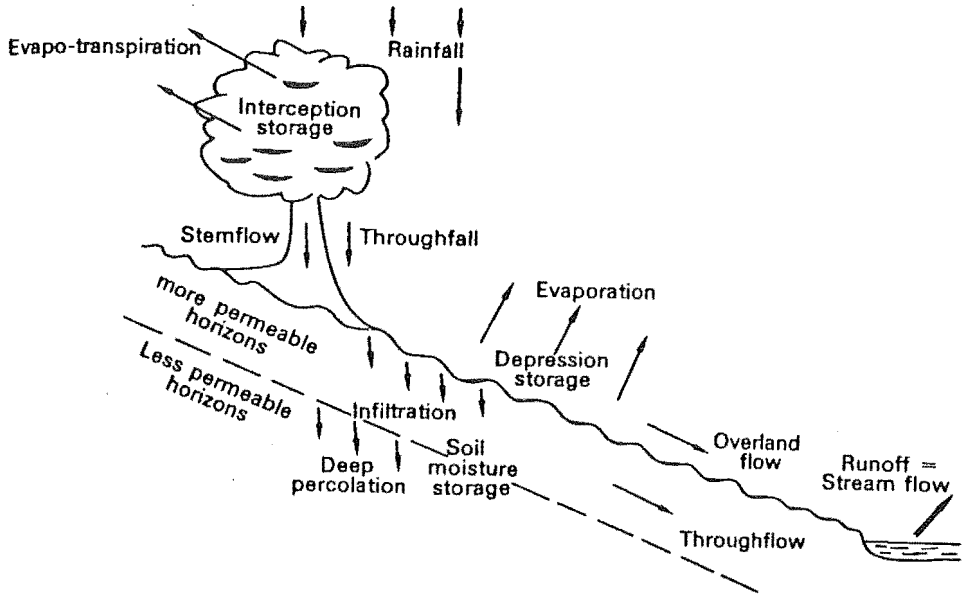

Fig. 4.26: Schematic components in near-surface hydrologic balance (from Carson and Kirky, 1972, Fig.3.11)

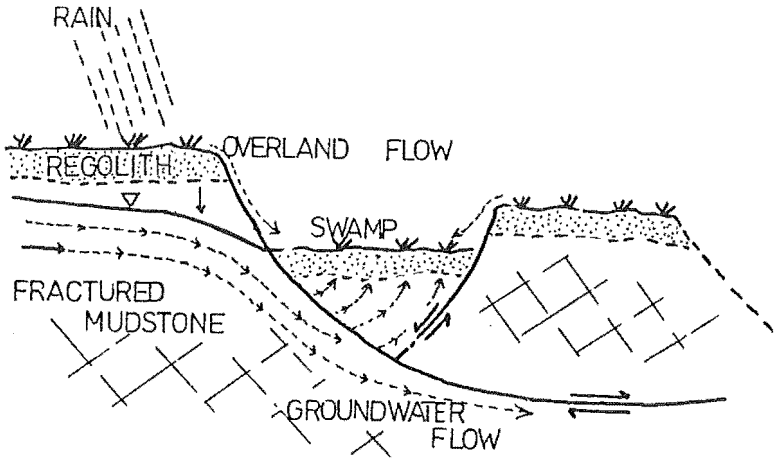

Fig. 4.27: Hypothetical schematic graben structure and inferred groundwater flow patterns which facilitate swamp development.

provide impermeable barriers concentrating flow around their margins.

Ponding within the mudstone formations is predominantly attributed to overland flow draining higher relief, concentrating within depressions. The two areas of significant ponding in the field area, are both in the Davids Road region and developed in graben structures formed by slope failure. These downfaulted "blocks" form ideal surface runoff catchments and alter ground water patterns, facilitating ponding (Fig. 4.27).

4.6.3 Coastal Erosion

Wave action together with fluctuating water levels are resulting in active coastal erosion along the northern coastline of Moeraki Peninsula. Wave induced erosion is dynamic, changing with time and dependent on:

- wave climate (wind velocity, duration and direction)
- nearshore and offshore bathymetry
- shore orientation
- water level

and lithology of coastline.

Outcropping igneous rocks form resistant headlands, restricting longshore current and erosion is principally from buffeting wave action. Alternating water levels have an indirect effect by accelerating mudstone slaking, thus the onset of localised slope failure.

Waves entering the nearshore zone will be slowed, shortened and steepened, as they move into shallow water (process known as shoaling). Waves arriving at an angle are bent or refracted towards alignment with the underwater contours. Quantitative procedures using these parameters can be used to evaluate wave energy plus erosion rate, however they involve extensive field calibration and only give a probabalistic result hence were not attempted.

Coastline comparisons made from vertical aerial photography reveal minimal coastal retreat between 1947 and 1978.

Benson (1946b) describes severe coastal erosion to the west of Tawitiatauka Point between 1860 and 1945 (Millers Bay). He notes, although in a very sheltered spot, wave action has cut back low mudstone cliffs at the rate of a few feet per year so the 1945 coastline is not only a hundred yards inland of its position in 1860 but is nearly fifty yards inland of the railway embankments former position, built in 1876.

However, comparison of the 1863 survey plan with a 1982 precisely scaled vertical aerial photograph indicates no net regression over the last 120 years, inferring the coastline has equilibrated with tide and wave action (Tonkin and Taylor, 1982).

Low mudstone coastal batters are "actively" degraded via composite debris flow-slide features induced by inadequate drainage plus wave buffeting. Higher mudstone cliffs erode predominantly by "toppling" failure and accumulate extensive aprons of talus debris (Fig. 4.28).

Slope colluvium is perpetually removed by offshore currents to maintain the constant coastline profile; rudimentary remedial construction attempting to alter "equilibrium profile" has invariably failed (Fig.4.29).

Fig.4.28: Retrogression of steep Kurinui mudstone cliffs principally via "toppling" failure amassing talus colluvium. Looking east from 6950E,0400N.

Fig.4.29: Remedial sea-walls have proven ineffectual in preventing retrogression of the peninsula's northern coastline to "equilibrium profile". Viewing west from 7700E,0500N.

CHAPTER FIVE

STABILITY INVESTIGATIONS

5.1 INTRODUCTION

Comprehensive investigations on slope instability were carried out in two areas where active failure is causing extensive damage to roading and jeopardizing housing; regions chosen for study were the Motor Camp and Davids Road areas.

Detailed research on shallow slope failure for both districts is described under sections on piezometric monitoring, surveying plus stability assessment, with collated data used as a basis to suggest remedial options which will minimise hazardous slope deformation. Consideration of this chapter should be made in conjunction with cross-sections and survey plans within the map enclosure.

5.2 MOTOR CAMP AREA

5.2.1 Introduction

The Motor Camp Area is located within the Eastern Slide Complex and refers to that zone formed by a deep-seated stabilized translational slide (Motor Camp Slide, Fig. 3.10). The region extends from the Peninsula's northern coastline 280 m southward encompassing an area of approximately 4.3×10^4 square metres. Bedrock geology comprises homogeneous Hampden mudstone exposed along the shore platform in the north and within major escarpments to the south. There is no evidence of faulting or folding in the vicinity which could influence slope instability.

Two fundamental morphological regimes are recognized:

1) A principal escarpment; delineating the region of concern.

2) A stabilized slide mass; forming the bulk of the Motor Camp Area. (Fig.5.1)

Principal Escarpment

A semi-circular escarpment, partially degraded and varying in height (5 m to 20 m) encloses the Motor Camp area. The escarpment, developed within incompetent mudstones, has a steep, salient, southern section eroded by debris flow-slides accumulating talus aprons of colluvium with the most active of these slides retrogressing and encroaching onto the local school domain. The principal scarp's eastern lateral margin has a low subdued relief (<10 m) and is cloaked in dense vegetation cover (conifers). Morphology of the western escarpment section is extensively altered to facilitate Motor Camp accommodation however the original trend can still be discerned. (Fig.5.2)

Localised temporary surface runoff ponding occurs in deflated areas but does not significantly affect instability.

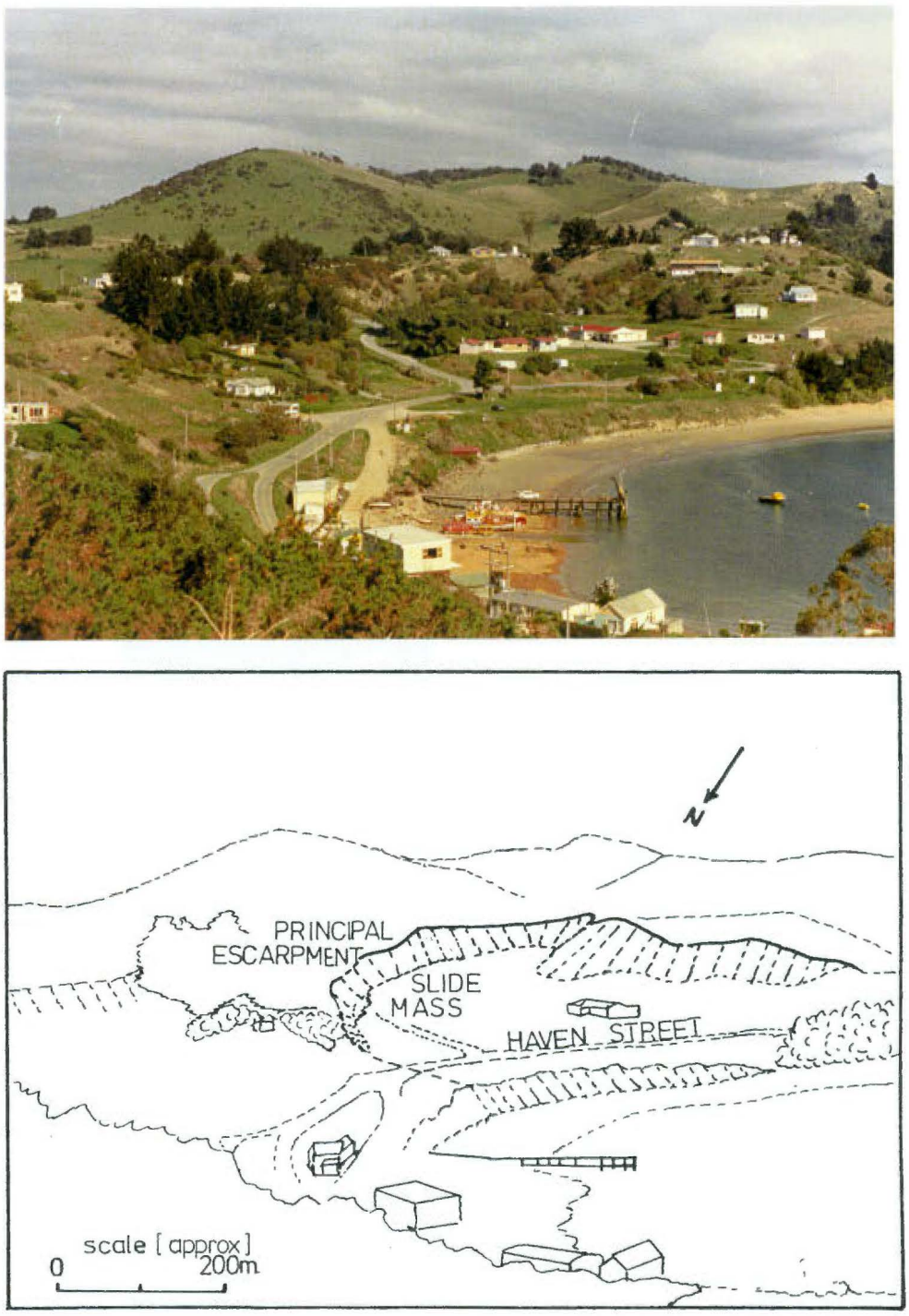

Fig. 5.1: Oblique view of the Motor Camp area principal escarpment and slide mass. Looking south from 7800E,0600N.

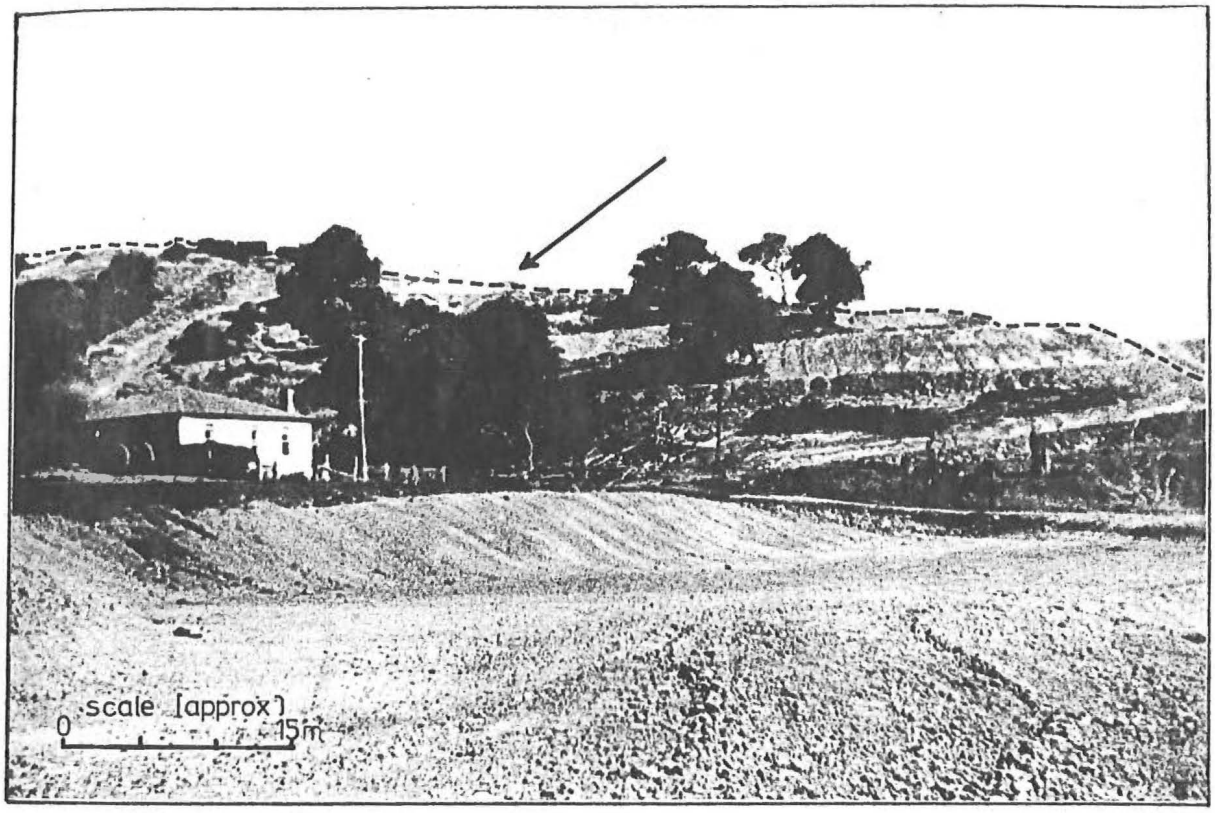

Fig. 5.2 : Extensive regrading of the Motor Camp Slide's western lateral escarpment to form "benches" enabling the construction of additional cottages. Note original trend of the principal scarp is easily discerned (dashed line). Looking west from 7600E,0400N.

Photograph: Mr P. Kedsley (dated about 1940's)

Slide Mass

The slide mass encompassed within the principal escarpment ostensibly consists of a triangular area with gentle relief (<5 m) gradually sloping down to the peninsula's northern coastline. Natural topography has been considerably modified by re-levelling to create a series of benches in the central region enabling construction of Motor Camp cottages (Fig. 5.1).

Haven Street runs parallel to and 40 m inland of the northern coastline; in plan, dividing the area into two unequal sections. The street actively subsides along well defined shear boundaries creating a traffic hazard and requires annual repairs (Fig. 5.3, 5.4).

Drainage of excess water from all Motor Camp housing is concentrated behind Haven Street in the lower mid-section of the slide mass. Water is channelled into a slotted P.V.C. culvert which allows dissipation of drainage into roading substrate (Fig. 5.5). During summer months when Motor Camp accommodation is full, massive quantities of water are concentrated in this zone causing frequent ponding adjacent to the downhill slide of Haven Street.

Geomorphology

Detailed investigations described in this chapter pertain to shallow slope instability affecting roading and/or housing, hence only surficial geomorphology relating to this contingency is discussed in this section (ie. for information on the deep-seated Moeraki Slide refer to Chapter Three).

Four shallow boreholes (<7 m) forming a line, in plan view, down the centre of the slide mass were augered into Hampden mudstone to obtain subsurface data (refer to map enclosure, engineering geology maps for borehole locations). Slide mass, overburden mantle, has a confused stratigraphy comprised of regolith plus colluvium horizons varying in weathering intensity and organic content.

Subsurface data for individual auger holes is outlined in Appendix 7 and presented with geomorphological interpretation

Fig.5.3: Haven Street, depicting significant and well defined (dashed) subsidence which poses a traffic hazard and requires annual repairs. Looking east from 7500E,0450N.

Fig.5.4: Prominent shear zone propagating across Haven Street. Viewing south from 7550E,0450N.

Scale

0 2 m

Fig.5.5(a): Culvert (PVC) amidst chaotic gravel-clay roading substrate; note previous subsided road levels. Viewing north from 7550E,0450N.

Fig.5.5(b): Portraying the extent of gravel "drain" channelling Motor Camp effluent into Haven Street culvert. Looking east from 7500E,0450N.

on a surveyed profile of the Motor Camp area, scale 1:100 (refer map enclosure).

A sharp basal boundary between oxidised yellow-brown regolith/colluvium and blue-grey mudstone can be traced from the coast uphill (dip 5^{o}) 200 m to the south (via boreholes 2, 3 and P_1), and is assumed to depict a relict ground water table (refer Chapter Four, section 4.3.6). Information from auger hole 1, neighbouring the southern escarpment, showed no sign of the inferred projected boundary, but instead comprised a sequence of colluvial/organic horizons. The anomalous absence of this continuing bedrock-overburden margin is ascribed to a graben structure associated with the Motor Camp Slide. Based on stereoscopic analyses (1947 aerial survey) an extensive slope failure eroded the Motor Camp Slide's principal escarpment in the southwest and colluvial debris associated with this failure produced a hummocked topography over the southern region of the Motor Camp Slide mass. Utilizing this information to interpret auger hole profiles (1, 3 and P_1) it seems the cryptic succession of organic horizons represent paleosols delineating the extent of failed debris (refer map enclosure, surveyed Motor Camp Area cross-section). Unfortunately no carbon dating which may have determined absolute ages of shallow mass movement was possible.

Comparison of aerial surveys (1947, 1978) confirms that active slope degradation has intensified over the last thirty years, remaining unchecked in some parts by ineffectual remedial measures.

5.2.2 Ground Water Monitoring

Introduction

Piezometers are devices which measure changes in pore pressures at specific horizons within the profile and were utilized in the Motor Camp Area to monitor ground water. They vary in sophistication, but esentially are sealed tubes of small diameter, extending from ground surface to pertinent horizons, in which the water level or pressure can be observed.

Principal aims of piezometric monitoring in the Motor Camp Area were:

1) To establish seasonal ground water fluctuations within the mudstone regolith.

2) To determine if artesian pore pressures exist within paleosol horizons.

To achieve this a simple open ended design was adopted, since

1) Permeability of the material in which they are installed was estimated as sufficient for an adequate response time using this type of device.

2) The design was inexpensive and easy to construct.

Two piezometers, constructed of P.V.C. conduit (12 mm) were installed at relevant horizons down a borehole located in the centre of the Motor Camp Area. To ensure measurement of pore pressure at the required level each piezometer was sealed by bentonite and/or cement aggregate mix (refer Appendix 8 for construction details). Positive pressures were recorded by measuring maximum piezometric head (water level) using a well depth indicator; a probe was lowered down each conduit tube which upon immersion in water completed a circuit causing deflection of an amp meter. Piezometric head was then calculated from the distance the probe was lowered immediately prior to deflection.

Two horizons were monitored:

1) A narrow zone corresponding to a saturated paleosol (depth 2 m to 2.5 m).

2) A wide zone of regolith (depth 4 m to 6.5 m) on top of relatively unweathered mudstone (Fig. 5.6).

Results

Both horizons monitored were equivalent in all 20 piezometric head readings taken. The highest water level was recorded during August 1981 at 31 cm below ground surface, the lowest in September 1982 at 60 cm below the surface (refer to Appendix 8)

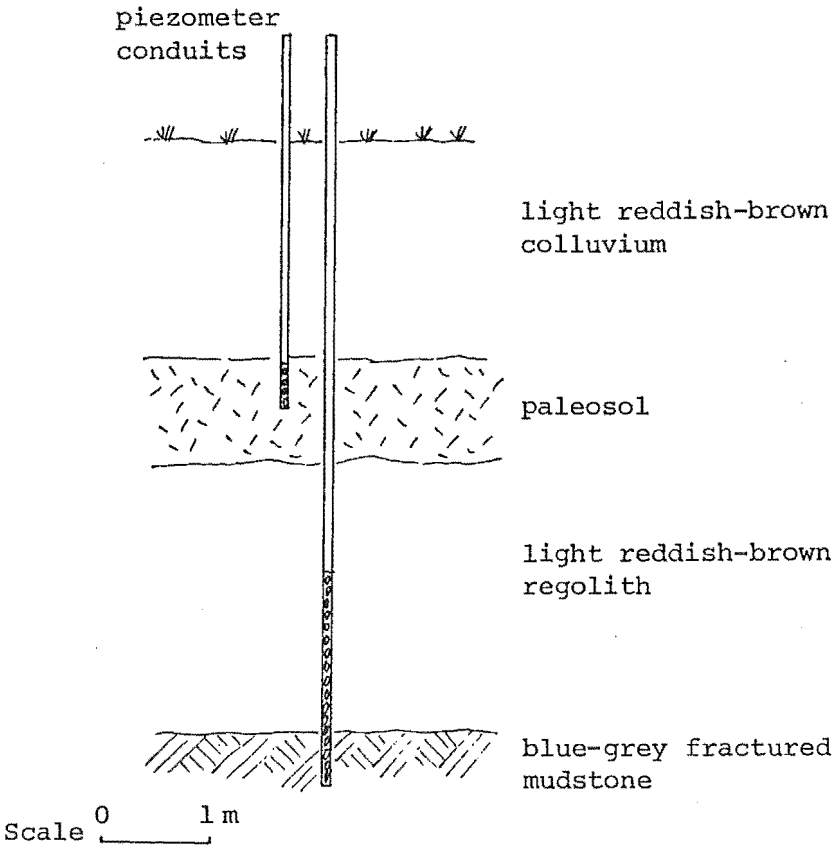

Fig. 5.6: Schematic representation of regolith/colluvium horizons monitored in the Motor Camp area. Refer to appendix 7 for comprehensive borehole log (P_1). Location 7500E,0400N.

Conclusions

The monitoring period from August 1981 to August 1982 was sufficient but the number of recordings provided an inadequate data base to establish seasonal ground water fluctuations. The three months of relatively continuous records (August, October 1981 and September 1982) were correlated with daily rainfall and two tentative conclusions drawn:

1) No artesian pressure appears to exist within the paleosol horizon.

2) A time lag of six to seven days exists between heavy rainfall and observable increased ground water pressures; speculatively attributed to the response time for the monitoring device. Transient excess pore pressures may have significantly changed during this period hence the magnitudes recorded should not be used in effective stress stability analyses.

5.2.3 Surveying

Introduction

A survey network was established over the Motor Camp Area with principal aims of:

1) Ascertaining activity of the deep-seated translational slide on which the Motor Camp is based.

2) Delineating relatively active regions within the area plus their rates of movement.

3) Providing further insight into the mechanisms and modes of instability affecting the area.

The system, comprising 21 points in total, is "tied" into the regional network (Geodetic Datum 1949) to establish if points assumed "stable" beyond the salient boundaries of shallow instability are in actuality moving via deep-seated deformation.

The Motor Camp network consists of four "control" points outside the limits of active slope failure with four "base" points, in plan, down the slide mass central region and lines

of subsidiary "monitoring" points across the coastal district plus southern escarpment (refer map enclosure, plan of Motor Camp Area survey network).

Bench marks are in public areas hence concealed below ground level to avoid disturbance. Control points were constructed of galvanised pipe in 1.8 m lengths and surrounded by concrete to a minimum depth of 2.0 m (designed to avoid seasonal creep movement). Base points consist of metal pipes set within a bowl of concrete to a depth of not less than 80 cm. Subsidiary monitoring points comprise short lengths of galvanised conduit hammered below ground surface and consealed with turf mats (Fig. 5.7, 5.8).

Nine surveys were completed over a period of one year from August 1981 to August 1982. Initial and final measurements were taken with the assistance of Mr A. Greig and J. Hermann using a Wild T_2 theodolite plus Wild DI3 distomat, the intervening surveys using a Wild T_6 theodolite in conjunction with DI3 distomat. Measurements of horizontal survey point displacement involved alignment of theodolite in combination with distomat over each of the four "base" points A, B, C, and D, then distances plus appropriate angles (three full sets; left and right face) were observed to "control" and pertinent "monitoring" points (refer Appendix 9 for detailed methodology). Based on equipment used a maximum survey uncertainty of ±1 cm is assumed.

Results

Total measured movement for all base and monitoring points is drawn in vector form on the Motor Camp survey plan (refer map enclosure).

Results highlight two relatively active zones:

1) A debris flow slide eroding the southern escarpment containing monitoring point A_2, exhibiting movement in the order of 24 cm per year (denoted the School Slip).

2) A coastal domain slide to the north of and including Haven Street, incorporating points D, D_1, D_2 and C_2

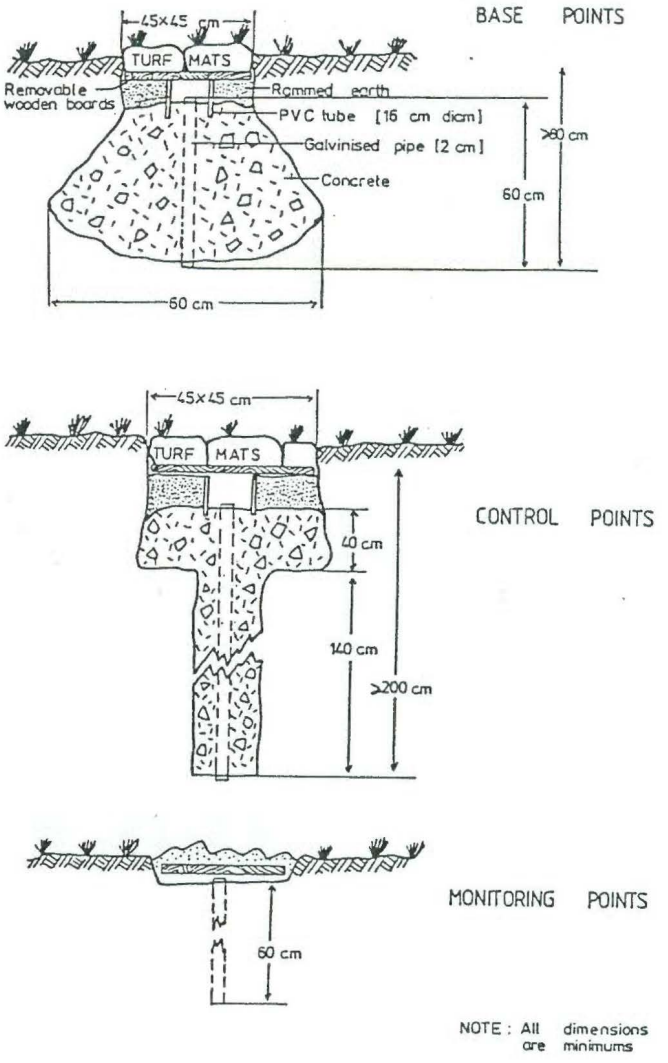

Fig.5.7: Construction details for benchmarks utilized in survey network.

Fig.5.8: Concealed "base" point C, Motor Camp area survey network. (7550E,0400N)

Scale
0 10 cm

exhibiting movement rates in the order of 5 cm to 15 cm per year.

No "control" point displacement was observed and the central region embracing points A, B, B_1 and C appears comparatively stable with total surveyed movement in the order of 2 cm to 4 cm per year.

Conclusions

Trends of measured survey displacement with respect to rainfall are inferred for the three areas. Movement of the relatively "stable" central region shows a marked increase during February and March (1982) following a period of inactivity (December 1981, January 1982)(Fig.5.9). Displacement is ascribed to surficial "creep", the acceleration of which is probably in response to raised ground water levels furnished by heavy rainfall over the preceding two months (December 1981, January 1982). During summer, evaporation is significantly higher and thus prolonged rainfall is necessary to raise ground water levels. In contrast, throughout the winter months (June, July, August), evaporation is low with less precipitation needed to increase subsurface water tables and so trigger movement. This may account for displacements during months of low rainfall from August to November 1981, inclusive.

The comparatively active School Slip exhibits the same general trends and displacement is probably via "drained" failure in reaction to ground water table fluctuation (Fig. 5.10). Accelerated movements during April to August 1982 are most likely the result of drainage from the local school's septic tank pouring effluent into the failure's principal escarpment.

Instability of the domain region is analogous to base points A, B, and C except during December 1981 and January 1982 when displacement rates increase (Fig. 5.11). Accelerated movement is not preceded by months of heavy rainfall and for this reason chiefly attributed to inefficient drainage from Motor Camp accommodation via the centrally located Haven Street culvert.

CENTRAL REGION, MOTOR CAMP AREA

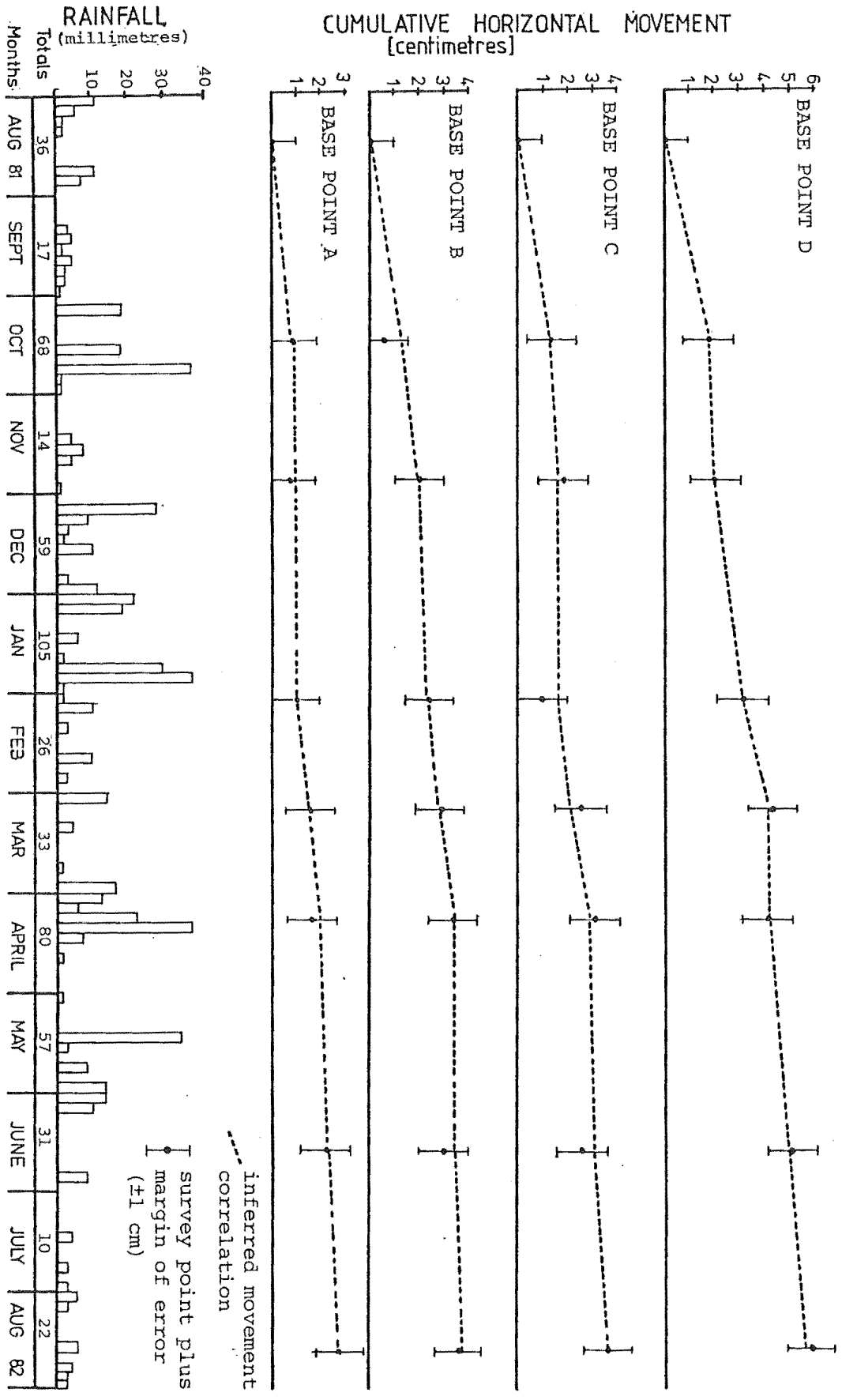

Fig.5.9 : Central Region survey data correlated with rainfall measurements taken by Mr and Mrs Kedsley.

SCHOOL SLIP, MOTOR CAMP AREA

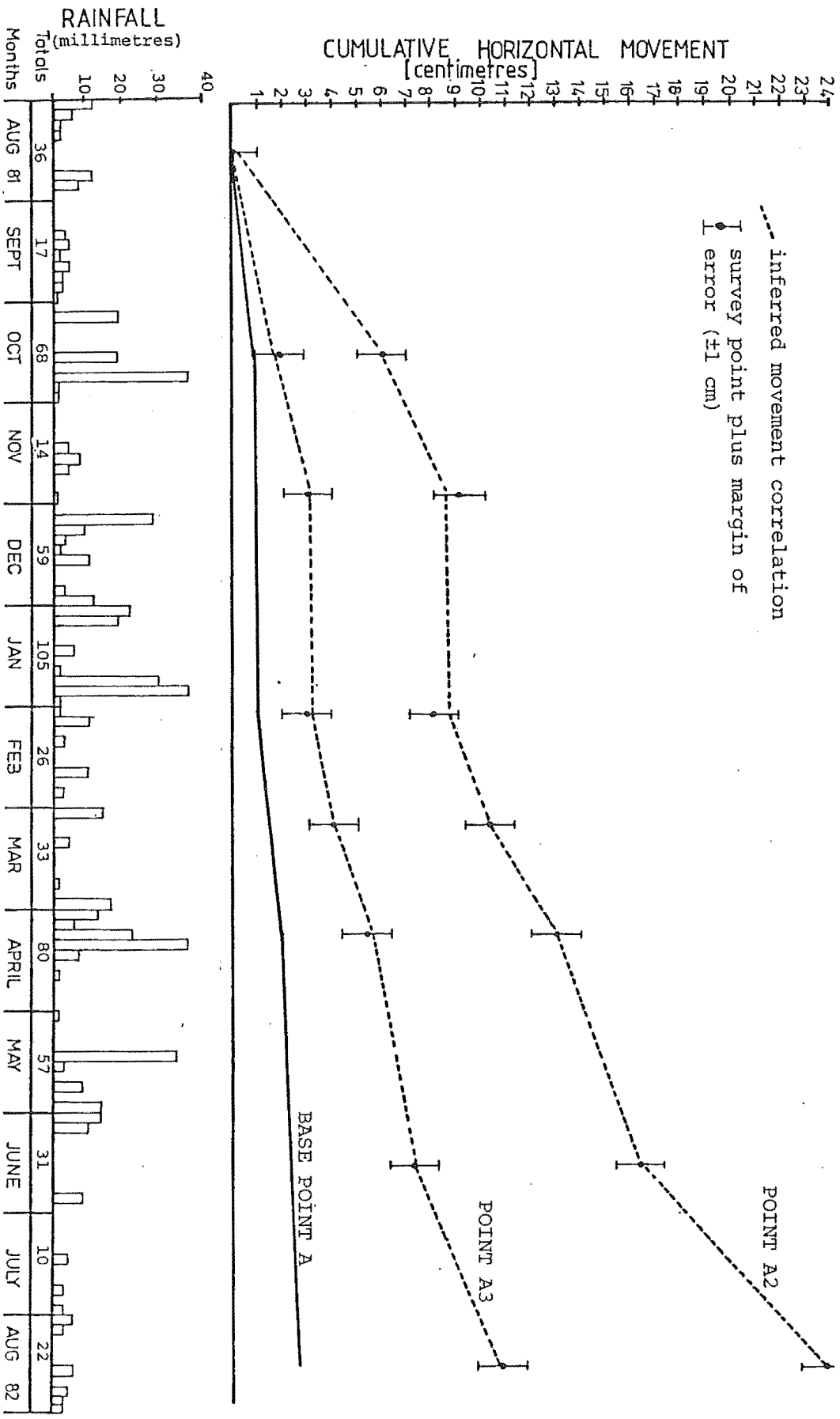

Fig.5.10: School Slip survey data correlated with rainfall measurements taken by Mr and Mrs Kedsley.

DOMAIN REGION, MOTOR CAMP AREA

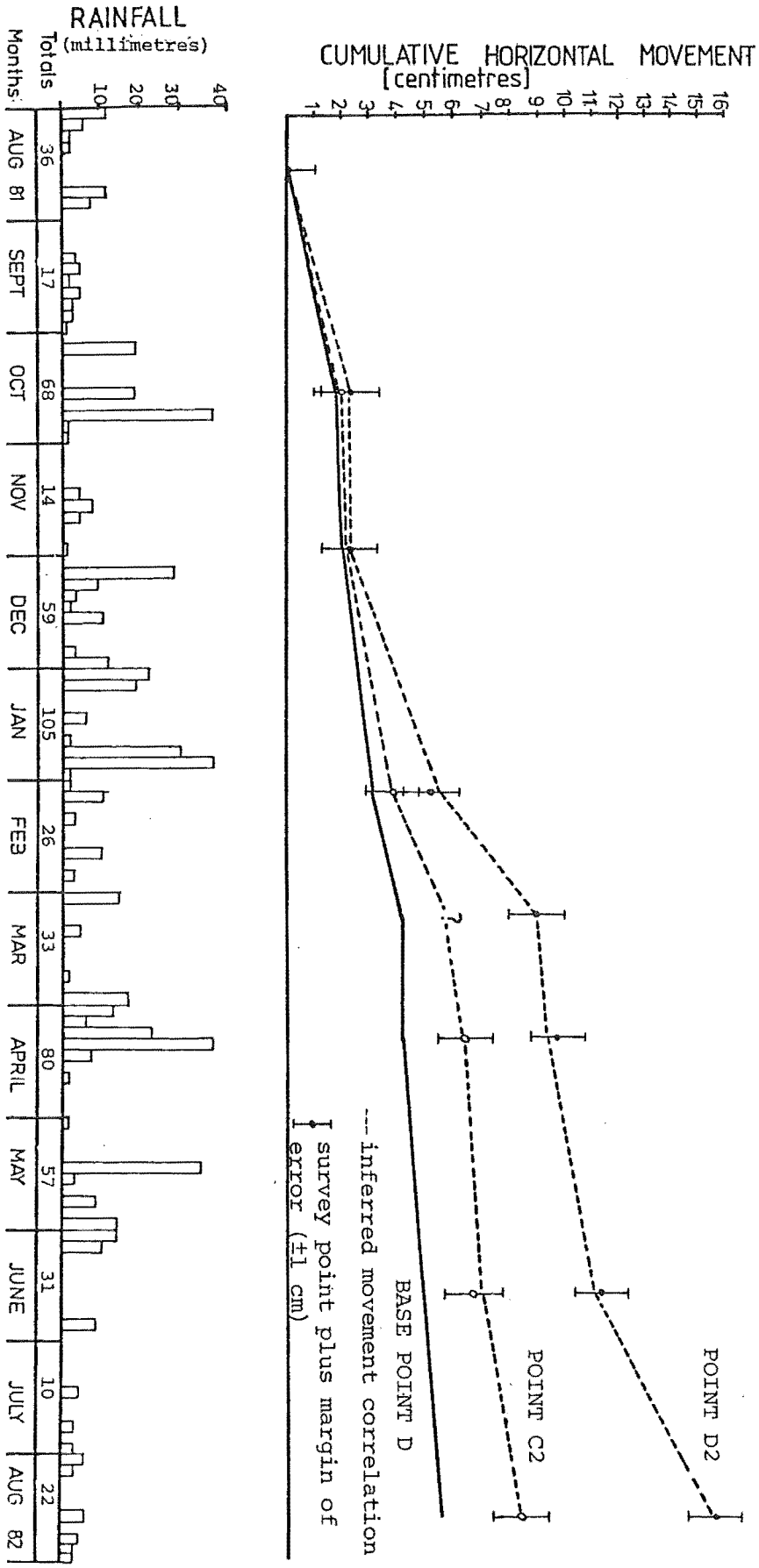

Fig.5.11: Domain Region survey data correlated with rainfall measurements taken by Mr and Mrs Kedsley.

In summary, high ground water levels accelerate slope movement in the area. There are two distinct "active" zones of displacement within the region, each apparently controlled by separate phenomena and unrelated to deep-seated failure. The Moeraki Slide mass is tenatively considered stabilized but exhibits seasonal creep movement.

5.2.4 Stability Assessment

Introduction

Slope stability and the relative effects of various remedial measures are assessed using numerical analyses. The degree of safety against ultimate failure is usually expressed in terms of a Factor of Safety.

$$F = Tf/\tau$$

where F = Factor of Safety, Tf = shear strength along some shear surface, τ = equilibrium shear stress along the same shear surface.

In general, the purpose of analysis is to obtain the minimum value for F, for a given set of parameters. Some important tacit assumptions made prior to analysis are:

1) The concept of "limiting equilibrium" is invoked. At the moment of incipient failure every point along the rupture (shear) surface, whether circular or noncircular, simultaneously attains the maximum (inputed) strength. This is equivalent to assuming that the stress-strain curve of the material acts as a "rigid plastic" and the actual stress-strain relationship does not enter into the method of analysis (Lo, 1972).
   A state of limiting equilibrium exists when
   $$\tau = Tf/F \quad \text{or} \quad F = 1.$$

2) The undrained or drained strengths used in analysis are "isotropic", ie. independent of the direction of applied stresses or plane of rupture (Lo, 1972).

3) Three dimensional effects are not incorporated. Analyses only consider stresses on one vertical cross section through the slope.

4) Factor of Safety is assumed uniform along the entire slip surface.

Conventional computations of instability are divided into two general categories:

1) Short term assessment, where no drainage is assumed to occur (inputed strength evaluated by total stress parameters).

2) Long term assessment, where time allows drainage and the subsequent equilibration of pore pressures (inputed strength assessed in terms of effective stress parameters).

If surface profiles or stratigraphy are irregular, stability is usually evaluated numerically by a method of slices. Each method divides the sliding body into a number of vertical slices with the equilibrium of each individual slice considered separately; the main difference between methods being assumptions made on inter-slice forces.

Analyses of slope failures in the field area were carried out on computer using Janbu's (1973) Generalised Procedures of Slices, assuming:

1) Plane strain conditions apply.

2) Equilibrium shear stress along the shear surface is given by the equation

$$\tau = Tf/F$$

3) The total resultant ΔN is assumed to cut where $\Delta W = \Delta W + q\Delta x + \Delta P$ intersects the base (Fig. 5.12).

4) Positioning of the thrust line for the total side force E is assumed to be known.
NOTE: Investigations reveal changing thrust line position over wide margins has insignificant effects on the computed Factor of Safety (Janbu, 1973).

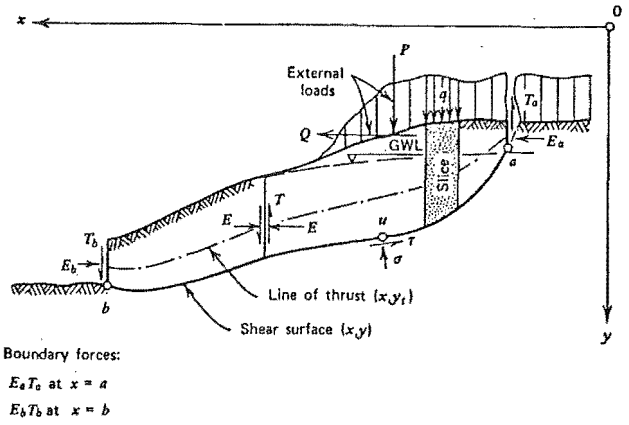

Fig.5.12a: Definitions and notations used for the Generalised Procedure of Slices (Janbu, 1973, Fig.18).

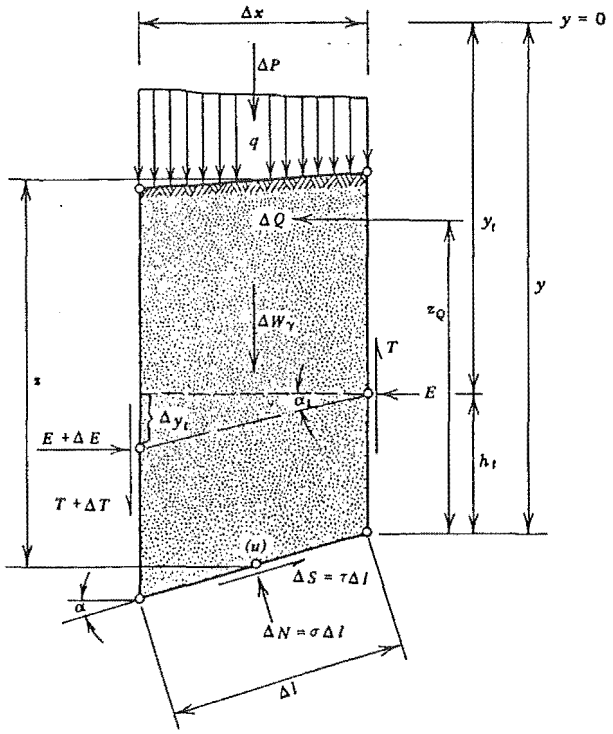

Fig.5.12b: Forces acting on the boundaries of a single slice (Janbu, 1973, Fig.19)

Assumptions made on field conditions for long-term stability assessment are:

1) Drained conditions exist throughout the slope profile (strength evaluated in terms of effective strength parameters). A hypothesis supported by survey data, ie. movement occurs months after heavy rain.

2) No confined zones of high pore pressure are present, ie. water table is equivalent to the phreatic surface.

   Permeability is assumed isotropic with steady seepage parallel to ground surface and pore pressures are derived from a simple orthagonal flow net. Effects of forces exerted by water flowing through overburden are not considered.

These simplistic assumptions are necessary due to the lack of reliable field pore pressure measurement.

Skempton (1977) noted negative pore pressures within the fissured London clay may take in excess of 50 years to equilibrate following excavation. However these conclusions were based on deeper-seated instability where permeability was decreased by high effective normal pressures closing mudstone defects. The shallow Hampden regolith/colluvium failures occur in zones where secondary permeability (attributed to fracturing) is high (fissures open), and accentuated by organic "aquifer" horizons, thus the limiting conclusion is not considered applicable.

More accurate information for stability analyses regarding pore pressure magnitude would mean long term monitoring using expensive sensitive piezometers and is probably unwarranted.

Therefore, although the assumptions made are felt realistic, it must be noted stability analyses show "relative" rather than absolute effects on stability for changing ground water conditions.

Domain Slide

The coastal domain region comprises an ill-defined zone imperceptibly moving seaward, possibly associated with well delineated subsidence of Haven Street. Survey data implies displacement is triggered by localised high ground water levels adjacent to a Haven Street culvert.

Stereoscopic analyses of aerial photography plus the lack of salient mass movement morphology imply incipient slope failure. Skempton (1964) and Bjerrum (1967) note first time slides in over-consolidated clays, such as the Hampden Formation, are generally associated with "fully softened" strength. For this reason, effective stress parameters to utilize in stability analyses were determined for "softened" Hampden mudstone. Strength was evaluated by undrained triaxial testing on samples taken in the immediate vicinity of a shear zone and thus assumed "fully softened" (refer to section 4.3.7). Two interpretations of test results are plausible:

$$\phi' = 17^{o} \text{ with } c' = 8 \text{ kPa}$$
$$\text{or } \phi' = 18^{o} \text{ with } c' = 0$$

Variations in the degree of softening within mudstone means some parts undoubtedly retain limited effective cohesion (developed by over-consolidation); should this be released both strength parameters c' and ϕ' for the material would be reduced (ϕ' from associated increase in strain). Deviation in triaxial test results could reflect incomplete softening of material analysed and for this reason ϕ' and c' may not represent "fully softened" strength for the Hampden Formation.

A surveyed profile of the coastal region was drawn, divided into eight segments and analysed by computer based on the following assumptions:

1) The failure zone propagated along the saturated boundary between yellow-brown regolith and blue-grey mudstone (refer Appendix 7, auger hole 3).

2) Assuming the preceding assumptions on conditions of failure (p.135) the worst ground water conditions prevailed (almost total saturation).

3) Effective stress parameters were $\phi' = 18^{o}$ and $c' = 0$; based on Skempton's (1970, 1977) conclusion cohesion is zero at "fully softened" strength (refer section 4.3.7).

The resultant Factor of Safety was 1.84 inferring a stable slope, which is inconsistent with survey and field observation of displacement during periods of ground saturation (Fig. 5.13).

To verify the validity of effective stress parameters ($\phi' = 18^{o}$, $c' = 0$), they were subsequently utilized to analyse a well exposed "active" slope failure whose basal shear zone could accurately be inferred.

A large debris flow-slide degrading the northern coastline within the Davids Road area was chosen (Fig. 5.14). A surveyed profile, including the slip's likely failure surface, was compiled and divided into seven sections for computer analysis (Fig. 5.15). Given that $\phi' = 18^{o}$, $c' = 0$, and the worst ground water conditions prevailed, the computed Factor of Safety was 1.26.

Strength parameters required for movement to occur (F=1) under identical ground water conditions are $\phi' = 13^{o}$, $c' = 0$ (found by iteration). The appreciably lower ϕ' value may indicate:

1) Excess pore pressures develop as a result of shear displacement. Triaxial testing of regolith caused initial dilatancy and resultant negative pore pressures within the sample which were followed by significant excess pressures developing prior to failure. By analogy, if displacement within the landslides shear zone was sufficiently rapid, to prevent drainage via ambient softened mudstone, transient excess pressures may develop along the zone of shear and account for the low backcalculated ϕ value.

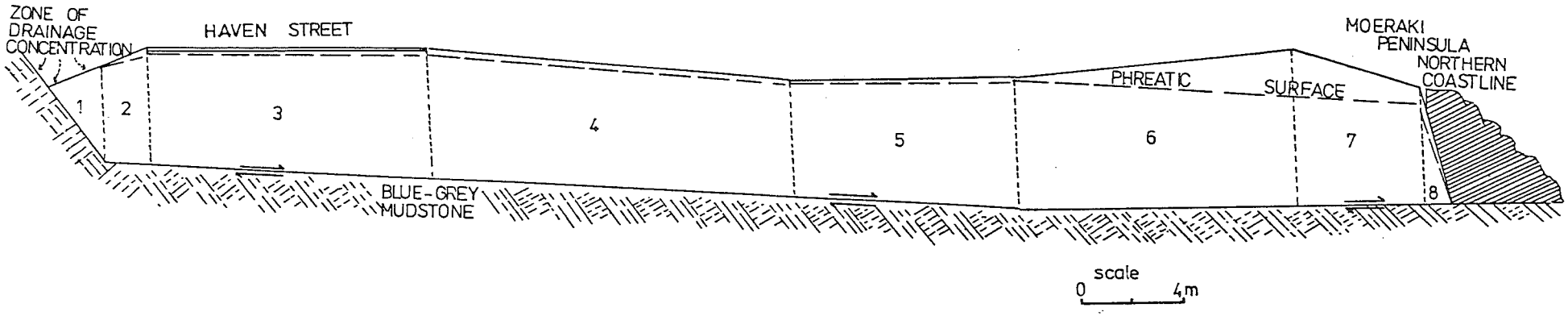

Fig. 5.13 Surveyed profile of Domain Slide, Motor Camp area; note active coastal instability (cross-hatched zone) provided minimal butress support hence was not included in computation. Limit equilibrium analysis of the incipient failure utilizing the marked phreatic surface and strength parameters of $\phi'=18^{\circ}$,$c'=0$ gave a Factor of Safety equal to 1.84 (7550E,0450N).

Fig.5.14: Oblique view, coastal debris flow-slide, well delineated by prominent escarpment (dashed); note well exposed basal shear plane facilitating accurate inference of subsurface failure geometry. Cross-sectioned denoted X-Y. Looking southwest from 7300E,0450N.

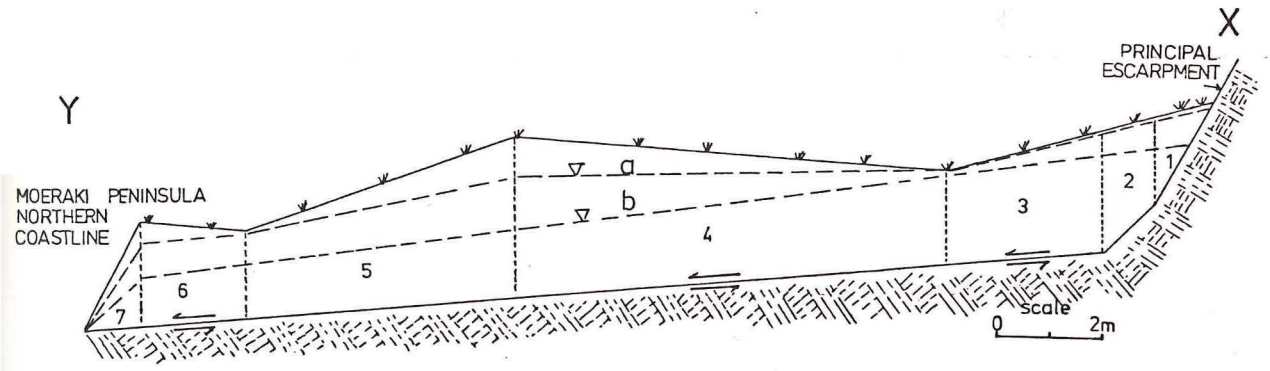

Fig.5.15: Surveyed profile (X-Y), coastal debris flow-slide; divided into seven segments for computer analyses which utilized two subsurface water table levels (marked ∇) (7250E,0350N)

Strength parameters	Phreatic Surface	Factor of Safety
ϕ'=13, c' =0	a	1.03
ϕ'=13, c' =0	b	1.23

2) An increased slope surcharge from an abrupt rise in ground water levels could create temporary high pore pressures within the slide mass shear zone.

3) Salient morphology clearly indicates the slide has been moving for sufficient time to define a discrete basal shear "zone" along which high strain may have adequately orientated particles such that ϕ' approaches the residual value.

Based on stability analyses results parameters $\phi' = 13^{o}$, $c' = 0$ probably more closely approximate mudstone strength at failure than $\phi' = 18^{o}$, $c' = 0$.

Limit equilibrium computations yield relative rather than "absolute" stability assessment. Hence, even if failure is undrained, once backcalculated parameters for slope movement are known comparative effects of ground water fluctuations on stability can be appraised.

Analyses show a drop of about 1 m in the water table would stabilize the debris flow-slide, assuming parameters of $\phi' = 13^{o}$ and $c' = 0$ (Fig. 5.15).

The "active" coastal domain region, in the Motor Camp area, was then re-analysed, based on original assumptions pertaining to conditions of failure (p.136) but utilizing effective stress parameters of $\phi' = 13^{o}$, $c' = 0$. The calculated Factor of Safety was 1.28, again inconsistent with field and survey observation of instability.

However when divided and analysed individually as separate "sections", assuming the same conditions (ground saturation, $\phi' = 13^{o}$, $c' = 0$), a plausible mechanism of slope failure emerges (Fig. 5.16).

Section one	: Definitely unstable,	F = 0.98
Section two	: Unstable	F = 1.11
Section three	: Unstable	F = 1.07
Entire coastal domain region	: Stable	F = 1.28

Domain Section	Strength Parameter	Phreatic Surface	Factor of Safety
4	$\phi'=18^{o},c'=0$	a	1.84
	$\phi'=13^{o},c'=0$	a	1.23
	$\phi'=13^{o},c'=0$	b	1.63
3	$\phi'=13^{o},c'=0$	a	1.07
	$\phi'=13^{o},c'=0$	b	1.42
2	$\phi'=13^{o},c'=0$	a	1.11
	$\phi'=13^{o},c'=0$	b	1.44
1	$\phi'=13^{o},c'=0$	a	0.98
	$\phi'=13^{o},c'=0$	b	1.30

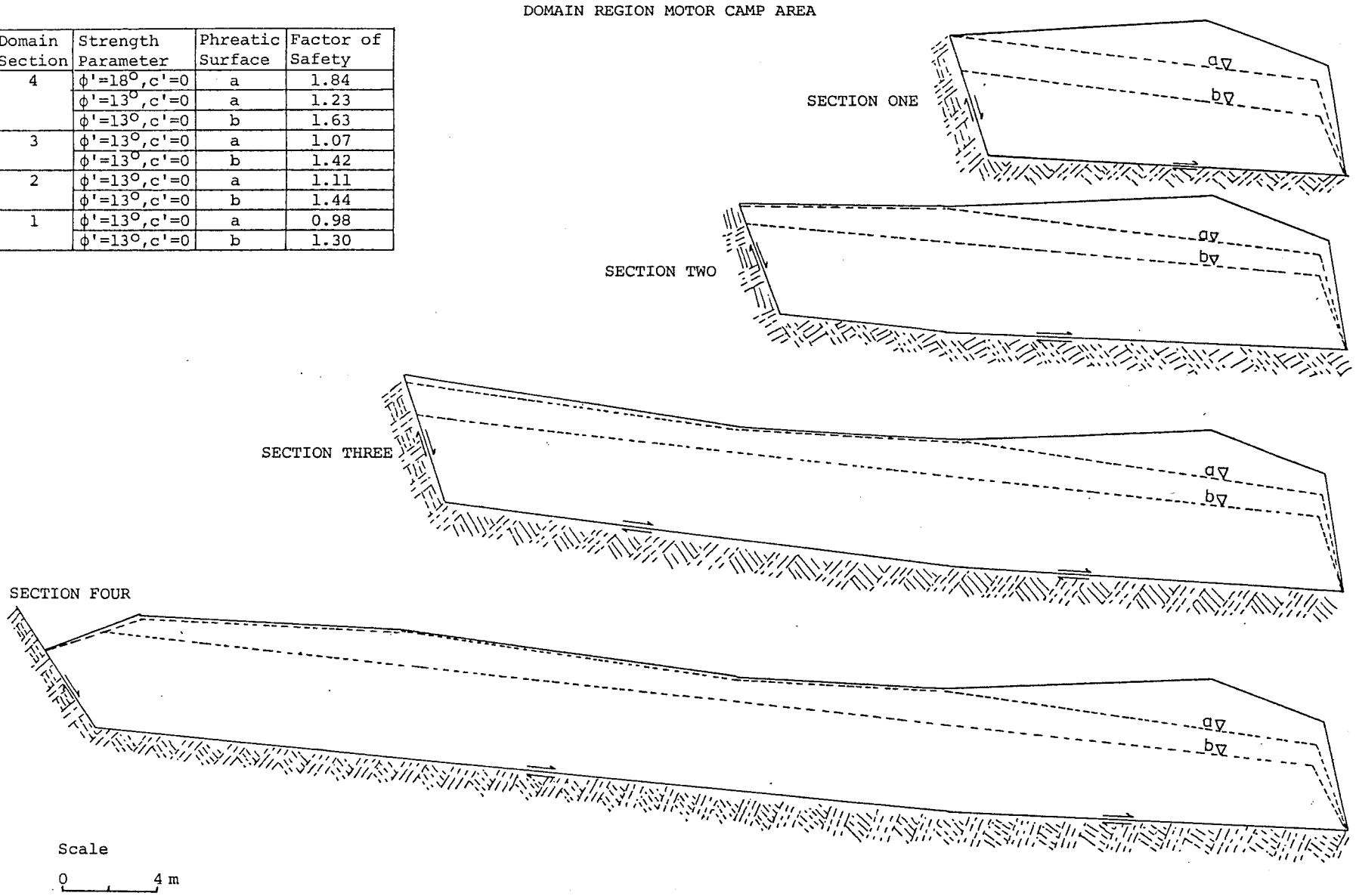

Fig.5.16: Domain Region assessed as four separate sections by limit equilibrium analyses; results suggest "progressive slope failure" with downslope buttress support being removed causing subsidence of Haven Street.

Movement downslope of material encompassing section three (unstable at high ground water levels) would remove laterial support, ultimately resulting in subsidence of adjacent material higher upslope. The proposed mechanism accounts for field observation of horizontal displacement along the coast and subsidence of Haven Street.

Note, relative stability of all sections would be achieved by a comparatively small drop in ground water levels (Fig. 5.16).

Slope movement is advancing by "PROGRESSIVE FAILURE" of individual units which can be represented by a hypothetical four stage "model" (Fig. 5.17).

STAGE I : LOCAL FAILURE Induced principally by lack of buttress support (coastal erosion) plus high pore pressures.

STAGE II and III : PROGRESSIVE FAILURE Zone of movement retrogressing due to removal of lateral support; triggered by high ground water levels.

STAGE IV : "EN-MASSE" FAILURE Development of an upslope graben structure and movement of the entire slide mass as one unit.

The preceding analyses highlight the inherent dangers of limit equilibrium methods in slope stability assessment of over-consolidated materials subject to strain softening ie. the slide when analysed as a whole is apparently stable yet anomalously in the field obviously unstable.

The following intrinsic analysis assumptions prove invalid for strain softening materials:

1) The concept of limiting equilibrium is not invoked ie. stress-strain relationships do affect analysis.

2) The resultant Factor of Safety is not uniform along the entire slipe surface.

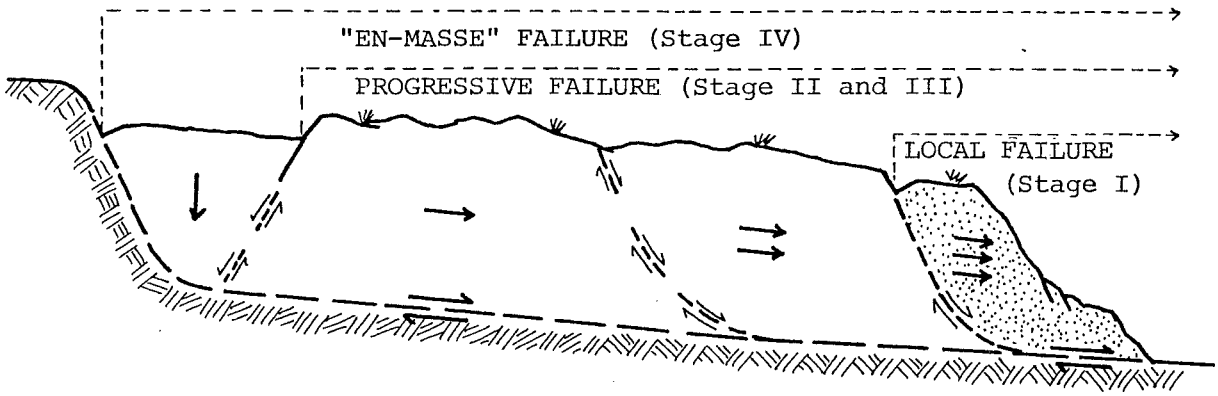

Fig.5.17: Hypothetical schematic four stage model for "progressive" slope failure within over-consolidated strain softening clay sediments.

The concept of "progressive slope failure" was originally developed to explain the peculiarity of first time slides within over-consolidated clays occurring well below peak strength (Skempton, 1964; Bjerrum, 1967). The theory was extended to "soft clays" by Lo (1972) who defined the phenomenon as "the process of successive failure of individual elements in a soil mass; requiring space and time to occur."

A mathematical model accounting for the phenomenon was developed by Bjerrum (1967), and is presented in Appendix 10.

School Slip

The School Slip is a slow moving cohesive debris flow-slide whose displacement is principally attributed to concentration of septic tank drainage (Fig. 5.18).

Effluent pours directly into the slip's principal escarpment having a two fold effect:

1) Increasing local ground water levels causing slip movement to be more rainfall responsive. ie. less precipitation necessary to exceed the threshold required to initiate movement.

2) Lowering shear strength in the escarpment vicinity facilitating retrogression of the failure into school grounds.

Salient morphology indicates the slide has been moving for sufficient time to establish a discrete basal rupture "zone" hence parameters initially utilized for stability computations are founded on analyses of the Davids Road area coastal slide ($\phi' = 13^{o}$, $c' = 0$).

A surveyed profile of the School Slip was compiled including the most probable failure surface and the slide divided into eight segments for computer analyses.

Assuming the original assumptions made on conditions of failure are valid (p.135), the Factor of Safety was calculated for two low ground water tables; both implied the slope unstable (Fig. 5.19).

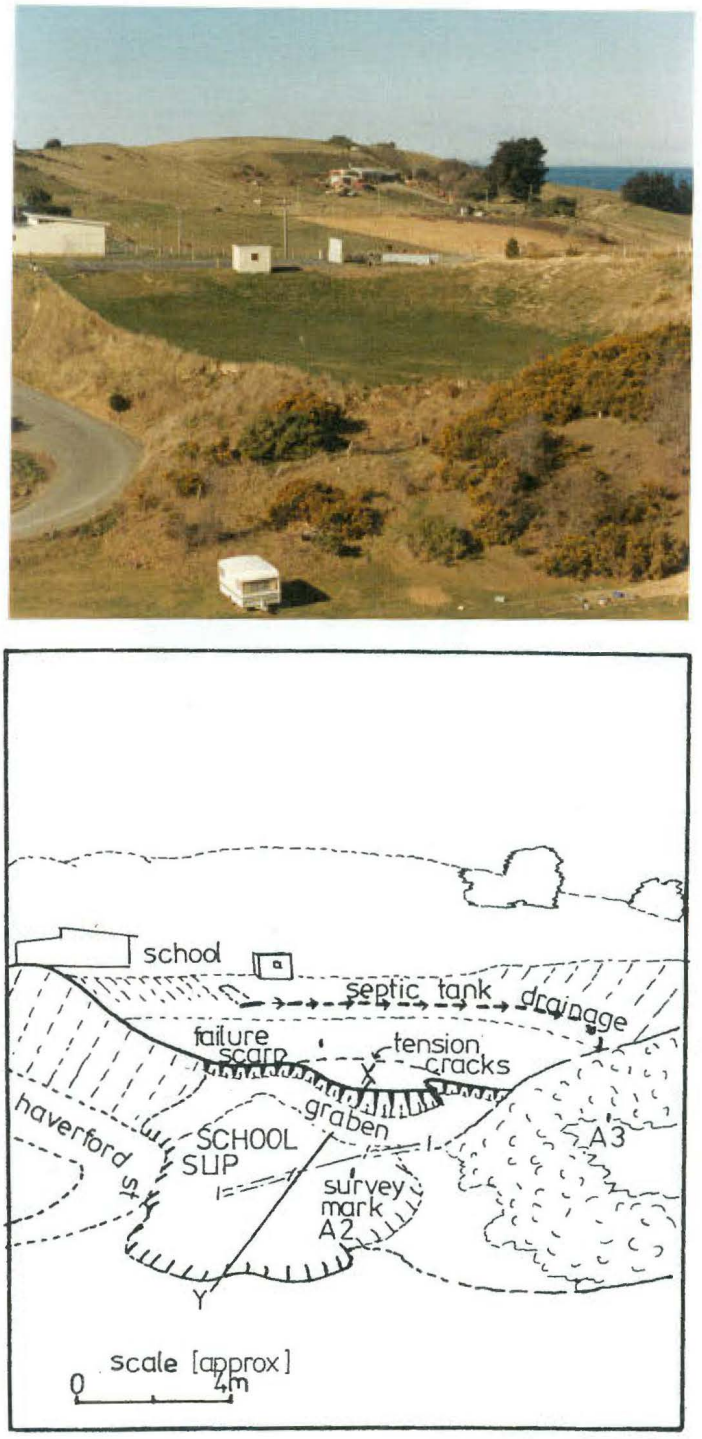

Fig. 5.18: School Slip delineating by salient escarpment actively retrogressing into the playground area. Surveyed profile marked X-Y. Viewing east from 7500E,0300N.

Strength Parameters	Phreatic Surface	Factor of Safety
$\phi'=13^{o}$	a	0.60
	b	0.79
$\phi'=18^{o}$	a	0.90
	b	1.11

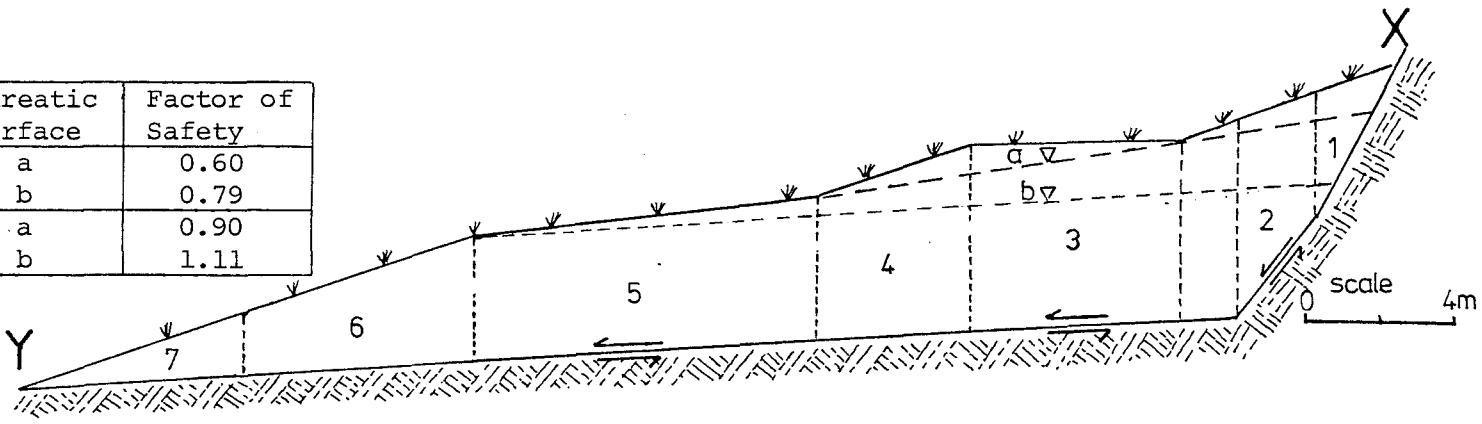

Fig.5.19: Surveyed profile of the School Slip (X-Y). Limit equilibrium analyses utilizing parameters $\phi'=18^{o}$,c'=0 for both phreatic surfaces marked appear to best "model" in-situ behaviour as determined from survey data (7550E,0300N).

Field observation indicated higher ground water tables were necessary to initiate failure, hence the slide was re-analysed utilizing "softened" mudstone parameters of $\phi' = 18^{o}$, $c' = 0$.

Subsequent effective stress analyses implied almost total ground saturation was required to initiate movement with a drop of about 1 m in subsurface water levels necessary to attain stability.

Two conclusions are drawn:

1) Stability analyses incorporating strength parameters for softened Hampden mudstone ($\phi' = 18^{o}$, $c' = 0$) "model" field behaviour of the School Slip more realistically than utilizing values approaching residual strength ($\phi' = 13^{o}$, $c' = 0$). Thus strain over "principal rupture surfaces" may not have sufficiently orientated particles below the "fully softened" strength.

2) Bearing in mind computations reflect relative slope activity, stability would most likely be restored by a lowering of ground water levels in the order of 1 m.

5.2.5 Remedial Options

The principal aim of remedial design for the Motor Camp area is lowering of ground water levels. Regrading of morphology to reduce driving forces and create buttressing support is of minor importance since field evidence clearly demonstrates slides mobilize at extremely low angles in saturated ground (Domain Slide, School Slip).

1) Drainage concentrating water at the crest of any slope (stable or unstable) should be avoided.

2) A dense cover of shrub vegetation is recommended for currently active shallow failures (School Slip, coastal batter slope) to minimise seasonal ground water fluctuations and increase surficial overburden strength.

3) Drainage of the school's septic tank via clay tile conduit should be relocated, channelling effluent well clear from the School Slips principal escarpment.

4) The Haven Street culvert should furnish a continuous, unimpeded channel for Motor Camp drainage through the domain area to the coast. Two or three horizontal drains parallel to the culvert, extending 10 m to 15 m back from the coastal batter would encourage lower ground water levels. ie. narrow 1 m to 2 m deep trenches, containing perferated flexible P.V.C. tubing, backfilled with permeable sand/pebble aggregate.

5.3 DAVIDS ROAD AREA

5.3.1 Introduction

The Davids Road Area is located in the vicinity of the Davids Road Slide and refers to that triangular section extending east of Davids Road northward to the coast (refer map enclosure, engineering geology plans). The region extends from Tenby Street, 240 m to the south, including 130 m of shoreline and encompasses an area of 1.6×10^4 square metres.

Bedrock geology is the homogeneous Hampden Formation, confined in exposure to the shore platform in the north and isolated outcrops within scarps to the south. A northeast-southwest trending normal fault is situated west of the area but does not influence, hazardous, local, shallow mass movement. No folding which could affect instability has been identified within the Hampden mudstones.

Three rudimentary morphologic regimes are recognized:

1) A head region; well delineated, of relatively high elevation.
2) A coastal zone; sharply bound and narrow.
3) A coastal tract; ill-defined and with low elevation.

(Fig. 5.20)

Head Region

The head region, situated in the south of the area, comprises a distinctive eliptical escarpment, open to the north, varying in height (5 m to 15 m) and enclosing a triangular area of subdued, undulatory, topography. Shallow instability degrades the escarpment, amassing talus margins of colluvium.

Morphology provides an ideal catchment for precipitation runoff and the flat triangular district of land encompassed by the scarp is predominantly swampy and often ponded.

Central Zone

The central zone divides the Davids Road area into two equal parts of different elevation; an upper head region and further to the south, a lower coastal "tract".

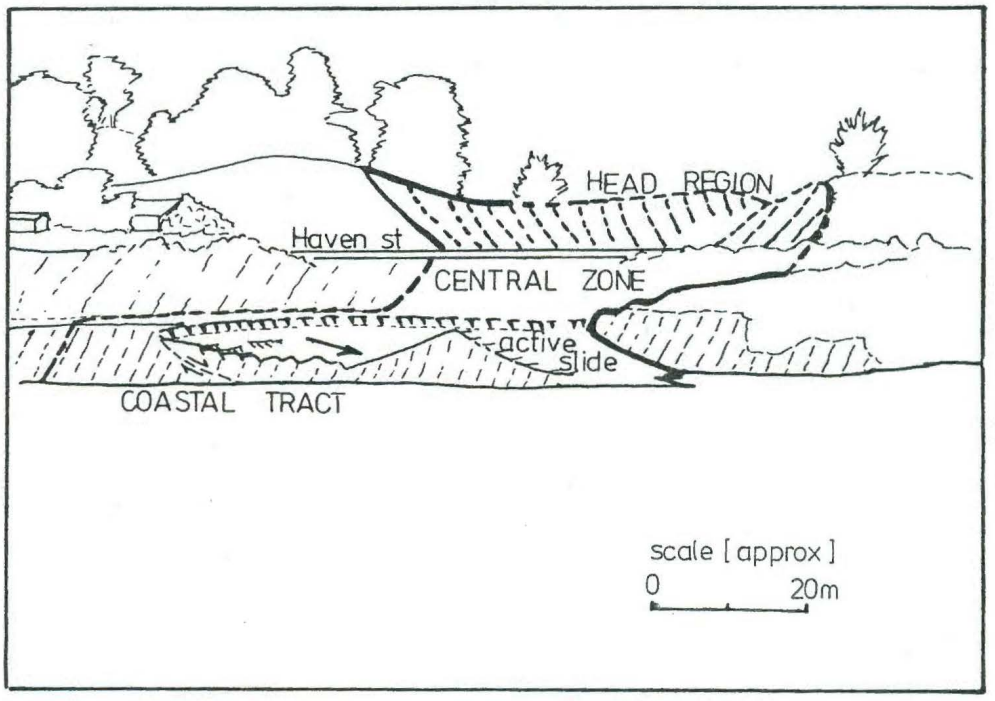

Fig. 5.20: Principal morphological regimes comprising the Davids Road area; note extent of active debris flow-slide eroding the "coastal tract". Looking southeast from 7100E,0600N.

The central zone embodies Haven Street plus affiliated batter slope; the batter of chaotic gravel-colluvial fill (height 10 m) uniformly slopes 30^{o} to 25^{o} facing north. Batter slope morphology is subdued, hummocked (relief <3 m) and partially masked in places by dense exotic shrub cover.

Haven Street is tarsealed and prone to sudden subsidence along well defined rupture (shear) zones, jeopardising traffic (Fig. 5.21, 5.22). Two twelve inch culverts channel drainage from the head region below Haven Street, emptying effluent onto the batter. Both drains are aligned with features in the head regio one a buried swamp in the east, the second with swampy ground toward the centre (refer map enclosure, engineering geology plans).

Coastal "Tract"

The coastal tract comprises an ill-defined area, essentially horizontal and with little relief (<3 m), adjacent to the central zone and bound by a low coastal cliff to the north. The coastal slope is actively eroded by composite debris flow-slide features, the largest of which encroaches an area of about 500 square metres.

A narrow district of permanently ponded water exists and neighbours the central zone. Originating in part from rainfall runoff and in part spring fed, the ponding is ineffectually drained by a shallow ditch extending to the coast; otherwise runoff draining higher relief results in temporary ponding amidst gently deflated areas.

Geomorphology

Geomorphology described in this section only relates to shallow mass movement affecting housing and/or roading (refer to section 3.6. for details of the deep-seated Davids Road Slide).

Subsurface information on overburden stratigraphy was collated from six bore holes (five auger, <8 m, one drill, 9 m) arranged in plan, to form a line through the centre of the area. Subsurface data plus geomorphological interpretation is presented on a surveyed profile of the Davids Road area, scale 1:100 (refer to map enclosure). Description of individual

Fig.5.21: Haven Street, Davids Road area depicting zone effected by well delineated batter slope failure (dashed) prone to abrupt subsidence. Viewing northwest from 7300E,0250N.

Fig.5.22: Rupture zone propagating through Haven Street defining batter failure (7250E,0250N).

Scale

0 1 m

bore holes is outlined in Appendix 7.

Profiles within the head region comprise thick sequences of successive paleosol/yellow-brown mudstone layers. These successions are interpreted as numerous debris failures which have eroded principal escarpments of the Davids Road Slide; hence the ostensibly triangular area of subdued relief in the head region on which Haven Street is based, comprises colluvial fill.

Bore hole data from the lower coastal "tract" implies the presence of a buried graben structure adjacent to Haven Street, probably affiliated with the Davids Road Slide. The deflated zone, has subsequently been infilled with debris, but nevertheless most likely structurally governs the extent of overlying permanently imponded water in its vicinity.

It must be noted subsurface stratigraphy within regolith/colluvium overburden has been confused by episodic slope failure and alternate plausible interpretations of bore hole data are likely.

Active erosion in the area appears to have remained unimpeded over the last thirty years. Ineffectual remedial measures (road re-sealing, occasional new culverts) have failed to check continual subsidence of Haven Street. Extensive "active" erosion amidst the coastal slope is gradually encroaching increasing amounts of land used for recreation purposes.

5.3.2 Ground Water Monitoring

Introduction

Piezometers together with standpipes were installed at two locations in the Davids Road area to monitor ground water pressures. Piezometers record pore pressure at specific levels as compared to the simpler standpipe device which registers unconfined ground water pressure.

Principal objectives of the first installation situated adjacent to the coast were:

1) To establish seasonal ground water fluctuations within the mantle of yellow-brown mudstone regolith/colluvium.

2) To ascertain if a thick sequence of organic detritus causes different flow regimes within mudstone regolith/colluvium.

To achieve this two horizons were monitored (Fig.5.23a).

1) A thick organic horizon (0 m to 3 m depth) via a standpipe.

2) A 1 m zone of yellow-brown mudstone (6 m to 7 m depth) via a piezometer.

(Refer to Appendix 7 for detailed profile description).

Main aims of the second installation, located above Haven Street within an active debris flow-slide were:

1) To establish seasonal fluctuations within three separate horizons in "actively moving" yellow-brown mudstone colluvium.

2) To determine if softened mudstone layers result in separate flow regimes and if so, their inter-relationship.

To accomplish this, three horizons were observed (Fig. 5.23b).

1) Yellow-brown fissured mudstone (0 m to 3 m depth) via a standpipe.

2) Softened yellow-brown mudstone (3.1 m to 3.6 m depth) via a piezometer.

3) Yellow-brown fissured mudstone (4 m to 4.7 m) via a piezometer.

(Refer to Appendix 7 for detailed profile description).

Piezometers were constructed of 19 mm P.V.C. conduit placed in augered holes then sealed to relevant depths by bentonite and/or cement aggregate mix; standpipes within the same holes comprised perforated 19 mm conduit encased in filter cloth (refer Appendix 8 for construction details). Water levels in

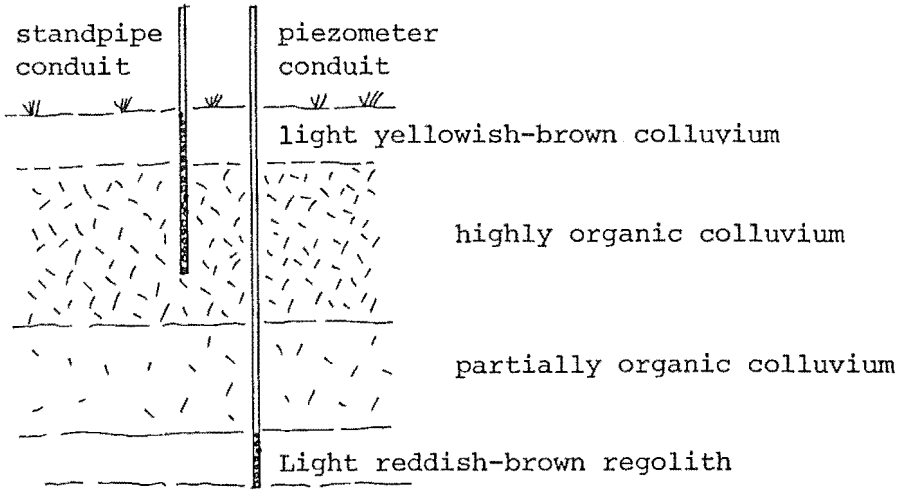

Fig.5.23(a) Coastal Installation (P_2) (7250E,0350N)

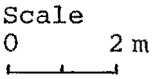

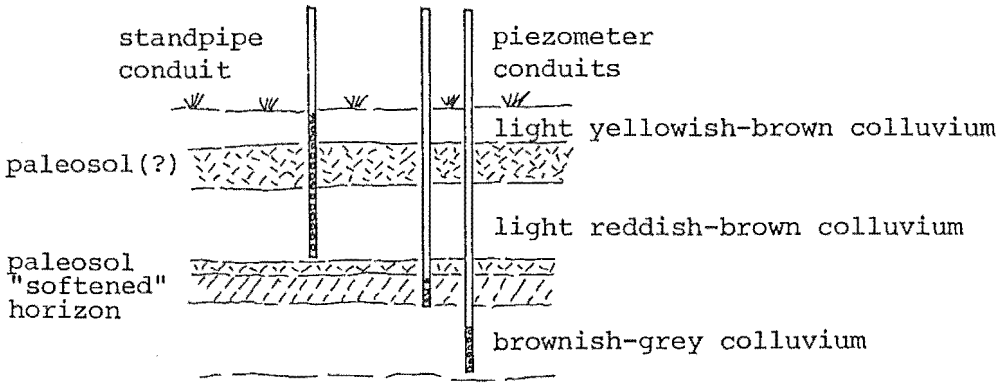

Fig.5.23(b): Debris Slide Installation (P_3). Refer Appendix 7 for comprehensive borehole logs. Location 7300E,0200N

both devices was measured using a well depth indicator.

Location of the two monitoring sites meant recording of ground water pressures would probably be infrequent hence a method to note maximum interim pore pressure between readings was developed. This involved pouring cork dust down piezometer/standpipe conduit and inserting a flexible graduated section of clear P.V.C. tubing (Appendix 8). Cork dust, floating, rose with increasing ground water pressure and then as pressures subsided a residue of cork fragments remained adhereing to the clear tubing. Prior to the next pressure reading, the clear tubing was extracted and maximum pressure noted.

Results

Coastal Installation:

Fifteen recordings of the two horizons monitored were made, revealing two ground water pore pressure regimes; both maximising in August 1981 and minimising in March 1980.

Debris Slide Installation:

Fifteen readings of the three levels monitored showed markedly different ground water pressures. The upper-most layer varied markedly whilst the lower-most zone maintained relatively constant pressure. The piezometer within the intervening "softened" mudstone horizon was dry for at least the first month, indicating the zone's impermeability and emphasising the inadequacy of this type of device in low permeability materials.

(Refer Appendix 8 for data record).

Note: Cork dust method of recording maximum interim pore pressure proved tedius and inaccurate so was abandoned.

Conclusions

The monitoring period from August 1981 to August 1982 was sufficient but the fifteen readings taken furnish an inadequate data base for conclusive determination of seasonal ground water patterns. However results were correlated with daily rainfall and tentative conclusions made:

Coastal Installation:

Two ground water flow regimes were recognized, correlating to the levels monitored. Following a month's moderate rainfall (August 1981), pore pressures within the lower mudstone horizon were significantly higher than the overlying organic layer. In contrast, during a month of low rainfall (August 1982), pressures were equivalent. The conclusion drawn is that the overlying organic layers initially retain precipitation, causing undrained loading on the less permeable underlying material which requires time to equilibrate.

Debris Slide Installation:

Three ground water flow regimes were recognized within the profile, corresponding with horizons monitored. The upper fluctuated more readily with rainfall than the lower. Response to precipitation of the intermediate, softened layer, could not be established from the type of device used.

Response time for piezometers and standpipes appeared in the vicinity of seven days. As transient pore pressures may have significantly changed during this time magnitudes recorded were not used for effective stress stability analyses.

5.3.3 Surveying

Introduction

A survey network was established over the Davids Road Area with principal objectives of:

1) Delineating relatively active zones plus their rates of movement.

2) Helping establish movement mechanisms for the Haven Street batter slope failure.

The network essentially comprises a central line of six "monitoring" points in conjunction with three adjoining rows; one row monitoring land immediately behind Haven Street, the second Haven Street itself, and the third the lower coastal tract. Two "control" points plus one "base" point are installed outside principal escarpments defined by the Davids Road Slide. The system, consisting of 18 points in total,

is "tied" to the Motor Camp network, hence Geodetic Datum 1949 (refer map enclosure, plan of Davids Road Area survey network).

Bench mark construction follows designs outlined for the Motor Camp Area with the exception of control point 13, which is concreted to a depth of 1.5 m amidst volcanic bedrock.

Nine surveys were completed over a period of one year (August 1981 to August 1982). Initial and final measurements were taken with the help of Mr A. Greig and J. Hermann, utilizing a Wild T_2 theodolite plus Wild DI3 distomat. Interim surveys employed a Wild T_6 theodolite in conjunction with DI3 distomat.

Individual surveys involved positioning of the theodolite in combination with distomat over "base" point 11, followed by alignment with points 12 and 10 to ensure no lateral movements of the mark (point 11) had occurred. Distances plus relevant angles (three full sets, left and right face), were then observed to all "control" and "monitoring" points. Only horizontal displacement was calculated except for three Haven Street points where vertical movement was also noted. Detailed survey methodology and analyses of data are outlined in Appendix 9.

Based on equipment used a maximum survey error of ±1 cm is assumed.

Results

Measured displacement for all monitoring points is shown in vector form on a plan of the Davids Road Area survey network (refer map enclosure).

Three relatively "active" regions are recognized:

1) A slowly advancing debris flow-slide, above Haven Street, progressing at a measured rate of 5.5 cm per year (point C).

2) A well defined Haven Street batter slope failure, horizontal movement of 14.3 cm, vertical of 10.7 cm per year (points H, I and J).

3) An ill-defined zone adjacent to the coast with measured displacement in the order of 4 cm to 9 cm per year (points K, L, M and P).

No displacement of "control" points was discerned with remaining "monitoring" points exhibiting movement in the order of 2 cm to 4 cm per year.

Conclusions

The active debris flow slide above Haven Street is like the School Slip in bedrock lithology, salient morpholpgy and failure mode, hence mechanism of movement is assumed similar (ie. principally by drained failure in response to rising ground water levels).

Measured displacement was correlated with rainfall data for the remaining two active regions.

Both vertical and horizontal movement of the Haven Street failure maximised during months of high rainfall (December 1981, January, April and May 1982). Thus displacement probably results from undrained conditions created immediately following heavy precipitation (Fig. 5.24).

Data interpreted for the coastal region shows increased movement (February, March 1982) up to one month after heavy rainfall (December 1981, January 1982)(Fig. 5.25). For this reason accelerated displacement is attributed to slowly rising ground water levels, under drained conditions.

Movement of the remaining points is ascribed to surficial regolith/colluvium "creep".

In summary, the Davids Road area contains active mass movement triggered by heavy precipitation (drained failures within the head and coastal area, plus an undrained slide developed in the Haven Street batter). The entire area exhibits "creep" movement confusing speculation relating to activity of the deep-seated Davids Road Slide, which if considered as one unit, is tentatively assumed stable.

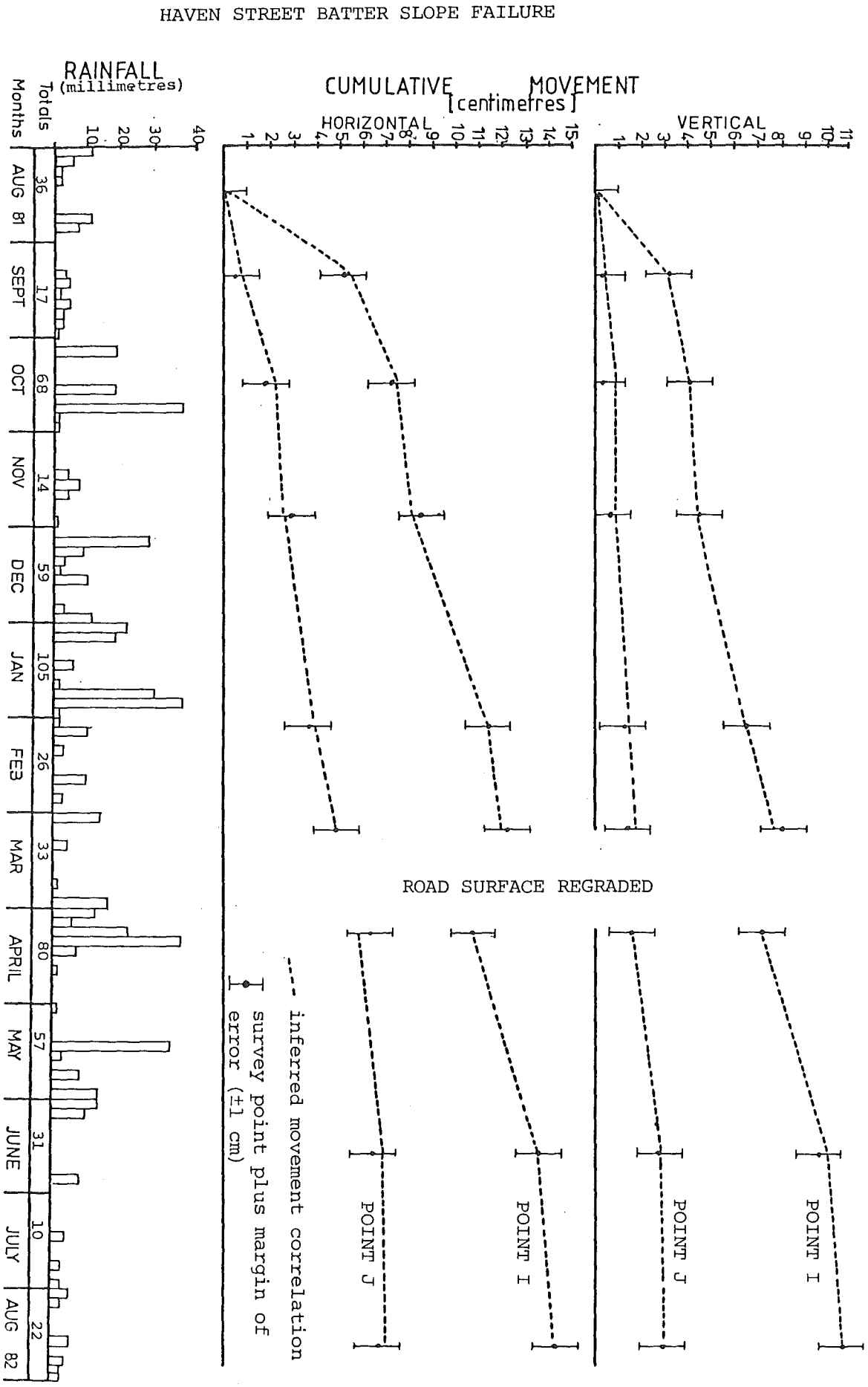

Fig.5.24: Haven Street survey data correlated with rainfall measurements taken by Mr and Mrs Kedsley.

COASTAL REGION, DAVIDS ROAD AREA

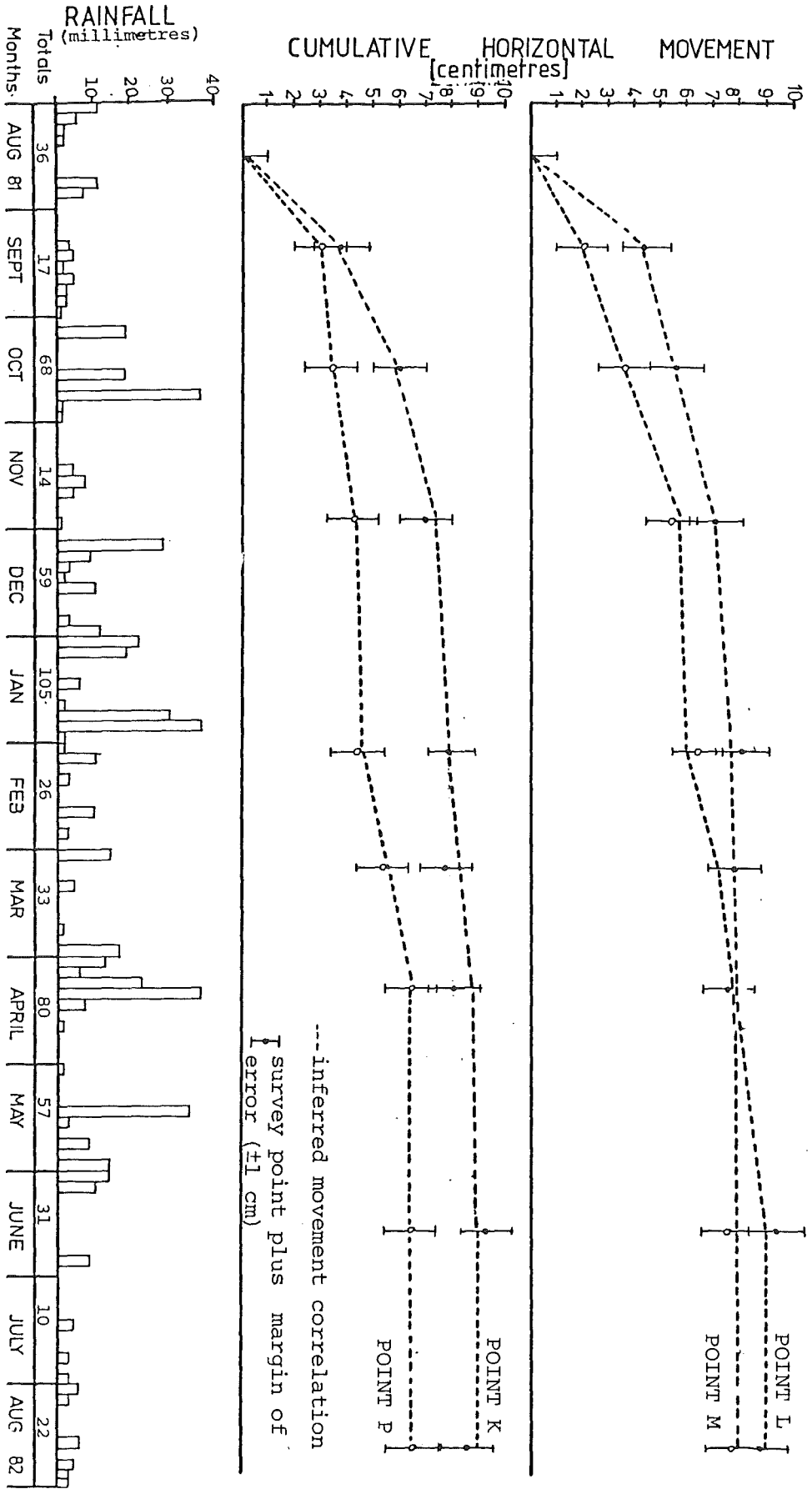

Fig.5.25:Coastal Region survey data correlated with rainfall measurements taken by Mr and Mrs Kedsley.

5.3.4 Stability Assessment

Introduction

Limit equilibrium analyses were not utilized for stability assessment of the active coastal or Haven Street regions due to:

1) Lack of subsurface data.
   a) Basal failure surface of the Haven Street batter slide is presumed circular but may in fact be partially controlled by debris within the profile (previous sections of roading or culverts).

   b) No tentative failure surface has been defined for the coastal region.

2) Lack of relevant geotechnical parameters.
   a) Movement of Haven Street occurs in undrained conditions most likely at residual strength and neither $\phi'r$ or appropriate pore pressures magnitudes are known.

   b) The coastal piezometer installation revealed different flow regimes within mudstone overburden which undoubtedly influence local instabilities yet effects cannot realistically be incorporated in analyses.

However, enough information has been collated to establish movement mechanisms hence the causes of slope failure in the two areas.

Haven Street

The Haven Street batter failure developed within chaotic gravel-colluvial "fill", is well defined and moves in abrupt response to severe rainfall.

Following heavy precipitation, overland flow is concentrated and usually imponded behind Haven Street; ground water is subsequently channelled via permeable horizons (paleosols) into Haven Street roading substrate. An undrained situation results when infiltration of the clay rich foundation "fill"

is exceeded, creating excess pore pressures and initiating sudden failure. Movement continues until pore pressures dissipate along the rupture (shear) surface; the failure zone probably predetermined and at residual strength from large strains developed during preceding months.

Ground water south of Haven Street may accumulate within a single, horizontal paleosol layer (approximate depth, 2 m), the presence of which is tentatively extrapolated from bore hole data (refer map enclosure, Davids Road Area surveyed profile). Drainage of the region proves inadequate since:

1) Culvert intakes are too shallow (approximately 1.3 m) with the majority of ground water flow bi-passing the structures, draining via permeable horizons below.

2) Having concentrated drainage culvert outlets direct water onto the Haven Street batter further encouraging movement.

Retrogression of the failure is hindered by a sequence of tarsealed layers marking previous subsided road levels.

Coastal Region

The active coastal region comprises an ill-defined zone which based on survey data, moves via drained failure in response to rising ground water levels.

The section monitored is construed as a rafted "block" associated with the Davids Road Slide (refer map enclosure, surveyed profile, Davids Road Area). Movement may indicate a re-activation of this blocks western margin and is tentatively ascribed to:

1) The removal of buttressing support by an active coastal debris flow-slide the displacement of which is accelerated by drainage into its principal escarpment (refer section 5.2.4 for limit equilibrium analysis).

2) Increased pore pressures attributed to adjacent thick organic horizons channelling ground water into the rafted "block".

5.3.5 Remedial Options

The chief objective of remedial design for the Davids Road area is effective reduction in ground water pressures.

1) The encouragement of dense shrub vegetation cover to minimise seasonal ground water fluctuations and strengthen shallow overburden is recommended for
   a) the entire head region within the Davids Road Area,
   b) the area comprising the active coastal debris flow-slide,
   c) coastal batter slopes.

2) A cut off drain (2 m to 3 m deep, 15 m to 20 m long) bisecting the section of swampy ground, south of Haven Street, channelling ground water directly into a road culvert (2 m to 3 m deep). Outflow from the road culvert should be directed beyond the batter slope.

3) Filling in the present shallow ditch draining imponded water adjacent to the Haven Street batter. Subsequent installation of a collector drain (approximately 10 m x 5 m, 4 m in depth) neighbouring the zone of ponded water and within organic horizons exposed by the coastal piezometer; the drain emptying effluent beyond the coastal scarp via a connecting impervious section of P.V.C. conduit.

CHAPTER SIX

SLOPE STABILITY ASSESSMENT

6.1 INTRODUCTION

Slope stability investigations have highlighted the extent and current "activity" of mass movement influencing the northern coastline of Moeraki Peninsula.

Classical limit-equilibrium analyses are known to be incapable of coping with real world scenarios such as "progressive slope failure" hence a subjective approach of slope stability evaluation for the township are was chosen. Treatment of instability assessment is in five parts.

The first section comprises a hypothetical model for slope failure within the Hampden mudstone formation and is based on integrated data from detailed research on two unstable areas (Motor Camp and Davids Road areas).

Slope failures jeopardizing township housing and/or roading were identified as principally shallow-seated. Hence the second section describes the compilation of shallow mass movement susceptibility maps (scale 1:1000) for hazard mitigation; susceptibility evaluation being based on the preceding failure model. Examination of this section should be made with reference to susceptibility plans within the map enclosure.

Thirdly, recommendations for land-use zoning founded on susceptibility mapping are submitted, and finally, there is a concise outline of further investigation required.

6.2 MODEL FOR SLOPE FAILURE WITHIN THE HAMPDEN FORMATION

6.2.1 Introduction

A hypothetical model for slope failure within the Hampden Formation has been derived from collated geomorphological, geological and geotechnical data.

The explanation of natural continuums such as mass movement, manifested on a variety of scales, in terms of isolated groups (slides, flows, topples) is thought unrealistic and inadequate. For this reason mechanisms and modes of slope failure salient within the mudstone unit are represented in the form of a dynamic, "evolving" failure model.

The model is developed in three sections:

1) Inherent Mudstone Properties; highlighting intrinsic elements which contribute to slope failure.

2) Instability Development; describing a hypothetical evolution of mass movement starting with deep-seated displacements and culminating in shallow, flow failure.

3) Stability Criteria; outlining factors which influence shallow slope movement.

Hazardous instability affecting Moeraki township is confined to the Kurinui and Hampden Mudstone Formations. Failure mechanisms and modes within both mudstone units are tacitly assumed alike due to the lithological similarity of both Formations, hence the failure model outlined is representative of slope processes over the entire study area and thus can be used as a basis for susceptibility mapping.

6.2.2 Inherent Mudstone Properties

The Hampden Formation is a silty-clay, over-consolidated to form an homogeneous soft rock, with no significant lithological variation (11% sand, 42% silt, 47% clay). Water absorbing smectite minerals comprise the majority of the clay fraction and in conjunction with stress history, account for

characteristic intrinsic properties which influence slope instability.

1) Stress-Strain Behaviour
   Mudstone stress-strain characteristics are typical of "brittle" substances rather than strain hardening and perfectly plastic material, ie. a pronounced peak strength followed by abrupt fall to residual value well below peak upon increasing strain (refer section 4.3.7).

   Hence mudstones are "sensitive" and a small displacement beyond peak results in significant reduction in strength.

2) Latent Strain
   Deformation of flexible plate like clay minerals due to over-consolidation is partially recoverable thus mudstone contains "latent" strain energy. Bjerrum (1967) notes the greater the quantity of swelling clays the greater the potential for recoverable strain.

   Liberation of strain energy results in dilatancy and increased moisture content, the combination of which significantly reduces strength.

3) Plasticity
   Pliability or capacity for remoulding is attributed to the plate like nature of clays and lubricating yet binding influence of absorbed water. For this reason, mudstones containing clays rich in water of hydration (smectites) exhibit the greatest plasticity.

Geotechnical parameters of the Hampden mudstones reflect inherent properties:

Moisture content, coherent mudstone - 24% to 26%
In-situ density, coherent mudstone (fractured) - 1.1 t/m^3

Moisture content, softened mudstone - 30% to 40%
In-situ density, softened mudstone - 1.1 t/m^3 to 1.89 t/m^3
In-situ undrained strength, softened mudstone
- 1.5 t/m^2 to 4 t/m^2

Shrinkage limit = 8%
Liquid limit = 65%
Plasticity index = 41

6.2.3 Instability Development

Hypothetical development of instability within the Hampden Formation is portrayed on an evolving "model" of slope failure.

Deep-Seated Instability (Fig. 6.1)

1) Instability is initiated in response to:
   a) Fluctuating base levels (glacio-eustatic effects) and associated coastal erosion.
   b) Influences of regional uplift (seismotectonic effects).

   Erosion causing relaxation of horizontal stress results in latent strain release (flexural bulging) and consequent deep-seated "creep" movement. Propagation of "plastic" deformation is expedited by mudstones inherent philability and stress-strain characteristics. ie. "sensitivity" facilitating creep deformation.

2) Precursory deep-seated "creep" eventually culminates in complete slope failure producing a slide mass sheared into tilted coherent mudstone "blocks"; with movement intensifying mudstone fracturing and strain softening along zones of significant displacement.

3) Episodic rotational reactivation of "juxtaposed blocks" yields an acutely varied topography.

4) Changing geomorphic conditions (man's influence) results in slope degradation predominantly via shallow mass movement.

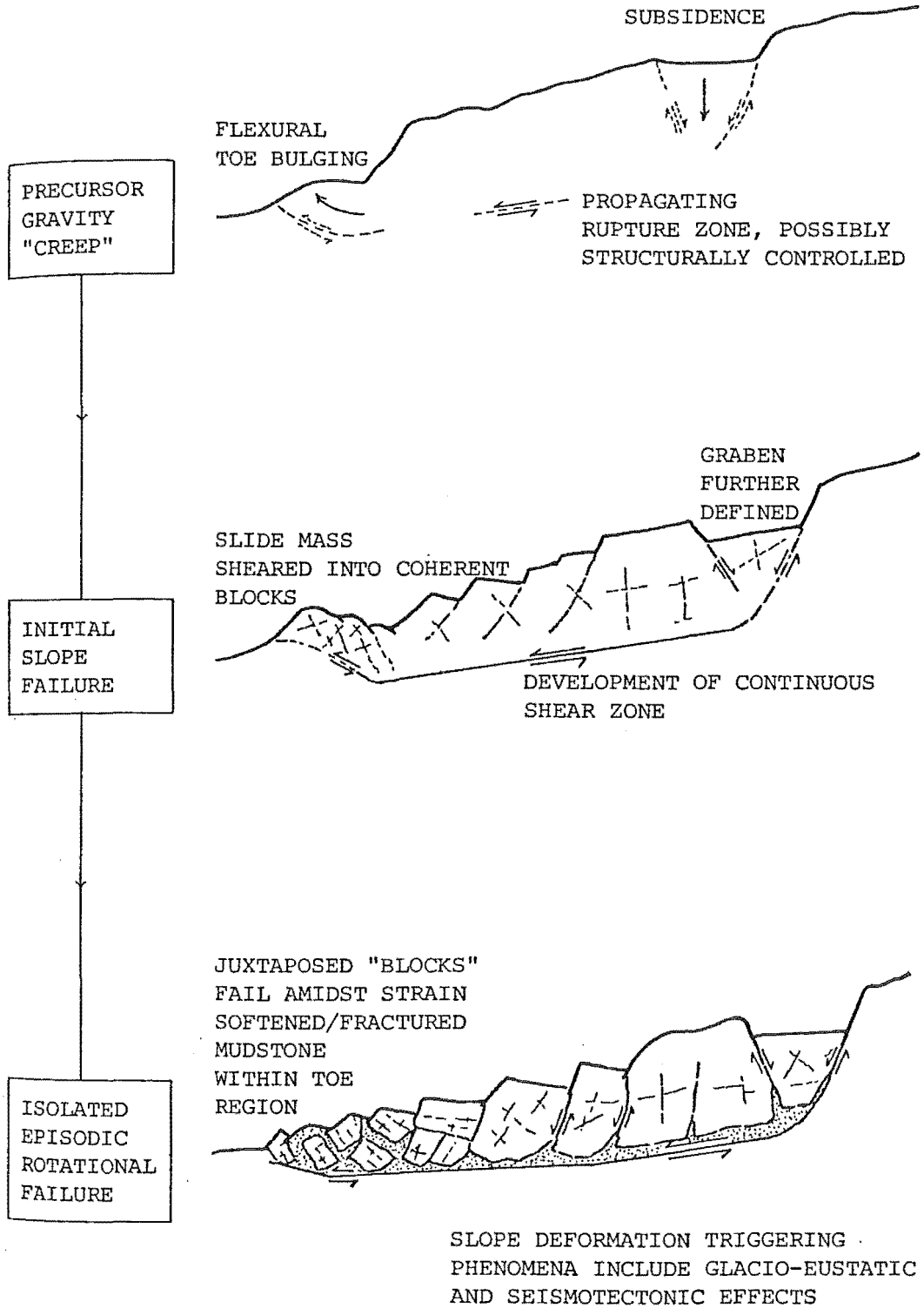

Fig. 6.1: Hypothetical sequential development of deep-seated slope failure amidst Hampden mudstone

Shallow Instability (Fig. 6.2)

5) Mudstone fracturing intensifying toward the surface produces gradational mantles of disaggregated blocks.

Material above the zone of permanent saturation becomes oxidised and "softened" to form a yellow-brown regolith (refer section 4.3.6). Weathering (mainly via slaking) progressively breaks cohesive bonding formed by over-consolidation, causing dilatancy and elevated moisture contents thus reducing regolith strength; a process accelerated by fluctuating ground water (desiccation/saturation) and drainage concentration (increasing pore pressures) (refer section 4.3.6).

Slaking may concentrate along weathered/unweathered mudstone discontinuities producing "weak" horizons susceptible to slope deformation.

6) During periods of high evaporation subsurface water tables drop and desiccation of the surface forms deep cracks as clay minerals contract losing water; in this state the slopes are stable.

7) If subsurface water tables rise the elevated slope surcharge promotes instability due to:
   a) Increased gravity related forces acting on the slope.
   b) Decreased slope shear strength (attributed to raised pore pressures).

Investigations indicate prolonged moderate rainfall is required to elevate ground water tables; brief intense storms cause saturation of surface layers creating an impermeable barrier and precipitation is transported as "overland flow" rather than "through flow".

8) If increased shear stress exceeds reduced shear strengths slope failure occurs; initial movement possibly controlled by areas of "softened" mudstone since:

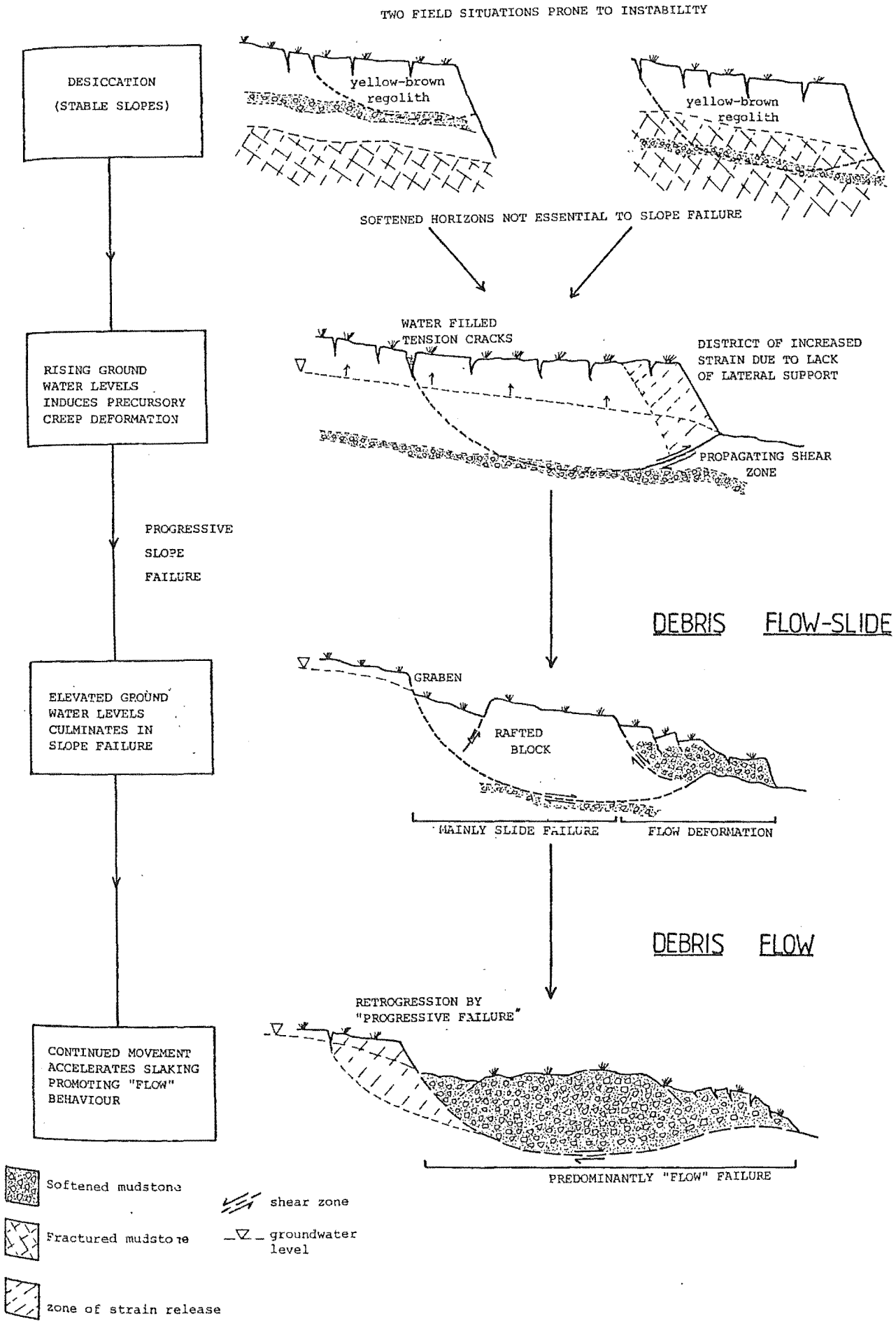

Fig.6.2: Hypothetical evolution of shallow mass movement within the Hampden mudstone.

a) they exist at softened strength and as such are "weak" zones within the profile;
b) they are relatively impermeable in comparison to uniquitous regolith/colluvium hence may be associated with transient excess pore pressures.

Initially slope movement is via slow plastic deformation (precursory creep) as shear strength is gradually exceeded by rising ground water levels. Continued "creep" propagates a basal rupture zone and eventually culminates in "slide" failure. Salient failure morphology comprises a principal escarpment, graben structure and an adjacent rafted block in the centre of the slide mass.

Note, field evidence suggests shallow slope failure initiates equally well within fractured blue-grey/yellow-brown mudstones and principal mass movement controls are the extent of mudstone softening in conjunction with ground water levels.

Field observation reveals failure of low angle slopes results in predominantly translational movement, whilst failure of higher angled slopes is mainly rotational (refer section 4.6.1).

9) Slope movements accelerate softening amidst the failure mass reducing permeability and thus accentuating development of transient excess pore pressures, ultimately leading to "flow" deformation. Salient morphology consists of a lobe shaped failure mass of subdued relief with prominent turf mat rippling.

Obviously a continuous gradation exists between the failure mechanisms (slide, flow) with the majority of mass movement a combination of both slide and flow behaviour, ie. "Plug Flow" (Hutchinson, 1970).

10) Retrogression occurs by "progressive failure" due to the removal of lateral support as adjacent

material is displaced downslope (refer section 5.2.4, Appendix 10).

Thus the final scenario is of shallow flow/slide failures "superimposed" on deep-seated mass movement; a situation analogous to the present in-situ state along the northern coastline of Moeraki Peninsula.

6.2.4 Stability Criteria

Factors influencing shallow slope instability within the Hampden Formation are derived from the preceding simplified model to provide a basis for susceptibility mapping.

1) Terrain Activity
   a) Currently active areas are prone to retrogression via "progressive failure" hence districts in their immediate encompassing vicinity are unstable.

   b) Slope failure disrupts structure within the slide mass accelerating mudstone softening, reducing strength and thus encouraging further movement. For this reason even "inactive" mass movement may exist as areas of inherent weakness.

2) Ground Water Levels
   a) High subsurface water tables accentuate the likelihood of slope failure by:
      - increasing stress promoting movement
      - reducing slope shear strength
      - accelerating softening (elevated pore pressure influencing slaking).

   b) Ground water fluctuations expedite mudstone softening lowering strength in the zone of alternate desiccation/saturation.

6.3 MASS MOVEMENT SUSCEPTIBILITY MAPPING

6.3.1 Introduction

Present day topography within Moeraki township is chiefly inherited from a complex sequence of deep-seated failures which indicate that the landscape has an intrinsic susceptibility to slope movement. The township's history of shallow instability has emphasised the critical necessity of knowledge relating to slope processes in the initial stages of town planning; in order to foresee effects of land utilization and to avoid supplementary costs (perhaps unexpected protection and remedial works).

Moeraki town planning has proceeded without such rudimentary information, consequently man's activities have undoubtedly accelerated and triggered further instability which now threatens housing and roading in some areas (original survey plan of 1863 is still adhered to as a basis for residential development).

Increasing urban expansion has necessitated a comprehensive assessment of slope processes. Information facilitating town planning in this regard is best depicted on maps dealing with a specific phenomenon. Data collated from detailed investigations suggests active shallow mass movement poses the predominant threat to township housing and roading, hence plans delineating risk of or susceptibility to surficial slope failure have been compiled for hazard mitigation. Maps entail analysis of the field area via a "blanket" type approach and consequently are no substitute for site-specific investigation.

Stabilization of potential or active landslide terrain is unique to each location and not depicted on this variety of generalised planning aid. Thus the principal aim of susceptibility mapping is to provide guidelines for residential development facilitating long term planning which will minimise further slope instability.

6.3.2 Approach

The problems of mass movement susceptibility mapping within New Zealand has been approached in a number of ways.

O'Byrne (1967) devised eight lithologic groups characterised by increasing severity of erosion. He correlated rock type with soils, topography and erosion to produce maps of the Gisborne-East Cape region at a scale of 1:250,000.

Leslie (1974) used three causal factors (basement lithology, regolith and slope angle) to formulate five classes of landslip potential in the Otago region.

Pettinga (1980) evaluated soil failure susceptibility on a scale of 1:15,000 based on three parameters; geomorphology, likelihood of movement in terms of five susceptibility units (extreme, very high, high, moderate, and low).

Overseas hazard mapping pertaining to slope instability generally follows one of two approaches.

For evaluating large areas (000's square km) "relative stability assessments" based on landslide abundance are accepted methods. Baker and Chieruzzi (1959) assigned stability ratings on a regional basis founded on landslide frequency, size of displaced mass and repair costs. Brabb *et.al.* (1972) correlated landslide inventory mapping with lithologic type to produce relative tendencies of bedrock units to failure.

The second principal method, adopted for appraisal of smaller areas (0's square km), emphasises significant physical processes acting in conjunction with failure mechanisms. Blanc and Cleveland (1968) considered slope angle, strength, stream erosion and susceptibility of different lithologies to erosion.

Hoexter *et.al.* (1978) made relative stability analyses founded on detailed geological mapping which differed in two aspects to approaches outlined above:

1) Areas were classified as stable, potentially unstable, or moving ground rather than in terms of a continuous numerical scale.

2) Evaluation was based on detailed field work without the backup of statistical appraisals on rock type and slope angle.

Hoexter *et.al.* (1978) adopted this approach for "relative stability" mapping in the San Francisco Bay area, stressing assessment parameters plus map scale are site specific and determined by ultimate objective.

Coelho (1979) proposed a three stage process; initially the identification and mapping of slope instability phenomena, secondly the production of risk maps via synoptic evaluation (utilizing lithology, structure and morphology parameters) and thirdly, verification of these zones by stability analyses.

Stevenson and Sloane (1980) adopt a two tier land-use zoning system whereby areas are "descriptively" evaluated in terms of geology and geomorphology to produce guidelines for development and subsequently "proscriptively" zoned when advice on slope stability is ineffectual and compulsive restraints are necessary.

Based on this limited literature review, two common themes on slope deformation mapping emerge:

1) Mass movement assessment parameters are site specific and require detailed local knowledge of field area processes. ie. cannot arbitrarily apply mapping methodology developed for one region to extraneous areas.

2) Content and method of map preparation should be tailored to meet specific requirements.

Bearing these factors in mind a four stage approach was adopted for "relative stability" mapping based on evaluation of active physical process rather than landslide inventory (Fig.6.3).

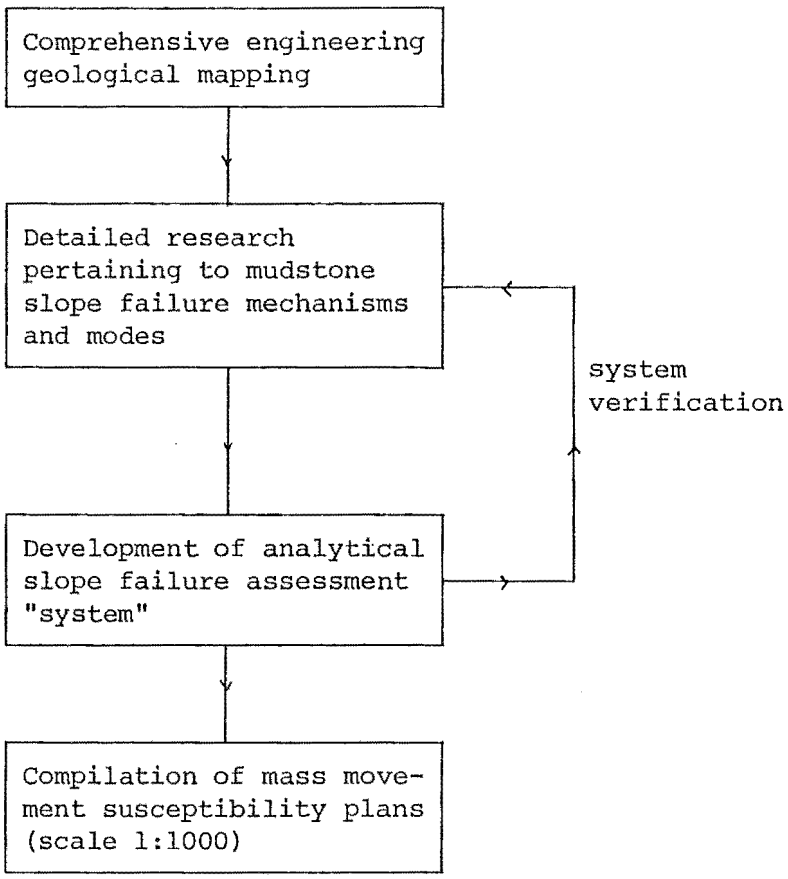

Fig.6.3: Approach adopted for shallow mass movement susceptibility mapping of Moeraki township area.

The first stage entailed comprehensive engineering geological mapping, collating data on slope stability, hydrology, structure and geology. Mass movement in the study area comprises "superimposed" failures evident over a continuum of scales. Field mapping disclosed active hazardous instability was shallow seated and confined within the Kurinui and Hampden Formations.

The second phase involved detailed investigation into failure mechanisms and modes of two representative regions and culminated in the evolution of a "model" of slope failure within the Hampden Formation.

The third step involved synthesising data compiled in phase two to develop a mass movement susceptibility assessment "system". The subjective system evaluates the likelihood of shallow slope failure by appraisal of three principal factors (geology, geomorphology and hydrology). System verification was by application to areas whose stability was estimated from limit equilibrium analyses carried out during phase two. The inherent bias that assessment factors pertain solely to mudstone instability is justified by the fact no significant active slope failure occurs within other lithologies in the field area.

The fourth stage involved a "blanket" application of the stability evaluation system and the compilation of mass movement susceptibility plans (scale 1:1000).

Aim of susceptibility mapping was to "describe" relative instability within the Moeraki township which could subsequently be used as a basis to develop "proscriptive" zoning.

6.3.3 Scale

The ultimate map objective governs precision and complexity of information presented, which in turn dictates map scale.

Geologic hazard plans are commonly compiled on the following scales:

1) Synoptic maps (at a scale 1:100,000 and smaller)

2) Medium scale maps (1:25,000 and 1:50,000)
3) Large scale maps (1:10,000 to 1:5000)
4) Details maps (on scales 1:2000 to 1:500)

Active mass movement affecting housing and/or roading within Moeraki township occurs on a variety of scales ranging from 10 to about 3000 square metres. To adequately portray minor hazardous zones which threaten individual houses, mapping was conducted on the detailed scale of 1:1000 (facilitates correlation with engineering geology plans).

6.3.4 Methodology

The approach chosen was evaluation of mass movement susceptibility via physical process, rather than landslide inventory, thus methodology comprises relative assessments of pertinent natural elements controlling slope deformation.

Processes effecting instability are complex, interrelated natural continuums and for the purposes of this study are isolated into three principal groups:

1) Geologic Factor; accounting for inherent bedrock properties, ie. composition and structure.
2) Geomorphic Factor; depicting landscape "condition" ie. terrain activity.
3) Hydrology Factor; ostensibly appraising chief triggering phemonena, ie. increasing ground water pressure.

Assessment was achieved utilizing an analytical "system" in which factors are numerically weighted depending on importance (Fig. 6.4). Factor quantum was subjectively deduced rather than founded on extensive statistical slope parameter studies, initial appraisal being based on data collated from detailed investigations (mainly a model for mudstone slope failure).

Each principal factor is evaluated by parameters numerically weighted in multiples of five. Once summed, multiples provide a "susceptibility rating" which is categorised into one of four units of "relative stability"; active, unstable,

TERRAIN ASSESSMENT SYSTEM

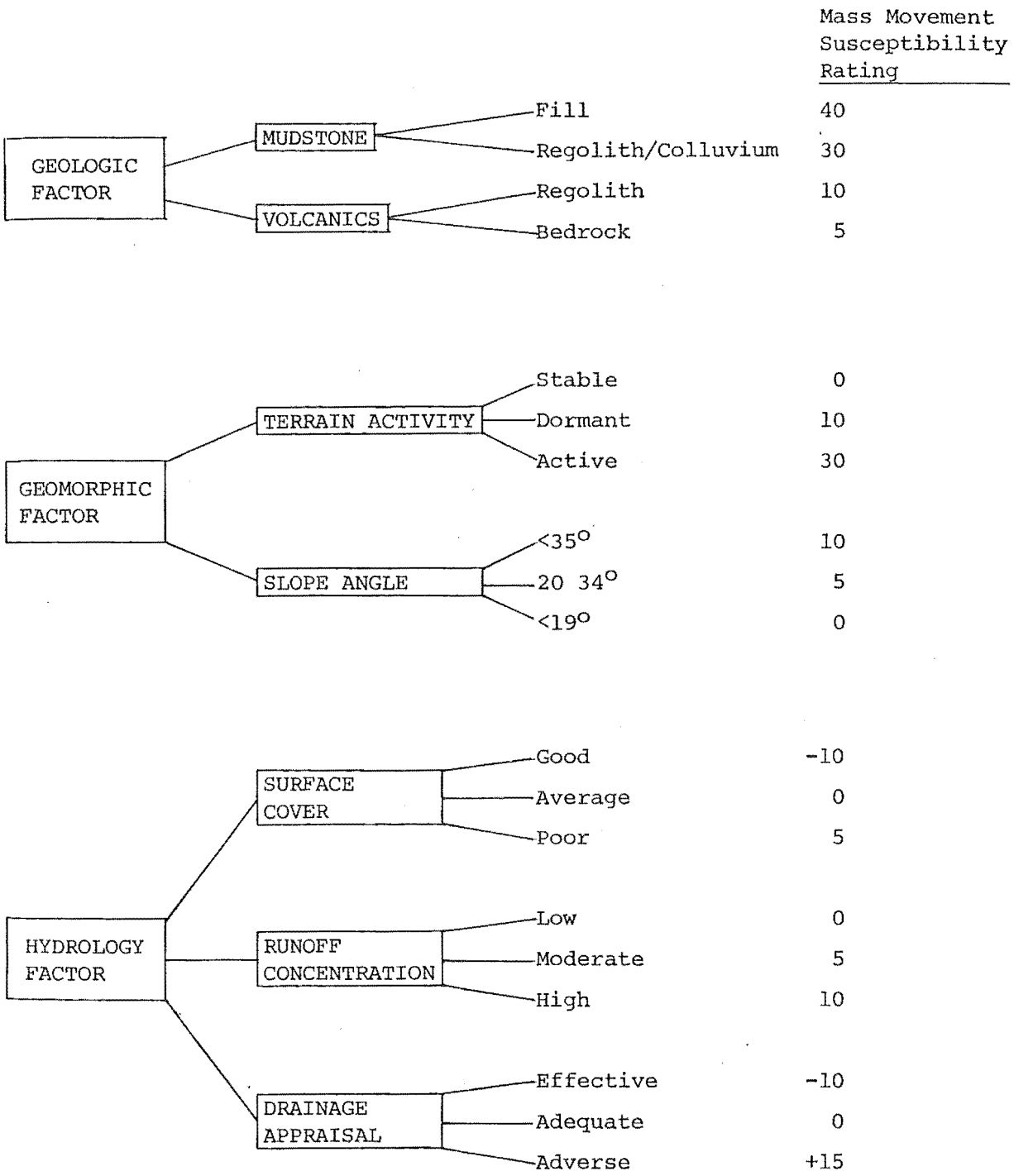

Fig.6.4: Analytical system applied to assess susceptibility to shallow slope failure within the field area; districts assessed are subsequently grouped into "relative stability" units based on summed susceptibility ratings.

potentially unstable and stable. Ultimate parameter and susceptibility unit ratings were determined by iteration in conjunction with application of the system to areas of known stability (ascertained by stability analyses).

Geologic Factor

Structure plus intrinsic properties (mass and material) of bedrock and surficial deposits, significantly influence degradation processes and for this reason the geologic factor is evaluated on lithological rather than Formational boundaries.

Four categories are established:

1) Mudstone Regolith/Colluvium
2) Mudstone Fill
3) Volcanic Bedrock
4) Volcanic Regolith/Colluvium.

Mudstone formations due to their composition (presence of smectites) and intense fracture profiles, are extremely prone to slope failure. No distinction between colluvium, yellow-brown and blue-grey mudstones is made since:

1) Geotechnical parameters of "softened", mudstone/colluvium/regolith are ostensibly the same (refer section 4.5).

2) Field evidence suggests softened yellow-brown and blue-grey mudstones are equal in susceptibility to shallow slope failure (refer section 6.2.3).

Fill (uncompacted or re-compacted) originating from disrupted in-situ mudstone is often exposed in the study area as zones of instability. Obliteration of natural structure, and disaggregation of coherent mudstone by machinery, expedites weathering (softening) reducing strength and thus markedly raises the chances of slope failure.

Weathering of volcanic intrusives produces surficial regoliths of different composition and structure increasing the likelihood of shallow instability and for this reason the lithology is subdivided into two groups; bedrock and regolith/colluvium.

Geomorphic Factor

The geomorphic factor incorporates assessment of currently unstable areas plus topography conducive to ensuing slope failure. This is attained via two parameters.

Terrain Activity

The single most important parameter is terrain activity, which relates to mass movement susceptibility by differentiating the following:

1) High risk regions; areas currently moving or about to move.
2) Moderate risk regions; regions where previous slope movement has increased the chance of ensuing failure (ie. expediting weathering, reducing strength and raising infiltration by disruption of surface runoff).
3) Low risk regions; stable districts not previously involved in slope failure and unlikely to move in present in-situ conditions.

Terrain activity was categorized active, dominant and stable according to Varnes (1978) and refers to classification of shallow slope deformation (refer section 3.3.5).

Whether "failed" material approaching residual value can ever increase in strength with the passage of time is unknown, but obviously of great interest in this context. For the purposes of this study strength is assumed non-recoverable, hence the determination of slope failure "age" is unnecessary.

To attain plausible mass movement susceptibility assessment areas exhibiting major "creep" movements were classified, dormant, whilst defined areas of displacement encompassed by rupture (tension, shear) zones were classified active.

Slope Angle

High slope angles enhance tendencies for mass "creep" and progressive slope failure (refer to Appendix 10), hence the inclusion as a separate parameter.

No statistical evaluation of "critical" mudstone slope angles was carried out so assessment is purely subjective.

Field evidence suggests slope angle in a subordinate influence on slope instability with the principal factors being ground water levels and extent of mudstone softening, ie. steep slopes, if well drained remain stable whilst there are numerous active, low angle failures in areas of ground water concentration (ie. Domain and School Slips).

The entire study area predominantly faces north and is subject to the same prevailing climate with minor changes in outlook not significantly influencing slope profile or deposits. For this reason slope aspect was not incorporated in assessment.

No coastal erosion parameter was felt necessary since all significant shoreline slope failure appears controlled by poor drainage rather than wave action (refer section 4.6.3).

Hydrology Factor

Shallow slope deformation appears predominantly via drained failure chiefly as a result of increased ground water levels.

High water tables elevate pore pressures and accelerate softening, both of which reduce strength facilitating failure. Raised ground water levels, triggering movement are associated with increased regolith/colluvium "through flow". Through flow is governed by an interaction of elements which was assessed by three parameters.

Surface Cover

Surface cover dealt with estimation of comparative drainage infiltration rates, ie. poor denoted little spasmodic grass vegetation, average refers to dense grass plus occasional shrubs, and good applies to roading, housing and dense clusters of vegetation.

Runoff Concentration

Surface ponding following heavy precipitation occurs in deflated zones resulting in localised increased ground water levels. Evaluation of this parameter was largely based on topography, eg. amphitheatre escarpments often result in "high" runoff accumulation at their base as opposed to free draining areas of flat morphology causing "low" or minimal runoff ponding.

Drainage Appraisal

This parameter assessed the efficiency of any drainage related structure. Drainage was denoted "effective" for an area should a specific structure (culvert) result in the lowering of ground water levels. Similarly should "through flow" within regolith (via a permeable horizon), elevate the water table, drainage in the area affected was described as "adverse".

6.3.5 Map Compilation

Susceptibility mapping was on compilation base plans collating terrain activity, slope angle, vegetation and drainage data. A geomorphological approach for base map preparation was used to facilitate correlation with in-situ morphology and engineering geology plans (scale 1:1000) depicting shallow instability. Mass movement susceptibility map construction was in four phases:

1) The field area was divided into zones of similar relief, terrain activity and drainage to form "geomorphic regimes".

2) Each "regime" was individually assessed and susceptibility ratings ascribed using the "system" outlined.

3) Ratings were contoured into four relative mass movement susceptibility units.

4) The final overlay maps were draughted and checked for any anomalous susceptibility zoning.

6.3.6 Limitations

1) The phenomenon of mass "creep" manifested amidst mudstone formations results in a movement continuum from imperceptible (mm/year) to rapid (cm/day) making classification into isolated susceptibility units difficult. For this reason overlap between mass movement susceptibility units is inevitable and unit boundaries are transitional.

2) Regions are assessed as isolated pockets without reference to effects of surrounding areas, ie. an anomalously stable zone may be encompassed by potentially unstable areas. However such idiosyncrasies are corrected following initial map compilation.

3) Numerical evaluation of physical parameters is subjective. This can only be overcome by exhaustive statistical studies comparing relative importance and inter-relationships of each parameter.

4) Susceptibility mapping is based on 1981 to 1982 in-situ conditions and subsequent alterations to topography or drainage may change susceptibility ratings.

6.3.7 Relative Mass Movement Susceptibility Units

Relative mass movement susceptibility within Moeraki township was delineated on geomorphological maps (scale 1:1000) in terms of four units; active, unstable, potentially unstable and stable.

Active (numerical rating >60)

Regions actively moving under current in-situ conditions within and along well delineated zones of shear. Movements in excess of 10 cm/year.

Active mass movement occurs as isolated plots predominantly in areas of concentrated ground water. Onset of instability is normally preceded by development of tension cracks concentric in plan and concave downslope, ensuing plastic

deformation of the encompassed area evolves into a slowly expanding (concurrently retrogressing and advancing) debris flow-slide with movement principally via drained failure.

Active areas delineated are hazardous to roading and housing. Movement of most "active" zones can be attributed to a single cause (eg. drainage concentration) which often can be alleviated by appropriate remedial measures.

Dense shrub vegetation increases stability by minimising ground water fluctuation, ie. reduces infiltration plus water loss via evaporation. Landscaping of presently "active" areas (altering the centre of gravity relative to the failure mass) would probably have little effect on displacement rates. ie. intrinsic mudstone properties mean slides can propagate at low angles and any zones of mudstone "fill" would be very susceptible to slope failure. Established "active" regions generally exist at strengths approaching residual value so following stabilzation of movement would still exist as zones of high "risk" and should not be considered stable for surface construction.

Unstable Areas (numerical rating 51 to 60)

Regions prone to slope failure under current in-situ conditions within and along broadly manifested zones of shear. Subject to significant creep movement in the order of 5 cm to 10 cm/year.

Unstable zones comprise peripheral transitional districts generally associated with active slope failure. Delineated by discontinuous rupture (tension or shear) zones, they exist as areas of significant intermittent creep which may ultimately result in slope failure. Displacement is generally under drained conditions as a result of:

1) Removal of buttressing support, ie. by adjacent active mass movement.

2) Drainage concentration.

Areas are "high risk" jeopardizing roading and housing. Appropriate remedial work (drainage, vegetation) will stabilize

most zones if considered with regard to surrounding terrain, ie. incorporate neighbouring active instability in corrective measures.

Potentially Unstable Areas (numerical rating 40 to 50)

Zones either subject to or prone to significant mass "creep" displacement under present in-situ conditions (2 cm to 5 cm/year).

In the main, these are regions of moderate to steep relief where slope angle sufficiently increases gravity related stresses to induce significant creep. Active and unstable regions undergo movement principally ascribed to a specific cause; potentially unstable areas exist in a "meta stable" state attributed to the sum of a number of in-situ factors (intrinsic mudstone properties, terrain activity, slope angle, drainage). Hence under adverse conditions the region will most likely become progressively unstable and finally active (ie. influences such as drainage concentration, vegetation removal, human activity, excess precipitation).

Stable Areas (numerical rating <40)

Comparatively stable areas possibly subject to mass "creep" movements in the order of 2 cm to 4 cm/year.

Predominantly regions of subdued relief within mudstone and volcanic terrain where adequate local drainage ensures stability.

6.3.8 Susceptibility Map Criticism

1) The majority of septic tank locations and associated areas of adverse drainage were not included in assessment.

2) Revegetation following extensive regrading of original topography has masked some potentially unstable zones of mudstone fill; zones not accounted for in assessment.

3) Comprehensive appraisal of stability is only made in two regions; the Motor Camp and Davids Road areas where subsurface data is known

6.4 RECOMMENDATIONS ON LAND-USE ZONING

1) Mass movement susceptibility mapping should be utilized as the principal basis for "proscriptive" land-use zoning for hazard mitigation within Moeraki township.

   Deep-seated slope failure affecting the township area, if active, is envisaged as slow creep displacement of large coherent mudstone "blocks", hence does not jeopardize housing/roading to the same extent as active shallow mass movement but nevertheless must be considered in ultimate land-use zoning.

2) The generalised analytical approach of stability assessment means susceptibility mapping is no substitute for site specific investigations.

3) Mass movement "risk" depicted on susceptibility plans should be made plain to building owners in the proximity of "active" and "unstable" areas so they may take prudent precautions such as remedial drainage and the avoidance of deep earthworks.

4) Active and unstable areas delineated on mass movement susceptibility maps require further engineering geological input to confirm stability evaluation and determine appropriate remedial measures.

5) If areas depicted unstable or active on susceptibility maps are effectively stabilized by remedial measures they will remain as inherently weak zones having been associated with increased strain and hence careful consideration should be given prior to utilization for surface construction.

6) Residential development in areas portrayed "potentially unstable" on susceptibility plans is technically feasible on low angle slopes, but would require site specific design and on the steeper slopes ($>20^{o}$) is not recommended.

7) Development of areas outlined "stable" on mass movement susceptibility maps is deemed safe regarding shallow slope failure, but should be recessed from escarpments a minimum of 15 m.

8) All surface structure design should allow for significant mass "creep" deformation in the order of 2 cm to 4 cm/year.

9) Drainage concentration should be avoided whenever possible and never allowed to accumulate behind steep scarps or in the vicinity of mass movement depicted active/dormant on detailed engineering geology plans (scale 1:1000).

6.5 FURTHER INVESTIGATION REQUIREMENTS

1) Comprehensive analyses of all Moeraki township cadestral survey data (1890 to the present) with the object of delineating areas of relative instability pertaining to deep-seated slope failure (creep deformation).

2) Continued re-appraisal of survey information to check movement rates and if possible the formation of networks surveyed annually in "dangerously" unstable areas.

3) Site-specific investigations to develop design "criteria" for future buildings and to determine appropriate remedial options for zones portrayed currently "active" on mass movement susceptibility plans.

CHAPTER SEVEN

CONCLUSIONS

1) Moeraki township is established on a complex sequence of deep-seated slope failures developed within underlying mudstones.

2) Damage to housing and/or roading is attributed principally to shallow slope failure confined within the Kurinui and Hampden mudstone formations, outcropping over the western section of Moeraki township.

3) The mudstone units are over-consolidated, containing significant quantities of smectite clays and are subject to strain softening. The "softening" phenomenon, is accelerated by high ground water pressures and results in shallow "progressive slope failure".

4) Surficial instability within the township is mainly via cohesive flow-slide behaviour with salient "active" zones moving at rates in excess of 15 cm/year.

5) Drainage is the principal control of shallow mass movement within mudstone formations.

   Ground water concentration accentuates gravity related forces promoting slope failure, reduces drained strength by increasing pore pressure, accelerates the "softening" process and for this reason markedly increases the likelihood of mass movement.

6) Comparatively stable mudstone regolith/colluvium at low slope angles can be expected to exhibit "creep" displacements in the order of 2 cm to 4 cm/year.

7) Residential development of Moeraki township can safely continue provided a "proscriptive" land use zoning scheme is adopted for hazard mitigation.

REFERENCES

REFERENCES

ARMAN, A. 1970: Engineering classification of organic soils, Highway Res. Rec., No.310: 75-89.

ATTERBERG, A. 1911: Die Plastizitäi der Tone, Int. Mitt. für Bodenjunde, I: 10-43.

BADGER, C., CUMMINGS, A. and WHITMORE, R. 1956: The Disintegration of shales in water. J.N. Inst. of Fuel: 417-423.

BAKER, R.F. and CHIERUZZI, R. 1959: Regional concept of landslide occurrence. Highway Res. Bd. Bull., 216: 1-16.

BARTON, N. 1973: Review of a new shear-strength criterion for rock joints. Eng. Geol. 7: 287-332.

BENSON, W.N. 1940: Landslides and Allied Features in the Dunedin District in Relation to Geological Structure, Topography, and Engineering. Trans. Roy. Soc. N.Z. Vol.70: 249-263.

_____ 1941: Basic Igneous Rocks of Eastern Otago and the Tectonic Environment, Part 1. Trans. Roy. Soc. N.Z. Vol. 71: 208-222.

_____ 1942: Basic Igneous Rocks of Eastern Otago and the Tectonic Environment, Part 2. Trans. Roy. Soc. N.Z. Vol. 72: 85-110.

_____ 1943: Basic Igneous Rocks of Eastern Otago and the Tectonic Environment, Part 4, Section A. Trans. Roy. Soc. N.Z. Vol. 73: 116-138.

_____ 1944: Basic Igneous Rocks of Eastern Otago and the Tectonic Environment, Part 4, Section B. Trans. Roy. Soc. N.Z. Vol. 74: 71-133.

_____ 1945: Basic Igneous Rocks of Eastern Otago and the Tectonic Environment, Part 4, Section C. Trans. Roy. Soc. N.Z. Vol. 75: 288-318.

_____ 1946a: Basic Igneous Rocks of Eastern Otago and the Tectonic Environment, Part 5. Trans. Roy. Soc. N.Z. Vol. 76: 1-32.

_____ 1946b: Landslides and their Relation to Engineering in the Dunedin District, New Zealand. Econ. Geol., Vol. XLI, No. 4.

BIRKLAND, P. 1980: Pedology, Weathering and Geomorphological Research. Oxford University Press. 285p.

BISHOP, A.W. and HENKEL, D.J. 1957: The Measurement of Soil Properties in the Triaxial Test. Edward Arnold Ltd (London). 228p.

BJERRUM, L. 1967: Progressive failure in slopes of over-consolidated plastic clay and clay shales. Journ. Soil Mech. Found. Div., Proc. ASCE 93, No.SM5: 3-49.

BLANK, R.P. and CLEVELAND, G.B. 1968: Natural slope stability as related to geology, San Clemente area, Orange and San Diego Counties, California. Calif. Div. Mines Geol., Spec. Rep.98, 19p.

BLOOMFIELD, C. 1953: A Study of Podzolization: Part II. The Mobilization of Iron and Aluminium by the Leaves and Bark of *Agathis Australis* (Kauri). J. Soil Sci. 4: 17-23.

BOUCHARDT, G.A. 1977: Clay mineralogy and slope stability. Calif. Div. Mines Geol., Spec. Rep.133. 15p.

BRABB, E.E., PAMPEYAN, E.H. and BONILLA, M.G. 1972: Landslide susceptibility in San Mateo County, California. In: San Francisco Bay Region Environment and Resources Planning Study - Basic Data Contrib. 43; U.S.G.S. Misc. Field Stud. Map, MF-360.

BROWN, D.A. 1959: Kurinui Formation. In Lexique Stratigraphique International, Vol. 6, FASC 4 (ed. Fleming, C.A.).

_____ : Moeraki Subdivision. Geo. Surv. Bull. No. 44. (unpub).

BROWN, I.R. and MARTIN, G.R. 1977: Methods for the investigation and design of cut slopes in fractured rock. NRB Report.

BUCKMAN, H.O. and BRADY, N.C. 1969: The Nature and Properties of Soils. The Macmillan Company (7th Edition).

CADLING, L. and ODENSTAD, S. 1950: The vane borer: an apparatus for determining the shear strength of clay soils directly in the ground. Roy. Swedish Geotech. Inst. Proc. 2.

CARROLL, D. 1970: Clay minerals; a guide to their X-ray identification. G.S.A. Special Paper 126.

CARSON, M.A. and KIRKBY, M.J. 1972: Hillslope Form and Process. Cambridge University Press (London), 425p.

CASAGRANDE, A. 1932: The structure of clay and its importance in foundation engineers. J. Boston. Soc. Civil Eng. 19, No.4. 168p.

CHANDLER, R.J. 1972: Lias clay: weathering processes and their effect of shear strength. Géotechnique 22, No. 3: 403-431.

COELHO, A. 1979: Engineering geological evaluation of slope stability for urban planning and construction. Bull. Int. Assoc. Eng. Geol., No. 19: 75-78.

COOMBS, D.S. and DICKEY, J.S. 1965: The Early Tertiary Petrographic Province of North-East Otago: Waiareka and Deborah Volcanic Formations. In N.Z. Volcanology, South Island. (ed. B.N. Thompson and L.O. Kermode). NZ D.S.I.R. Info Series, No.51.

COOMBS, D.S. and NORRIS, R.J. 1981: The East Abbotsford, Dunedin, New Zealand, Landslide of August 8, 1979, An Interim Report. Bull. Liaison Labo. P. et Ch., Special X, jan v. 1981. p27-34.

COX, S.H. 1883: On the Shag Valley. Rep. Geol. Explor. 15: 55-57.

FINLAY, H.J. and MARWICK, J. 1940: The Divisions of the Upper Cretaceous and Tertiary in New Zealand. Trans. Roy. Soc. N.Z. 70: 77-135.

FLAATE, K. 1966: Factors Influencing the Results of Vane Tests. Canadian Geotech. Jol. 3, No. 1: 18-31.

FOOKES, P.G., DEARMAN, W.R. and FRANKLIN, J.A. 1971: Some Engineering Aspects of Rock Weathering with Field Examples from Dartmoor and Elsewhere. Q. Joul. Eng. Geol., Vol. 4: 139-85.

GAGE, M. 1957: The Geology of Waitaki Subdivision. N.Z. Geol. Surv. Bull. 55.

GIBBS, B.J. 1965: Error due to Segregation in Quantitative Clay Mineral X-ray Diffraction Mounting Techniques. Amer. Min., Vol. 50: 741-51.

HAAST, J. von. 1872: Report on Shag Point Coal Fields, Otago. Rep. Geol. Explor. 7: 148-153.

HECTOR, J. 1862: Dept. Reports, Session XVI, Otago Prov. Govt. Gazette: 13-15.

_____ 1866: First General Report on the Coal Deposits of New Zealand. Rep. Geol. Explor. 1: 1-46.

_____ 1877: Progress Report. Rep. Geol. Explor 10.

_____ 1884: Progress Report, 1883. N.Z. Geol. Surv. Rep. Geol. Explor. 1883-4, 16, XIV (Waiareka Tufas, Series).

HOEXTER, D.F., HOLZHAUSEN, G. and SOTO, A.E. 1978: A Method of Evaluating the Relative Stability of Ground for Hill-slide Development. Eng. Geol., No. 12: 319-336.

HOLMES, A. 1965: Principals of Physical Geology. Thomas Nelson and Sons Ltd. 3rd edition.

HUTCHINSON, J.N. 1970: A Coastal Mudflow on the London Clay Cliffs at Beltinge, North Kent. Géotechnique, Vol. 20, No. 4: 412-438.

HUTTON, F.W. 1875: Geology of Otago, Part 1 of Report on the Geology and Gold Fields of Otago. 151p, 7 plates.

JACKSON, M.L. 1956: Soil Chemical Analysis - Advanced Course. Pub. by author, Dept. of Soils, Univ. of Wisconsin.

JANBU, N. 1973: Slope Stability Computations. In Embankment Dam Engineering, Casagrande Volume. John Wiley and Sons Ltd.

KER, D.S. 1970: Renewed movement on a slump at Utiku. NZ J. of Geol. and Geophys 13: 996-1017.

LESLIE, D.M. 1974: Effects of Basement Lithology, Regolith and Slope on Landslide Potential, Otago Peninsula, New Zealand. Soil. Bur. Scient. Rep. 12. 25p.

LEWIS, D.W. 1981: Practical Sedimentology. Apteryz.

LO, K.Y. 1972: An Approach to the Problem of Progressive Failure. Canadian Geotech. Jol. 9: 407-428.

MacEWAN, D. 1946: The identification and estimation of montmorillonite group of minerals, with special reference to soil clays. J. Soc. Chem. Ind. 65: 298-305.

McDONALD, K.C. 1940: History of North Otago. Oamaru Mail Coy. Ltd. 275p.

McLEAN J.D. 1976: A Systematic Method of Soil Description. N.Z. Geol. Surv. Eng. Geol. Rep. EG265. 14p.

McKAY, A. 1877: Oamaru and Waitaki Districts. N.Z. Geol. Surv. Rep. Geol. Explor. 1876-77, 52 (Hampden Beds).

_____ 1877: On the Younger Secondary and Tertiary Formations of Eastern Otago - Moeraki to Waikouaiti. N.Z. Geol. Surv. Rep. Geol. Explor. 1886-87, 18: 1-23.

MANTELL, G.A. 1850: Notice of the remains of the Dinornia and other birds. Q. Joul. Geo. Soc. (London), 6: 319-342.

MARWICK, J. 1926: Molluscan fauna of the Waiarekan Stage of the Oamaru Series. Trans. N.Z. Inst. 56: 307-16.

MILLAR, P.J. 1982: The Triaxial Test Method. MOW Central Laboratories Report No. 2-82/8.

MOERAKI CENTENARY SOUVENIR 1836-1936. Whitcombe and Tombs Ltd, L 6406.

MORGENSTERN, N.R. 1970: Discussion on Black Shale Heaving at Ottawa, Canada. Canadian Geotech. J.L. 7: 114-115.

MORGENSTERN, N.R. and TCHALENKO, J.S. 1967: Microscopic Structures in Kaolin Subjected to Direct Shear. Géotechnique 17: 309-328.

MUTCH, A.R. 1963: Sheet 23, Oamaru (1st ed) Geological Map of New Zealand 1:250,000. D.S.I.R.

NAKANO, R. 1967: On Weathering and Change of Properties of Tertiary Mudstone Related to Landslide. Soils and Found.7: 1-14.

NEW ZEALAND SOIL BUREAU 1972: Soil Bureau Laboratory Methods. N.Z. Soil Bureau Scientific Report 10.

O'BYRNE, T.N. 1967: A correlation of rock types with soils, topography, and erosion in the Gisborne-East Cape region. N.Z. Joul. Geol. and Geophys 10: 217-31.

PATTERSON, B.R. 1980: Moeraki Township, Slope Instability. N.Z. Geol. Surv., D.S.I.R. J42/16 (unpub).

PETTINGA, J.R. 1980: Geology and Landslides of the Eastern Te Aute District, Southern Hawkes Bay. Unpub. Ph.D. Thesis, University of Auckland. 602p.

_____ in prep. The Waipoapoa Landslide: A Deep-Seated Complex Wedge Failure in Tertiary 'Soft-Rock' Flysch; Southern Hawke's Bay, New Zealand.

SCHRODER, J.F. 1971: Landslides of Utah. Utah Geol. Min. Sur. Bull., No. 90. 51p.

SHARP, C.F.S. 1938: Landslides and Related Phenomena: A Study of Mass Movements of Soil and Rock. Columbia Univ. Press (New York). 137p.

SKEMPTON, A.W. 1953: The Colloidal Activity of Clays. Proc. 3rd Int. Conf. Soil Mech. and Found. Eng. Vol. 1: 57.

_____ 1964: Long-Term Stability of Clay Slopes. Géotechnique Vol. 14, No. 2: 77-101.

_____ 1966: Some Observations on Tectonic Shear Zones. Proc. 1st. Int. Conf. Rock Mech., Lisbon 1: 329-335.

_____ 1970: First-Time Slides in Over-Consolidated Clays. Géotechnique, Vol. 20: 320-324.

_____ 1977: Slope Stability of Cuttings in Brown London Clays. Proc. 9th Int. Conf. Soil Mech. and Found. Eng. (Tokyo): 261-269.

SKEMPTON, A.W. and PETLEY, D.J. 1967: The Strength along Structural Discontinuities in Stiff Clays. Proc. Geotech. Conf., Oslo, Vol. 2: 29-46.

SMALE. D., van der LINGEN, D.J. and BELL, D.H. 1982: A Landslide near Mt. Vulcan, North Canterbury, New Zealand. J.L. Geol. Geophy. 25: 397-404.

SPANGLER, M.G. and HANDY, R.L. 1973: Soil Engineering. 3rd edition. Harper and Row.

STEVENSON, P.C. and SLOANE, D.J. 1980: The Evolution of a Risk-Zoning System for Landslide Areas in Tasmania, Australia. In 3rd Aust-NZ Geomech. Conf. on Geomech (Wellington).

STOUT, M.L. 1971: Landslides in the Kilmog Hill-Sea Cliff area, South Island, New Zealand. NZ Geol. Surv. Rep (unpub), D.S.I.R.

TAYLOR, N.H. and POHLEN, I.J. 1979: Soil Survey Handbook. A New Zealand Handbook for the Field Study of Soils. N.Z. Soil Bur. Bull. 25. 242p.

TAYLOR, R. and SPEARS, D. 1970: The Breakdown of British Coal Measures. Int. Jl. Rock Mech. Min. Sci. 7: 481-501.

TERZAGHI, K. and PECK, R.B. 1967: Soil Mechanics and Engineering Practice. John Wiley and Sons. 729p.

TONKIN and TAYLOR, 1982: Land Use Management Plan Moeraki Township, Waitaki County. Unpub. Rep. 12p.

TRAIL, C. 1869: On the Tertiary Series of Oamaru and Moeraki. Trans. Roy. Soc. of N.Z. Vol. 2: 166-169.

UNITED STATES BUREAU OF RECLAMATION EARTH MANUAL 1974: U.S. water resources technical publication. U.S. Government Printing Office (Washington).

VARNES, D.J. 1958: Landslide Types and Processes. In Landslides and Engineering Practice. High. Res. Board Spec. Rep. 29: 20-47.

_____ 1978: Slope Movement Types and Processes. In Landslides Analysis and Control. Trans. Res. Board Spec. Rep. 176.

VAUGHAN, P.R. 1969: A Note on Sealing Piezometers in Boreholes. Géotechnique, 19: 405.

VAUGHAN, P.R. 1974: The Measurement of Pore Pressures with Piezometers. In Field Instrumentation in Geotec Engineering. John Wiley and Sons (New York-Toronto): 411-422.

WELLMAN, H.W. 1979: An Uplift Map for the South Island of New Zealand, and a Model for Uplift of the Southern Alps. Roy. Soc. N.Z. Bull. 18 (Walcott and Cresswel, eds.).

WHITTIG: L.D. 1965: X-ray Diffraction Techniques for Mineral Identification and Mineral Composition. In Methods of Soil Analysis Part 1. (eds. Black, C.A., Evans, D.D., White, J.L., Ensminger, L.E., Clark, F.E.) Published by Am. Soc. of Agronomy (No. 9): 568-577.

WINTERKORN, H.F. and FANG, H. 1975: Foundation Engineering Handbook. Van Nostrand Reinhold Ltd. 626p.

APPENDICES

APPENDIX 1

GEOLOGICAL TIME SCALE

NEW ZEALAND GEOLOGIC TIME SCALE

UPPER MESOZOIC-QUATERNARY

SYSTEM	T (my)	SERIES	STAGE	SUB STAGE	MAP SYMBOL	INTERNATIONAL EQUIVALENT	
QUATERNARY	0·001		ARANUIAN		Quor	HOLOCENE	
	0·07		OTIRAN		Quti	WURM	PLEISTOCENE
	0·16		OTURIAN		Qutu	NEOTYRRHENIAN	
			WAIMEAN			RISS	
	0·25	HAWERA	TERANGIAN			EUTYRRHENIAN	
			WAIMAUNGAN			MINDEL	
			WAIWHERAN			PALEOTYRRHENIAN	
	0·28		PORIKAN			GUNZ	
	0·45		CASTLECLIFFIAN	PUTIKIAN	Wu Wc	SICILIAN	
	1·06			OKEHUAN	Wk	DONAU	
	1·60	WANGANUI	NUKUMARUAN	MARAHAUAN	Wa Wn	EMILIAN	
	1·79			HAUTAWAN	Wh	CALABRIAN	
TERTIARY			WAITOTARAN	MANGAPANIAN	Wm Ww	ASTIAN	PLIOCENE
				WAIPIPIAN	Wp		
	5·0		OPOITIAN		Wo	PLAISANCIAN	
		TARANAKI	KAPITEAN		Tk	MESSINIAN	MIOCENE UPPER
	10·5		TONGAPORUTUAN		Tt		
		SOUTHLAND	WAIAUAN		Sw	TORTONIAN	MIOCENE MID
	14·0		LILLBURNIAN		Sl		
			CLIFDENIAN		Sc	HELVETIAN	
		PAREORA	ALTONIAN		Pl	BURDIGALIAN	MIOCENE LOWER
	22·5		OTAIAN		Po	AQUITANIAN	
		LANDON	WAITAKIAN		Lw	CHATTIAN	OLIGOCENE
			DUNTROONIAN		Ld	RUPELIAN	
			WHAINGAROAN		Lwh	LATTORFIAN	
	36·0	ARNOLD	RUNANGAN		Ar	BARTONIAN	EOCENE UPPER
			KAIATAN		Ak		
			BORTONIAN		Ab	LUTETIAN	EOCENE MID
	46·5	DANNEVIRKE	PORANGAN		Dp		
			HERETAUNGAN		Dh	YPRESIAN	EOCENE LOWER
			MANGAORAPAN		Dm		
	53·5		WAIPAWAN		Dw	THANETIAN	PALEOCENE
			TEURIAN		Dt	DANIAN	
UPR MESOZOIC	65·0	MATA	HAUMURIAN		Mh	MAASTRICHTIAN	CRETACEOUS UPPER
			PIRIPAUAN		Mp	CAMPANIAN	
		RAUKUMARA	TERATAN		Rt	SANTONIAN	
			MANGAOTANEAN		Rm	CONIACIAN	
			AROWHANAN		Ra	TURONIAN	
						CENOMANIAN	
	95·0	CLARENCE	NGATERIAN		Cn	ALBIAN	CRETACEOUS LOWER
			MOTUAN		Cm		
			URUTAWAN		Cu	APTIAN	
			KORANGAN		Ck		
						NEOCOMIAN	
	135·0						

APPENDIX 2

CLIMATALOGICAL DATA

A2.1 CLIMATE

Rainfall, wind direction and minimum temperature were recorded daily by Mr and Mrs Kedsley (Pembroke Street) from August 1981 through to October 1982.

Minimum temperature, taken 0.25 m above ground level, indicated frosts chiefly occur during months June, July and August.

Maximum rainfall was recorded in January 1981 (105 mm) and the minimum in July 1982 (10 mm).

Data correlates well with information from the nearest meteorological station established at Trotters Creek (Lat. 45°23'S, Long. 170°49'E). The meteorological station recorded 499 mm of rainfall from August 1981 to August 1982 as compared to 558 mm noted for the study area. Based on data registered at Trotters Creek, 1981 was slightly wetter than average (647 mm, the mean being 623 mm) and 1982 much drier (547 mm).

A2.2 CLIMATOLOGICAL DATA

MONTH	Aug	Sept	Oct	Nov	Dec	Jan	Feb	Mar	Apr	May	Jun	Jul	Aug	Sept	Oct
RAIN (mm)	36	17	68	14	59	105	26	33	80	57	31	10	22	28	104
MIN TEMP (°C)	3	4	7	9	11	10	11	9	6	5	3	2	3	4	5
	TROTTERS CREEK														
RAIN (mm)	50	24	51	11	76	70	35	35	58	25	17	9	28	15	115

Fig. A2.1: Summary of climatological data, recorded daily for the study.

APPENDIX 3

CONSISTENCY LIMITS

Introduction

A3.1 Atterberg Limits

A3.2 Shrinkage Limits

- 3.2.1 Methodology
- 3.2.1 Moisture content
- 3.2.3 Hygroscopic water content
- 3.2.4 Shrinkage limit
- 3.2.5 Linear shrinkage

A3.3 Tabulated Data

INTRODUCTION

Consistency limit testing involved determination of Liquid, Plastic and Shrinkage Limits together with Hygroscopic water content. Testing was on "whole" samples thoroughly remoulded with coarse detritus removed (rock fragments, plant debris). Samples containing considerable quantities of organic matter proved difficult to test and results were ignored in some cases; soil cakes slide "en-masse" without deformation in the liquid limit apparatus cup and relevant moisture content determination was hindered by the presence of unabsorbed water which may have contributed to liquidity or plasticity of samples.

A3.1 ATTERBERG LIMIT DETERMINATION

Whole samples were thoroughly remoulded and saturated with distilled water to about the Liquid Limit, left for three days in covered containers and tested according to NZS 4402, Part 1, 1980.

A3.2 SHRINKAGE LIMIT DETERMINATION

Testing to establish Shrinkage Limit, Linear Shrinkage and Hygroscopic water content were carried out on saturated samples prepared for Atterberg Limit determination. A simplified method of obtaining dried soil pat volume was devised which avoided the use of mercury, hence only approximate parameters are quoted.

A3.2.1 Methodology

1) Soil was thoroughly mixed with distilled water to a consistency fluid enough to be readily worked into a shrinkage dish without the inclusion of air bubbles.

2) Shrinkage dishes of known volume were coated on the inside with a thin layer of grease (silicone based) to prevent soil pat adhesion upon drying.

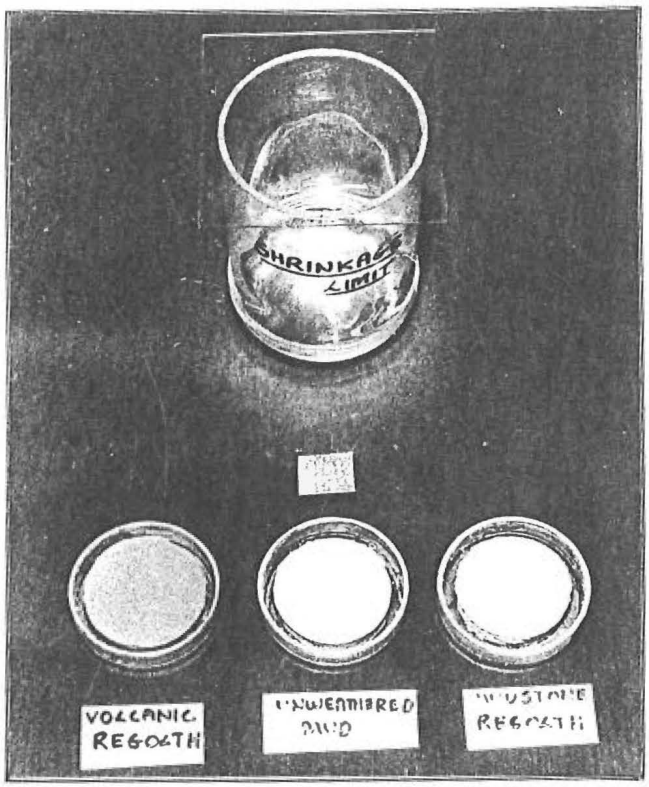

Fig.A3.1: Volume determination apparatus together with symmetrical dried soil pats. Note relative amounts of shrinkage associated with mudstone/volcanic materials.

(dishes are all the same)

3) Dishes were then weighed to 0.000 gms.

4) One third of the dish was then filled with remoulded soil and the dish gently tapped on a firm surface to remove air bubbles; the process was repeated until the dish was filled. The upper surface was then trimmed flush using a spatula and excess soil wiped off.

5) Dish plus soil was weighed to 0.000 gms.

6) Samples were left to air dry for ten days and re-weighed to 0.000 gms.

7) Shrinkage dishes were subsequently placed in an oven ($110^{o}C$) for 24 hours, cooled in a desiccator and re-weighed to 0.000 gms.

8) Estimation of dried soil pat volume was by water displacement. A glass jar, with ground upper edges was weighed to 0.00 gms (M_1) then filled with water and sealed by sliding a glass plate slowly over the upper edge ensuring no trapped air remained in the jar. It was then re-weighed to 0.00 gms (M_2). Symmetrical dried soil pats were sprayed with polyurethane clear plastic and allowed to dry. Coated pats were then immersed and sealed within the jar filled with water and the jar re-weighed to 0.00 gm (M_3). (Fig.A3.1)

The mass of individual plastic coats was assumed negligible and dried pat volume was estimated from the quantity of water displaced calculated by:

$$V_0 = (M_2-M_1)-M_3$$

where V_0 = volume of dried soil pat.

A3.2.2 Moisture Content (W%)

Moisture content of the soil at time it was placed in the dish expressed as a percentage of the dry soil mass was calculated as follows:

$$W\% = [(W-W_0)/W_0] \times 100$$

where W = mass of wet soil pat obtained by subtracting shrinkage dish mass from mass of dish plus wet soil.

W_0 = mass of oven dried soil obtained by subtraction of shrinkage dish mass from mass of dish plus oven dried pat.

A3.2.3 Hygroscopic Water Content (H_W%)

Water retained within the air dried soil cake at room temperature expressed as a percentage of the dry soil mass was calculated by:

$$H_W\% = [(W_1-W_0)/W_0] \times 100$$

where W_1 = air dried pat mass obtained by subtracting shrinkage dish mass from mass of dish plus air dried pat.

To enable H_W comparisons air dried pats were weighed in the same day ie. samples equibrated to same air humidity.

A3.2.4 Shrinkage Limit (SL%)

Shrinkage Limit of a soil is the maximum water content at which a reduction in water content will not cause a decrease in volume of the soil mass.

ASTM D427-61 (1973)

$$SL\% = W-([(V-V_0)/W_0] \times 100)$$

where W = Initial moisture content of wet soil pat.
V = Volume of wet soil pat.
V_0 = Volume of dry soil pat.
W_0 = Mass of oven dried soil pat.

A3.2.5 Linear Shrinkage ($L_S\%$)

Linear shrinkage of a soil is the decrease in one dimension of that soil mass expressed as a percentage of the original dimension when the water content is reduced from a given value to the shrinkage limit (ASTM D427-61, 1974).

$$L_S\% = 100[1-\sqrt[3]{100/(V_S + 100)}]$$

where V_S = The volumetric shrinkage and is calculated from

$$V_S = (W_1-SL)R$$

where R, the Shrinkage ratio is calculated from

$$R = W_0/V_0.$$

A3.3 TABULATED DATA

Data is presented in tabulated format; appropriate corresponding profile descriptions outlined in Appendix 7.

GEOTECHNICAL PARAMETERS

LOCATION: MOTOR CAMP AREA HOLE NO. 1

LITHOLOGY: Mudstone Colluvium (Refer Appendix 7 for Comprehensive, Log)

Sample Depth	Description	Sand %	Silt %	Clay %	Colloid %	PL%	LL%	PI	SL%	L_S%	HW% x10^{-2}	PI/% Clay
0.35		5	44	51	46	30	79	49	14.6	25.2	6.1	0.96
0.50	yellowish-brown mudstone	5	50	45	40	25	65	40	10.5	22.7	6.2	0.88
1.75		6	46	48	39	24	68	44	11.3	28.0	7.7	0.92
1.80	highly organic mudstone	5	47	48	40	40	78	38	7.1	26.1	6.5	0.79
2.30		3	60	37	33	22	51	31	4.5	22.1	4.3	0.84
2.6		4	60	36	32	19	47	28	6.4	19.9	3.9	0.77
3.0	yellowish-brown mudstone	8	57	35	30	25	55	30	9.3	17.0	4.0	0.86
4.2		6	39	55	49	28	77	49	9.3	23.9	7.2	0.89
4.6		6	40	54	49	28	78	50	9.8	24.9	7.2	0.93
5.3		6	44	50	45	27	73	52	10.7	25.2	6.9	1.04
5.7		5	44	51	46	36	85	49				0.96
6.3	highly organic mudstone	6	48	46	41	39	79	40				0.87
6.4		5	57	39	35	42	77	35				0.89
6.42		8	46	46	43	45	87	42	5.4	25.3	4.9	0.91

LOCATION: MOTOR CAMP AREA HOLE NO. P_1

LITHOLOGY: Mudstone Colluvium (Refer Appendix 7 for Comprehensive, Log)

Sample Depth	Description	Sand %	Silt %	Clay %	Colloid %	PL%	LL%	PI	SL%	L_S%	HW% x10^{-2}	PI/% Clay
0→1 m		10	67	34	20	20	39	19	9.6	16.4	2.6	0.83
1.0 m	light reddish-brown mudstone	7	53	40	36	27	62	35	9.7	22.6	4.6	0.88
2.0 m		8	50	42	38	29	68	41	5.5	27.0	5.5	0.98
2.5 m	highly organic mudstone	6	49	45	40	32	80	48	6.6	27.9	5.3	1.06
3.0 m		5	50	45	41	36	78	42	9.3	23.0	4.8	0.93
4.5 m		7	53	40	35	30	68	38	5.0	26.8	5.7	0.95
5.5 m		2	43	55	47	30	78	48	5.1	28.7	6.1	0.87
6.5 m	blue-grey mudstone	7	43	50	46	26	72	46	6.4	26.3	6.1	0.92

LOCATION: DAVIDS ROAD AREA HOLE NO. P_2

LITHOLOGY: Mudstone Colluvium (Refer Appendix 7 for Comprehensive, Log)

Sample Depth	Description	Sand %	Silt %	Clay %	Colloid %	PL%	LL%	PI	SL%	L_S%	HW% x10^{-2}	PI/% Clay
0→1 m	light yellowish-brown mudstone	7	48	45	39	28	65	37	9.7	19.9	5.2	0.82
1→4 m	highly organic mudstone	10	42	48	44	30	79	49	8.8	29.1	6.3	1.02
4→6 m	partly organic mudstone	10	38	52	38	23	68	45	13.6	26.3	7.1	0.87
6→7 m	light reddish-brown mudstone	11	37	55	45	25	72	47	8.5	28.2	7.1	0.85

GEOTECHNICAL PARAMETERS

LOCATION: DAVIDS ROAD AREA HOLE NO. P_3

LITHOLOGY: Mudstone Colluvium (Refer Appendix 7 for Comprehensive, Log)

Sample Depth	Description	Sand %	Silt %	Clay %	Colloid %	PL%	LL%	PI	SL%	L_S%	HW% x10^{-2}	PI/% Clay
60 cm		6	43	51	45	24	67	43	13.3	22.3	6.4	0.84
1.3	yellowish-brown mudstone (partly organic in places)	5	60	25	20	25	47	22	10.6	17.3	2.6	0.88
2.0		9	67	24	17	20	40	20	7.7	18.7	3.2	0.83
2.6	highly organic mudstone	12	62	26	21	20	45	25	9.5	16.2	2.6	0.96
2.85		5	55	40	37	22	56	34	10.3	20.5	6.1	0.85
3.25		5	44	51	45	26	75	49	4.8	28.0	7.7	0.96
4.1	light yellowish-brown mudstone	9	51	40	31	26	64	38	8.3	25.9	5.0	0.95
4.6		8	49	43	33	31	68	37	7.0	26.8	6.7	0.86
4.7		10	47	43	36	27	60	33	7.9	24.6	6.1	0.77

BLUE-GREY HAMPDEN MUDSTONE

(COLLECTED FROM "SOFTENED" HORIZONS EXPOSED ALONG SHORE PLATFORM)

Sand %	Silt %	Clay %	Colloid %	PL%	LL%	PI	SL%	L_S%	HW% x10^{-2}	PI/% Clay
12	38	50	44	26	78	44	11.1	27.0	6.5	0.88
11	47	42	36	23	60	37	8.2	24.0	4.1	0.88
9	44	47	38	24	65	41	5.3	26.2	5.0	0.87
13	41	46	39	21	63	42	6.5	27.6	6.2	0.91
9	42	49	43	26	66	40	9.1	26.1	6.1	0.82

DRIED, WEATHERED REGOLITH

Sand %	Silt %	Clay %	PL%	LL%	PI	PI/% Clay
4	66	30	20	32	12	0.41
8	45	47	25	47	22	0.47

VOLCANIC REGOLITH
(RANDOM SAMPLES)

Sand %	Silt %	Clay %	Colloid %	PL%	LL%	PI	SL%	L_S%	HW% x10^{-2}	PI/% Clay
28	38	34	30	20	41	21	10.0	14.0	4.5	0.63
28	29	33	31	19	43	24	13.0	14.6	4.8	0.73
35	36	29	26	19	42	23	12.3	14.2	4.6	0.79
38	34	28	26	18	35	17	8.6	14.5	3.9	0.61
25	53	22	19	17	31	14	8.6	12.8	3.5	0.64
34	47	29	27	20	41	21	13.9	13.5	3.9	0.72
55	25	20	14	19	34	15	9.8	13.0	2.4	0.75
53	25	22	19	19	35	16	11.0	13.3	2.7	0.71
57	29	14	11	19	29	10	6.5	12.0	1.6	0.71
31	39	30	27	18	39	21	7.0	14.3	3.8	0.69

APPENDIX 4

GRAIN-SIZE ANALYSES

A4.1 Methodology

A4.2 Analysed Data

A4.1 METHODOLOGY

Grain-size analyses of samples were performed utilizing techniques outlined in Lewis (1981). Sand fractions were dry sieved (using 1Ø intervals in the 1 to 4Ø range) with silt and clay tested by pipette analyses. There is a tendency for coarse aggregates and partially weathered material to break up with continued dry sieving hence to avoid bias all samples were sieved for a standard period of 15 minutes.

Disaggregation for pipette analyses was done by hand in a solution of distilled water and Calgon (sodium hexametaphosphate) then subjected to 10 minutes ultrasound treatment.

Samples with excessive organic matter were treated with dilute (10-15%) HCl prior to boiling in 10% H_2O_2 as outlined by Lewis (1981); the initial removal of $CaCO_3$ necessary to prevent formation of Ca oxalates.

Carbonate content of fifteen, fifty gram samples were calculated from weight reduction after treatment with 15% HCl.

A4.2 ANALYSED DATA

To facilitate interpretation of data, results were presented adjacent to consistency limit data in Appendix 3.

Grain-size distributions are relatively consistent for both mudstone and volcanic materials tested; two representative profiles are drawn solely for comparative purposes.

Typical Waiareka Regolith grain-size distribution

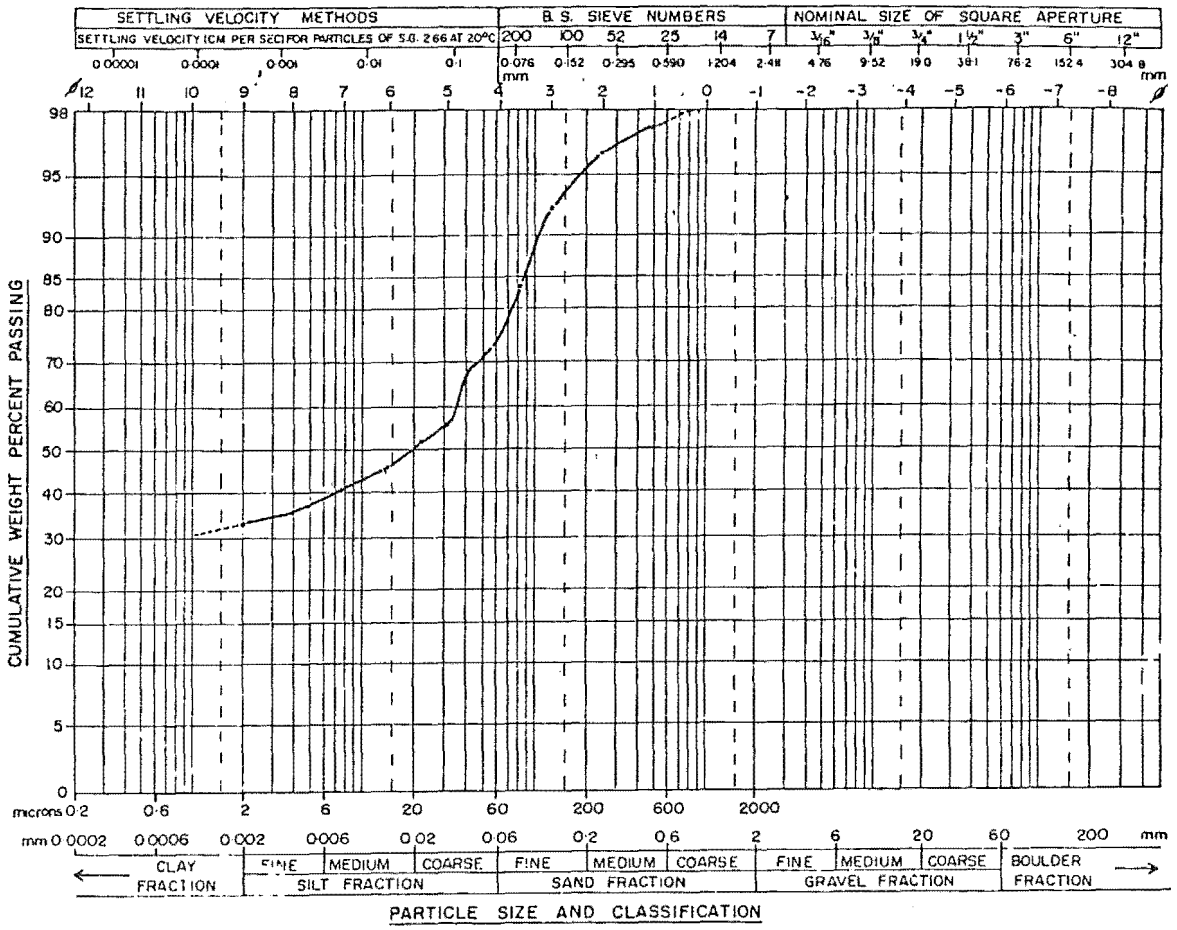

Typical grain-size distribution for Hampden Formation.

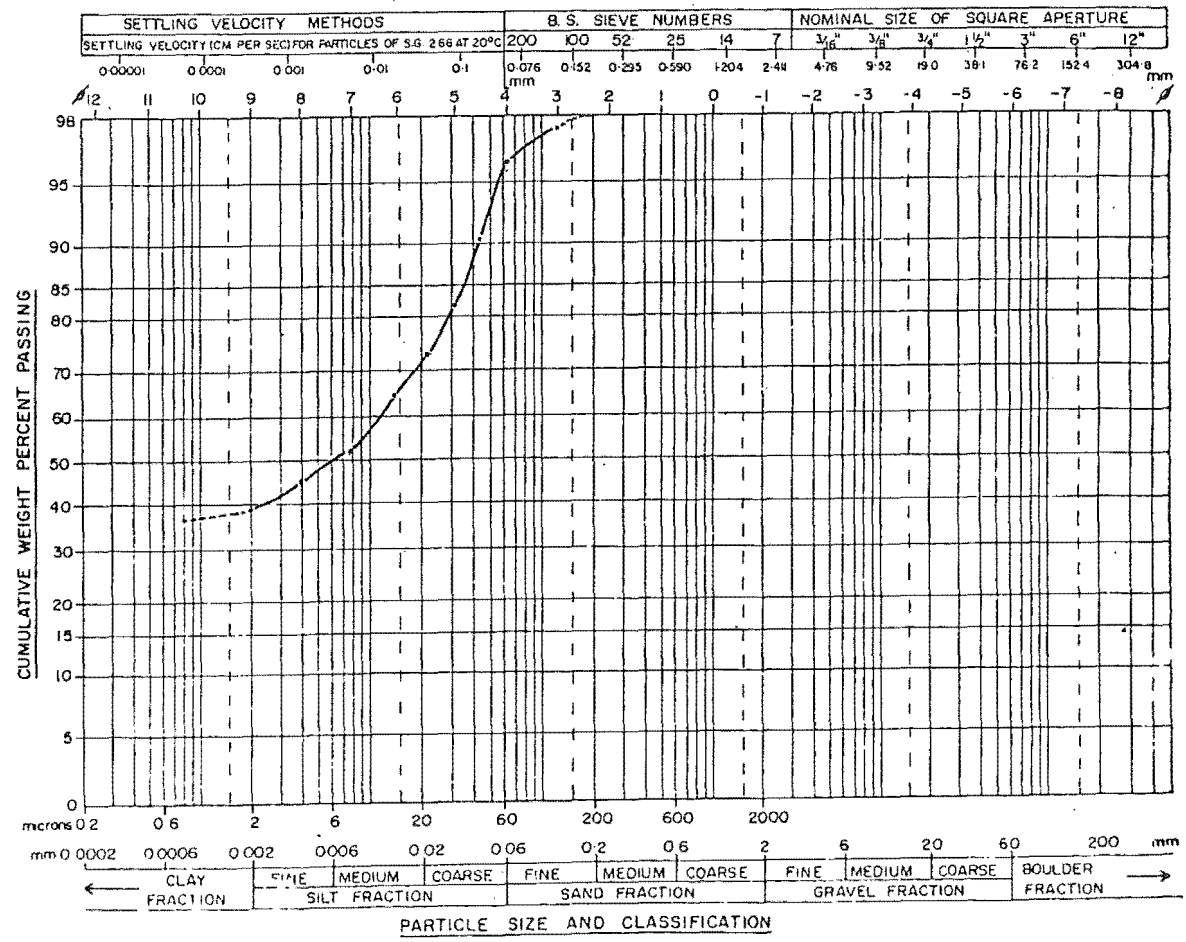

APPENDIX 5

CLAY MINERAL IDENTIFICATION

A5.1 Methodology Exposition

A5.2 Methodology

- 5.2.1 Pretreatments
- 5.2.2 Clay Sampling
- 5.2.3 Ion Saturation
- 5.2.4 Mount Preparation
- 5.2.5 Glycerolation
- 5.2.6 Heating
- 5.2.7 Analysis
- 5.2.8 Identification

A5.1 METHODOLOGY EXPOSITION

Pretreatments and preparation of samples for clay mineral X-ray diffraction are largely dependant on sample type and accuracy required. Lack of standardization in the literature means a brief discussion on methodology adopted is warranted.

Initially sampling for clay mineral identification was from a grain size column during pipette analysis but results were subsequently ignored for two main reasons:

1) Only clays reaching the columns top section during initial agitation are sampled and not the whole clay fraction.

2) Normally sodium hexa-metaphosphate (Calgon) was utilized as a peptizer however results subsequently proved Calgon reacted with swelling clays producing unsatisfactory diffractograms with broad diffuse peaks. Jackson (1956) notes phosphate decomposes oxides plus aluminosilicates and may produce crystalline CaC_2O_4 which would interfere with analyses.

Ensuing analyses were on material sampled from the whole clay fraction with clay flocculation prevented by Na_2CO_3 (PH approximately 5).

Peptizers prevent flocculation by increasing PH (raising relative quantity of OH^- ions) so clay particles electronegativity is maximised causing micelle repulsion. Compounds of hydrated monovalent ions such as sodium are frequently used since these ions do not effectively reduce clay negative charge (Buckman and Brady, 1969).

$$X\boxed{\begin{matrix}\text{clay}\\ \text{micelle}\end{matrix}} + 2H_2O + Na_2CO_3 \rightleftarrows Na\boxed{\begin{matrix}\text{clay}\\ \text{micelle}\end{matrix}} + 2OH^- + H_2CO_3$$

Note: mudstone samples had high quantities of smectites so separation of the clay particles into size fractions as suggested

by Jackson (1956) as an essential aid to establish their presence was unnecessary.

Cementing agents such as carbonates, oxides, organic matter, amorphous silica and alumina are normally removed by "pretreatment" of samples prior to testing since their presence:

1) Prevents effect dispersion and hence hinders separation of the clay fraction.

2) Act as dilutants, thus reducing diffraction intensity of crystalline minerals present (Whittig, 1965).

3) Prevents effective orientation during slide preparation.

4) Decreases sensitivity by lowering the ratio of diffracted maxima to background, ie. copper radiation was used which Fe compounds would absorb, flourece and emit non directional radiation adding to overall background.

Chemical pretreatments were kept to a minimum. Carbonates and soluble salts were removed with a NaOA buffer (PH=5). Carbonate extraction is essential since:

1) Carbonate presence increases diffractogram scatter.

2) Carbonate compounds form upon ion saturation (M^{+}, Mg^{2+})

Different cations may retain different quantities of water of hydration hence it is necessary clay samples be concentrated with common ions so hydration is uniform within each clay type to enhance accurate identification (Whittig, 1965). Since preparation of orientated mounts involves air drying, cations which minimise interlayer absorption due to relative fluctuations in humidity were chosen to saturate samples; these were magnesium and potassium (potassium having a higher bonding energy than other monovalent ions thus low hydration).

Saturation with potassium also tests for closure of smectites and some vermiculite while leaving chlorite expanded.

Samples saturated with Mg ions allows uniform interlayer absorption of water (Whittig, 1965) when air drying and distinction of smectites when saturated with glycerol. Montmorillonite (Mg^{2+}) absorbs double sheets of glycerol molecules amidst layers expanding to 17.7→18 Å separating it from vermiculites and chlorites which remain at 14→15 Å. For this reason glycerol was preferred to ethelene glycol which yields expansion of both smectites and vermiculites to approximately 17 Å. Montmorillonite readily forms complexes with other polar molecules of moderate size (Whittig, 1965) but without the advantages of glycerol assimilation which are:

1) Intense first order basal diffraction, well separated from other peak maxima.
2) Spacing and peak itensity of basal diffraction remaining unaffected by large variation in water content.
3) Low volatility of glycerol resulting in an extremely stable complex.

(MacEwan, 1946)

X-ray diffraction of samples was on prepared orientated slide mounts, the orientation of flaky clay minerals enhancing diagnostic basal (001) diffraction patterns and obscuring less characteristic (hkl) refraction.

Mounts were produced by evaporating flocculated samples from a medium of 95% ethanol. Segregation of clays was minimised due to quick drying and settling interference caused by flocculated clay. Both smear (outlined by Gibbs, 1965) and drop mounts gave similar results and since no quantitative analyses were attempted "drop mounting" was preferred due to ease of preparation and consistency of results.

Heating of potassium saturated samples to 580°C for one hour enabled distinction between chlorites and vermiculites. Vermiculites contain non-exchangeable interlayer hydroxol

complexes which collpase at less than 300°C, whilst Kaolinite becomes amorphous at 550→600°C (Carroll, 1970). Chlorite if present remains after heating having a first order peak of 14 Å and a second order maxima of 7.14 Å.

Diffraction intensity maxima are related to the number of diffraction planes therefore relative intensities should provide an estimation of mineral concentration. However assuming no "screening effect" and "perfect" thickness is achieved in slide preparation a number of other factors apart from mineral concentration influence intensity maxima.

1) Particle size
2) Chemical composition
3) Crystalinity
4) Amorphus substances
5) Variation in orientation

(outlined in detail by Jackson, 1956)

Overlapping of diffractogram peaks, especially at low 2θ angles (mixed layer assemblages) makes it difficult to differentiate background scatter and estimate a base line necessary for measurement of peak intensity and area.

Based on this reasoning no quantitative X-ray diffraction analyses of clays was carried out.

A5.2 METHODOLOGY

5.2.1 Pretreatment

Removal of Carbonates and Soluble Salts

Reagents: Sodium acetate: IN adjusted to PH5 with acetic acid

Saturated NaCl

Samples (10 gm) were placed in 90 mls centrifuge tubes with 50 mls of sodium acetate buffer added to each. The solution was stirred and tubes placed in a water bath for approximately 30 minutes. Sediment was "settled" by centrifuging at 1500 rpm for 5 minutes, supernatant liquid was then poured off and sampled "washed" by adding 50 mls of distilled water, stirring and re-centrifuging (1500 rpm for 5 minutes). If the supernatant liquid remained cloudy a few mls of saturated sodium chloride was added and the sample re-centrifuged (1500 rpm for 5 minutes). (As specified by Jackson, 1956, NZSBS 1972).

HCl was not used for carbonate removal due to its reaction with chlorite minerals.

5.2.2 Clay Sampling

Sampling of the whole clay fraction was carried out using a Multex centrifuge by the method outlined in Fig. A5.2.

5.2.3 Ion Saturation

Samples were saturated with either Magnesium or Potassium ions as outlined in Fig. A5.3. Care was taken to remove all chlorites prior to mounting otherwise salts ($MgCl_2$) may have precipitated onto slides with evaporation.

5.2.4 Mount Preparation

Following ion saturation a mixture of approximately 50% flocculated clay and 50% solution of 95% ethanol was thoroughly mixed. Mounts were formed by placing samples drop by drop onto glass slides ensuring surface tension was not exceeded, then leaving to air dry. Thickness was assumed approximately correct if a felt tipped pen mark on the underside of the glass mount was obscured when placed horizontal on a bench yet visible if held to the light.

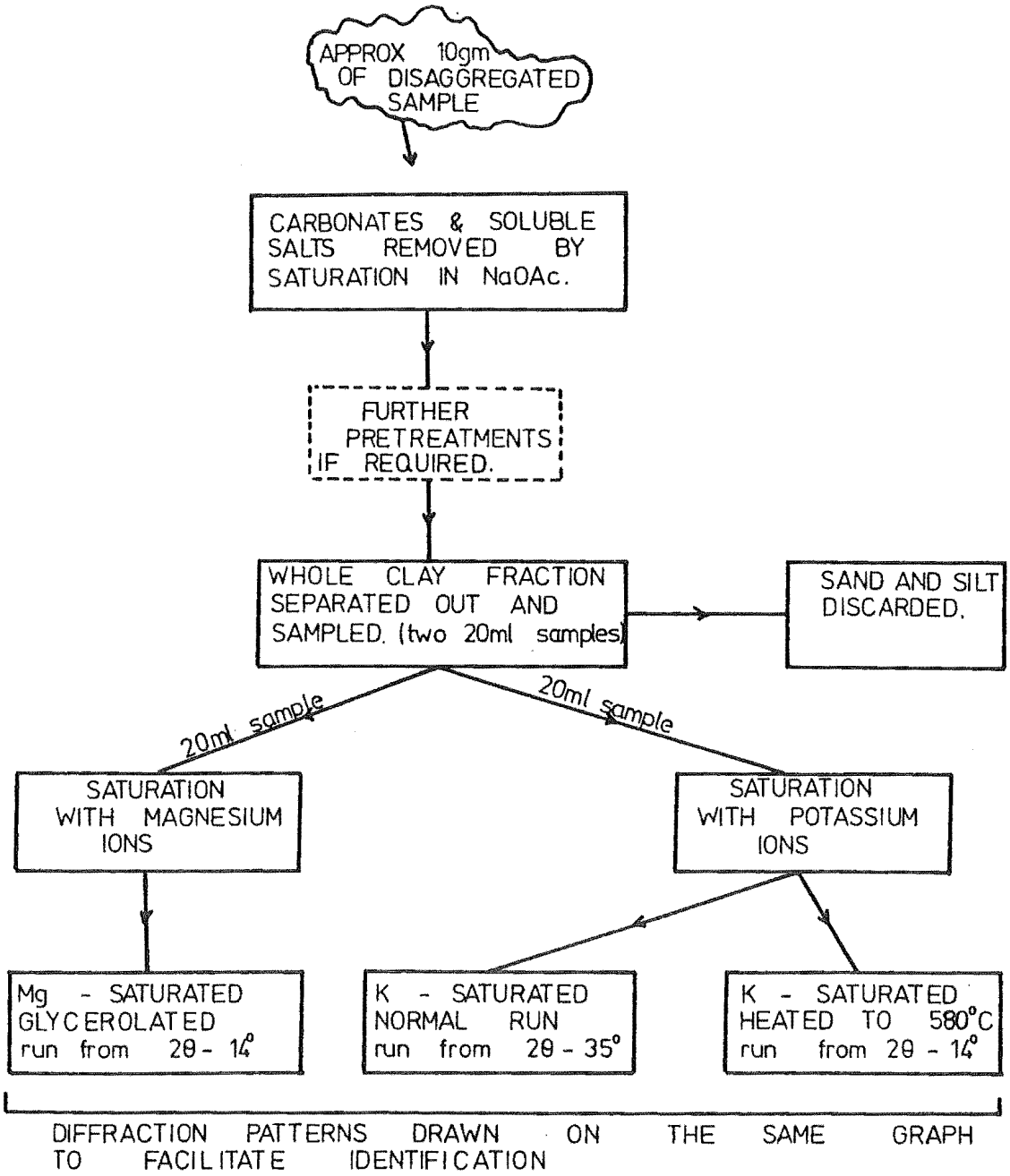

Fig.A5.1: Flow diagram showing methodology adopted for clay mineral analyses.

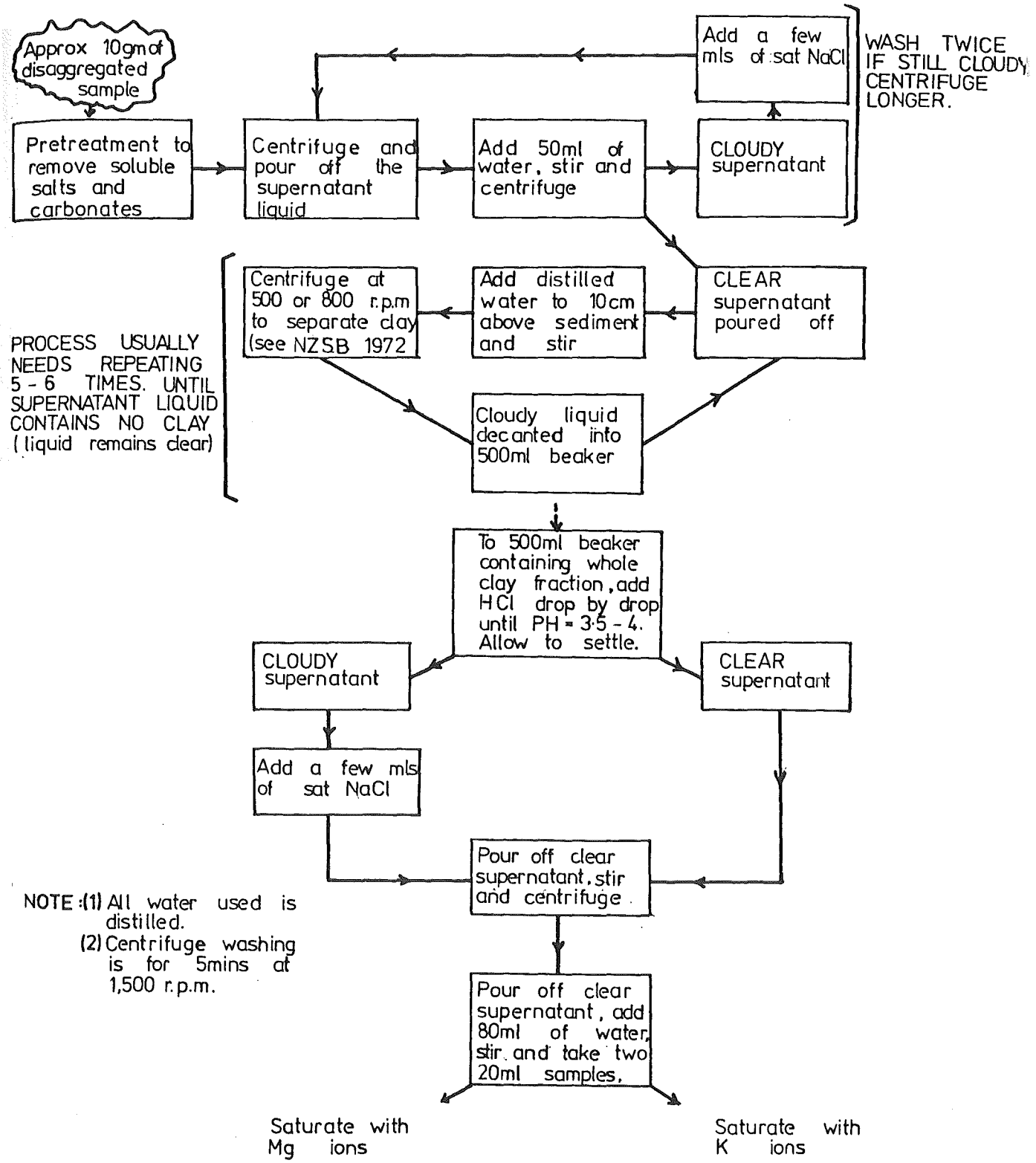

Fig.A5.2: Flow diagram showing methodology for sampling of whole clay fraction.

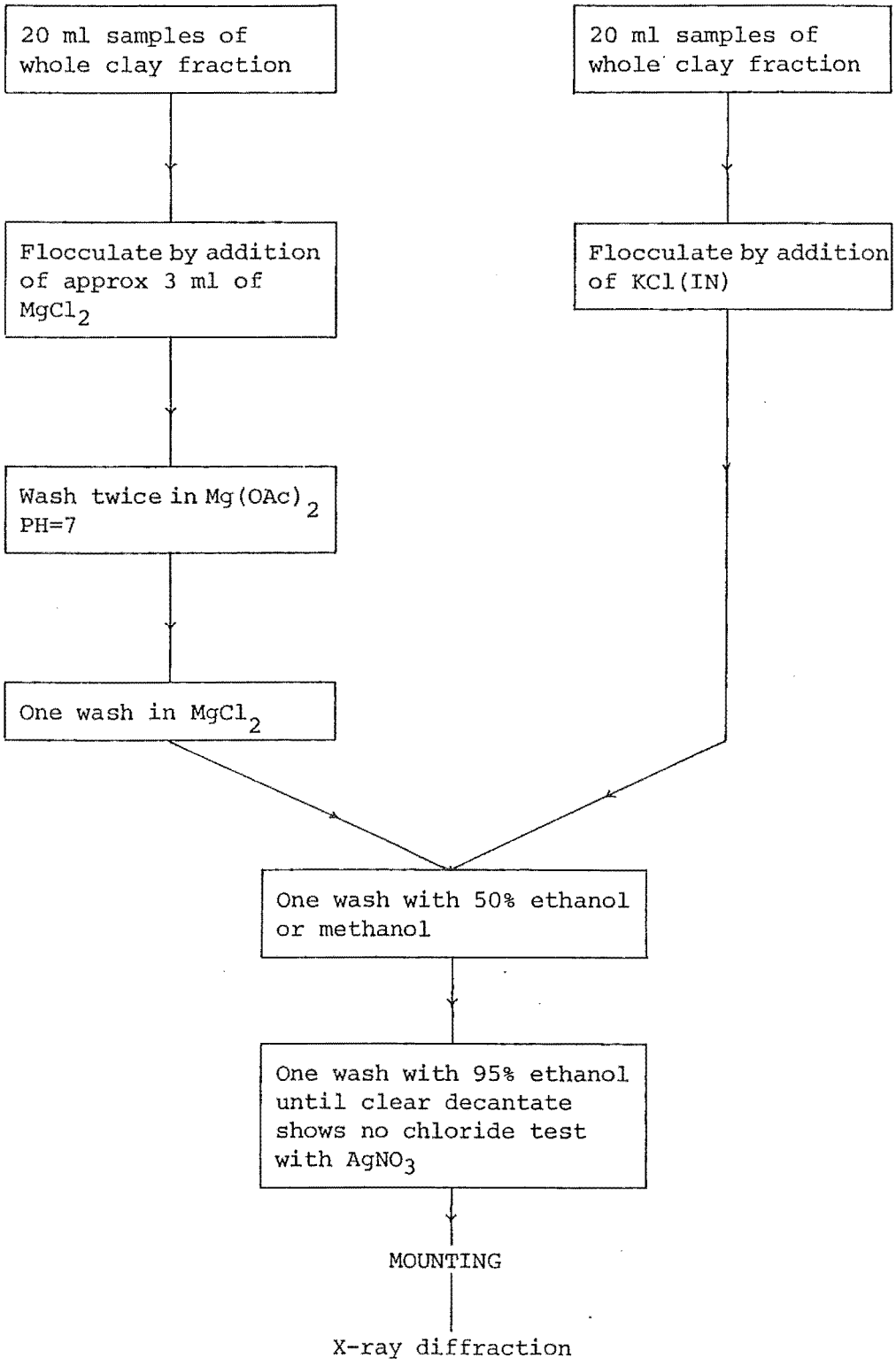

Fig.A5.3: Ion saturation methodology

5.2.5 Glycerolation

Glycerol quantity required to expand smectites is dependant on abundance. The glycerolated mount should have a 'moist' appearance if not more glycerol is required, if excessively 'wet' too much has been applied (Jackson, 1956).

Two methods were adopted for glycerolation:

1) Prior to mounting a glycerol drop was stirred into the clay, ethanol mixture.
2) A drop of glycerol was added to the orientated mount before completely air dry.

5.2.6 Heating

Slide mounts were placed on asbestos tiles and heated to approximately 580^{o}C for one hour. Slow heating and cooling minimised sample 'curling' and peeling.

Rehydration was avoided by transferring the cooling tile plus slides to an oven set at 100^{o}C from which the mounts were moved to the diffractometer for analysis as soon as possible.

5.2.7 Analysis

X-ray diffraction was carried out with a Phillips X-ray diffractometer using CuKα radiation maintained by a 1^{o} divergence slit, a 0.2 mm receiving slit and a 1^{o} anti scatter slit. The Norelco tube was run at 34 Ku and 34 mZ and diffraction patterns recorded at a scan rate of 1^{o} min^{-1}.

Untreated Potassium saturated mounts were run from 20 to 35^{o} to detect quartz, feldspar, calcite, plus other non clay minerals.

Magnesium saturated gylcerolated samples were run from 14 to 20^{o} as were Potassium saturated, heated mounts.

Three diffraction patterns for each sample were recorded on the same graph (Potassium normal, Magnesium glycerolated, Potassium heated) using different colours to expedite indentification. For practical purposes treatments (glycerolation, heating) do not alter the orientations within samples and direct

comparisons of peak intensities can be made.

5.2.8 Identification

Clay minerals are identified through a process of elimination by comparing all three X-ray diffraction patterns (Fig. A5.4, A5.5).

Representative diffractograms for mudstone samples tested are presented; the identification process illustrated by annotating basal diffraction peaks with appropriate letters

S = smectite
V = vermiculite
I = Illite
K = kaolinite
(S/I) = mixed layer, inferred smectite with illite.

Fig.A5.4: X-ray diffraction spacings (obtained) from (001) planes of layer-silicate species as related to sample treatment (Whittig, 1965, Table 49.1).

Diffraction spacing (Å.)	Mineral (or minerals) indicated
	Mg-saturated, air-dried
14-15	Montmorillonite, vermiculite, chlorite
9.9-10.1	Mica (illite), halloysite
7.2- 7.5	Metahalloysite
7.15	Kaolinite, chlorite (2nd-order maximum)
	Mg-saturated, glycerol-solvated
17.7-18.0	Montmorillonite
14-15	Vermiculite, chlorite
10.8	Halloysite
9.9-10.1	Mica (illite)
7.2- 7.5	Metahalloysite
7.15	Kaolinite, chlorite (2nd-order maximum)
	K-saturated, air-dried
14-15	Chlorite, vermiculite (with interlayer aluminum)
12.4-12.8	Montmorillonite
9.9-10.1	Mica (illite), halloysite, vermiculite (contracted)
7.2- 7.5	Metahalloysite
7.15	Kaolinite, chlorite (2nd-order maximum)
	K-saturated, heated (500° C.)
14	Chlorite
9.9-10.1	Mica, vermiculite (contracted), montmorillonite (contracted)
7.15	Chlorite (2nd-order maximum)

Fig.A5.5: X-ray diffractions spacings (Å) obtained from (001) planes of binary, regularly alternating, layer-silicate species as related to sample treatment. (Whittig, 1965, Table 49.2).

Interstratified mixture	Mg-saturated, air-dried	Mg-saturated, glycerol-solvated	K-saturated, heated (500° C.)
	diffraction spacings, Å.		
Mica-vermiculite	24	24	10
Mica-chlorite	24	24	24
Mica-montmorillonite	24	28	10
Vermiculite-chlorite	28	28	24
Vermiculite-montmorillonite	28	32	10
Montmorillonite-chlorite	28	32	24

DIFFRACTOGRAMS FOR "DRIED"
HAMPDEN MUDSTONE

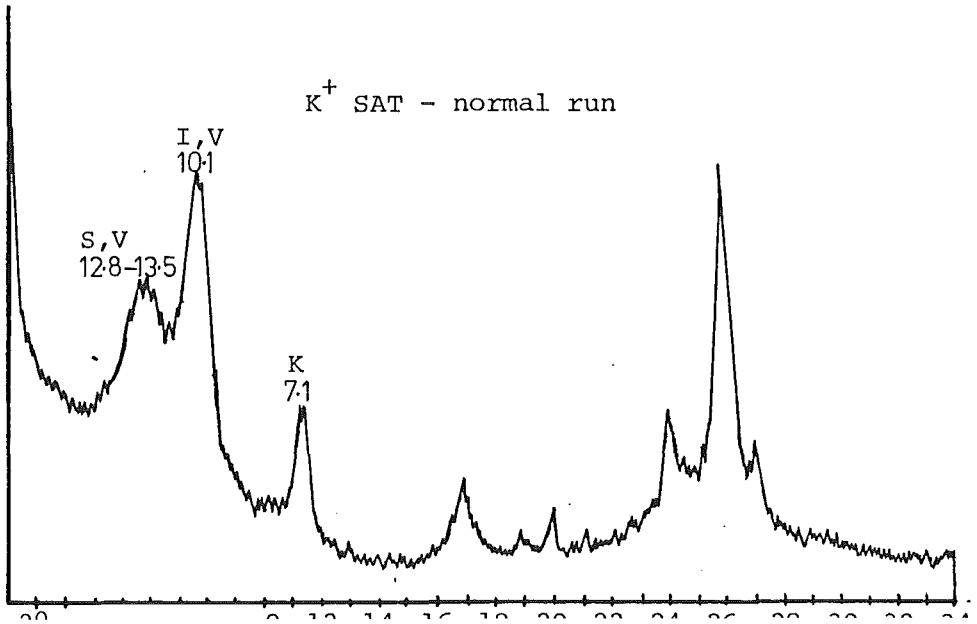

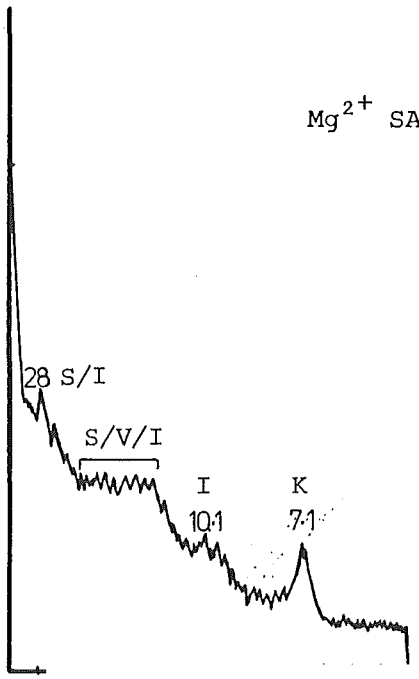

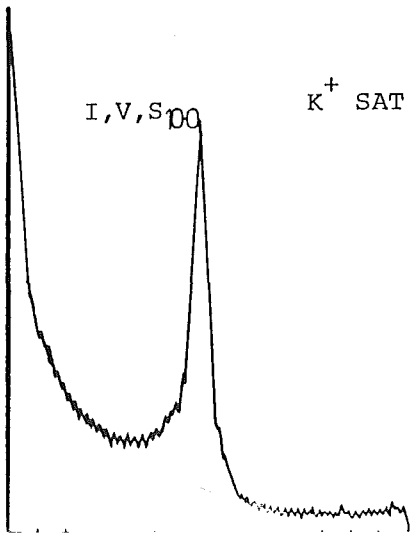

Clay Mineral Assemblage

Kaolinite
Illite
Interlayered Vermiculite/
Smectite/Illite

Peak reference enumeration
in Ångströms.

DIFFRACTOGRAMS FOR "SOFTENED" BLUE-GREY MUDSTONE

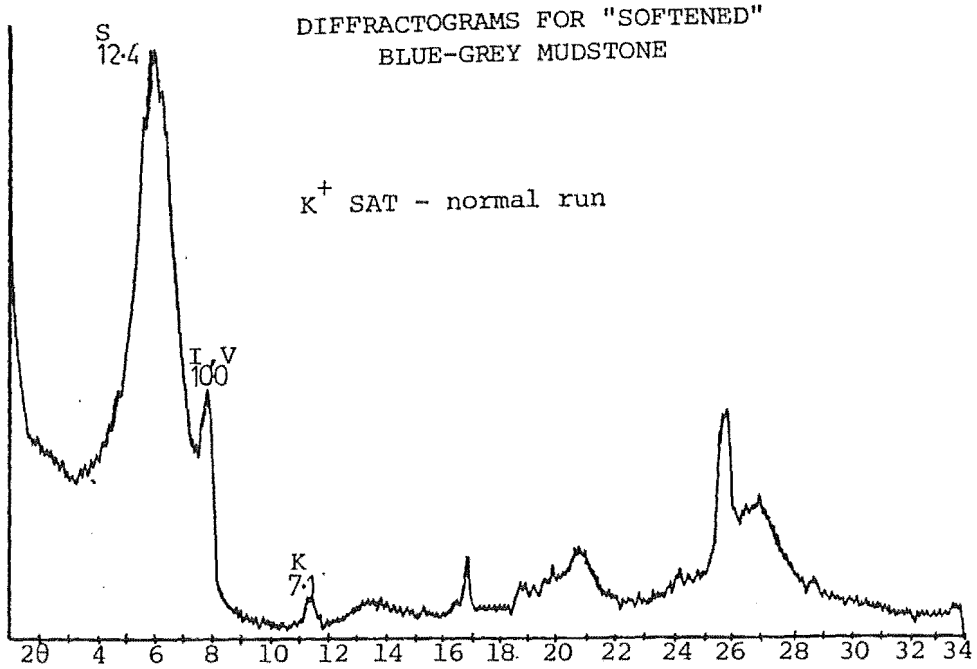

K^+ SAT - normal run

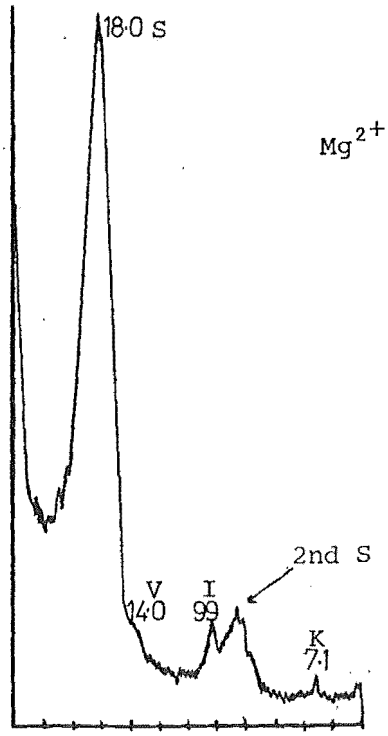

Mg^{2+} SAT - glycerolated run

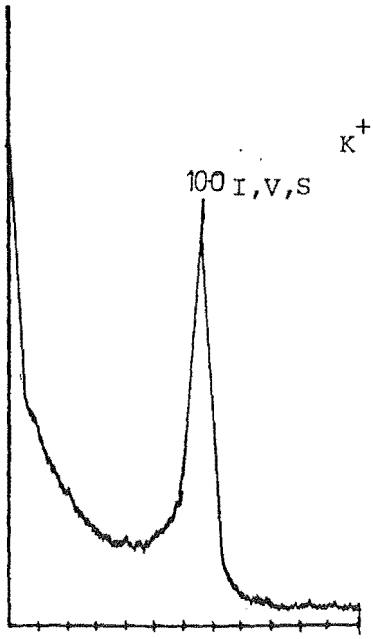

K^+ SAT - heated

Clay Mineral Assemblage

Smectite
Vermiculite
Illite
Kaolinite

Peak reference enumeration in Ångströms.

DIFFRACTOGRAMS FOR VOLCANIC REGOLITH

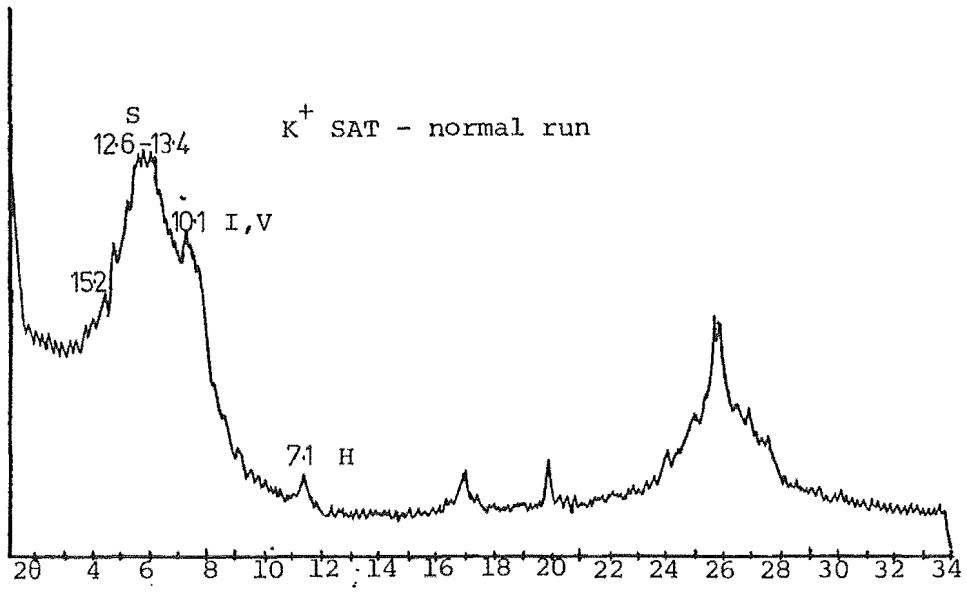

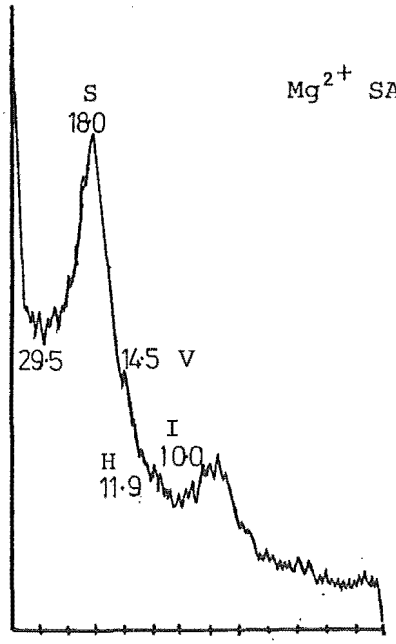

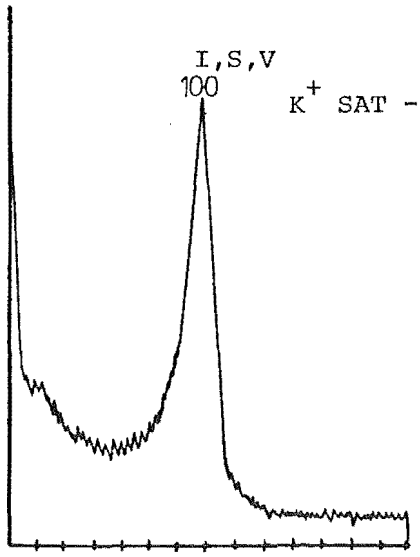

Clay Mineral Assemblage

Smectite
Vermiculite
Hallyosite
Illite

Random interlayering between M/V/I

Peak reference enumeration in Ångströms

DIFFRACTOGRAMS FOR "SOFTENED" YELLOW-BROWN MUDSTONE

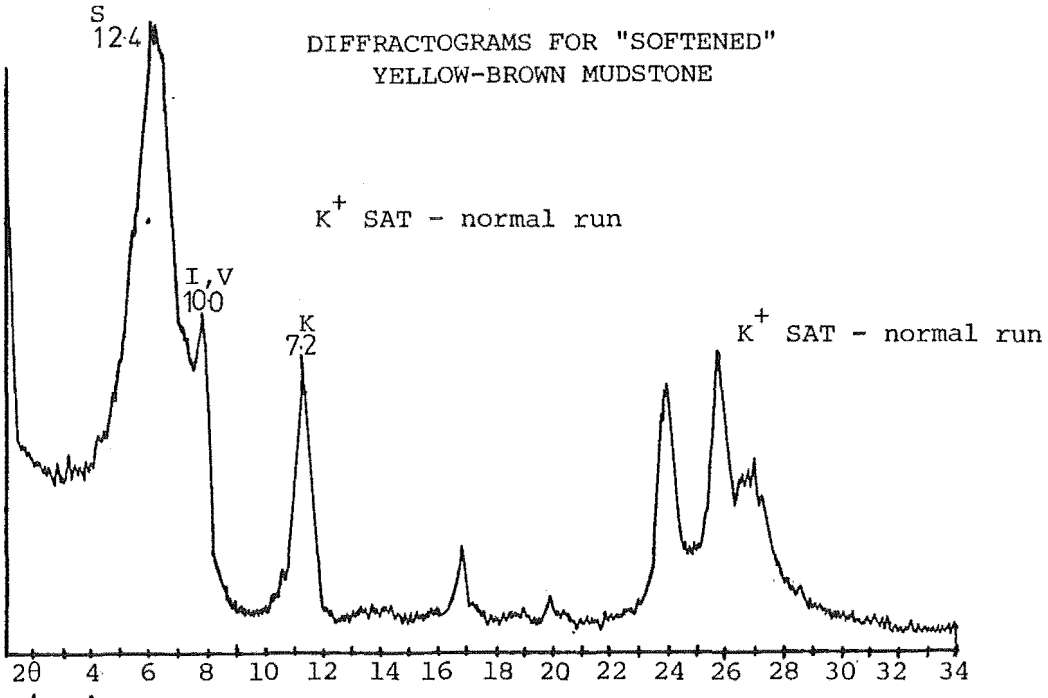

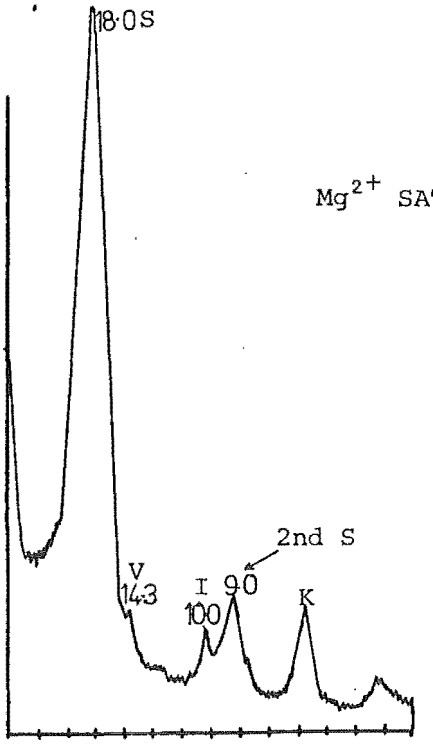

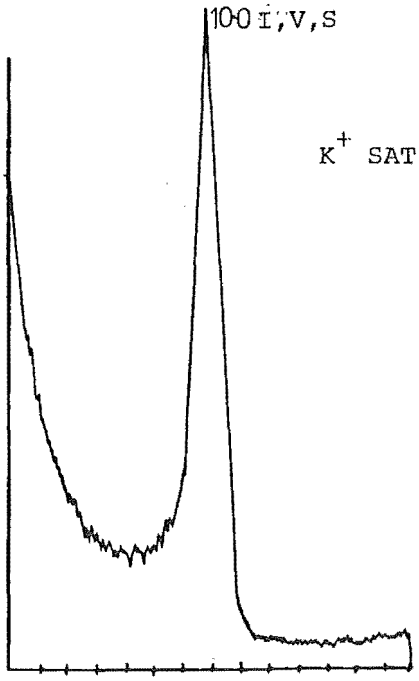

Clay Mineral Assemblage

Smectite
Vermiculite
Illite
Kaolinite

Peak reference enumeration in Ångströms.

APPENDIX 6

STRENGTH TESTING

A6.1 Triaxial Testing

Introduction
6.1.1 Mohr Failure Criterian
6.1.2 Apparatus
6.1.3 Methodology
6.1.4 Analysed Data

A6.2 Vane Testing

Introduction
6.2.1 In-situ Vaning
Methodology
Field Vane Profiles
6.2.2 Laboratory Vaning
Methodology

A6.1 TRIAXIAL TESTING

Triaxial test apparatus enables measurement of stress-strain characteristics for core samples within a controlled two dimensional stress field.

Three consolidated, undrained tests with pore pressure measurement were performed to establish strength parameters for "softened" Hampden mudstone. Each test involved analysing a cylindrical specimen, sealed in a water tight membrane enclosed within a perspex cell and subjected to a pre-determine all round fluid pressure. Initially consolidation of samples was allowed to the confining fone by allowing drainage of pore fluid out both ends of the specimen. Full saturation of fine grained samples was expedited by application of a back pressure to the core which also dissolved any entrapped air. Once consolidated, drainage was prevented and an axial load applied to the sample at a predetermined rate, creating shear stress.

Major principal stresses (σ_1) are simulated by the axial load; the intermediate and minor stresses by the ubiquitous fluid pressure ($\sigma_2 = \sigma_3$). Thus shear stress within cores is equivalent to the deviator stress ($\sigma_1 - \sigma_3$). To obtain effective stress parameters pore pressure was measured during shear.

Main differences between in-situ and triaxial test conditions can be summarised as:

1) The isotropic consolidation pressures ($\sigma_1 = \sigma_2 = \sigma_3$) and biaxial shearing pressures ($\sigma_1 > \sigma_2 = \sigma_3$) applied during triaxial testing differ from conditions in a natural slope ie. in the field situation material generally consolidates when $\sigma_1 > \sigma_3$.

2) Core samples may not be representative of strength within larger in-situ masses ie. presence of partially "softened" mudstone may affect strength considerably within a small core sample.

3) The imperceptible increase of stress in the field till incipient failure cannot be practically simulated during testing.

Nevertheless, despite limitations the triaxial test is widely used because of advantages in controlling and monitoring pore pressure, drainage and volume changes in the sample.

Only principal stresses are applied to specimen boundaries in this equipment hence the state of stress on other principal planes must be established via indirect means. Shear strength of triaxial core samples, or the state of stress on a propagating shear surface at incipient failure, is determined by application of the Mohr Failure Criterion.

6.1.1 Mohr Failure Criterion

A Mohr circle is a continuous set of points representing stress on different sections through a single point in a mass for a particular two dimensional stress field; thus at least one point on a Mohr circle must represent the normal and shearing stress associated with failure (Fig.A6.1). If a series of Mohr circles are plotted for varying stress conditions it is apparent the resultant envelope encompassing these circles represents the locus of points associated with failure. The "rupture line" or "Mohr envelope" through failure loci is generally curved but often approximated by a straight line utilizing Coulombs equation.

$$\tau = c + \sigma n \, \mathrm{Tan}\, \phi$$

where τ = shear strength
c = cohesion
σn = normal stress
ϕ = angle of internal friction.

In terms of effective stress Terzaghi's equation is applied.

$$\tau' = c' + (\sigma n - \mu) \mathrm{Tan}\, \phi'$$

where τ' = effective shear strength
c' = effective cohesion
ϕ' = effective angle of internal friction
μ = pore pressure
σn = normal stress

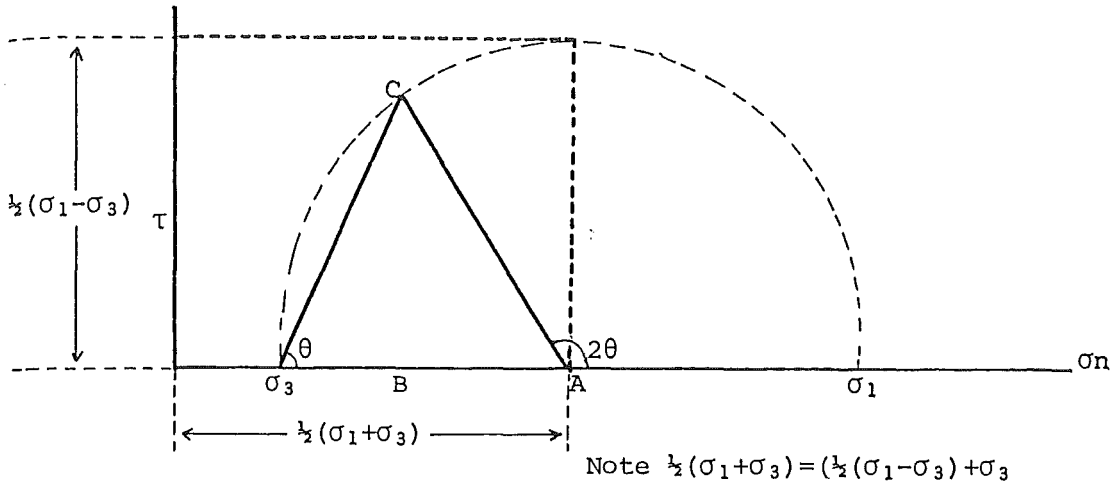

Shear stress (τ) at point C

$\tau = \overline{CB} = \overline{AC}$ Sine 2θ

AC is the radius of the circle = $\frac{1}{2}(\sigma_1-\sigma_3)$

$\therefore \tau = \frac{1}{2}(\sigma_1-\sigma_3)$ Sine θ

The normal stress (σn) at point C

$\sigma n = \overline{OA} + \overline{AB} = \overline{OA} + \overline{AC}$ Cos 2θ

$\therefore \sigma n = \frac{1}{2}(\sigma_1+\sigma_3)+\frac{1}{2}(\sigma_1-\sigma_3)$Cos 2θ

Fig.A6.1(a): Mohr circle for a two dimensional stress field where $\sigma_1>\sigma_2=\sigma_3$, point C represents the state of stress at failure, and θ the angle of rupture to the horizontal.

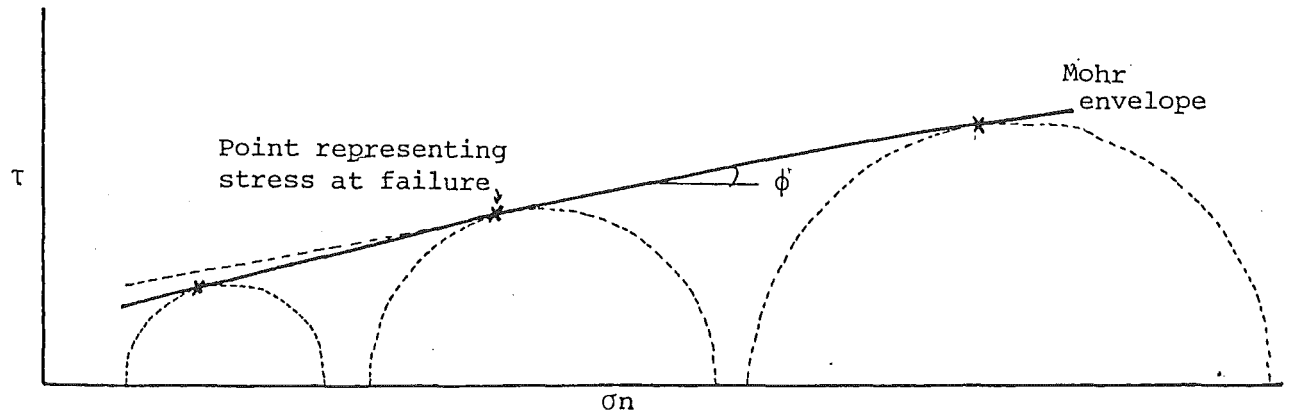

Fig.A6.1(b): Mohr failure envelope; often curved at low stresses.

6.1.2 Apparatus

Apparatus and equipment layout utilized for testing is shown in Fig. A6.2.

Testing required two separate pressure systems:

1) To maintain constant confining pressure. ($\sigma_2=\sigma_3$)

2) To apply uniform backpressure.

Confining pressure was maintained by compressing air within a loading frame chamber to the desired level which remained open to ubiquitous specimen fluid ($\sigma_2=\sigma_3$).

The second pressure system was connected via regulators, volume change burettes and de-aired water supply to a constant air source.

Pressure dissipation via the loading ram was minimised by a 1 cm layer of viscous oil floating on the cell fluid.

Pore pressure was measured utilizing diaphragm pressure type transducers at the top and base of core samples.

6.1.3 Methodology

Undisturbed samples were extruded from 35 mm cores and trimmed normal to their axis using fine wire.

To hasten pore pressure equalization 'filter drains' (made from Whatmans No.54) encased each sample reducing the distance water had to travel for pore pressure dissipation (Fig.A6.3)(Design outlined in Bishop and Henkel, 1957).

Specimens were backpressure saturated and consolidated prior to testing. Backpressures of 250 kPa were applied in 50 kPa increments with corresponding increases in cell pressure to avoid consolidation; pressure equibration being monitored via transducers at the top and bottom of each specimen. Effective consolidation pressures (350 kPa, 150 kPa, 100 kPa) were then applied and volume changes recorded using twin burettes. Consolidation was considered complete when volume change ceased which generally took a minimum of 24 hours.

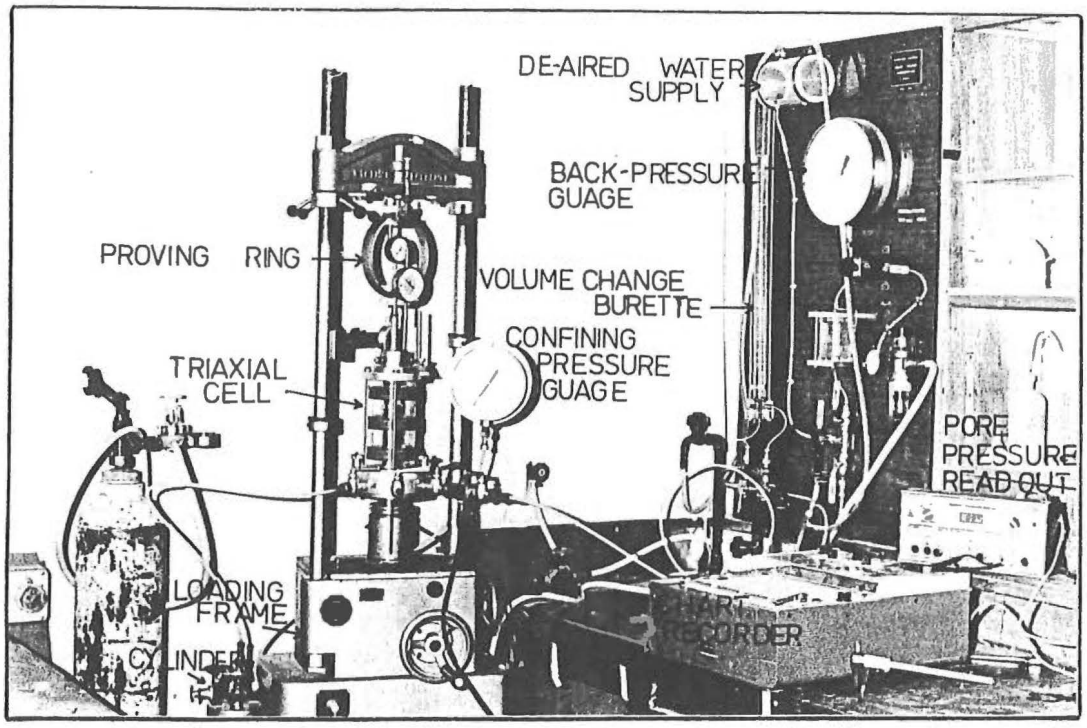

Fig. A6.2: Triaxial Test Apparatus

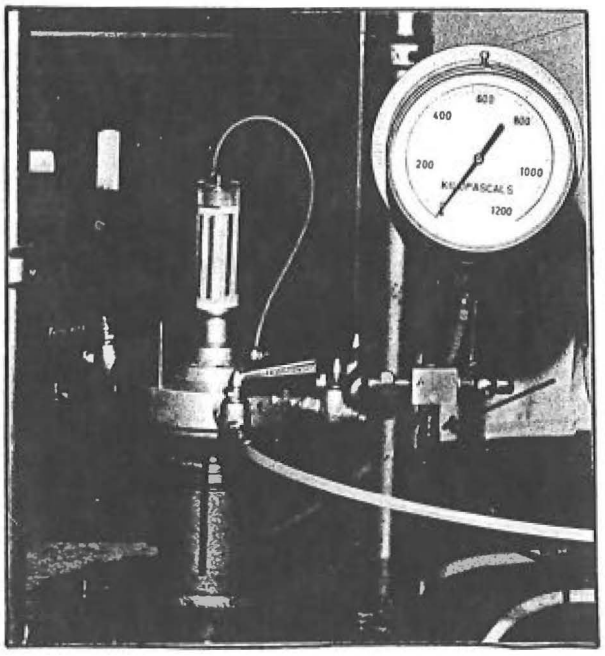

Fig. A6.3: Prepared triaxial sample encompassed by filter drain; arrows denote transducers used to measure pore pressure at the top/bottom of specimen.

For reliable strength measurements a strain rate to obtain at least 95% consolidation was calculated from the method outlined by Bishop and Henkel (1957).

$$\text{time to failure} = \frac{20\ h^2}{\eta\ Cv}$$

Drainage is radial and from both ends of the sample.

where $\eta = 35$

$h = \frac{1}{2}$ the sample height

$$Cv = \frac{\pi h^2}{100\ t_{100}}$$

t_{100} is extrapolated from a plot of $\sqrt{t}$ in minutes versus change in volume during consolidation.

Based on this, increasing strain was applied at a rate of 1.097×10^{-1} mm per hour.

Methodology and test procedure is outlined in Millar (1982) and Bishop and Henkel (1957).

6.1.4 Analysed Data

All samples exhibited plastic failure after 6.9% to 10% strain, consistent with expected behaviour of "softened" mudstone.

Effective stress parameters are derived graphically from Mohr circle plots (refer section 4.3.7).

UNDRAINED TRIAXIAL TEST THREE

Effective Confining Cell Pressure = 100 kPa

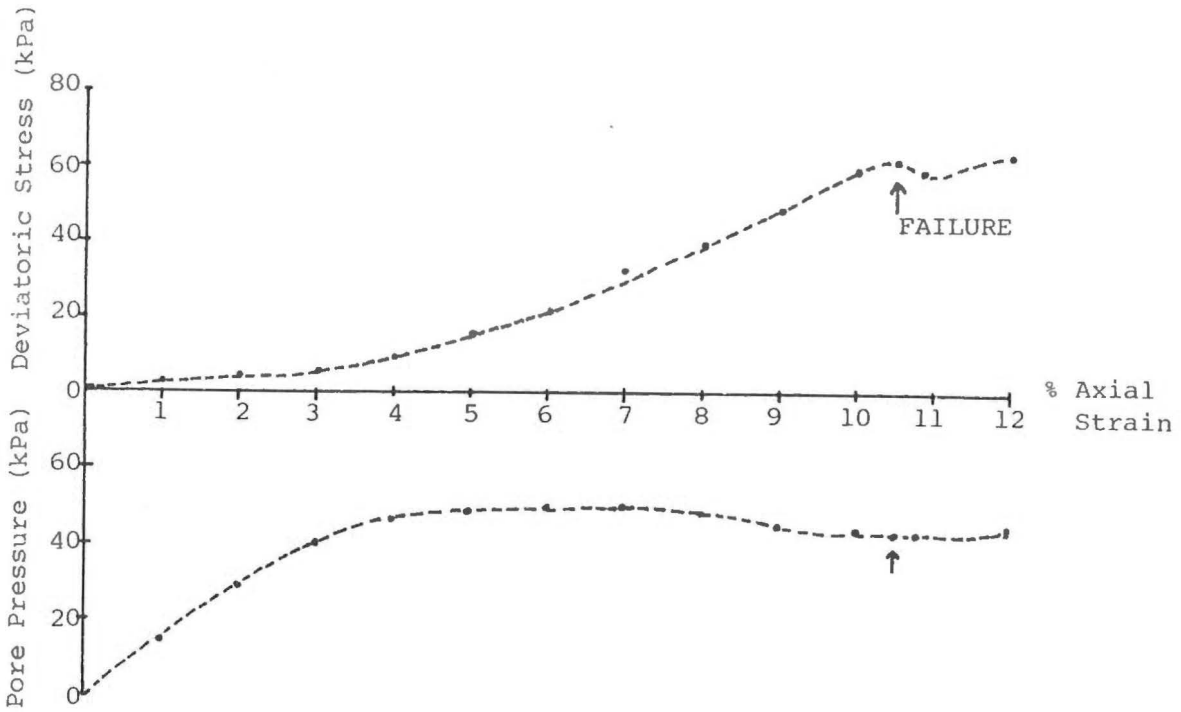

ANALYSED DATA

INITIAL	length	71 mm
	diam	35 mm
	ρd t/m^3	1.37
	W%	34.6

STRAIN RATE = 1.097×10^{-1} mm/hr

TIME TO FAILURE = 64.2 hr

FAILURE MODE = Plastic

FINAL	length	58 mm
	diam	42 mm
	W%	33.3
	ε%	20

AT FAILURE	
$\frac{1}{2}(\sigma_1'+\sigma_3')$	80.62 kPa
$\frac{1}{2}(\sigma_1'-\sigma_3')$	23.6 kPa
μ	43 kPa
ε%	10.5

UNDRAINED TRIAXIAL TEST TWO
Effective Confining Cell Pressure = 150 kPa

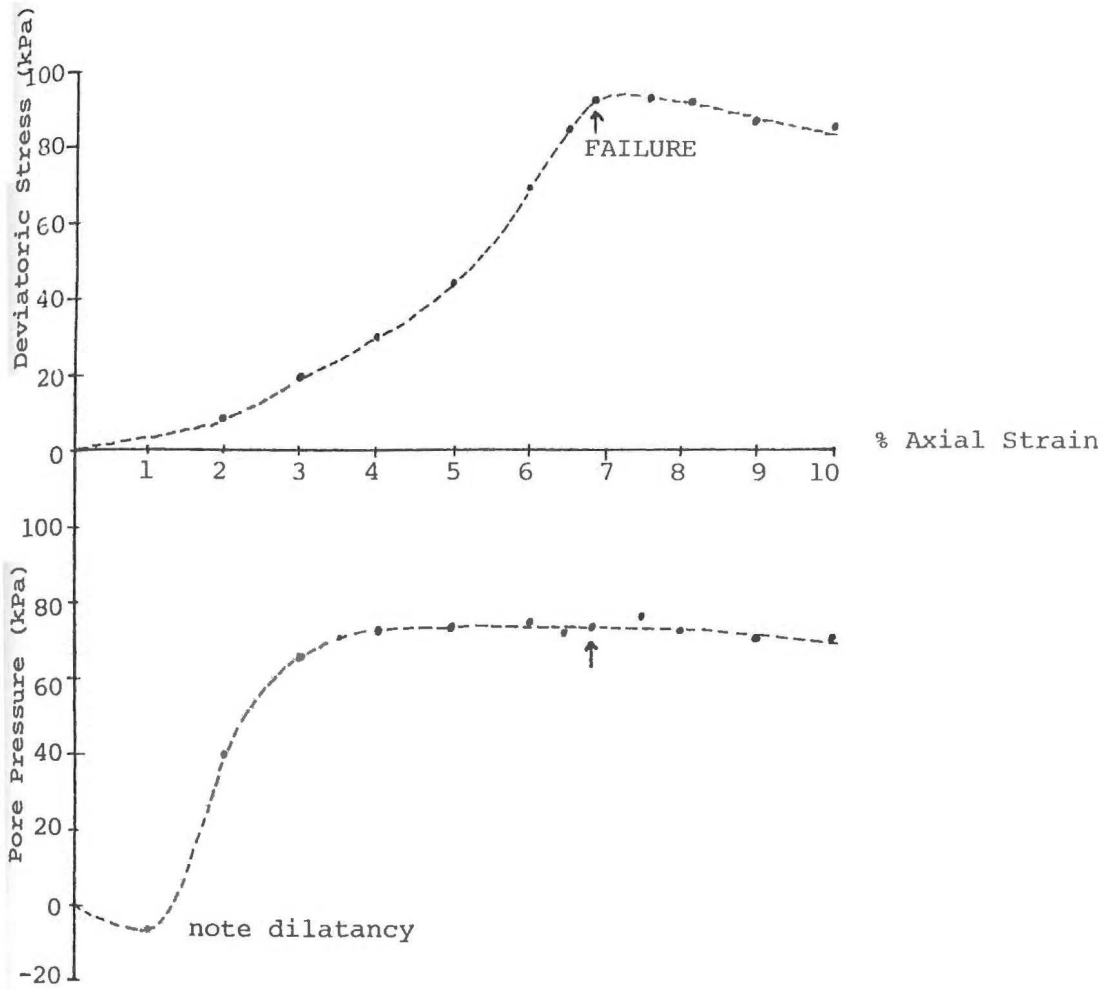

INITIAL	length	73 mm
	diam	35 mm
	ρd t/m^3	1.36
	W%	35.5

STRAIN RATE = 1.097×10^{-1} mm/hr
TIME TO FAILURE = 45.5 hr
FAILURE MODE = Plastic

FINAL	length	58 mm
	diam	44 mm
	W%	34.1
	ε%	20

AT FAILURE	
$\frac{1}{2}(\sigma'_1+\sigma'_3)$	115.47 kPa
$(\sigma'_1-\sigma'_3)$	39.5 kPa
μ	76 kPa
ε%	6.9

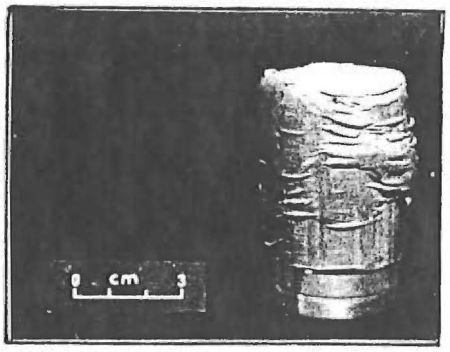

UNDRAINED TRIAXIAL TEST ONE

Effective Confining Cell Pressure = 350 kPa

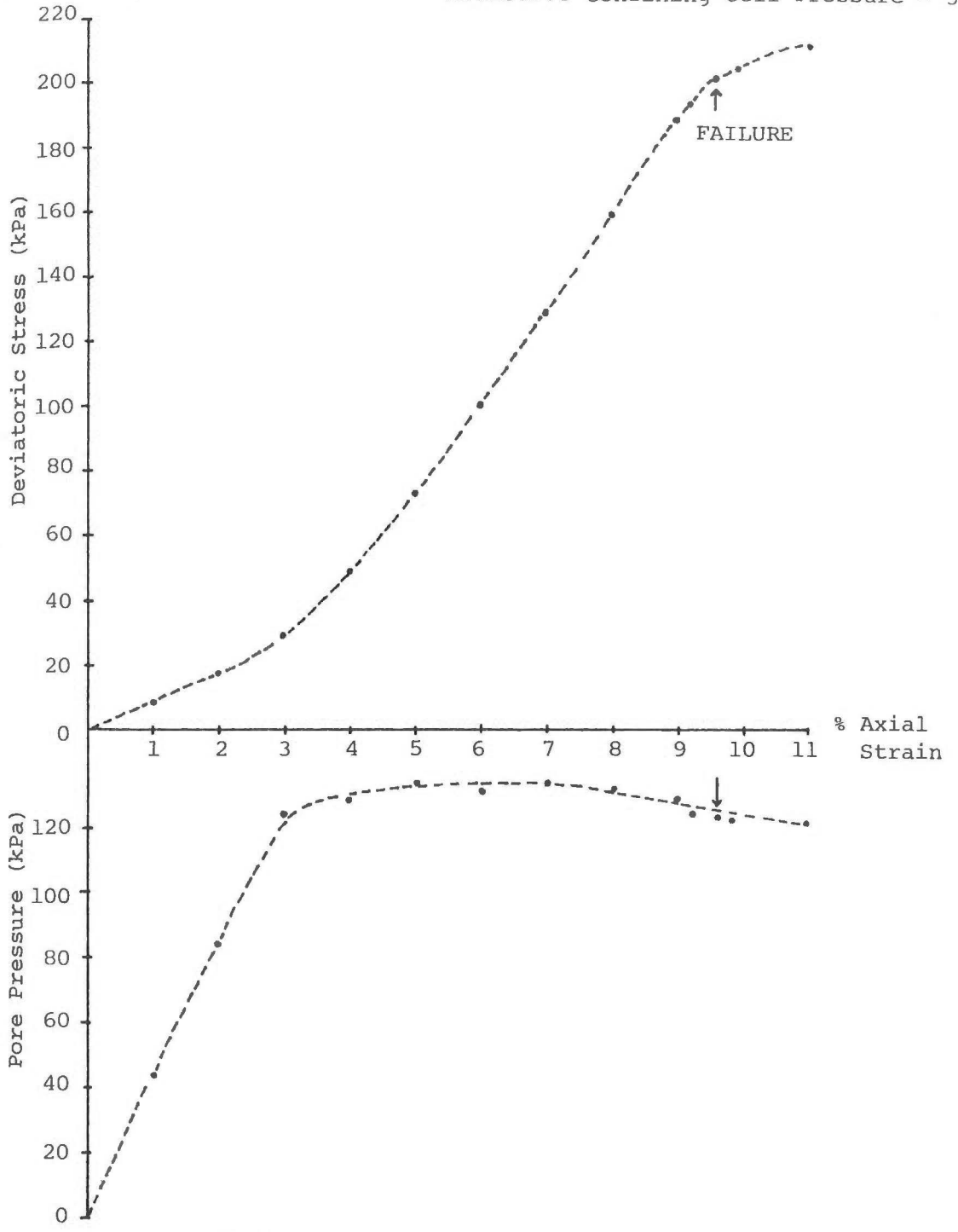

ANALYSED DATA

INITIAL	length	72 mm
	diam	35 mm
	ρd t/m^3	1.41
	W%	33.3

STRAIN RATE = 1.097×10^{-1} mm/hr

TIME TO FAILURE = 56.8 hr

FAILURE MODE = Plastic

FINAL	length	52 mm
	diam	42 mm
	W%	32.7
	ε%	20

AT FAILURE	
$\frac{1}{2}(\sigma_1'+\sigma_3')$	327.96 kPa
$\frac{1}{2}(\sigma_1'-\sigma_3')$	100.96 kPa
μ	123 kPa
ε%	9.6

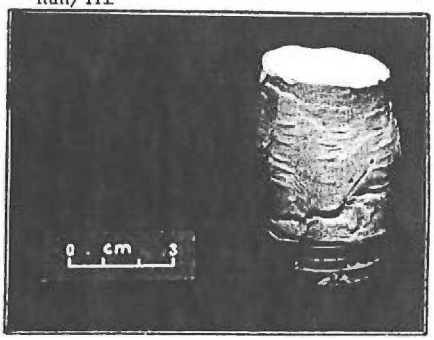

A6.2 VANE TESTING

Principal objectives of in-situ vane testing is determination of accurate, undrained shear strength values for clays by minimising stress changes in the soil due to sampling. Interpretation of results is based on a number of assumptions:

1) Soil failure is along the surface of the cylinder circumscribing the vane.

2) Shear strength is fully mobilized on all surfaces and no progressive failure takes place.

3) The remoulded zone around the vane is very small and has no effect on stress-strain properties of the tested mass.

4) The undrained strength is the same in both vertical and horizontal directions.

5) No drainage occurs during testing.

Obviously some of these assumptions will not always apply hence vane testing should not be relied on for exact undrained strength values.

6.2.1 In-Situ Vaning

Field testing was at standard intervala (usually 25 cm) down three shallow profiles using a Geonor vaneborer with an estimated accuracy of ±10%.

Four inch diameter holes were augered to roughly 0.5 mm above sampling depth and the Geonor instrument carefully inserted to the required level. The 50 cm penetration depth (appeoximately 5 x the diameter of the hole) avoids stress relief changes caused by augering (Cadling and Odenstad, 1950).

The following procedure was adopted for each sampling interval.

1) Hole augered to the required depth.

2) Vane shaft with dummy head is slowly pushed in approximately 45 cm, rotated and a rod friction component taken.

3) A 16 x 32 mm vane was pushed to the required depth, without twisting, and subsequently rotated slowly at a constant rate until failure giving the undisturbed strength. Flaate (1966) notes any time lag of greater than 5 minutes from initial penetration to vane testing can alter strength values.

4) The vane was turned at least 25 full revolutions and two more readings taken, the minimum of which was recorded as remoulded strength.

5) Material from the relevant depth was then described from remoulded auger samples.

Undrained strength was calculated by subtracting rod friction and multiplying vane readings by a constant.

6.2.2 Laboratory Vaning

Samples were tested using a Geonor laboratory vane by the following procedure:

1) Samples (400 gm) were mixed with distilled H_2O to approximately the liquid limit on a glass plate, then left for four days to equilibrate in plastic beakers (500 gm beakers).

2) Specimens were then "jarred", by gentle tapping on a firm surface, to remove all air pockets and obtain even density, (orientation of particles and size segregation due to this is assumed negligible).

3) A 2 x 4 cm vane was then lowered into the sample, making sure the vane was totally submerged, and subsequently rotated at 0.1 degree per second until failure (recommended rate by Cadling and Odenstad (1950)).

LOCATION: Davids Road Area VANE HOLE No. 1 (adjacent to P_2)

LITHOLOGY: Mudstone Colluvium

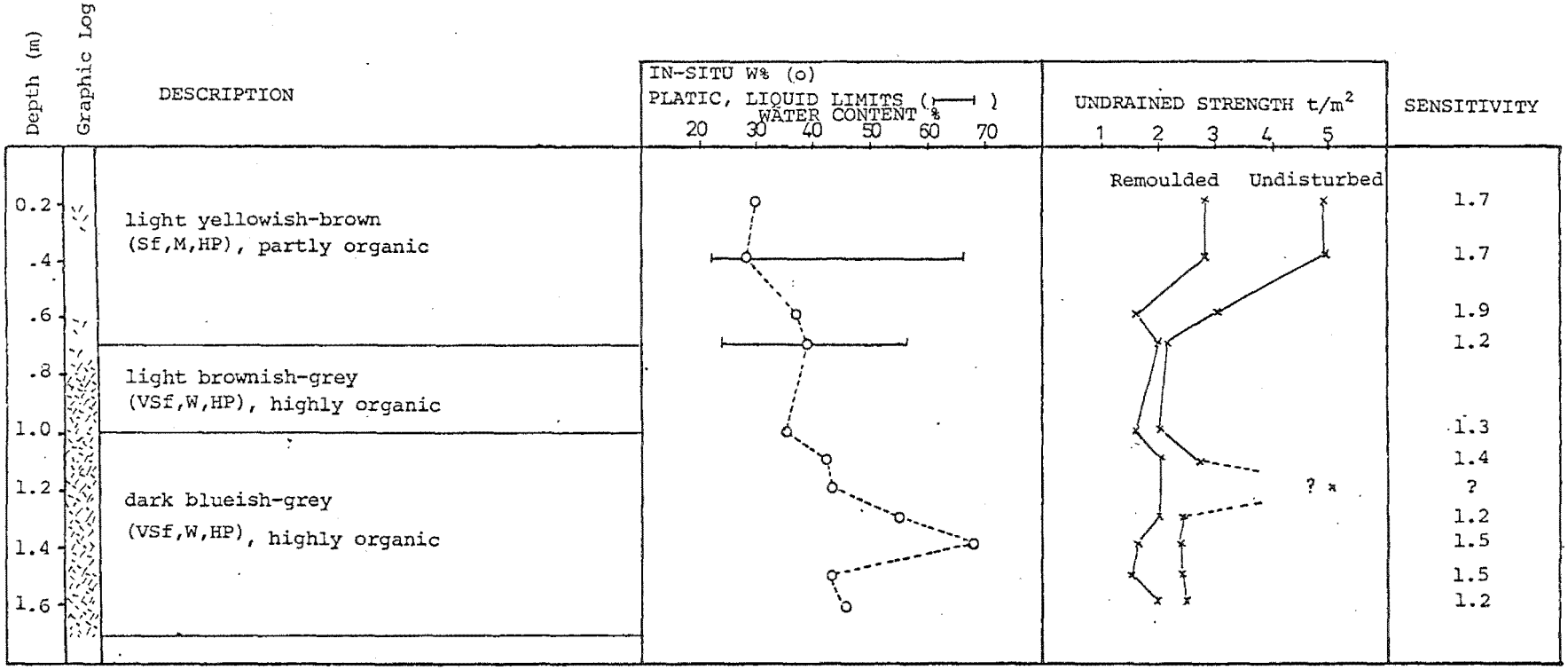

Graphic log depicting relative abundance of organic matter.

LOCATION: Motor Camp Area VANE HOLE NO. 2 (neighbouring auger hole 3)

LITHOLOGY: Mudstone Regolith

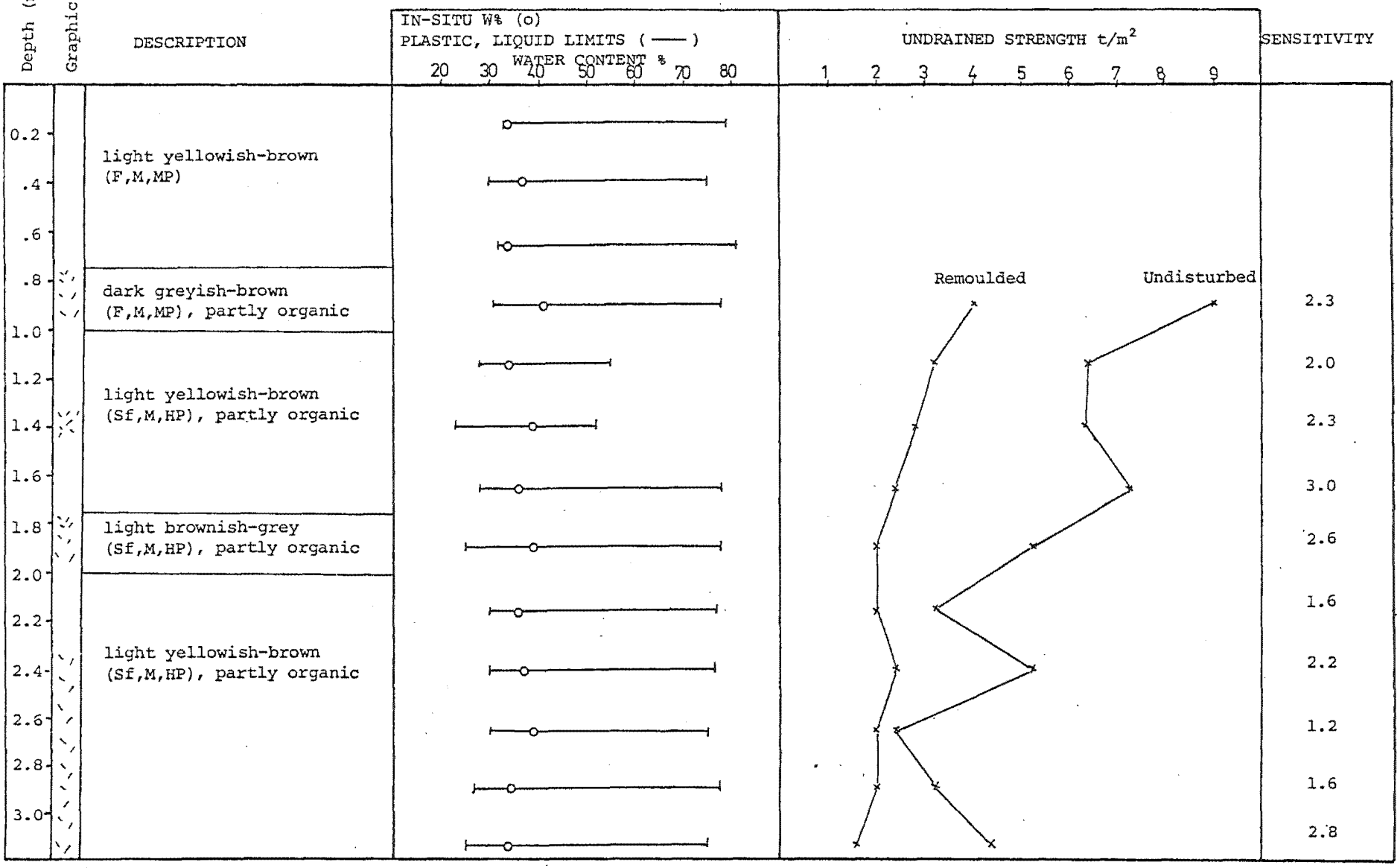

LOCATION: Motor Camp Area VANE HOLE NO.3 (neighbouring auger hole 1)

LITHOLOGY: Mudstone Colluvium

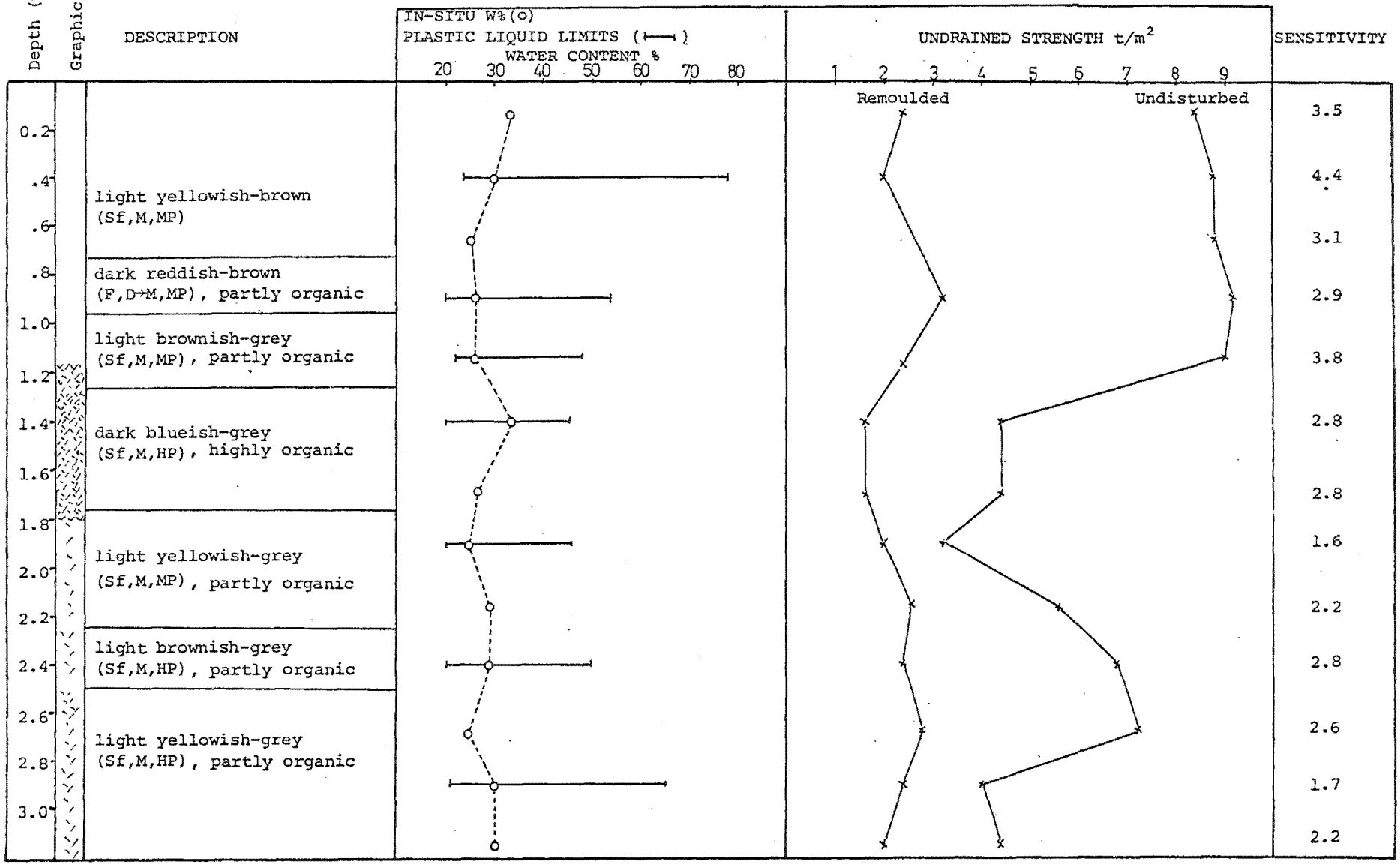

The vane was removed, cleaned, the sample "re-agitated" and another reading taken; the final value recorded being averaged from three such tests.

4) Moisture content samples were taken from vane blades after the final extrusion.

5) Samples were then spread on glass plates and dried up to 5 minutes by a fan; re-mixed for 5 to 10 minutes then put back into 500 gm plastic beakers and the process from step (2) repeated for a drier moisutre content.

APPENDIX 7

SUBSURFACE DATA

A7.1 Introduction

A7.2 Borehole logs

A7.1 INTRODUCTION

Subsurface data on mudstone regolith and colluvium within the two study areas was obtained from ten boreholes (six augered and one drill hole).

An Iwan 4" hand auger was used with aluminium extensions capable of augering to depths of 8 m. Maximum depth was seldom attained due to:

1) hole pinching below the water table,
2) rock fragments plus plant debris preventing auger head biting into overburden.

A Caldwell rig with 2' bucket was utilized for the drill hole.

Description of remoulded samples was based on the charts shown in Figs A7.1 to A7.7.
No weathering terms was assigned due to the difficulty of ascertaining texture plus in-situ from colluvial material for thoroughly remoulded samples. However oxidation was outlined in terms of gleying and mottling based on New Zealand Soil Survey Method (1970) (Fig.A7.7).

Characteristic greyish or blueish colours of gleyed horizons are produced by reduction of iron and maganese within the profile. Reduction is most active within grey zones which on air exposure tend to change to yellowish or brownish colours yielding a distinctive colour intermixing known as mottling (Taylor and Pohlen, 1979). In may places the change is rapid and marked, in others scarcely detectable, apparently because ferrous iron is able to form stable compounds with other soil constituents (Bloomfield, 1953). The same mottling effect is produced if conditions are part oxidising and part reducing as in a zone of water table fluctuation.

Organic material and the Unified Soil Symbol were assigned to material by methods outlined in ASTM D2488-69 (Fig.A7.7).

Significant horizons are highlighted in a generalized graphic log adjacent to profile description.


organic material


mass movement debris


blue-grey mudstone

DESCRIPTION TERMINOLOGY UTILIZED

Fig.A7.1: Cohesive soil strength (after McLean, 1976, Table 4).

TERM	DIAGNOSTIC FEATURES	UNCONFINED COMPRESSIVE STRENGTH KPa (1kPa = 145 x 10-3 lb/in^2 = 9.32 x 10-3 T/ft^2)
Hard	Difficult to indent by thumbnail	> 450
Very Stiff	Indented by thumbnail	300 - 450
Stiff	Indented by thumb pressure	150 - 300
Firm	Indented only by strong finger pressure	75 - 150
Soft	Easily indented by fingers	35 - 75
Very soft	Exudes between fingers when squeezed	< 35

Fig.A7.2: In-situ moisture content (after McLean, 1976).

Moisture Content*

A simple, objective classification based on appearance and 'feel'. The terms are mainly self-explanatory.

Dry — Looks and feels dry; cohesive soils usually hard, powdery or friable, granular soils run freely through hands.

Moist — Soil feels cool, darkened in colour; granular soils tend to cohere, cohesive soils usually weakened by moisture presence but one gets no free water on hands when re-moulding.

Wet — Soil feels cool, darkened in colour; granular soils tend to cohere, cohesive soils usually weakened and free water forms on hands when handling.

Saturated — A special case of 'wet', applicable only to soil below the water table.

Fig.A7.3: Plasticity scale (after McLean, 1976, Table 6).

TERM	PI	DRY STRENGTH (Air Dried)	CUBE TEST RESULT
Non Plastic	0 - 3	Very low	Falls apart easily
Sightly Plastic	4 - 15	Slight	Easily crushed with fingers
Moderately Plastic	15 - 25	Medium	Difficult to crush
Highly Plastic	> 25	High	Impossible to crush with fingers

Plasticity Determination and Terms (Refers to -36# fraction)

UNIFIED SOIL CLASSIFICATION
INCLUDING IDENTIFICATION AND DESCRIPTION

FIELD IDENTIFICATION PROCEDURES (Excluding particles larger than 3 inches and basing fractions on estimated weights)				GROUP SYMBOLS [1]	TYPICAL NAMES	INFORMATION REQUIRED FOR DESCRIBING SOILS	LABORATORY CLASSIFICATION CRITERIA
COARSE GRAINED SOILS — More than half of material is larger than No 200 sieve size [2] (The No. 200 sieve size is about the smallest particle visible to the naked eye)	GRAVELS — More than half of coarse fraction is larger than No 4 sieve size (For visual classifications, the ¾" size may be used as equivalent)	CLEAN GRAVELS (Little or no fines)	Wide range in grain size and substantial amounts of all intermediate particle sizes	GW	Well graded gravels, gravel-sand mixtures, little or no fines.	Give typical name; indicate approximate percentages of sand and gravel; max. size; angularity, surface condition, and hardness of the coarse grains; local or geologic name and other pertinent descriptive information; and symbol in parentheses.	Determine percentages of gravel and sand from grain size curve. Depending on percentage of fines (fraction smaller than No 200 sieve size) coarse grained soils are classified as follows:- Less than 5 %: GW, GP, SW, SP. More than 12 %: GM, GC, SW, SC. 5 % to 12 %: Borderline cases requiring use of dual symbols.
			Predominantly one size or a range of sizes with some intermediate sizes missing.	GP	Poorly graded gravels, gravel-sand mixtures, little or no fines.		$C_U = \frac{D_{60}}{D_{10}}$ Greater than 4; $C_C = \frac{(D_{30})^2}{D_{10} \times D_{60}}$ Between one and 3. Not meeting all gradation requirements for GW. Atterberg limits below "A" line, or PI less than 4. Atterberg limits above "A" line with PI greater than 7. Above "A" line with PI between 4 and 7 are borderline cases requiring use of dual symbols.
		GRAVELS WITH FINES (Appreciable amount of fines)	Non-plastic fines (for identification procedures see ML below)	GM	Silty gravels, poorly graded gravel-sand-silt mixtures.	For undisturbed soils add information on stratification, degree of compactness, cementation, moisture conditions and drainage characteristics.	
			Plastic fines (for identification procedures see CL below).	GC	Clayey gravels, poorly graded gravel-sand-clay mixtures.		
	SANDS — More than half of coarse fraction is smaller than No 4 sieve size (For visual classifications, the ¾" size may be used as equivalent to the No 4 sieve size.)	CLEAN SANDS (Little or no fines)	Wide range in grain sizes and substantial amounts of all intermediate particle sizes.	SW	Well graded sands, gravelly sands, little or no fines.	EXAMPLE:- Silty sand, gravelly; about 20% hard, angular gravel particles ½"-in maximum size; rounded and subangular sand grains coarse to fine; about 15% non-plastic fines with low dry strength; well compacted and moist in place; alluvial sand; (SM)	$C_U = \frac{D_{60}}{D_{10}}$ Greater than 6; $C_C = \frac{(D_{30})^2}{D_{10} \times D_{60}}$ Between one and 3. Not meeting all gradation requirements for SW. Atterberg limits below "A" line or PI less than 4. Atterberg limits above "A" line with PI greater than 7. Above "A" line with PI between 4 and 7 are borderline cases requiring use of dual symbols.
			Predominantly one size or a range of sizes with some intermediate sizes missing.	SP	Poorly graded sands, gravelly sands, little or no fines.		
		SANDS WITH FINES (Appreciable amount of fines)	Non-plastic fines (for identification procedures see ML below)	SM	Silty sands, poorly graded sand-silt mixtures.		
			Plastic fines (for identification procedures see CL below).	SC	Clayey sands, poorly graded sand-clay mixtures.		
FINE GRAINED SOILS — More than half of material is smaller than No 200 sieve size. (The No. 200 sieve size is about the smallest particle visible to the naked eye)	IDENTIFICATION PROCEDURES ON FRACTION SMALLER THAN No. 40 SIEVE SIZE	DRY STRENGTH (CRUSHING CHARACTERISTICS)	DILATANCY (REACTION TO SHAKING)	TOUGHNESS (CONSISTENCY NEAR PLASTIC LIMIT)			Use grain size curve in identifying the fractions as given under field identification.
	SILTS AND CLAYS — Liquid limit less than 50	None to slight	Quick to slow	None	ML	Inorganic silts and very fine sands, rock flour, silty or clayey fine sands with slight plasticity.	Give typical name; indicate degree and character of plasticity, amount and maximum size of coarse grains; color in wet condition, odor if any, local or geologic name, and other pertinent descriptive information; and symbol in parentheses. For undisturbed soils add information on structure, stratification, consistency in undisturbed and remolded states, moisture and drainage conditions. EXAMPLE:- Clayey silt, brown; slightly plastic; small percentage of fine sand; numerous vertical root holes; firm and dry in place; loess; (ML)
		Medium to high	None to very slow	Medium	CL	Inorganic clays of low to medium plasticity, gravelly clays, sandy clays, silty clays, lean clays.	
		Slight to medium	Slow	Slight	OL	Organic silts and organic silt-clays of low plasticity.	
	SILTS AND CLAYS — Liquid limit greater than 50	Slight to medium	Slow to none	Slight to medium	MH	Inorganic silts, micaceous or diatomaceous fine sandy or silty soils, elastic silts.	
		High to very high	None	High	CH	Inorganic clays of high plasticity, fat clays.	
		Medium to high	None to very slow	Slight to medium	OH	Organic clays of medium to high plasticity.	
HIGHLY ORGANIC SOILS		Readily identified by color, odor, spongy feel and frequently by fibrous texture.			Pt	Peat and other highly organic soils.	

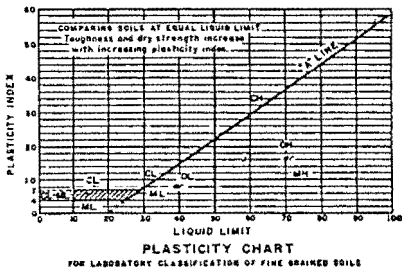

PLASTICITY CHART
FOR LABORATORY CLASSIFICATION OF FINE GRAINED SOILS

[1] Boundary classifications:- Soils possessing characteristics of two groups are designated by combinations of group symbols. For example GW-GC, well graded gravel-sand mixture with clay binder.

[2] All sieve sizes on this chart are U.S. standard.

ADOPTED BY:- CORPS OF ENGINEERS AND BUREAU OF RECLAMATION - JANUARY 1952

Fig.A7.4: Unified Soil Classification (ASTM D2488)

Fig.A7.5: Mottling Terminology (Taylor and Pohlen, 1979)

Contrast

The relative contrast may be described as:

Faint – Mottles are indistinct and recognisable only by close examination. Soil colours in both the matrix and the mottles are similar.

Distinct – Although not striking, the mottles are readily seen. The colour of the matrix is easily distinguished from that of the mottles.

Prominent – The mottles are conspicuous and mottling is one of the outstanding features of the horizon.

Size

The relative size of mottles is expressed in terms of their greatest diameters as follows:

Fine – Less than 5 mm.

Medium – 5–15 mm (0·2 to 0·6 in.).

Coarse – Greater than 15 mm.

Abundance

The relative number of mottles can be expressed by the words few, many, abundant, and profuse:

Few – Mottles occupy less than 2 per cent of the exposed surface.

Many – Mottles occupy 2–20 per cent of the exposed surface.

Abundant – Mottles occupy more than 20 per cent of the exposed surface, and are set in a definite matrix.

Profuse – Mottles occupy almost the whole of the exposed surface, and there is no clear matrix colour.

Fig.A7.6: Gleying descriptions (Taylor and Pohlen, 1979)

Weakly gleyed	– Few gley mottles (less than 2 per cent).
Moderately gleyed	– Many gley mottles (2–20 per cent).
Strongly gleyed	– Abundant gley mottles (more than 20 per cent, but not completely gley mottled).
Very strongly gleyed	– Almost or completely gleyed (profuse gley mottles or diffusely gleyed).

Fig.A7.7: Organic classification based on ASTM D2488.

Highly Organic Soils–Contains fibrous plant debris in various stages of decay; when moist are dark-brown-black with soft spongy feel; distinctive odour.

Partly Organic Soils–Composed predominantly of inorganic material; often dark brown-grey with some odour.

LOCATION: MOTOR CAMP AREA

DATE: 13/8/81

METHOD: Hand Auger (4 inch)

Lithology: Mudstone colluvium

Hole No: 1

DEPTH	GRAPHIC LOG	COLOUR	STRENGTH	MOISTURE CONTENT	PLASTICITY	UNIFIED SOIL SYMBOL	ADDITIONAL DESCRIPTION
0		Dark brown topsoil					
0.3	REGRADED MATERIAL	Dark yellowish brown	F	M	MP	CH	Few medium faint mottles; some decomposed root fragments
0.5		Light yellowish brown	Sf	S	HP	CH	Many medium faint mottles; some decomposed root fragments
1.0		Light yellowish brown	Sf	W	HP	CH	Many medium distinct mottles; some decomposed plant material.
1.5		Light yellowish brown	Sf	W	HP	CH	Abundant medium prominent mottles; small quantity of undecomposed plant material.
1.75	paleosol ?	Dark greyish brown	Sf	S	HP	OH	Highly organic; many coarse distinct mottles; moderate gleying.
2.3	MASSMOVEMENT DEBRIS	Dark brownish grey	Sf	S	HP	CH	Partially organic, some decomposed material; few medium distinct mottles; moderate gleying.
2.6		Dark yellowish grey	F	W	MP	CH	Some carbonaceous material; few coarse faint mottles; Clasts of indurated mudstone.
3.0		Dark brownish grey	F	W	MP	CH	Many medium distinct mottles.
3.5		Dark brownish grey	F	W	MP	CH	Few coarse distinct mottles.
4.0		Dark brownish grey	F	W	MP	CH	Many coarse distinct mottles.
4.2		Light yellowish grey	F	W	MP	CH	Many medium distinct mottles.
4.6							

DEPTH	GRAPHIC LOG	COLOUR	STRENGTH	CONTENT MOISTURE	PLASTICITY	UNIFIED SOIL SYMBOL	ADDITIONAL DESCRIPTION
4.6	MASSMOVEMENT DEBRIS	Light yellowish grey	F	W	MP	CH	Abundant coarse prominent mottles; dark brown intensely oxidised zones?
5.3	MASSMOVEMENT DEBRIS	Light yellowish grey	F	W	MP	CH	Many coarse faint mottles; moderate gleying; dark brown intensely oxidised zones (?)
5.7	Paleosol ?	Dark brownish grey	F	W	HP	OH	Partially organic; many coarse faint mottles; dark brown intensely oxidised patches (?)
6.3	Paleosol ?	Dark brownish grey	F	W	HP	OH	Partially organic; few medium faint mottles; remnants of a paleosol (?)
6.4	Paleosol ?	Dark brownish black	VSf	S	HP	OH	Highly organic; contains clasts of indurated mudstone.
6.5							

LOCATION: MOTOR CAMP AREA

DATE: 4/2/82

METHOD: Hand Auger (4 inch)

Lithology: Mudstone colluvium

Hole No: 2

DEPTH	GRAPHIC LOG	COLOUR	STRENGTH	MOISTURE CONTENT	PLASTICITY	UNIFIED SOIL SYMBOL	ADDITIONAL DESCRIPTION
0	REGRADED MATERIAL	Light yellowish brown	F	M	SP	CH	Compact fill; stones of various sizes within matrix.
0.2		Light greyish brown	Sf	M	MP	CH	Many medium faint mottles.
0.3		Light reddish brown	F	M	MP	CH	Many coarse distinct mottles.
0.5		Light reddish brown	F	M	MP	CH	Many coarse prominent mottles.
1.0		Light reddish brown	F	M	MP	CH	Many medium prominent mottles.
1.5		Light reddish brown	F	M	MP	CH	Abundant medium prominent mottles.
2.0		Light reddish brown	F	M	MP	CH	Abundant coarse prominent mottles
2.5		Light reddish brown	F	M	MP	CH	Abundant coarse prominent mottles.
3.0	paleosol	Light greyish brown	F	M	HP	OH	Many medium distinct mottles. Partly organic
3.5	MASSMOVEMENT DEBRIS	Dark yellowish grey	F	M	HP	CH	Many coarse distinct mottles.
4.0		Dark reddish grey	F	M	HP	CH	Many coarse distinct mottles.
4.7		Dark yellowish brown	F	M	MP	CH	Many coarse distinct mottles.
5.0							

DEPTH	GRAPHIC LOG	COLOUR	STRENGTH	MOISTURE CONTENT	PLASTICITY	UNIFIED SOIL SYMBOL	ADDITIONAL DESCRIPTION
5.0	MASS MOVEMENT DEBRIS	Dark yellowish grey	F	M	MP	CH	Partly organic; many medium distinct mottles.
5.5	paleosol?	Dark blueish grey	F	M	MP	OH	Highly organic, some undecomposed material; moderate gelying; volcanic rock fragments
6.0		Dark grey	S	M	MP	CH	Clasts of indurated mudstone augered up.
6.5							

LOCATION: MOTOR CAMP AREA

DATE: 5/2/82

METHOD: Hand Auger (4 inch)

Lithology: Mudstone regolith

Hole No: 3

DEPTH	GRAPHIC LOG	COLOUR	STRENGTH	MOISTURE CONTENT	PLASTICITY	UNIFIED SOIL SYMBOL	ADDITIONAL DESCRIPTION
0	REGRADED MATERIAL	Dark brown topsoil					
0.3		Light brownish grey	Sf	M	HP	CH	Partly organic; many medium distinct mottles.
0.6	ORGANIC	Dark blackish grey	VSf	S	HP	OH	Highly organic; moderately gleyed.
1.2	REGOLITH	Light yellowish brown	Sf	S	HP	CH	Abundant corase faint mottles.
2.0		Dark yellowish brown	Sf	S	HP	CH	Abundant coarse faint mottles.
3.0		Dark yellowish grey	Sf	S	HP	CH	Abundant medium distinct mottles.
4.0		Dark grey	VSf	S	HP	CH	Clasts of mudstone within a saturated matrix; shear zone (?) approximately 25 cm thick.
4.25							

LOCATION: DAVIDS ROAD AREA

DATE: 16/2/82

METHOD: Hand Auger (4 inch)

Lithology: Mudstone overburden

Hole No: 4

DEPTH	GRAPHIC LOG	COLOUR	STRENGTH	MOISTURE CONTENT	PLASTICITY	UNIFIED SOIL SYMBOL	ADDITION DESCRIPTION
0		Dark brownish grey	F	M	MP		
0.2	ORGANIC DEBRIS	Light brownish grey	VSf	S	HP	CH	Partly organic; many coarse distinct mottles.
1.0		Light brownish grey	VSf	S	HP	CH	Partly organic; many medium distinct mottles; moderately gleyed.
1.5		Light brownish grey	VSf	S	HP	CH	Partly organic; many medium distinct mottles; weakly gleyed.
2.0		Dark brownish grey	VSf	S	HP	CH	Partly organic; more decomposed material; many medium distinct mottles; weakly gleyed.
2.5		Dark blackish grey	VSf	S	HP	CH	Partly organic; carbonaceous material; moderately gleyed.
3.2		Light greyish brown	Sf	W	HP	CH	Many coarse distinct mottles.
3.3		Dark blackish grey	VSf	S	HP	OH	Highly organic; carbonaceous material; moderately gleyed.
3.7		Dark greyish brown	Sf	S	HP	CH	Partly organic, numerous decompoased plant material; many coarse distinct mottles. Paleosol ?
4.0		Dark blackish grey	VSf	S	HP	OH	Highly organic.
4.2	MASSMOVEMENT DEBRIS	Dark reddish brown	F	M	HP	CH	Abundant coarse prominent mottles.
4.7		Dark reddish brown	F	M	HP	CH	Abundant coarse prominent mottles.
5.8							

DEPTH	GRAPHIC LOG	COLOUR	STRENGTH	MOISTURE CONTENT	PLASTICITY	UNIFIED SOIL SYMBOL	ADDITIONAL DESCRIPTION
5.8	ORGANIC	Light blackish grey	F	W	HP	OH	Highly organic; moderately gleyed.
6.0		Light blackish grey	F	S	HP	OH	Highly organic; moderately gleyed.
6.5							

LOCATION: DAVIDS ROAD AREA

DATE: 9/2/82

METHOD: Hand Auger (4 inch)

Lithology: Mudstone colluvium

Hole No: 5

DEPTH	GRAPHIC LOG	COLOUR	STRENGTH	MOISTURE CONTENT	PLASTICITY	UNIFIED SOIL SYMBOL	ADDITIONAL DESCRIPTION
0		Dark brown topsoil	Sf	M	SP		
0.2		Dark brownish grey	F	M	HP	CH	Partly organic; many medium distinct mottles.
0.65		Light brownish grey	F	M	HP	CH	Partly organic; some undecayed material; abundant coarse distinct mottles; weakly gleyed.
1.2		Light reddish grey	VSf	S	HP	CH	Partly organic; many coarse distinct mottles; weakly gleyed.
1.8		Light brownish grey	F	M	HP	CH	Many medium distinct mottles; partly organic.
2.0	paleosol	Light grey	F	W	HP	OH	Few medium faint mottles; partly organic.
3.8	MASSMOVEMENT DEBRIS	Light reddish grey	F	M	HP	CH	Many medium distinct mottles.
4.0		Light yellowish brown	F	M	MP	CH	Many coarse distinct mottles.
5.0		Dark yellowish brown	F	M	MP	CH	Abundant medium prominent mottles.
6.0		Dark yellowish brown	F	M	MP	CH	Abundant medium prominent mottles.
7.3		Dark grey	F	D	MP	CH	Clasts of mudstone; apparently sharp boundaries between horizons.
7.4		Dark yellowish brown	F	M	MP	CH	Abundant medium prominent mottles.
7.75							

DEPTH	GRAPHIC LOG	COLOUR	STRENGTH	MOISTURE CONTENT	PLASTICITY	UNIFIED SOIL SYMBOL	ADDITIONAL DESCRIPTION
7.75	MASSMOVEMENT DEBRIS	Dark grey	F	D	MP	CH	Clasts of mudstone; apparently sharp boundaries between horizons.
7.8		Dark yellowish brown	F	M	MP	CH	Abundant coarse prominent mottles.
8.3		Dark grey	F	D	MP	CH	Clasts of mudstone
8.5		Dark yellowish brown	F	M	MP	CH	Many coarse prominent mottles
8.6							

LOCATION: DAVIDS ROAD AREA

DATE: 17/2/82

METHOD: Hand Auger (4 inch)

Lithology: Mudstone colluvium

Hole No: 6

DEPTH	GRAPHIC LOG	COLOUR	STRENGTH	MOISTURE CONTENT	PLASTICITY	UNIFIED SOIL SYMBOL	ADDITIONAL DESCRIPTION
0		Dark brown topsoil	Sf	M	SP		
0.2		Dark brownish grey	F	M	MP	CH	Partly organic; abundant coarse prominent mottles.
0.6		Light yellowish brown	Sf	S	HP	CH	Abundant coarse prominent mottles.
0.7	paleosol	Dark blackish grey	VSf	S	HP	OH	Highly organic.
1.1	MASSMOVEMENT DEBRIS	Light yellowish grey	Sf	S	HP	CH	Many medium distinct mottles.
1.2		Dark blackish grey	VSf	S	HP	OH	Highly organic; numerous undecayed plant fragments. Moderate gleying.
2.1		Dark blackish brown	VSf	S	HP	OH	Highly organic; possibly an old soil horizon.
3.2		Dark brownish grey	Sf	W	HP	CH	Partly organic; some undecayed plant material. Moderately gleyed.
3.6		Dark yellowish brown	F	W	HP	CH	Many medium distinct mottles.
5.5		Dark yellowish brown	F	W	HP	CH	Many coarse distinct mottles.
6.0		Dark yellowish brown	F	W	HP	CH	Abundant medium prominent mottles.
7.0		Dark yellowish grey	F	W	HP	CH	Many medium distinct mottles; clasts of mudstone colluvium matrix.
7.5							

DEPTH	GRAPHIC LOG	COLOUR	STRENGTH	MOISTURE CONTENT	PLASTICITY	UNIFIED SOIL SYMBOL	ADDITIONAL DESCRIPTION
7.5 8.0	MASS MOVEMENT DEBRIS	Dark yellowish grey	F	M	HP	CH	Many medium distinct mottles; clasts of mudstone colluvium matrix.

LOCATION: DAVIDS ROAD AREA, base of batter slope

DATE: 15/2/82

METHOD: Caldwel Rig; two foot bucket; Remoulded samples taken every 50 cm.

Lithology: Mudstone regolith

Hole No: B1

DEPTH	GRAPHIC LOG	COLOUR	STRENTH	MOISTURE CONTENT	PLASTICITY	UNIFIED SOIL SYMBOL	ADDITIONAL DESCRIPTION
0		Dark brown topsoil	Sf	M	SP		
0.5	REGOLITH	Dark yellowish brown	F	M	HP	CH	Partly organic; many medium distinct mottles; rock fragments; shells.
1.0		Dark yellowish brown	F	M	HP	CH	Many medium distinct mottles; volcanic rock fragments; shells.
1.5		Dark yellowish brown	F	M	HP	CH	Partly organic; some undecayed material; many coarse distinct mottles; moderate gleying.
2.0		Dark yellowish brown	F	M	HP	CH	Many medium distinct mottles.
2.5		Dark greyish brown	F	M	HP	CH	Few medium faint mottles; clasts of mudstone within regolith matrix.
3.0		Dark greyish brown	F	M	HP	CH	Few medium faint mottles; large clasts of mudstone within regolith matrix.
3.5		Dark blue grey	F	M	HP	CH	Few medium distinct mottles; large clasts of mudstone within regolith matrix.
4.0		Dark blue grey	F	M	HP	CH	Few medium distinct mottles; large clasts of mudstone within regolith matrix.
4.5		Dark blue grey	F	M	HP	CH	Few coarse distinct mottles; large clasts of mudstone within regolith matrix.
5.0		Dark blue grey	F	W	HP	CH	Few coarse prominent mottles; large clasts of mudstone within regolith matrix.
5.5		Dark blue grey	F	W	HP	CH	Few coarse distinct mottles; large clasts of mudstone within regolith matrix
6.0							

DEPTH	GRAPHIC LOG	COLOUR	STRENGTH	MOISTURE CONTENT	PLASTICITY	UNIFIED SOIL SYMBOL	ADDITIONAL DESCRIPTION
6.0 9 m		Dark blue grey	F	M	H	CH	Hard, unweathered mudstone.

LOCATION: MOTOR CAMP AREA

DATE: 15/8/81

METHOD: Hand Auger (4 inch)

Lithology: Mudstone colluvium

Hole No: P1

DEPTH	GRAPHIC LOG	COLOUR	STRENGTH	MOISTURE CONTENT	PLASTICITY	UNIFIED SOIL SYMBOL	ADDITIONAL DESCRIPTION
0		Dark brown topsoil					
0.2	REGRADED MATERIAL	Light reddish brown	F	M	SP	CH	Many coarse distinct mottles.
1.0		Light reddish brown	F	M	SP	CH	Many medium prominent mottles.
1.5		Light reddish brown	F	M	SP	CH	Abundant medium prominent mottles.
2.0	paleosol	Light greyish brown	VSf	S	HP	OH	Partially organic, some undecomposed material; few coarse distinct mottles; weak gleying.
2.5		Light blueish grey	F	M	MP	OH	Partially organic; some undecomposed material; coarse distinct mottles; weak gleying.
3.0	REGOLITH	Light reddish brown	F	M	MP	CH	Abundant medium prominent mottles.
3.5		Light reddish brown	F	M	MP	CH	Abundant coarse prominent mottles.
4.0		Light reddish brown	F	M	MP	CH	Abundant coarse prominent mottles.
4.5		Light reddish brown	F	M	MP	CH	Many coarse distinct mottles.
5.0		Light reddish brown	F	M	MP	CH	Many medium distinct mottles.
5.5		Light blueish grey	Sf	M	MP	CH	Few coarse distinct mottles.
6.0							

DEPTH	GRAPHIC LOG	COLOUR	STRENGTH	MOISTURE CONTENT	PLASTICITY	UNIFIED SOIL SYMBOL	ADDITIONAL DESCRIPTION
6.0 6.5		Light blueish grey	F	M	MP	CH	Many medium distinct mottles.

LOCATION: DAVIDS ROAD AREA

DATE: 10/8/81

METHOD: Hand Auger (4 inch)

Lithology: Mudstone regolith

Hole NO: P2

DEPTH	GRAPHIC LOG	COLOUR	STRENGTH	MOISTURE CONTENT	PLASTICITY	UNIFIED SOIL SYMBOL	ADDITIONAL DESCRIPTION
0	REGRADED MATERIAL	Dark brown topsoil	Sf	W	SP		
0.3		Light yellowish brown	VSf	W	HP	CH	Partly organic; some undecayed material; many coarse distinct mottles; weakly gleyed.
1.0		Dark blueish black	VSf	S	HP	OH	Highly organic; moderately gleyed.
2.0		Dark blueish black	VSf	S	HP	OH	Highly organic; strongly gleyed.
3.0		Dark blueish black	VSf	S	HP	OH	Highly organic; strongly gleyed.
4.0		Dark blueish grey	VSf	S	HP	CH	Partly organic; some undecayed material; many coarse distinct mottles; moderately gleyed.
5.0		Dark blueish grey	VSf	S	HP	CH	Partly organic; some undecomposed material; many medium distinct mottles; moderately gleyed.
6.0		Light reddish brown	VSf	S	HP	CH	Abundant medium prominent mottles.
7.0							

LOCATION: DAVIDS ROAD AREA

DATE: 12/8/81

METHOD: Hand Auger (4 inch)

Lithology: Mudstone colluvium

Hole No: P3

DEPTH	GRAPHIC LOG	COLOUR	STRENGTH	MOISTURE CONTENT	PLASTICITY	UNIFIED SOIL SYMBOL	ADDITIONAL DESCRIPTION
0		Dark brown topsoil	Sf	M	SP	CH	
0.25	MASSMOVEMENT DEBRIS	Light yellowish brown	F	M	MP	CH	Partly organic; many medium distinct mottles.
0.5		Dark brownish grey	F	M	MP	CH	Partly organic; some undecomposed root fragments; many medium distinct mottles; weak gleying.
1.5		Light reddish brown	F	M	MP	CH	Many medium prominent mottles.
2.8		Light brownish grey	F	M	MP	CH	Partly organic; abundant medium distinct mottles; moderate gleying.
3.1	softened horizon	Light yellowish brown	VSf	W	HP	CH	Abundant coarse distinct mottles; moderate gleying.
3.6	MASSMOVEMENT DEBRIS	Light brownish grey	F	M	MP	CH	Many coarse distinct mottles.
4.1		Light brownish grey	F	M	MP	CH	Many medium distinct mottles.
4.6		Dark brownish grey	F	M	MP	CH	Clasts of mudstone within regolith.
4.8		Light yellowish brown	F	M	MP	CH	Abundant medium prominent mottles.
5.0							

APPENDIX 8

GROUNDWATER MONITORING

Introduction

A8.1 Construction of Monitoring Devices

A8.2 Tabulated Data

INTRODUCTION

Piezometers in conjunction with standpipes were installed at three locations to monitor groundwater pressures over a one year period from August 1981 to August 1982.

Piezometric level at a point is the elevation to which water eventually rises within a small tube seated into the appropriate horizon. Groundwater pressure (μ) at a point is equal to the piezometric level (hp) minus the elevation of that point (h) multiplied by the unit weight of water (Yw)

$$\mu = Yw(hp-h)$$

Significance of data recorded from these types of device is largely dependant on 'response time' which apart from the physical properties of ambient material is dependant on:

1) size and permeability of drain surrounding the piezometer tip,

2) diameter of piezometer/standpipe tubing,

3) presence of entrapped air.

A8.1 CONSTRUCTION

Both piezometers and standpipes comprise lengths of P.V.C. conduit, perforated at selected intervals, and the porus sections encased in several layers of synthetic filter cloth. Generalised construction is depicted in Fig. A8.1.

Drains (approximately 10 cm diameter) enclosing piezometer tips were backfilled with very fine, well sorted sand to prevent clogging by ubiquitous clay. Drains were assumed to have negligible affect on measured pore pressures, ie. Vaughan (1969) notes drain permeability may be in the order of ten times greater than the surrounding material before causing significant influence on pore pressures. Thin layers of coarse gravel were incorporated within some drains, below the water table, to facilitate ramming of concrete/bentonite sealer horizons.

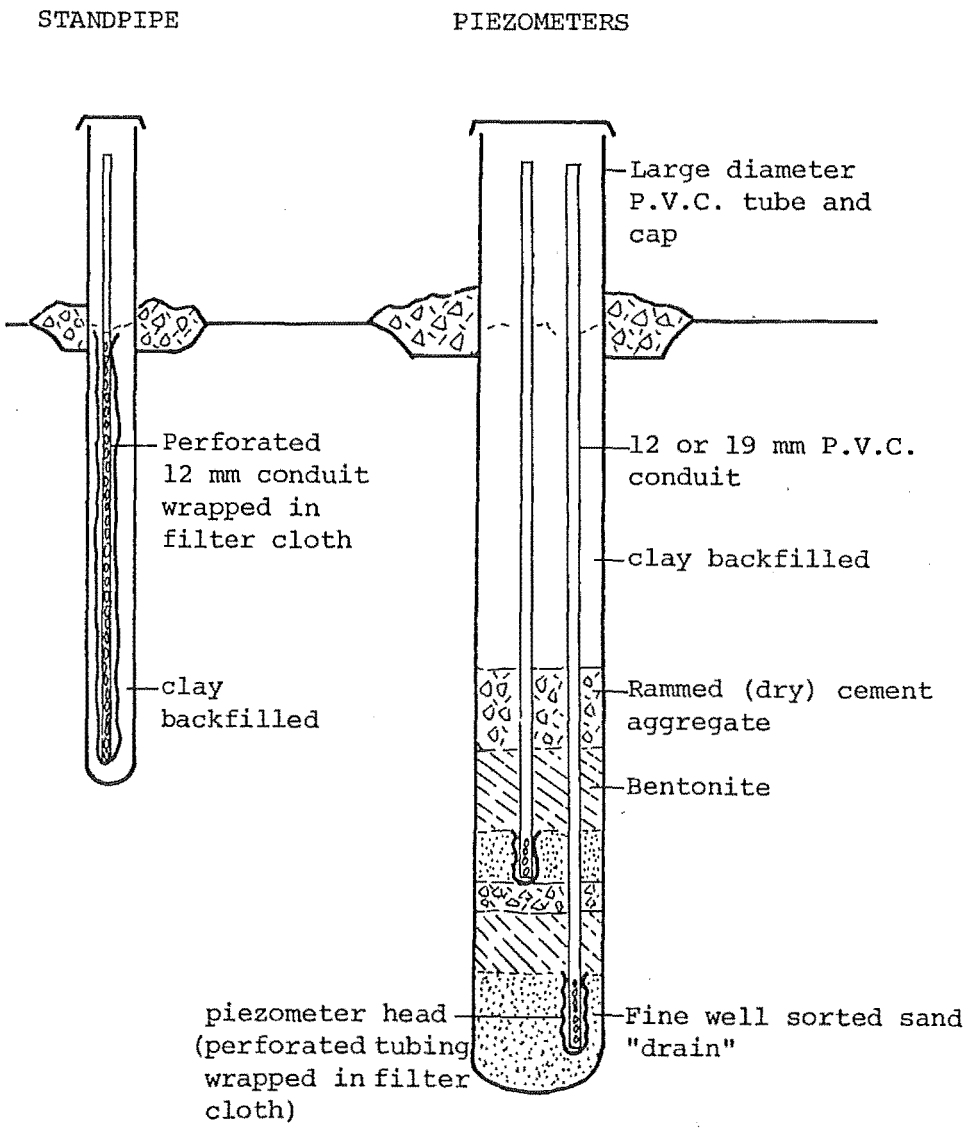

Fig.A8.1: Generalised construction details for ground water monitoring devices; note "drain" bentonite/aggregate thickness is site specific (diagram based on P_3).

Systems were assumed self de-airing with piezometer/ standpipe tubing of sufficient diameter to allow any entrapped air to rise freely to the air-water interface, ie. Vaughan (1974) states a 'clean' conduit diameter of 12 mm is the minimum for the self de-airing process.

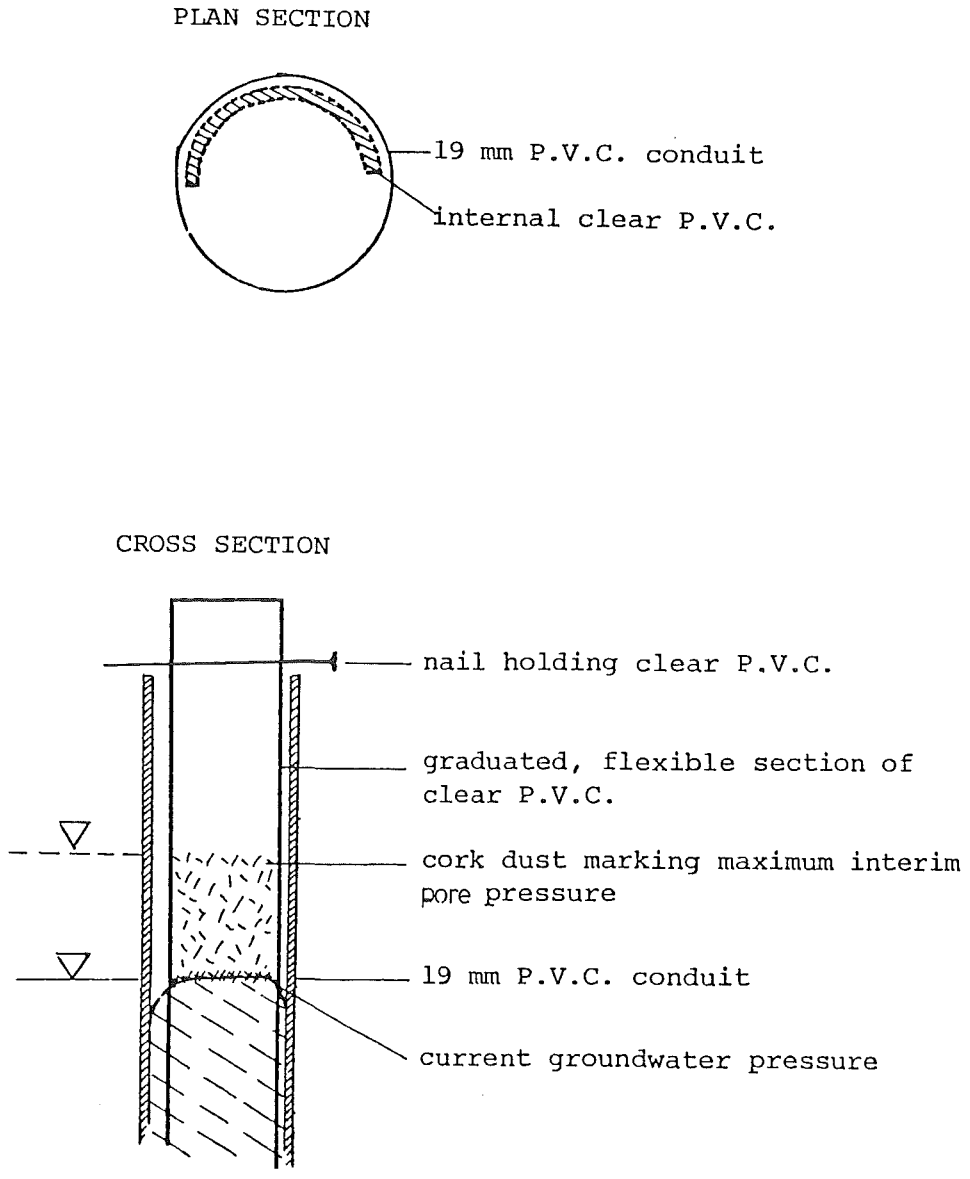

Fig.A8.2: Schematic diagram portraying 'cork dust' method of recording maximum interim pore pressure.

A8.2 TABULATED PIEZOMETER/STANDPIPE DATA

MOTOR CAMP AREA		
MOTOR CAMP INSTALLATION		
DATE	WATER LEVEL BELOW GROUND SURFACE	
	GREY TUBE	GREEN STRIPED TUBE
03.08.81	0.32 m	0.31 m
16.08.81	0.38	0.37
19.08.81	0.53	0.54
22.08.81	0.42	0.44
24.08.81	0.33	0.33
30.08.81	0.54	0.55
14.09.81	0.36	0.36
18.09.81	0.51	0.42
06.10.81	0.37	0.37
08.10.81	0.37	0.37
14.10.81	0.50	0.50
27.10.81	0.50	0.50
31.10.81	0.43	0.43
25.02.82	0.37	0.36
04.03.82	0.4	0.39
01.08.82	0.51	0.52
08.08.82	0.53	0.54
16.08.82	0.48	0.49
22.08.82	0.35	0.39
19.09.82	0.60	0.60

DAVIDS ROAD AREA					
	COASTAL INSTALLATION		DEBRIS SLIDE INSTALLATION		
DATE	WATER LEVEL BELOW GROUND SURFACE				
	GREY	GREEN	GREY	GREEN	BLUE
03.08.81	0.34 m	0.47 m		0.83 m	0
12.08.81	0.34	0.41		0.68	0
19.08.81	0.49	0.73	3.01	0.75	0
02.09.81	0.56	0.52	2.35	0.96	0
09.09.81	0.57	0.56	2.30	1.20	0
24.09.81	0.61	0.69	2.56	1.40	
05.10.81	0.71	0.60	2.46	0.91	
25.02.82	1.17	1.25	2.60	1.76	1.29
04.03.82	1.20	1.29	2.60	1.82	1.34
20.07.82	0.92	0.88	2.66	2.21	2.11
01.08.82	0.90	0.89	2.66	2.30	2.12
08.08.82	0.95	0.88	2.67	3.35	2.19
16.08.82	0.98	0.92	2.72	3.45	2.23
22.08.82	0.94	0.90	2.76	3.42	2.24
19.09.82	0.91	0.92	2.75	3.5	2.3

APPENDIX 9

SURVEYING

A9.1 Introduction

A9.2 Methodology

9.2.1 Initial and Final Surveys

Equipment
Control Points
Base Points
Monitoring Points - Motor Camp Area
Davids Road Area
Calculation of Resection
Analysed Data

9.2.2 Interim Surveys

Equipment
Motor Camp Area
Davids Road Area
Analysed Data

A9.3 Accuracy

A9.4 Survey Programme

A9.5 Cadestral Reports

A9.1 INTRODUCTION

Survey networks were established in two regions within Moeraki township; the Davids Raod area and the Motor Camp area. Monitoring was over a one year period from August 1981 to August 1982 and comprised nine individual surveys. Initial and final measurements, completed with assistance from Mr Greig and Mr Hermann, were more comprehensive and established if any "control points" taken as fixed during interim surveys had moved. The large number of network points (34) meant redundant measurements were kept to a minimum during monthly surveys with monitoring points 'fixed' by ties (angle and distance from known co-ordinates). Points considered stable after early measurements were not reobserved until the final survey.

Survey plans of both networks with total calculated movement expressed in vector form are presented in the map enclosure.

A9.2 METHODOLOGY

9.2.1 Initial and Final Surveys (August 1981, August 1982)

Equipment

Wild T2	Steel band
Wild T16 (with ED.M)	Prisms GDR31 single and triple
Wild D13 Distomat	

Control Points

Point 4 is assumed stable and utilized as the main control station. Using a "resection" absolute positioning of point 4 was determined in terms of Geodetic Datum 1949 (Observation Point). Orientation was then transferred to control point 1 and its co-ordinates held fixed. Control points 1, 2 and 3 were then traversed and adjusted. Accuracy was limited, due to lack of regard taken for atmospheric conditions in the initial survey measurement of base lines. This limitation has not affected relative accuracies to a large degree (atmospheric corrections are a function of

distance) but should be appreciated in the interpretation of results. With this understanding in mind Mark Nos 1 and 11 are assumed to have remained "fixed", as over distances involved it is not possible to discern displacement.

Base Points

From point 1, control point 10 and base point 11 were co-ordinated. In the Davids Road area to provide a quick method for showing transverse movement of point 11 during observation of monthly surveys point 12 (stable) was "lined in" with 10 and 11 to give a line over 10; movement of 11 would thus immediately be discerned upon re-alignment of the three survey markers.

In the Motor Camp area points A, B, C and D were fixed utilizing a measured line between control points as a base and measuring each of the three angles.

Monitoring Points

Motor Camp Area

Monitoring points were observed from base points A, B, C and D and fixed by "ties" (angle and distance) with the appropriate checks.

Davids Road Area

All monitoring points were observed and measured from base point 11 and fixed by "ties" with checks made from points 13, D and B and the triangles closed.

Points H, I and J were heighted with vertical angles from 11 (relative to arbitrary datum Mark No 10 = 100 m).

CALCULATION OF RESECTION

	MN	ME
L 12' QUAD	745 545.188	309 320.789
F Pillar	751 819.57	314 296.57
H 6' Trig (Adj for ecc)	755 478.51	315 450.71
Mt.Charles No.2 12' QUAD	764 843.385	312 705.717

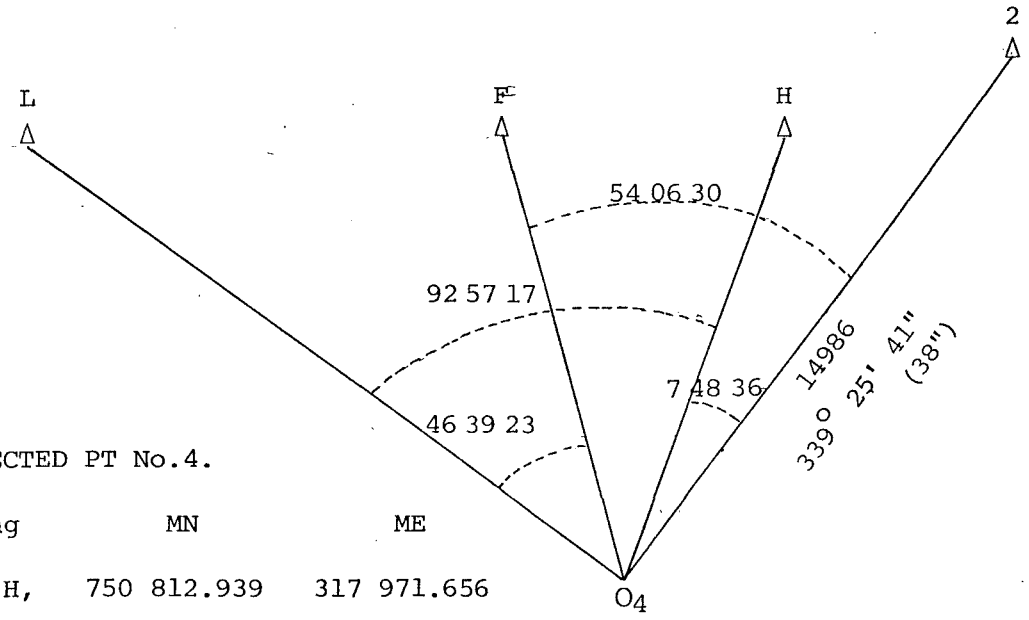

RESECTED PT No.4.

Using	MN	ME
L,F,H,	750 812.939	317 971.656
L,H,2	750 812.547	317 971.666
L,F,2	750 812.825	317 971.815
F,H,2	750 812.835	317 971.481

TRIAL PT 750 812.8N 317 971.6E

Nth Cut	Est Cut	STN	BRG	DIST
-0.251	+0.412	4 → L	238 39 48	10 128
+0.036	+0.131	4 → F	285 19 11	3 810
-0.092	-0.050	4 → H	331 37 05	5 303
+0.074	+0.028	4 → 2	339 25 41	14 986
				20.29

FINAL COORD OF 4

750 812.820 317 971.820

RESECTION OF CONTROL POINT 4

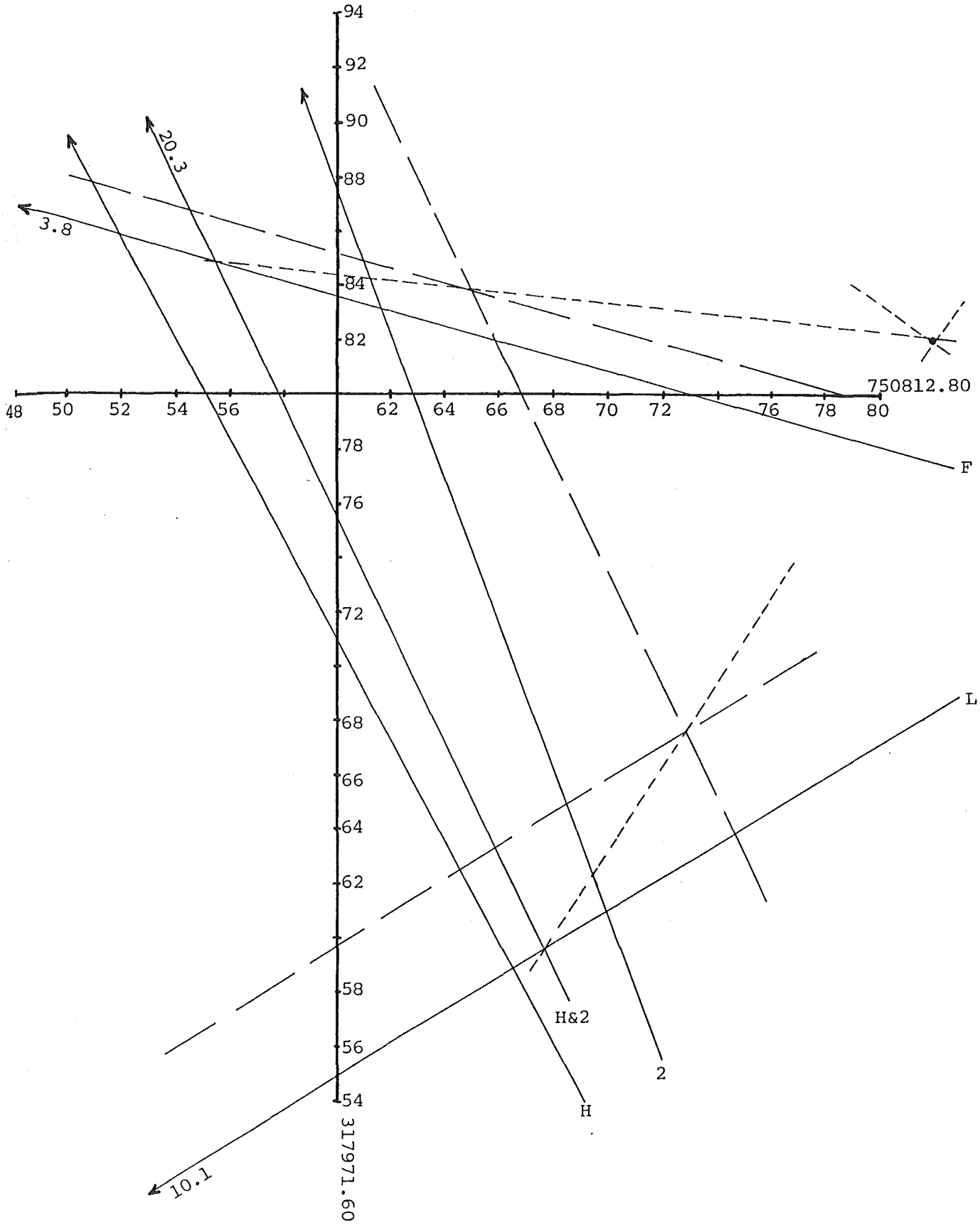

ANALYSED DATA

MOTOR CAMP AREA - COMPUTATIONS

AUGUST 1981

Motor Camp Base Control

IN Δ1,2,3

At 1	44°19'26"	4 → 3	266.108	199 38 36
At 2	115°23'23"	4 → 2	629.081	210 16 48
At 3	20°17'12"			
	180°00'01"			

Intersections (Motor Camp, coordinates from traverse sheet)

1,2,A

		Adj
Angles at 1	12°50'44"	39
2	13°30'52"	47
A	153°38'40"	34
	180°00'16"	

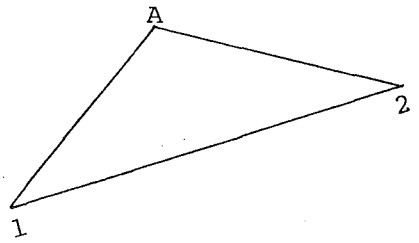

results on trav. sheet 1

1,2,B

Angles at 1	35°15'32"	33
2	35°22'40"	41
B	109°21'45"	46
	179°59'57"	

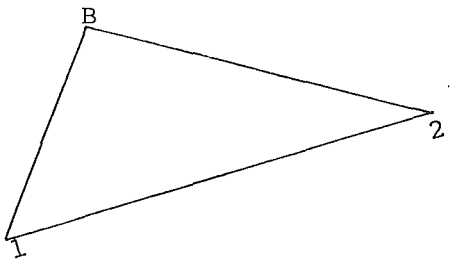

1,3,C

Angles at 1	13°27'48"	48
3	6°46'51"	51
C	159°45'37"	21
	180°00'16"	

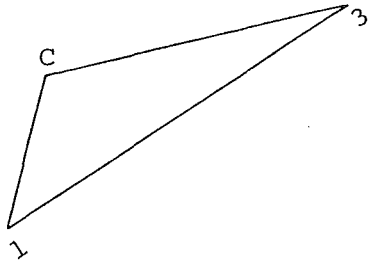

1,3,D

Angles at	1	$17^{\circ}35'46"$	50
	3	$17^{\circ}07'31"$	31
	D	$145^{\circ}16'39"$	39
		$179^{\circ}59'56"$	

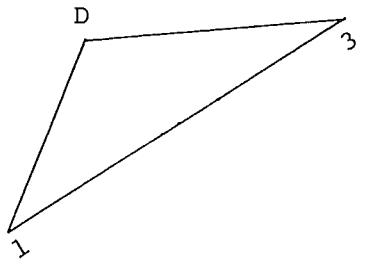

MOTOR CAMP AREA AUGUST 1981

	No. of Survey Mark	Bearing ° ' "	Distance Metres	Northing +N −S	Cor.	Easting +E −W	Cor.	Coordinates Metres N	Coordinates Metres E		No. of Survey Mark	Remarks, including source of coords.
1	4							750 812.820	317 971.820	1	4	Ref Resection
2	1	224 37 22	707.310	503.426		496.840		750 309.394	317 474.980	2	1	
3										3		
4	1				-		-	750 309.394	317 474.980	4	1	line 2 above
5	3	58 10 41	479.453	252.807	2	407.387	3	750 562.199	317 882.364	5	3	
6	2	217 53 29	370.810	292.635	1	227.739	3	750 269.563	317 654.622	6	2	
7	1	282 30 06	184.004	39.831		179.641	1	750 309.394	317 474.980	7	1	line 4 above
8				Misclose		1 in 135.000				8		
9	1		Intersection Programme					750 309.394	317 474.980	9	1	ℓ2 above
10	A	89 39 28	96.847 calc					750 309.973	317 571.825	10	A	
11										11		
12	2							750 269.563	317 654.622	12	2	ℓ6 above
13	A	296 00 54	92.131 calc					750 309.973	317 571.825	13	A	
14										14		
15	1							750 309.394	317 474.980	15	1	
16	B	67 14 34	112.921 calc					750 353.075	317 579.110	16	B	
17										17		
18	2							750 269.563	317 654.622	18	2	
19	B	317 52 48	112.589 calc					750 353.075	317 579.110	19	B	
20										20		
21	1							750 309.394	317 474.980	21	1	
22	C	44 42 53	163.602 calc					750 425.652	317 590.086	22	C	
23										23		
24	3							750 562.199	317 882.364	24	3	ℓ5 above
25	C	244 57 32	322.601 calc					750 425.652	317 590.086	25	C	
26										26		
27	1							750 309.394	317 474.980	27	1	
28	D	40 34 51	247.857 calc					750 497.639	317 636.216	28	D	
29										29		
30	3							750 562.199	317 882.364	30	3	
31	D	255 18 12	254.474 calc					750 497.639	317 636.216	31	D	
32										32		
33	2							750 269.563	317 654.622	33	2	line 6 above
34	A1	324 00 27	31.676	25.629		18.615		750 295.192	317 636.007	34	A1	
35										35		
36										36		

MOTOR CAMP AREA AUGUST 1981

	No. of Survey Mark	Bearing ° ' "	Distance Metres	Northing +N	Northing −S	Cor.	Easting +E	Easting −W	Cor.	Coordinates Metres N	Coordinates Metres E		No. of Survey Mark	Remarks, including source of coords.
1	A									750 309.973	317 571.825	1	A	
2	A2	104 52 57	28.491		7.318		27.535			750 302.655	317 599.360	2	A2	RADIAL (A)
3	A3	132 55 14	33.163		22.583		24.285			750 287.390	317 596.110	3	A3	
4	A4	189 57 05	39.479		38.885			6.822		750 271.088	317 565.003	4	A4	
5	A5	259 42 06	33.740		6.032			33.196		750 303.941	317 538.629	5	A5	
6	A6	172 13 30	9.733		9.644		1.317			750 300.330	317 573.142	6	A6	
7												7		
8	B									750 353.075	317 579.110	8	B	
9	B1	99 05 44	16.728		2.644		16.518			750 350.431	317 595.628	9	B1	RADIAL (B)
10	B2	283 34 27	18.632	4.373				18.112		750 357.448	317 560.998	10	B2	
11	B3	283 12 10	53.422	12.201				52.010		750 365.277	317 527.100	11	B3	
12												12		
13	C									750 425.652	317 590.086	13	C	
14	C1	82 03 50	40.774	5.630			40.383			750 431.282	317 630.469	14	C1	RADIAL (C)
15	C3	56 45 50	49.401	27.076			41.320			750 452.728	317 631.406	15	C3	
16	C4	349 24 14	26.355	25.906				4.846		750 451.558	317 585.240	16	C4	
17	C5	317 55 21	39.552	29.357				26.505		750 455.009	317 563.581	17	C5	
18	C6	264 44 02	15.890		1.458			15.823		750 424.194	317 574.263	18	C6	
19	C7	263 57 10	74.895		7.890			74.478		750 417.762	317 515.608	19	C7	
20	C8	260 01 59	108.238		18.734			106.604		750 406.918	317 483.482	20	C8	
21	C9	81 52 46	112.198	15.849			111.073			750 441.501	317 701.159	21	C9	
22												22		
23	D									750 497.639	317 636.216	23	D	
24	D1	81 14 12	23.680	3.608			23.404			750 501.247	317 659.620	24	D1	RADIAL (D)
25	D2	265 08 52	32.704		2.766			32.587		750 494.873	317 603.629	25	D2	
26	D3	258 16 55	81.062		16.463			79.373		750 481.176	317 556.843	26	D3	
27	C2	207 11 11	55.615		49.471			25.410		750 448.168	317 610.806	27	C2	
28												28		
29												29		
30												30		
31												31		
32												32		
33												33		
34												34		
35												35		
36												36		

DAVIDS ROAD AREA AUGUST 1981

	No. of Survey Mark	Bearing ° ' "	Distance Metres	Northing +N −S	Cor.	Easting +E −W	Cor.	Coordinates Metres N	Metres E		No. of Survey Mark	Remarks, including source of coords.
1	1							750 309.394	317 474.980	1	1	&2 trav-sheet 1
2	10	231 02 31	325.432	-204.616		-253.058		750 104.778	317 221.992	2	10	
3	11	27 17 05	179.097	159.171		82.100		750 263.949	317 304.022	3	11	
4	13	351 41 16	234.036	231.577		-33.834		750 495.526	317 270.188	4	13	
5	A	182 21 22	87.436	-87.362		-3.595		750 176.587	317 300.428	5	A	The coordinates
6	B	195 44 55	73.225	-70.476		-19.875		750 193.473	317 284.148	6	B	
7	C	210 26 03	60.104	-51.822		-30.446		750 212.126	317 273.577	7	C	of these points
8	D	243 56 51	93.595	-41.106		-84.085		750 222.842	317 219.937	8	D	
9	E	261 18 57	62.494	-9.436		-61.778		750 254.513	317 242.245	9	E	are derived
10	F	270 31 22	50.817	0.464		-50.815		750 264.412	317 253.207	10	F	
11	G	352 52 17	42.012	41.687		-5.214		750 305.636	317 298.809	11	G	directly from
12	H	263 36 27	88.584	-9.863		-88.033		750 254.086	317 215.989	12	H	
13	I	278 52 27	65.596	10.119		-64.811		750 274.068	317 239.212	13	I	point 11
14	J	299 12 41	58.192	28.400		-50.791		750 292.348	317 253.231	14	J	
15	K	289 04 27	136.101	44.477		-128.629		750 308.425	317 175.394	15	K	line 3 above
16	L	299 06 23	113.134	55.032		-98.847		750 318.981	317 205.175	16	L	
17	M	313 45 24	108.744	75.207		-78.544		750 339.156	317 225.478	17	M	
18	N	328 36 10	108.304	92.446		-56.423		750 356.394	317 247.599	18	N	
19	P	345 15 09	112.011	108.321		-28.513		750 372.270	317 275.509	19	P	
20										20		
21										21		
22										22		
23										23		
24										24		
25										25		
26										26		
27										27		
28										28		
29										29		
30										30		
31										31		
32										32		
33										33		
34										34		
35										35		
36										36		

ANALYSED DATA

MOTOR CAMP AREA - COMPUTATIONS

AUGUST 1982

Motor Camp Base Control

IN Δ1,2,3		Adj
At 1	44°19'31"	-2"
2	115°23'20"	-1"
3	20°17'14"	-2"
	180°00'05"	

Intersections (Motor Camp, coordinates from traverse sheet)

1,2,A		Adj
Angles at 1	12°51'46"	-10"
2	13°31'49"	-11"
A	153°36'57"	-11"
	180°00'32"	

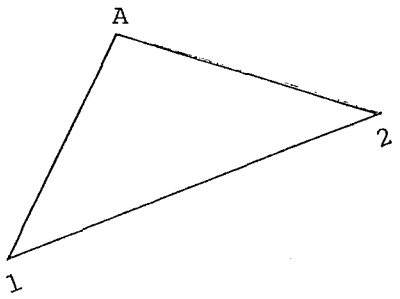

1,2,B		
Angles at 1	35°16'24"	-5
2	35°23'40"	-5
B	109°20'12"	-6
	180°00'16"	

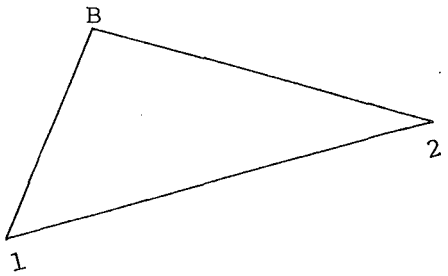

1,3,C		
Angles at 1	13°28'06"	
3	6°47'07"	
C	159°44'48"	-1
	180°00'01"	

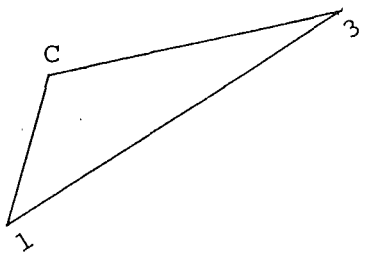

1,3,D

Angles at 1		$17^{\circ}36'28"$	+1
	3	$17^{\circ}08'15"$	+1
	D	$145^{\circ}15'13"$	+2
		$179^{\circ}59'56"$	

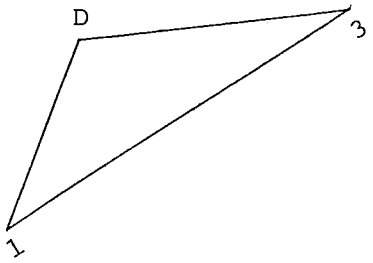

MOTOR CAMP AREA AUGUST 1982

	No. of Survey Mark	Bearing ° ' "	Distance Metres	Northing +N −S	Cor.	Easting +E −W	Cor.	Coordinates Metres N	Metres E		No. of Survey Mark	Remarks, including source of coords.
1	4							750 812.820	317 971.820	1	4	Ref previous
2	1	224 37 18	707.296	-503.425		-496.820		750 309.395	317 475.000	2	1	survey
3								750(309.394)	317(474.980)	3		
4	1							750 309.394	317 474.980	4	1	-accepted from
5	3	58 10 39	479.453	252.811	+1	407.384	+2	750 562.204	317 882.366	5	3	previous survey
6	2	217 53 27	370.818	292.643	-1	227.741	+2	750 269.560	317 654.627	6	2	
7	1	282 30 08	184.011	39.834		179.648	+1	750 309.394	317 474.980	7	1	
8				+(.002)		-(.005)		(1 in 192,000)		8		
9	1							750 309.394	317 474.980	9	1	
10	A	89 38 32	96.845 calc					750 309.999	317 571.823	10	A	
11										11		
12	2							750 269.560	317 654.627	12	2	
13	A	296 01 46	92.151 calc					750 309.999	317 571.823	13	A	
14										14		
15	1							750 309.394	317 474.980	15	1	
16	B	67 13 49	112.946 calc					750 353.107	317 579.124	16	B	
17										17		
18	2							750 269.560	317 654.627	18	2	
19	B	317 53 43	112.609 calc					750 353.107	317 579.124	19	B	
20										20		
21	1							750 309.394	317 474.980	21	1	
22	C	44 42 33	163.632 calc					750 425.685	317 590.097	22	C	
23										23		
24	3							750 562.204	317 882.366	24	3	
25	C	244 57 46	322.581 calc					750 425.685	317 590.097	25	C	
26										26		
27	1							750 309.394	317 474.980	27	1	
28	D	40 34 10	247.887 calc					750 497.693	317 636.198	28	D	
29										29		
30	3							750 562.204	317 882.366	30	3	
31	D	255 18 55	254.481 calc					750 487.693	317 636.198	31	D	
32										32		
33	2							750 269.560	317 654.627	33	2	
34	A1	324 00 04	31.697					750 295.204	317 635.996	34	A1	
35										35		
36										36		

ANALYSED DATA

MOTOR CAMP AREA AUGUST 1982

	No. of Survey Mark	Bearing ° ' "	Distance Metres	Northing +N −S	Cor.	Easting +E −W	Cor.	Coordinates Metres N	Metres E		No. of Survey Mark	Remarks, including source of coords.
1	A							750 309.999	317 571.823	1	A	
2	A2	104 40 56	28.298					750 320.827	317 599.197	2	A2	RADIAL
3	A3	132 55 44	33.073					750 287.473	317 596.039	3	A3	
4	A4	189 57 21	39.510					750 271.084	317 564.992	4	A4	
5	A5	259 41 09	33.723					750 303.961	317 538.645	5	A5	
6										6		
7	B							750 353.107	317 579.124	7	B	
8	B1	99 05 23	16.717					750 350.466	317 595.631	8	B1	RADIAL
9	B2	283 31 24	18.545					750 357.444	317 561.093	9	B2	*
10	B3	283 09 50	53.429					750 365.275	317 527.099	10	B3	
11										11		
12	C							750 425.685	317 590.097	12	C	
13	C1	82 01 40	40.768					750 431.339	317 630.471	13	C1	RADIAL
14	C3	56 44 37	49.408					750 452.780	317 631.413	14	C3	
15	C4	349 24 06	26.367					750 451.602	317 585.248	15	C4	
16	C5	317 54 32	39.532					750 455.021	317 563.598	16	C5	
17	C6	264 46 59	15.785	*						17	C6	*
18	C7	263 54 59	74.892					750 417.748	317 515.627	18	C7	
19	C8	260 00 15	108.241					750 406.897	317 483.499	19	C8	
20	C9	81 52 50	112.175					750 441.528	317 701.148	20	C9	
21										21		
22	D							750 497.693	317 636.198	22	D	
23	D1	81 16 34	23.703					750 501.288	317 659.627	23	D1	RADIAL
24	D2	265 16 12	32.598					750 495.005	317 603.711	24	D2	
25	D3	258 14 37	81.061					750 481.177	317 556.837	25	D3	
26	C2	207 11 05	55.581					750 448.252	317 610.805	26	C2	
27										27		
28										28		
29										29		
30										30		
31										31		
32										32		
33										33		
34										34		
35										35		
36										36		

DAVIDS ROAD AREA AUGUST 1982

	No. of Survey Mark	Bearing ° ' "	Distance Metres	Northing +N −S	Cor.	Easting +E −W	Cor.	Coordinates Metres N	Coordinates Metres E		No. of Survey Mark	Remarks, including source of coords.
1	1				mm		mm	750 309.394	317 474.980	1	1	Close of
2	10	231 02 30	325.424	204.612	-2	253.051	-5	750 104.780	317 221.924	2	10	Control to
3	11	27 17 10	179.097	159.169		82.104	-6	750 263.949	317 304.022	3	11	establish
4	13	351 41 10	234.045	231.585	-8	33.842	+8	750 495.526	317 270.188	4	13	any gross
5	4	65 40 02	770.023	317.277	+17	701.620	+12	750 812.820	317 971.820	5	4	errors
6				(503.419)		(496.831)		(503.426)	(496.840)	6		
7										7		
8										8		
9	11							750 263.949	317 304.022	9	11	
10	A	182 21 55	87.439					750 176.584	317 300.413	10	A	
11	B	195 46 14	73.218					750 193.487	317 284.122	11	B	
12	C	210 28 51	60.081					750 212.171	317 273.546	12	C	
13	D	243 58 05	93.599					750 222.871	317 219.919	13	D	
14	E	261 20 27	62.499					750 254.539	317 242.235	14	E	
15	F	270 33 09	50.812					750 264.439	317 253.212	15	F	
16	G	352 48 47	41.992					750 305.611	317 298.769	16	G	
17	H	263 38 18	88.583					750 254.134	317 215.984	17	H	
18	I	278 57 47	65.696					750 274.184	317 239.128	18	I	
19	J	299 13 22	58.256					750 292.390	317 253.180	19	J	
20	K	289 05 49	136.167					750 308.498	317 175.349	20	K	
21	L	299 07 28	113.214					750 319.051	317 205.122	21	L	
22	M	313 45 16	108.821					750 339.206	317 225.419	22	M	
23	N	328 35 21	108.331					750 356.404	317 247.563	23	N	
24	P	345 13 41	112.055					750 372.300	317 275.451	24	P	
25										25		
26										26		
27										27		
28										28		
29										29		
30										30		
31										31		
32										32		
33										33		
34										34		
35										35		
36										36		

9.2.2 Interim Surveys

Equipment

Wild T16

Wild D13 Distomat

Prisms GDR 31 single and triple.

Motor Camp Area

Co-ordinates of points 1, 2 and 3 were assumed "fixed". The T16 in conjunction with D13 distomat was set up on each of the base points A, B, C and D then distances measured to relevant control points (either points 1 and 2 or 1 and 3). Co-ordinates were subsequently determined by intersection of the three distances (refer calculator programme) utilizing the subtended angle observed between control points as a check. Should checks differ markedly from predicted values, three sets of co-ordinates for the base point are calculated and averaged out in the following manner:

Example: Base point B, survey 8, June 1982

In the field, to "fix" base point B:

Distances measured B → 1 was 112.943 m

B → 2 was 112.605 m

Subtended angle measured 1 $\hat{B}$ 2 = was 109.340°

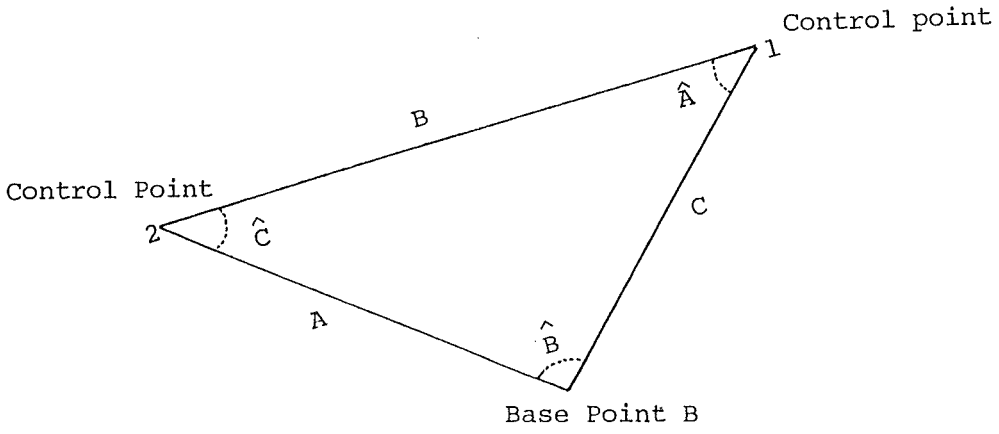

1) Using fixed distance B, measured distance C and subtended angle $\hat{B}$, angle $\hat{A}$ was calculated. Then co-ordinates for base point B were determined using co-ordinated control points 1 and 2, measured distance C and calculated angle $\hat{A}$ (utilizing calculator programme).

Measured Distance	Calculated angle	Co-ordinates mN	mE
112.943	32.268^{o}	353.100	579.124

2) Similarly using fixed distance B, measured distance A and angle $\hat{B}$, angle $\hat{C}$ was calculated. Subsequently co-ordinates for base point B were determined utilizing co-ordinated control points 1 and 3, measured distance A and calculated angle $\hat{C}$.

Measured Distance	Calculated angle	Co-ordinates mN	mE
112.605	35.390^{o}	353.101	579.116

3) Finally the co-ordinates of B were calculated by intersection using the two measured distances A and C in conjunction with co-ordinate control points 1 and 3.

Measured Distances	Co-ordinates mN	mE
112.943 112.605	353.106	579.121

The three co-ordinate sets north and east were averaged to obtain "adjusted co-ordinates" for the base point B:

353.103 mN, 579.120 mE.

Remaining monitoring points were co-ordinated by 'ties' (distance and a bearing) from the closest visible base point (either A, B, C or D).

Angles were observed using a T16 orientated onto the longest line to a control point; three full sets (left and right face) using different orientations (000,60°,20',120°) were taken and averaged.

Distance measurement was observed from the E.D.M. to:

- a pogo stick mounted G.D.R. single prism for all monitoring points (Fig.A9.1)
- a tripod mounted G.D.R. triple prisms for all base and control points.

Davids Road Area

T16 theodolite and D13 distomat were aligned over base point 11 and point 12 sighted with any base point (11) offset measured from control point 10 via a steel band. Base point positioning was determined by intersection using distances measured to points 10 and 13.

All monitoring points were subsequently fixed by "ties" to base point 11.

Vertical angles (both faces) were observed to points H, I and J, the adjusted angle used in heighting calculations; point 10 was held at 100 m.

Fig. A9.1

ANALYSED DATA - INTERIM SURVEYS

SURVEY 2: SEPTEMBER 7th-10th (1981)

SURVEY POINT	MEASURED distance (metres)	MEASURED subtended angle (degrees)	NEW COORDINATES metres N	NEW COORDINATES metres E	MOVEMENT from Survey 1
DAVIDS ROAD AREA			750,000+	317,000+	
11	179.098 (10)	144.404			
	234.033 (13)		263.951	304.019	0.4 cm
A	87.436	24.926	176.587	300.424	0.4
B	73.230	11.533	193.469	284.142	0.7
C	60.088	3.162	212.147	273.573	2.1
D	93.597	36.667	222.848	219.932	0.8
E	62.505	54.041	254.522	242.232	1.6
F	50.833	63.250	264.423	253.191	1.9
G	41.979	145.569	305.602	298.800	3.5
H	88.584	56.334	254.103	215.987	1.7
I	65.628	71.624	274.112	239.186	5.1
J	58.192	91.932	292.353	253.233	0.5
K	136.129	81.800	308.458	175.375	3.8
L	113.172	91.833	319.019	205.152	4.4
M	108.764	106.473	339.171	225.465	2.0
N	108.322	121.313	356.405	247.581	2.1
P	112.037	137.960	372.291	275.487	3.0

ANALYSED DATA - INTERIM SURVEYS

SURVEY 3: OCTOBER 12th-14th (1981)

SURVEY POINT	MEASURED distance (metres)	MEASURED subtended angle (degrees)	NEW COORDINATES metres N	NEW COORDINATES metres E	MOVEMENT from Survey 1
MOTOR CAMP AREA			750,000+	317,000+	
A	96.856 (1)	153.636			
	92.124 (2)		309.973	571.834	0.9 cm
A2	28.423	164.790	302.680	599.305	6.0
A3	33.137	136.732	287.405	596.098	1.9
A5	33.735	9.960	303.929	538.645	2.0
B	112.927 (1)	109.358	353.079	579.115	0.6
	112.589 (2)				
C	163.608 (1)	159.750	425.665	590.083	1.3
	322.598 (3)				
C3	49.392	8.207	452.744	631.391	2.2
C2	30.595	22.356	448.184	610.794	2.0
C4	26.355	75.565	451.570	585.233	1.4
C5	39.544	107.050	455.011	563.577	0.5
D	247.858 (1)	145.271	497.651	636.203	1.8
	254.483 (3)				
D2	32.676	170.149	494.892	603.644	2.4
D3	81.063	177.036	481.171	556.833	1.1
DAVIDS ROAD AREA					
11	179.095 (10)	144.402			
	234.037 (13)		263.947	304.020	0.3
A	87.435	24.922	176.588	300.418	1.0
B	73.233	11.531	193.467	284.139	1.1
C	60.090	3.164	212.146	273.571	2.1
D	93.595	36.667	222.849	219.934	0.8
E	62.515	54.047	254.527	242.221	2.8
F	50.834	63.261	264.433	253.190	2.7
G	42.012	145.564	305.634	298.792	1.7
H	88.585	56.342	254.115	215.984	2.9
I	65.639	71.639	274.131	239.177	7.2
J	58.207	91.936	292.364	253.222	1.8
K	136.142	81.808	308.480	175.369	6.0
L	113.182	91.836	319.029	205.146	5.6
M	108.778	106.478	339.188	225.461	3.6
N	108.327	121.317	356.413	247.585	2.4
P	112.039	137.958	372.292	275.483	3.4

ANALYSED DATA - INTERIM SURVEYS

SURVEY 4: NOVEMBER 24th-27th (1981)

SURVEY POINT	MEASURED distances (metres)	MEASURED subtended angle (degrees)	NEW COORDINATES metres N	NEW COORDINATES metres E	MOVEMENT from Survey 1
MOTOR CAMP AREA			750,000+	317,000+	
A	96.850 (1)	153.633			
	92.132 (2)		309.980	571.828	0.8 cm
A2	28.405	164.819	302.708	599.286	9.1
A3	33.135	136.728	287.414	596.091	3.1
A5	33.724	9.961	303.946	538.648	1.97
B	112.939 (1)	109.348	ADJUSTED COORDINATES		2.0
	112.597 (2)		353.093	579.119	
C	163.618 (1)	159.752	425.670	590.092	1.9
	322.588 (3)				
C3	49.391	8.204	452.746	631.400	1.9
C2	30.563	22.354	448.165	610.782	2.4
C4	26.358	75.568	451.578	585.240	2.0
C5	39.523	107.051	455.000	563.600	2.1
D	247.857 (1)	145.268	497.651	636.201	1.9
	254.485 (3)				
D2	32.692	170.140	494.896	603.625	2.3
D3	81.061	177.050	481.152	556.837	2.5
DAVIDS ROAD AREA					
11	179.093 (10)	144.402			
	234.034 (13)		263.949	304.012	1.0
A	87.432	24.925	176.591	300.422	0.7
B	73.228	11.528	193.473	284.137	1.1
C	60.077	3.179	212.166	273.564	4.2
D	93.600	36.676	222.860	219.923	2.3
E	62.512	54.054	254.535	242.223	3.1
F	50.839	63.267	264.438	253.185	3.4
G	42.025	145.561	305.647	298.788	2.4
H	88.586	56.347	254.123	215.983	3.8
I	65.645	71.650	274.144	239.174	8.5
J	58.218	91.939	292.372	253.214	2.9
K	136.150	81.810	308.488	175.363	7.0
L	113.196	91.839	319.041	205.137	7.1
M	108.798	106.475	339.197	225.443	5.4
N	108.338	121.314	365.420	247.575	3.5
P	112.043	137.954	372.294	275.474	4.2

ANALYSED DATA - INTERIM SURVEYS

SURVEY 5: FEBRUARY 1st-6th (1982)

SURVEY POINT	MEASURED distance (metres)	MEASURED subtended angle (degrees)	NEW COORDINATES metres N	NEW COORDINATES metres E	MOVEMENT from Survey 1
MOTOR CAMP AREA			750,000+	317,000+	
A	96.854 (1)	153.630			
	92.129 (2)		309.981	571.832	1.1 cm
A2	28.440	164.881	302.730	599.332	8.0
A3	33.133	136.724	287.415	596.092	3.1
A5	33.738	9.957	303.946	538.638	1.0
B	112.939 (1)	109.345	353.096	579.121	2.4
	112.597 (2)				
C	163.603 (1)	159.751	425.661	590.080	1.1
	322.603 (3)				
C3	49.409	8.203	452.746	631.403	1.8
C2	30.627	22.365	448.207	610.809	3.9
C4	26.372	75.551	451.584	585.233	2.7
C5	39.547	107.044	455.011	563.575	0.6
D	247.869 (1)	145.265	497.667	636.202	3.1
	254.480 (3)				
D2	32.692	170.125	494.923	603.625	5.0
D3	81.068	177.054	481.166	556.831	1.6
DAVIDS ROAD AREA					
11	179.093 (10)	144.403			
	234.034 (13)		263.949	304.012	1.0
A	87.441	24.922	176.582	300.417	1.2
B	73.224	11.522	193.479	284.131	1.8
C	60.091	3.183	212.156	273.553	3.8
D	93.606	36.681	222.864	219.914	3.2
E	62.524	54.058	524.537	242.210	4.3
F	50.843	63.272	264.443	253.181	4.1
G	42.028	145.550	305.649	298.780	3.2
H	88.579	56.353	254.133	215.989	4.7
I	65.670	71.664	274.164	239.151	11.4
J	58.222	91.944	292.379	253.213	3.6
K	136.144	81.817	308.501	175.374	7.9
L	113.202	91.844	319.052	205.137	8.1
M	108.808	106.478	339.208	225.440	6.4
N	108.340	121.314	356.421	247.574	3.7
P	112.042	137.953	372.293	275.472	4.4

ANALYSED DATA - INTERIM SURVEYS

SURVEY 6: MARCH 2nd-6th (1982)

SURVEY POINT	MEASURED distance (metres)	MEASURED subtended angle (degrees)	NEW COORDINATES metres N	NEW COORDINATES metres E	MOVEMENT from Survey 1
MOTOR CAMP AREA			750,000+	317,000+	
A	96.853 (1)	153.622			
	92.133 (2)		309.987	571.831	1.5 cm
A2	28.425	164.899	302.750	599.319	10.4
A3	33.130	136.721	287.423	596.089	3.9
A5	33.734	9.957	303.951	538.641	1.6
B	112.929 (1)	109.339			
	112.612 (2)		353.104	579.107	2.9
C	163.609 (1)	159.744	425.674	590.075	2.5
	322.602 (3)				
C3	49.415	8.208	452.765	631.402	3.7
C2					
C4	26.369	75.551	451.594	585.230	3.7
C5	39.548	107.044	455.026	563.570	2.0
D	247.879 (1)	145.260	497.680	636.202	4.3
	254.477 (3)				
D2	32.685	170.082	494.962	603.630	8.9
D3	81.070	177.064	481.168	556.833	1.3
DAVIDS ROAD AREA					
11	179.094 (10)	144.400			
	234.043 (13)		263.942	304.028	0.9
A	87.442	24.922	176.581	300.417	1.3
B	73.237	11.518	193.467	284.122	2.7
C	60.085	3.189	212.164	273.550	4.7
D	93.605	36.681	222.865	219.915	3.2
E	62.516	54.057	254.538	242.218	3.7
F	50.854	63.269	264.440	253.170	4.6
G	42.031	145.539	305.651	298.771	4.1
H	88.593	56.353	254.131	215.975	4.7
I	65.673	71.672	274.173	239.150	12.2
J	58.237	91.942	292.384	253.199	4.8
K	136.161	81.810	308.491	175.353	7.8
L	113.201	91.842	319.049	205.136	7.8
M	108.822	106.474	339.213	225.424	7.9
N	108.333	121.310	356.411	247.571	3.3
P	112.050	137.950	372.299	275.465	5.3

ANALYSED DATA - INTERIM SURVEYS

SURVEY 7: APRIL 6th-9th (1982)

SURVEY POINT	MEASURED distance (metres)	MEASURED subtended angle (degrees)	NEW COORDINATES metres N	NEW COORDINATES metres E	MOVEMENT from Survey 1
MOTOR CAMP AREA			750,000+	317,000+	
A	96.846 (1)	153.622			
	92.140 (2)		309.989	571.824	1.6 cm
A2	28.410	164.931	302.772	599.302	13.1
A3	33.120	136.717	287.430	596.074	5.4
A5	33.723	9.956	303.955	538.645	2.1
B	112.944 (1)	109.337			
	112.604 (2)		353.106	579.122	3.3
C	163.609 (1)	159.739			
	322.604 (3)		425.678	590.071	3.0
C3	49.420	8.206	452.769	631.404	4.1
C2	30.628	22.386	448.231	610.794	6.4
C4	26.364	75.547	451.594	585.229	3.8
C5	39.539	107.039	455.026	563.576	1.8
D	247.879 (1)	145.261			
	254.475 (2)		497.678	636.204	4.1
D2	32.693	170.063	494.970	603.623	9.7
D3	81.067	177.067	481.162	556.837	1.5
DAVIDS ROAD AREA					
11	179.097 (10)	144.401			
	234.041 (13)		263.945	304.030	0.9
A	87.433	24.922	176.590	300.418	1.0
B	73.221	11.514	193.484	284.122	2.8
C	60.087	3.189	212.162	273.549	4.6
D	93.603	36.681	222.866	219.917	3.1
E	62.509	54.056	254.538	242.226	3.1
F	50.844	63.267	264.438	253.180	3.8
G	42.041	145.533	305.660	298.766	4.9
H	88.582	56.350	254.128	215.986	4.2
I	65.654	71.667	274.165	239.168	10.7
J	58.254	91.936	292.387	253.181	6.3
K	136.164	81.811	308.494	175.351	8.1
L	113.202	91.839	319.044	205.132	7.6
M	108.819	106.469	339.204	225.420	7.5
N	108.342	121.308	356.417	247.563	4.3
P	112.050	137.942	372.295	275.450	6.4

ANALYSED DATA - INTERIM SURVEYS

SURVEY 8: JUNE 15th-18th (1982)

SURVEY POINT	MEASURED distance (metres)	MEASURED subtended angle (degrees)	NEW COORDINATES metres N	NEW COORDINATES metres E	MOVEMENT from Survey 1
MOTOR CAMP AREA			750,000+	317,000+	
A	96.844 (1)	153.617			
	92.144 (2)		309.994	571.822	2.1 cm
A2	28.384	164.951	302.794	599.278	16.1
A3	33.105	136.710	287.444	596.059	7.4
A5	33.714	9.957	303.959	538.653	3.0
B	112.943 (1)	109.340	ADJUSTED COORDINATES		
	112.605 (2)		353.103	579.120	3.0
C	163.615 (1)	159.745	425.676	590.081	2.5
	322.596 (3)				
C3	49.416	8.217	452.774	631.405	4.6
C2	30.627	22.399	448.234	610.797	6.7
C4	26.368	75.560	451.594	585.232	3.7
C5	39.541	107.058	455.017	563.574	1.1
D	247.882 (1)	145.257	ADJUSTED COORDINATES		
	254.47 (3)		497.685	636.200	4.9
D2	32.696	170.050	494.985	603.616	11.3
D3	81.050	177.069	481.172	556.850	0.8
DAVIDS ROAD AREA					
11	179.094 (10)	144.401			
	234.036 (13)		263.948	304.017	0.5
A	87.443	24.924	176.587	300.420	0.8
B	73.221	11.522	193.481	284.131	1.9
C	60.085	3.188	212.163	273.551	4.5
D	93.598	36.679	222.865	219.923	2.7
E	62.506	54.056	254.538	242.229	3.0
F	50.844	63.269	264.440	253.180	3.9
G	42.039	145.531	305.658	298.764	5.0
H	88.596	56.351	254.128	215.972	4.5
I	65.686	71.678	274.182	239.138	13.6
J	58.254	91.940	292.391	253.183	6.4
K	136.173	81.814	308.504	175.344	9.3
L	113.218	91.843	319.059	205.122	9.4
M	108.818	106.469	339.203	225.420	7.5
N	108.348	121.307	356.421	247.558	4.9
P	112.052	137.943	372.297	275.451	6.4

REDUCED LEVELS

$R.L._b$ = $R.L._a$ + Instrument height $\pm\Delta h$ - Target height

$\pm\Delta h$ = horizontal distance x tan V.A. (from 90°)

Height of IT 10 = 100.00 m (arbitrary datumn)

HEIGHTING

DAVIDS ROAD AREA

AUGUST 1981

Point	Horizontal distance	Vertical angle	H.I.	H.T.	Reduced level	movement
11→10	179.097	88.948	1.75	1.61	96.57	
11→H	88.584	102.573	1.75	0.05	78.513	
11→I	65.596	107.441	1.75	0.05	77.662	
11→J	59.192	109.736	1.75	0.05	77.393	

SEPTEMBER 1981

11→H	88.584	102.632	1.79	0	78.507	0.6 cm
11→I	65.628	107.530	1.79	0	77.630	3.2
11→J	58.192	109.812	1.79	0	77.396	0.3

OCTOBER 1981

11→H	88.585	102.620	1.77	0	78.506	0.7
11→I	65.639	107.518	1.77	0	77.621	4.1
11→J	58.207	109.790	1.77	0	77.396	0.3

NOVEMBER 1981

11→H	88.586	102.625	1.78	0	78.508	0.5
11→I	65.645	107.528	1.78	0	77.617	4.5
11→J	58.218	109.792	1.78	0	77.399	0.6

FEBRUARY 1982

11→H	88.579	102.648	1.81	0	78.502	1.1
11→I	65.670	107.562	1.81	0	77.596	6.6
11→J	58.222	109.833	1.81	0	77.381	1.2

MARCH 1982

11→H	88.593	102.622	1.76	0	78.491	2.2
11→I	65.673	106.753	1.76	0.98	77.581	8.1
11→J	58.237	109.786	1.76	0	77.379	1.4

APRIL 1982

Point	Horizontal distance	Vertical angle	H.I.	H.T	Reduced level	movement
11→H	88.582	102.602	1.74	0	78.506	0.7 cm
11→I	65.654	106.702	1.74	1.02	77.590	7.2
11→J	58.254	109.765	1.74	0	77.377	1.6

JUNE 1982

11→H	88.596	102.635	1.78	0	78.490	2.3
11→I	65.686	106.738	1.78	1.03	77.566	9.6
11→J	58.254	109.811	1.78	0	77.365	2.8

AUGUST 1982

11→10	179.097	88.930	1.73	1.63	96.56	
11→H	88.583	101.983	1.73	1.00	78.489	2.4
11→I	65.696	106.688	1.73	1.04	77.555	10.7
11→J	58.256	109.759	1.73	0	77.364	2.9

A9.3 ACCURACY

Whenever possible the same method and equipment was used to reduce calibration and calculation variations. Averaged sets of angles were assumed accurate to 10 seconds yielding an error of ±5 mm over a 100 m line. Since most "ties" were less than 100 m and the quoted accuracy of the Wild D13 is ±5 mm then a maximum survey error of ±1 cm was assumed.

Movement is shown on survey network plans by displacement vectors which are relative to either control point 1 in the Motor Camp area or base point 11 in the Davids Road area (refer map enclosure). Their orientation especially those up to 30 mm is greatly affected by a small variation normal to their direction, however general trends do show up.

A9.4 SURVEY PROGRAMME

(written for a Texas T159 calculator)

PROGRAMME DESCRIPTION

To find the rectangular coordinates of a third survey point by entering .....

1) the rectangular coordinates of two other survey stations;

and either 2) enter the two distances from these stations to the third survey point;

or 3) enter the distance from one survey station to the third point and the angle subtended between that distance and a line joining the two survey stations.

CONVENTIONS FOR ENTERING DATA

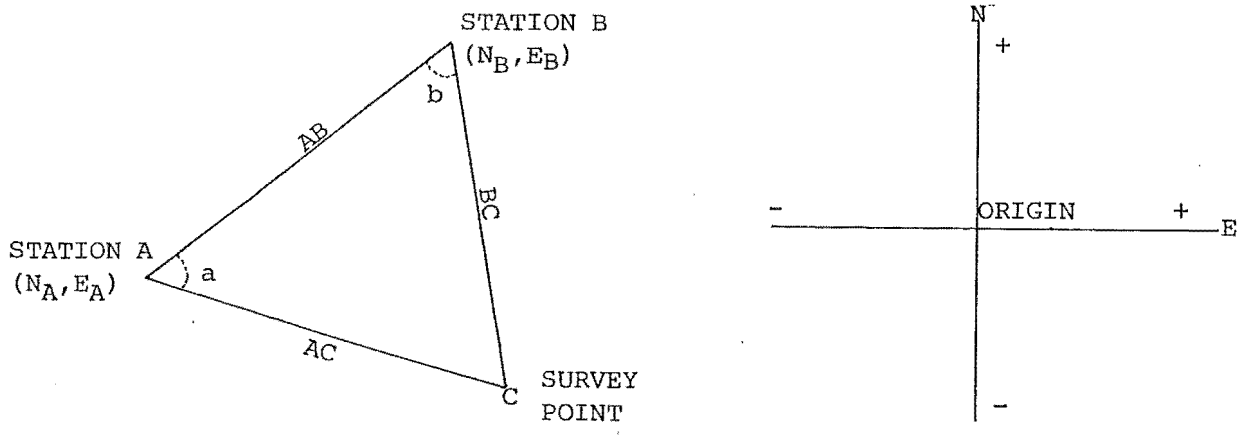

1) Rectangular coordinates are expressed in northings and eastings; + for north, - for south, + for east, - for west.

2) To avoid a wrong solution (two solutions are possible) data must be entered in either of the three following sequences to obtain the coordinates of survey point C.

1) If the distance BC and angle 'b' are known then enter;
coords of B → distance BC → angle 'b' → coords of A.

2) If the distance AC and angle 'a' are known then enter;
coords of B → angle 'a' → distance AC → coords of A.

3) If the two distances BC and AC are known then enter;
coords of B → distance BC → distance AC → coords of A.

USER INSTRUCTIONS

STEP	PROCEDURE	ENTER	PRESS	DISPLAY
1	Printer on, calculator on			
2	Read in program			
3	Enter northing of B (N_B)	eg400	A	400
4	Enter easting of B (E_B)	eg100	R/S	100
either 5	(1) Enter distance BC	eg670.8	R/S	670.8
	(2) Enter angle b		R/S	
or 6	(1) Enter angle a		R/S	
	(2) Enter distance AC	608	R/S	
or 7	(1) Enter distance BC		R/S	
	(2) Enter distance AC		R/S	
8	Enter northing of A (N_A)	eg-300	R/S	-300
9	Enter easting of A (E_A)	eg-200	R/S	-200
10	Run program; press [C] for step 5		CorEorB	
	[E] for step 6			
	[B] for step 7			
	Northing and Easting of C are printed in that order. For next triangle proceed from step 3.			

FORMULAE/CONVENTIONS

RECTANGULAR TO POLAR:

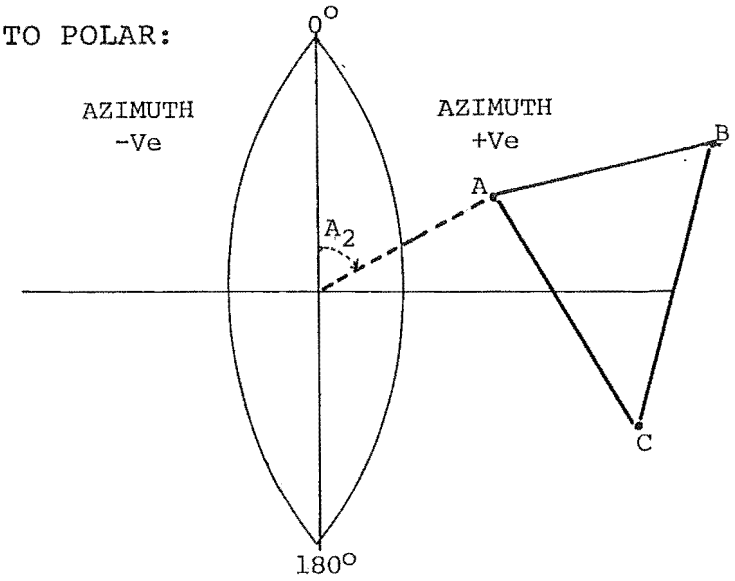

Triangle is treated as though B were at origin:

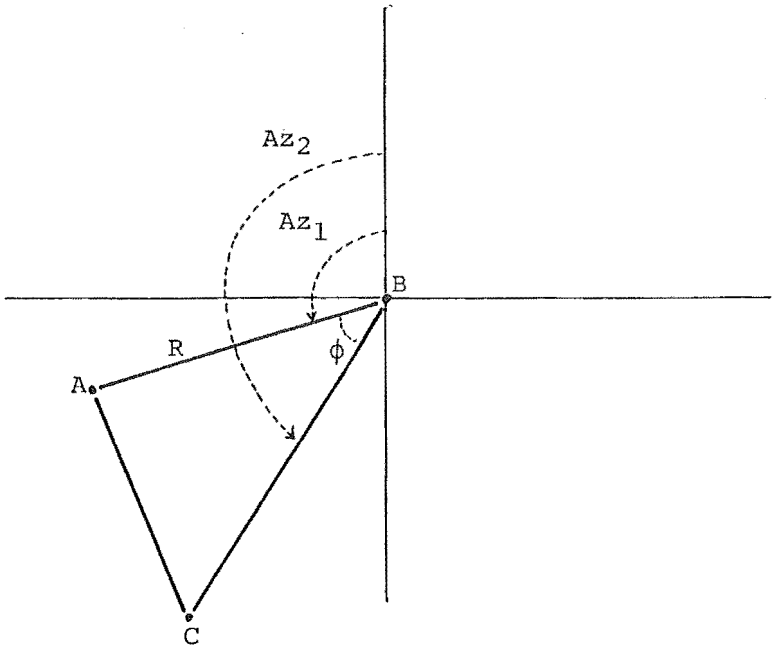

Rectangular to polar conversion derives Az_1 and radius R (AB)

e.g. -113·199°

$$\phi = \cos^{-1}\left(\frac{(AB)^2 + (BC)^2 - (AC)^2}{2 \times BC \times AB}\right)$$

e.g. $\phi = 43{\cdot}603^\circ$

$Az_2 = Az_1 - \phi$ = angular coord. of C

e.g. -113·199 - 43·603 = 156·802

Polar coords of C are converted back to rectangular coords.

CALCULATION OF SURVEY POINT MOVEMENT

To find out the distance between two sets of rectangular coordinates; either point can be entered first.

STEP	PROCEDURE	ENTER	PRESS	DISPLAY
1	Calculator on			
2	Read in program			
3	Enter Northing (N_A)		D	
4	Enter Easting (E_A)		R/S	
5	Enter Northing (N_B)		R/S	
6	Enter Easting (E_B)		R/S	

Point N_B and E_B is assumed to be the origin and distance between points is determined by rectangular to polar conversion; radius 'R' being the distance between points.

PROGRAMME FOR TEXAS T159
(G COATES)

000	76	LBL
001	11	A
002	42	STO
003	01	01
004	91	R/S
005	42	STO
006	02	02
007	91	R/S
008	42	STO
009	05	05
010	91	R/S
011	42	STO
012	06	06
013	91	R/S
014	42	STO
015	03	03
016	91	R/S
017	42	STO
018	04	04
019	91	R/S
020	76	LBL
021	12	B
022	43	RCL
023	04	04
024	75	-
025	43	RCL
026	02	02
027	95	=
028	32	X↕T
029	43	RCL
030	03	03
031	75	-
032	43	RCL
033	01	01
034	95	=
035	22	INV
036	37	P/R
037	75	-
038	09	9
039	00	0
040	95	=
041	94	+/-
042	42	STO
043	08	08
044	32	X↕T
045	42	STO
046	07	07
047	22	INV
048	87	IFF
049	01	01
050	23	LNX
051	71	SBR
052	22	INV
053	76	LBL
054	23	LNX
055	33	X²
056	85	+
057	43	RCL
058	05	05
059	33	X²
060	75	-
061	43	RCL
062	06	06
063	33	X²
064	95	=
065	55	÷
066	02	2
067	55	÷
068	43	RCL
069	05	05
070	55	÷
071	43	RCL
072	07	07
073	95	=
074	22	INV
075	39	COS
076	75	-
077	43	RCL
078	08	08
079	85	+
080	09	9
081	00	0
082	95	=
083	42	STO
084	09	09
085	43	RCL
086	05	05
087	32	X↕T
088	43	RCL
089	09	09
090	37	P/R
091	85	+
092	43	RCL
093	01	01
094	95	=
095	58	FIX
096	03	03
097	99	PRT
098	32	X↕T
099	85	+
100	43	RCL
101	02	02
102	95	=
103	99	PRT
104	98	ADV
105	81	RST
106	76	LBL
107	13	C
108	86	STF
109	01	01
110	61	GTO
111	12	B
112	76	LBL
113	22	INV
114	43	RCL
115	06	06
116	39	COS
117	65	×
118	43	RCL
119	05	05
120	65	×
121	43	RCL
122	07	07
123	65	×
124	02	2
125	95	=
126	94	+/-
127	85	+
128	43	RCL
129	05	05
130	33	X²
131	85	+
132	43	RCL
133	07	07
134	33	X²
135	95	=
136	34	ΓX
137	42	STO
138	06	06
139	43	RCL
140	07	07
141	92	RTN
142	76	LBL
143	14	D
144	42	STO
145	01	01
146	91	R/S
147	42	STO
148	02	02
149	91	R/S
150	42	STO
151	03	03
152	91	R/S
153	75	-
154	43	RCL
155	02	02
156	95	=
157	42	STO
158	04	04
159	43	RCL
160	03	03
161	75	-
162	43	RCL
163	01	01
164	95	=
165	42	STO
166	05	05
167	43	RCL
168	04	04
169	32	X↕T
170	43	RCL
171	05	05
172	22	INV
173	37	P/R
174	32	X↕T
175	91	R/S
176	76	LBL
177	15	E
178	43	RCL
179	02	02
180	75	-
181	43	RCL
182	04	04
183	95	=
184	32	X↕T
185	43	RCL
186	01	01
187	75	-
188	43	RCL
189	03	03
190	95	=
191	22	INV
192	37	P/R
193	32	X↕T
194	42	STO
195	10	10
196	33	X²
197	85	+
198	43	RCL
199	06	06
200	33	X²
201	75	-
202	53	(
203	02	2
204	65	×
205	43	RCL
206	06	06
207	65	×
208	43	RCL
209	10	10
210	65	×
211	43	RCL
212	05	05
213	39	COS
214	54	)
215	95	=
216	34	ΓX
217	42	STO
218	05	05
219	61	GTO
220	12	B

A9.5 CADESTRAL REPORTS

CLARK BREWSTER McDONALD & ASSOCIATES
REGISTERED LAND SURVEYORS, LAND DEVELOPMENT & PLANNING CONSULTANTS

ORIGINATING OFFICE:
56 Tennyson Street Dunedin
P.O. Box 5113
Telephone: 770-690

92 Esk Street, Invercargill
P.O. Box 1707
Telephone 55 063

14 Manley Street, Gore
P.O. Box 207
Telephone 7174

OUR REF:

DATE: 22 July 1981

Department of Geology
Canterbury University
Ilam
CHRISTCHURCH

ATTENTION: Mr D H Bell, Senior Lecturer, Engineering Geology

Dear Sir

GROUND MOVEMENT MOERAKI

A recent enquiry from Mr Ashley Muir of Mason & Wales, Architects, Dunedin, has resurrected a situation that occurred during the period July - October 1979 during which a survey was executed to re-establish the boundaries of Pt Sec 2 Blk XVI Town of Moeraki. Definition was based on reproduction from the original town layout plan to fix certain boundaries and it transpired that this definition was not accepted by the Chief Surveyor thus initiating correspondence and culminating in an investigation survey being carried out by the Lands & Survey Department in the Moeraki area at our request.

Mr Muir has been approached by his clients, the Mathiesons, whom we believe are now in possession of Certificate of Title 89/165 being Section 13 of the town of Moeraki. His clients are anxious in respect of earth movement in that area and we would here confirm that our survey originated in TENBY STREET and concluded in END STREET and the resultant discrepancies between a direct reproduction of the original section layout and its current position was of the order of 2m, said movement having taken place over a period from approximately 1890 to the present time. During the course of our investigations the opportunity was taken to refer to Mr Bensons reports of the area and on perusing and reading his comments, it was concluded that our survey had traversed one of a series of major faults referred to by him in his report.

We understand that Mr Molleneux is currently involved in research in the area and would here refer you to the Department of Lands & Survey, in particular the Chief Surveyor, for the documentation which is a matter of record and will be on their files, said file also containing our documentation in respect thereto.

...../2

Mr D H Bell

22 July 1981

The situation not only presents interesting geological implications but there are broader implications with respect to the land title system particularly in relation to the reproduction of titled boundaries where earth movement is recorded.

We trust that this information will be of interest to you and should the services of our firm be required we would be most happy to assist, but we would recommend that you contact the Chief Surveyor at the Lands & Survey Department who will, I am sure, be happy to assist in the first instance.

Yours faithfully

J G Brewster
Surveying Consultant

JGB:JO

L. & S. – F. 2

DEPARTMENT OF LANDS AND SURVEY

TELEGRAPHIC ADDRESS: 'LANDS'

FOR VERBAL INQUIRIES
PLEASE ASK FOR Mr Petre

TELEPHONE No. 770-650

OUR REFERENCE: 14/193

YOUR REFERENCE:

DISTRICT OFFICE,
P.O. BOX 896
DUNEDIN

16 October 1981

Geology

Mr M Molyneux
~~Engineering~~ Department
University of Canterbury
CHRISTCHURCH

Dear Sir

MOERAKI - LAND MOVEMENT

I have inspected the cadastral survey plans in Moeraki about the area you are investigating.

Plans are

Plan Number	Date	Remarks
SO 14577	1863	
SO 14579	1863	Old marks shown on subsequent plans show no sign of significant movement
SO 14576	Assume 1863	
	No date	
SO 14585	1922	
ML 75	1928	
SO 12356	1956	Indications that there is some movement supported by FB page 28 between 1922 to 1954
SO 12579	1957	
DP 10267	1961	
SO 13127	1961	
SO 13208	1962	
DP 10621	1962	
DP 10377	1962	Generally without calculations no significant change in positioning
DP 11016	1965	
DP 11464	1967	
DP 11746	1968	
SO 16979	1969	Discloses some differences
DP 15253	1973	
DP 15719	1975	Shows differences on marks established on DP 10377 Date 1962

Also some marks in FB 1495 page 28.

To make use of this information you would need to investigate closely the differences that may be disclosed and decide whether they are due to earth movement or survey differences. Equally significant is that there are little or no differences disclosed until 1928.

To properly assess this information is a major job however this memo gives you some idea of the records of survey that are available and if you wish to have any particularly small area looked at I may be able to assist you. The records are certainly available for your perusal.

Yours faithfully

R C Petre
Chief Surveyor

Attached are copies of two reports suggesting earth movement.

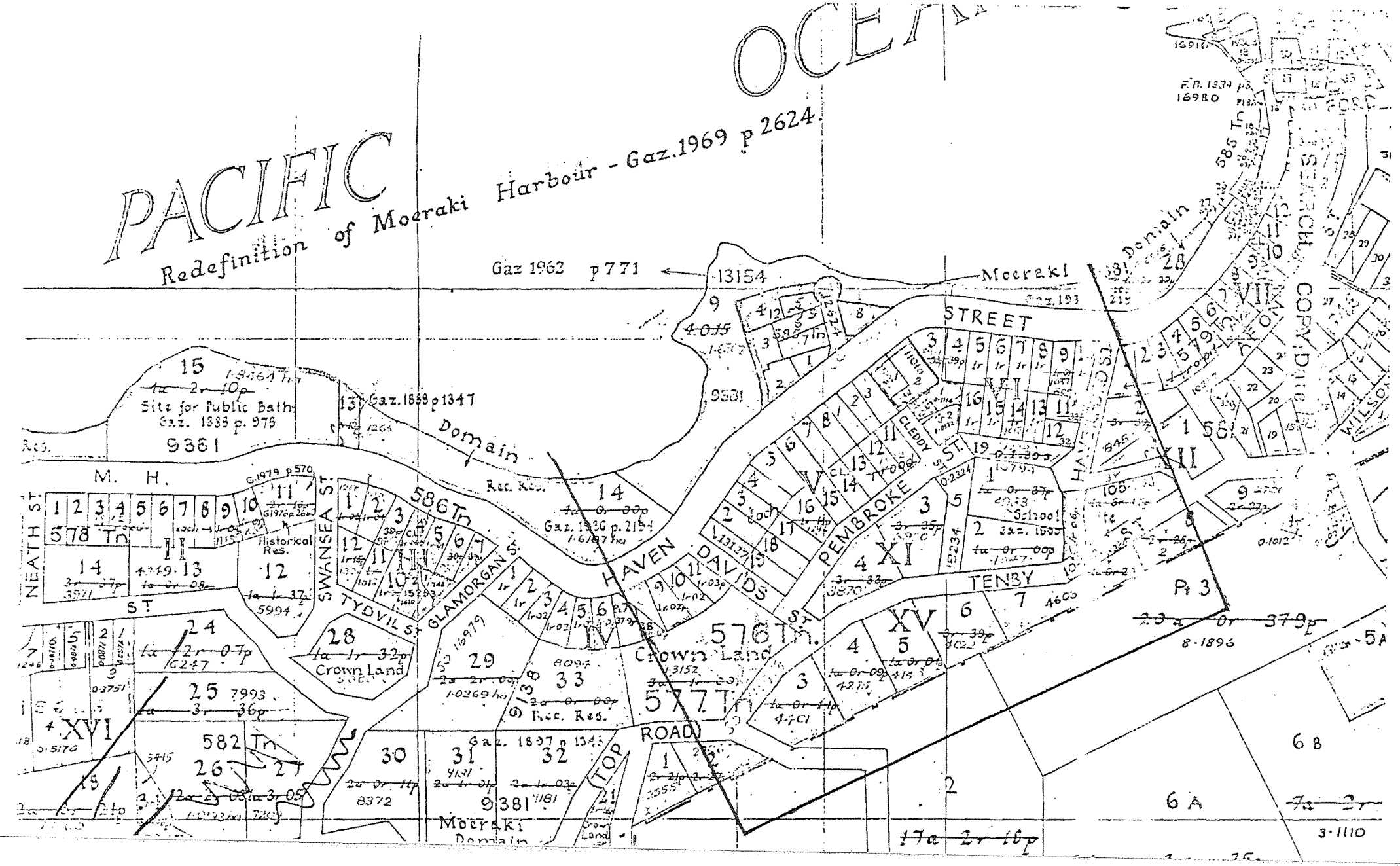
PACIFIC
Redefinition of Moeraki Harbour - Gaz.1969 p 2624.
Gaz 1962 p 771
13154
Moeraki
STREET
Domain
Rec. Res.
Gaz. 1888 p 1347
Site for Public Baths
Gaz. 1888 p. 975
9381
M. H.
Historical Res.
SWANSEA ST.
TYDVIL ST.
GLAMORGAN ST.
HAVEN
DAVIDS
PEMBROKE
CLEDDY
TENBY
NEATH ST.
586Tn
578Tn
576Tn.
577Tn.
582Tn
Crown Land
Gaz. 1897 p 1343
TOP ROAD
Moeraki Domain
SEARCH COPY DUNEDIN
WILSON
F.P. 1534 p3
16980
16910
585Tn
8·1896
3·1110
299

11/30

DUNEDIN.

27 April 1970

The Chief Surveyor,
OFFICE.

Survey file 69/68.

LEADING LIGHTS - MOERAKI SO 16979

In the fix of these marine beacons it was necessary to run traverses and place several survey marks. A plan has been drawn for survey information. A previous report is on folio 200.

Origin of bearings Trig E - Trig Shag Point
Origin of co-ordinates Trig E

Bearings and co-ordinates are in terms of geodetic datum. Rays were observed from trig E to OITX and OITY, ML66 and from the comparison obtained 40" has been added to all old bearings to bring the surveys in terms of geodetic datum.

Traverses have been run from trig E to connect with surveys in the Town of Moeraki and from adopted work co-ordinates have been obtained for several old marks including OITX ML66.

Where old work was tied to, it was difficult to establish agreement between any of the marks. Differences were so inconsistent this can only be put down to earth movement in the area.

The OIT shown south of ITXV is possibly ITIV SO12579. It was loose in the ground and protruding 1 inch. Neither ITIV nor the peg placed on section 4 could be found and it appears that the OIT found could be ITV shifted to another position. Other marks on SO12579 looked for were ITV which was not found and ITVIII which has been disturbed. The ray ITVII to ITXI is now blocked by a house.

M.H. Warburton
Senior Surveyor.

J. R. Park M.N.Z.I.S.
REGISTERED SURVEYOR

STRINGER'S BUILDING,
130 THAMES ST., (Cnr. Eden St.)
OAMARU.

SURVEY REPORT.

Sections 8 & 9 Blk 111 Town of Moeraki.

The Initial Bearing was between Trigs 'E' &'Y'.

The Position of O.P. S.O. 586 Town was accepted to fix the North Western corner. The original bearings and distances were accepted to fix the alignment of the Street frontages and original bearings and adjusted distances used on the other two boundaries.

I.T. 1V and I.T. V And the peg on the rear boundary of Section 4 as shown on S.O. 586 Town were searched for unsuccessfully.

The O.I.T. no Record could presumably be in Posn of O.P. V11 S.O.586 Tn but due to massive soil creep in this area the reliability of any old marks is questionable.

O.I.T. XX1 of S.O. 13127 was also searched for unsuccessfully,

J. R. Park.
Registered Surveyor.

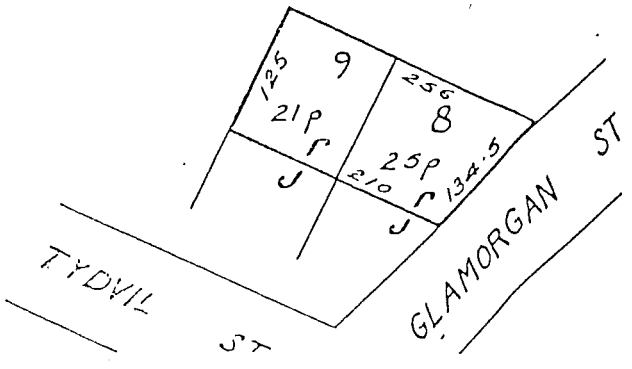

APPENDIX 10

PROGRESSIVE FAILURE

Introduction

A10.1 Mechanism of Progressive Failure (A Model)

A10.2 Susceptibility of Over-consolidated Clays to Progressive Failure

INTRODUCTION

The theory of progressive slope failure was originally developed by Skempton (1964) and Bjerrum (1967) to explain the apparent anomaly of first time slide in some over-consolidated clays occurring well below peak strength.

Skempton (1964) drew a number of important conclusions relating to the long term stability of clay slopes:

1) After a slide has taken place the strength along a slip surface is equal to the residual value. This value can be defined by the angle of shearing resistance ϕr and is the result of clay particle orientation.

2) ϕr is independent of the clays original strength and properties such as water content, liquidity index ...; its value dependent on size, shape and mineralogical composition of the particles.

3) Analysis of first-time slides in non-fissured clays showed failures initiated at strengths only slightly less than peak.

4) Back analyses of first time slides in fissured clays showed stress at failure nearly equal to the residual strength and therefore some method of "progressive failure" was required to take the clay past peak strength.

The rate at which a continuous sliding surface will develop by progressive failure can vary from one clay to another and in the stiffer clays the rate can be so small that the delay of a slide may be in the order of centuries (Bjerrum, 1967).

If the progressive failure phenomenon is ignored and stability is based on peak strength parameters a dangerously unstable slope may be assumed safe.

A10.1 MECHANISM OF PROGRESSIVE FAILURE (A Model)

Bjerrum (1967) developed a simple mathematical model for the propagation of a continuous rupture surface amidst "unfailed" clay slopes (Fig.A10.1).

Consider a simplified case of a small block (OO',AA') from a uniform stable slope of inclination α.

To initiate progressive failure there must be a discontinuity of some type somewhere in the slope. In this case it is assumed a cut with vertical walls is made exposing the face OO'. Removal of lateral support by excavation produces a redistribution of internal stresses; it is assumed AA' is sufficiently far away from the excavation so as not to be affected.

The difference between horizontal and vertical stress will maximise at point O so this represents the point of greatest shear stress (Fig.A10.1).

The question of whether excavation will initiate a progressive failure or not is dependant on whether increased shear stress exceeds peak strength of the clay. If it does a local failure will propogate along (O,P_1) until shear stress along this surface (due to the difference in horizontal and vertical stress) is less than peak strength of the clay. Assuming a large increase in strain accompanies failure across this zone (release of latent strain energy), clay strength will be taken well past peak and approach the residual value. If the residual strength is so low or the inclination of the slope (α) is so high that the block of clay on the already formed failure plane moves downhill, lateral pressures along (P,P_1') will be removed. shear stress concentrated at P_1 and the failure surface will progress backwards along P_1,A.

The assumption that progressive failure will progress approximately parallel to the slope is based on observations of actual slides rather than theoretical proof.

Based on this simplified model some pre-requisites for

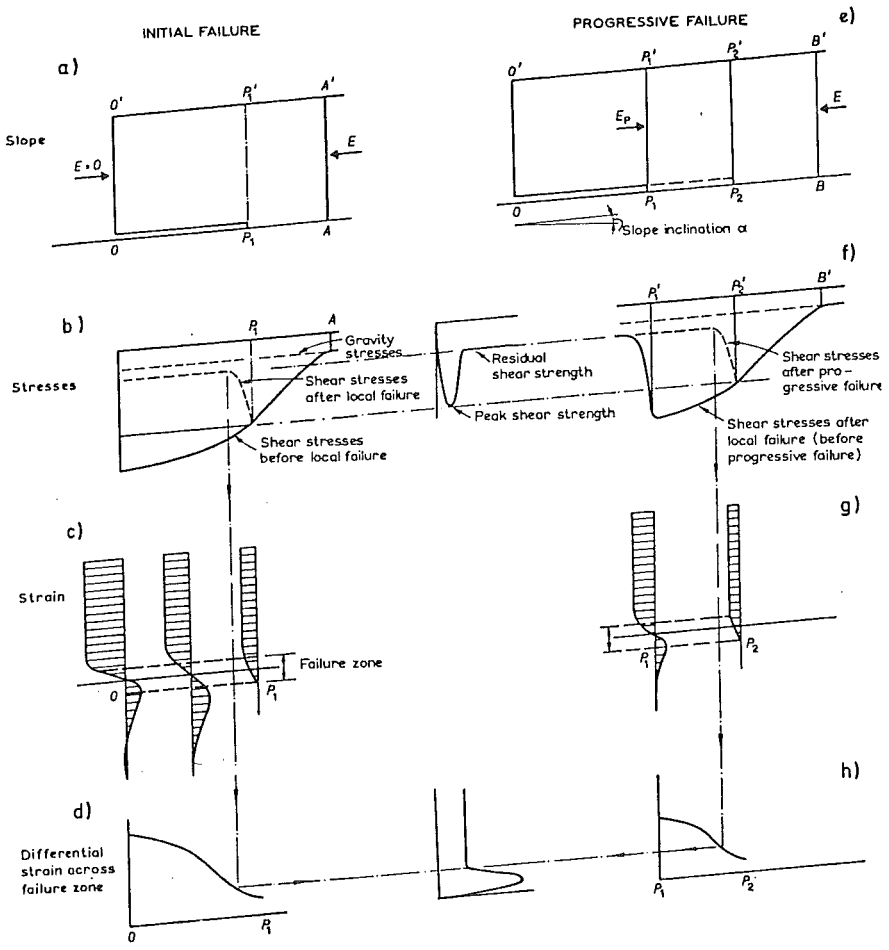

Fig.A10.1: Principle of development of continuous sliding surface by progressive failure. (Bjerrum, 1967, Fig.2).

	Overconsolidated plastic clay with weak bonds		Overconsolidated plastic clay with strong bonds		Overconsolidated clay with low plasticity
	unweathered	weathered	unweathered	weathered	
p_H / s_{peak}	2	3	0-1	3	1
$\epsilon_H / \epsilon_{peak}$	2	2	1	3	0-1
s_{peak} / s_{res}	2	1	3	2	0-1
Relative danger of progressive failure	High	High	Low	Very high	Very low

Potential for progressive failure of various types of clay, based on an evaluation of the degree to which the three significant ratios are fulfilled. Notations used:

0 Fulfillment not pronounced
1 Fulfillment less pronounced
2 Fulfillment pronounced
3 Fulfillment very pronounced

NOTE: lateral internal stress: : p_H
peak shear strength : s_{peak}
stored, recoverable strain energy: ϵ_H
failure stain : ϵ_{peak}
residual strength : $s_{residual}$

Fig.A10.2: Relative potential for progressive failure for differing degrees of over-consolidation. (Bjerrum, 1967, Table 3)

progressive failure can be specified.

1) There must be a discontinuity within the clay mass or at its boundary where failure can be initiated producing deformations which allow advancement of the failure surface (excavation, erosion, presence of fissures).

2) Local shear stress caused by this discontinuity must exceed the peak strength of the clay.

3) There must be sufficient strain to take the clay beyond peak strength and approach the residual value.

4) The clay must show a large and rapid decrease in shear strength with strain after failure, so shear resistance along the rupture zone allows sufficient displacement of the failed block to move the zone of stress concentration to neighbouring areas of unfailed clay (ie. material must have shear-stress behaviour showing a pronounced peak, characteristic of over-consolidated clays).

A10.2 SUSCEPTIBILITY OF OVER-CONSOLIDATED CLAYS TO PROGRESSIVE FAILURE

The more over-consolidated the clay, the more recoverable strain energy and consequently the greater the danger of progressive dailure. Also the steeper the slope and the deeper the cut to initiate failure the better the conditions for progressive failure.

However for the same degree of over-consolidation, and topography three main factors govern a clay's susceptibility to progressive failure:

1) strength of diagenetic bonds;
2) if the clay is weathered or unweathered;
3) if the clay is of high or low plasticity.

Bjerrum (1967) produced a chart indicating potential for progressive failure based on these three factors (Fig.A10.2).

In over-consolidated clays with weak bonds danger of progressive failure is large but with strong diagenetic bonds strain energy is locked in and therefore chances of progressive failure in the unweathered clay are small. Once bonding is gradually destroyed by weathering strain energy is released and danger of progressive failure increases.

For comparative purposes Bjerrum included a clay of low plasticity; danger of progressive failure is very low due to small percentages of active clay minerals (smectites) resulting in low recoverable strain energy and small strains accompanying failure, (ie. the clay is not brittle and does not show significant reduction in strength when strained beyond failure).

The rate of progressive failure, which determines time delay until slope failure is difficult to assess. However three sets of conditions are distinguished by Bjerrum (1967).

1) If the difference between lateral and vertical stress, due to the slope discontinuity, is large, resulting in a shear stress much greater than the undrained strength of the clay a progressive failure will develop rapidly.

2) If the discontinuity results in shear stresses smaller than undrained strength but larger than drained strength then progressive failure will not occur rapidly. In the zone of shear stress, the clay will dilate and increase in moisture content (depending on the availability of water) and with time decrease from the undrained to the drained strength. Therefore the rate at which progressive failure will proceed is dependent on time required to reduce from undrained strength to that of the acting shear stress.

3) If the discontinuity causes a shear stress (difference between vertical and horizontal stress) less than the drained strength there will be no failure.

It is also necessary to consider seasonal variations in the groundwater level causing changes in clays strength both in the unfailed portion and slip surface already developed.

Investigations pertaining to "rate" of progressive slope failure within the Hampden and Kurinui Formation have not been possible because of time restrictions imposed for thesis submission.